# Time-Optimal Control of the Bi-Steerable Robot

## A Case Study in Optimal Control of Nonholonomic Systems

Markus Mauder

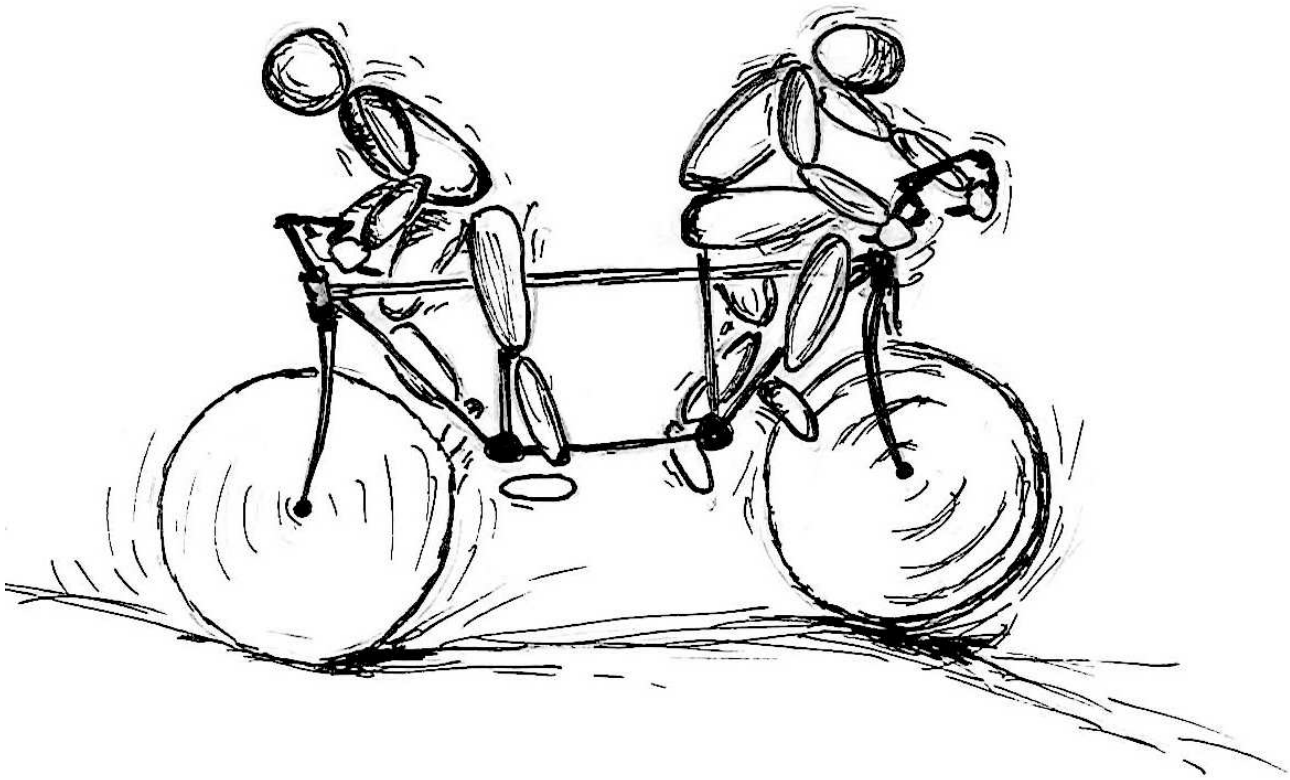

July 2012

# Time-Optimal Control of the Bi-Steerable Robot

## A Case Study in Optimal Control of Nonholonomic Systems


Dissertationsschrift zur Erlangung
des naturwissenschaftlichen Doktorgrads
der Julius-Maximilians-Universität Würzburg

vorgelegt von

**Markus Mauder**

aus

Bad Neustadt a. d. Saale

**Juli 2012**

Eingereicht am 06.07.2012

bei der Fakultät für Mathematik und Informatik
der Julius-Maximilians-Universität Würzburg

1. Gutachter: Prof. Dr. Uwe Helmke

2. Gutachter: Prof. Dr. Michael Zeitz

Tag der mündlichen Prüfung: 23.11.2012

# Vorwort

> *When you begin working on a Ph.D. you don't imagine what it means and how it will influence your life not only during the Ph.D. but also probably for the remainder of your life.*
>
> Eric Colon, Royal Military Academy

Die vorliegende Dissertation entstand während meiner Zeit als externer Doktorand am Lehrstuhl für Mathematik II der Fakultät für Mathematik und Informatik an der Julius-Maximilians-Universität Würzburg. Ausgangspunkt war das – scheinbar triviale – Problem, einen Roboter in minimaler Zeit von A nach B zu steuern. Die Lenkkinematik des Roboters entspricht der eines Fahrrads mit zwei Lenkern, die unabhängig voneinander das Vorder- und Hinterrad lenken können. Die Arbeit steht in der Tradition der Untersuchungen von L. E. Dubins (1957) und J. A. Reeds und L. A. Shepp (1990) über Bahnen minimaler Länge für den *car-like robot*.

Während meiner Promotion habe ich mit Menschen zusammengearbeitet, von denen ich viel gelernt und viel Unterstützung erfahren habe. Diesen Menschen möchte ich hier danken.

Zuerst danke ich Prof. Dr. Uwe Helmke, dass er die Betreuung meiner Promotion übernommen hat, obwohl ich Ingenieur und kein Mathematiker bin und anfangs nur eine vage Vorstellung meines Themas hatte. Prof. Dr. Helmke hat mich all die Jahre über wohlwollend begleitet und mir große Freiheiten bei der Entwicklung meiner Arbeit gelassen. In unseren sehr interessanten und intensiven Gesprächen stand er mir mit gutem Rat und seinem großen Erfahrungsschatz zur Seite. Weiterhin hat mich Prof. Dr. Helmke in den letzten Monaten durch seine Korrekturen und Anregungen wesentlich dabei unterstützt, die Arbeit erfolgreich abzuschließen.

Während meines Studiums in Stuttgart hat Prof. Dr. Michael Zeitz meine Faszination für nichtlineare Systeme geweckt. Bei ihm habe ich die Steuerbarkeit von Fahrzeugmodellen untersucht und bin erstmalig mit nichtholonomen Systemen in Berührung gekommen, noch ohne zu wissen, dass sie nichtholonom sind. Von Prof. Dr. Zeitz habe ich außerdem gelernt, dass man als Ingenieur nicht nur Problemlösungen finden, sondern auch stets seine Methodik weiterentwickeln muss. Hierfür und für das Erstellen des Mitberichts danke ich ihm herzlich.

Die Kollegen am Lehrstuhl II haben mich immer freundlich aufgenommen und unterstützt, so dass meine Aufenthalte in Würzburg sehr angenehm waren. Neben Prof. Dr. Helmke danke ich hierfür Dr. Martin Schröter, Dr. Jens Jordan, Dr. Gunther Dirr und Prof. Dr. Martin Kleinsteuber sowie allen anderen Kollegen am Lehrstuhl, die ich kennengelernt habe. Dr. Dirr danke ich außerdem dafür, dass er mir viele wertvolle Hinweise und Verbesserungsvorschläge für meine Arbeit gegeben hat. Dr. Schröter danke ich ebenfalls für seine Hinweise und Anregungen.

Ich danke meinem Freund Jochen Reinelt für sein wiederholtes geduldiges Korrekturlesen der Dissertation und sein immer hilfreiches Feedback.

Meinem Freund Stephan Szantho von Radnoth danke ich für die Gestaltung des Deckblatts.

Meinen Eltern Heidrun und Rudolf Mauder und meinen Geschwistern Stefanie und Christian danke ich für ihre Ermutigungen und ihr andauerndes Interesse an meiner Arbeit.

Der größte Dank gebührt meiner Frau Ursi, die mich all die Jahre unterstützt und mir den Rücken freigehalten hat. Sie hat meine Promotion mit Geduld und Wertschätzung begleitet, obwohl ich deshalb häufig wenig Zeit hatte. Gleichzeitig hat sie mir gezeigt, dass das Leben nicht nur aus (wissenschaftlicher) Arbeit besteht. Auch nach der Geburt unseres Sohnes Ben hat sie mir den nötigen Freiraum gewährt, um meine Arbeit fortführen und erfolgreich abschließen zu können. Hierfür, und für alles andere, danke ich ihr und widme ihr diese Arbeit.

Nürnberg, Juli 2012 Markus Mauder

# Abstract

In this thesis, time-optimal control of the bi-steerable robot (BSR) is addressed. The BSR, a vehicle with two independently steerable axles, is a complex nonholonomic system with applications in many areas of land-based robotics. Motion planning and optimal control are challenging tasks for this system, since standard control schemes do not apply.

The model of the BSR considered here is a reduced kinematic model with the driving velocity and the steering angles of the front and rear axle as inputs. The steering angles of the two axles can be set independently from each other. The reduced kinematic model is a control system with affine and non-affine inputs, as the driving velocity enters the system linearly, whereas the steering angles enter nonlinearly.

In this work, a new approach to solve the time-optimal control problem for the BSR is presented. In contrast to most standard methods for time-optimal control, our approach does not exclusively rely on discretization and purely numerical methods. Instead, the Pontryagin Maximum Principle is used to characterize candidates for time-optimal solutions. The resultant boundary value problem is solved by optimization to obtain solutions to the path planning problem over a given time horizon. The time horizon is decreased and the path planning is iterated to approximate a time-optimal solution. An optimality condition is introduced which depends on the number of cusps, i. e., reversals of the driving direction of the robot. This optimality condition allows to single out non-optimal solutions with too many cusps.

In general, our approach only gives approximations of time-optimal solutions, since only normal regular extremals are considered as solutions to the path planning problem, and the path planning is terminated when an extremal with minimal number of cusps is found. However, for most desired configurations, normal regular extremals with the minimal number of cusps provide time-optimal solutions for the BSR. The convergence of the approach is analyzed and its probabilistic completeness is shown. Moreover, simulation results on time-optimal solutions for the BSR are presented.

# Contents

# List of Figures

# List of Tables

# 1 Introduction

In classical mechanics, systems are studied which may have constraints that restrict their motion. The constraints may be holonomic or nonholonomic. Holonomic constraints are constraints on the configuration $q$ of a system. The configuration of a system describes its position, orientation, and internal shape. In contrast, nonholonomic constraints restrict the feasible velocities $\dot{q}$ and cannot be expressed as constraints on the configuration $q$. Nonholonomic constraints of mechanical systems are in general linear velocity constraints $A(q)\,\dot{q} = 0$. Systems subject to nonholonomic constraints are called nonholonomic systems. They can be represented locally by nonlinear ordinary differential equations. Nowadays, nonholonomic constraints and nonholonomic systems are considered apart from classical mechanics as well.

In the following, nonholonomic systems are addressed which are control systems, i. e., they have inputs to control their behavior. Such systems can be modeled as kinematic or dynamic systems. Nonholonomic kinematic systems are first-order systems with velocity inputs. For linear velocity constraints, they are driftless affine control systems $\dot{q} = g_1(q)\,u_1 + \cdots + g_m(q)\,u_m$. Nonholonomic dynamic systems are second-order systems with force inputs. For an introduction to nonholonomic systems, see [12, 22, 35, 80].

There is a great variety of nonholonomic systems. One of the simplest nonholonomic system is the Heisenberg system, also called Brockett's system or nonholonomic integrator. The nonholonomic constraint of the Heisenberg system with configuration $q = (q_1, q_2, q_3)$ is

$$\begin{bmatrix} q_2 & -q_1 & -1 \end{bmatrix} \begin{bmatrix} \dot{q}_1 \\ \dot{q}_2 \\ \dot{q}_3 \end{bmatrix} = 0. \tag{1.1}$$

For the inputs $u_1 = \dot{q}_1$ and $u_2 = \dot{q}_2$, the corresponding nonholonomic kinematic system is

$$\begin{bmatrix} \dot{q}_1 \\ \dot{q}_2 \\ \dot{q}_3 \end{bmatrix} = \begin{bmatrix} 1 \\ 0 \\ q_2 \end{bmatrix} u_1 + \begin{bmatrix} 0 \\ 1 \\ -q_1 \end{bmatrix} u_2. \tag{1.2}$$

All velocities $\dot{q} = (\dot{q}_1, \dot{q}_2, \dot{q}_3)$ of system (1.2) satisfy the nonholonomic constraint (1.1). The Heisenberg system discussed in [12, 18, 80] is a benchmark system for nonlinear control methods. Optimal control of the Heisenberg system with minimal control energy is related to the motion of a particle in a constant magnetic field.

Another simple mechanical system with a nonholonomic constraint is the rolling disk, also called rolling penny or unicycle. The constraint of the rolling disk arises from the assumption of ideal rolling of the disk over the ground without sliding. Due to this assumption, the disk can turn around its vertical axis and roll in its heading direction, but it cannot slide orthogonally to this direction. In robotics, the rolling disk is called unicycle and provides an example of a wheeled mobile robot with a nonholonomic constraint. It is addressed in Section 3.4.1. More complex wheeled mobile robots are the car-like robot discussed in the next section and the bi-steerable robot covered in this thesis. Other well-known nonholonomic systems are the differential drive, the car with $n$ trailers, the snakeboard, the roller racer, and the Chaplygin sleigh. For practical applications, nonholonomic systems play an important role in different fields like classical mechanics, quantum mechanics, or robotics. Besides wheeled mobile robots, robotic applications of nonholonomic systems include underwater vehicles and robotic manipulators.

Nonholonomic systems are interesting for both control theoretic aspects and practical applications. Controllability and optimal control lie at the heart of many studies on nonholonomic

systems. A kinematic system is controllable if it can be steered from any initial configuration $q_0$ to any desired configuration $q_d$. For a driftless kinematic system, controllability in the whole configuration space is equivalent to the fact that the constraint of the system is nonholonomic, as a nonholonomic constraint does not restrict the reachable configurations. In contrast, if the constraint is holonomic, the system can only evolve on the subset of the configuration space for which the constraint holds, i. e., it cannot reach any configuration $q_d$ from any configuration $q_0$.

The goal of optimal control of nonholonomic systems is to find solutions that satisfy the nonholonomic constraint and are optimal with respect to a given cost function. For kinematic models of wheeled mobile robots, shortest paths are studied most often. For this, solutions from an initial configuration $q_0$ to a desired configuration $q_d$ are searched which give the minimal path length

$$l = \int_0^T |v_t(\tau)| \, \mathrm{d}\tau.$$

Here, $|v_t|$ is the absolute translational velocity. Besides shortest paths, time-optimal solutions are considered to go from $q_0$ to $q_d$ in minimal time $T$. According to [108, 120, 124], time-optimal solutions are equivalent to shortest paths for kinematic models of wheeled mobile robots with constant absolute translational velocity and positive minimal turning radius, i. e., for robots which cannot turn on the spot. For nonholonomic dynamic systems, solutions with minimal control energy are mostly addressed. Necessary optimality conditions for optimal solutions of nonholonomic systems can be given by the Pontryagin Maximum Principle. For applications of the Maximum Principle to nonholonomic systems, see [2, 15, 106, 120].

There is a close connection between nonholonomic systems and differential geometry. As discussed below, fundamental results on shortest paths of wheeled mobile robots stem from the study of geodesics, i. e., locally length minimizing curves, which have bounded curvature. Nowadays, these paths are known as Dubins and Reeds-Shepp paths. More generally, optimal control problems for nonholonomic systems relate to problems in sub-Riemannian geometry. In sub-Riemannian geometry, geodesics are analyzed on smooth manifolds $M$ which are equipped with a sub-Riemannian metric $\mathbb{G}_S$ defined by a positive definite quadratic form on a subbundle $S$ of the tangent bundle $TM$. The configuration space of a nonholonomic system can be identified with a manifold $M$. The constraint distribution, which results from the nonholonomic constraint and describes the feasible velocities $\dot{q}$, can be identified with a subbundle $S$. Then, geodesics for a specific metric $\mathbb{G}_S$ give locally optimal solutions for a specific nonholonomic system. Here, $\mathbb{G}_S$ is chosen depending on the cost function of the optimal control problem. For an introduction to sub-Riemannian geometry, see [109], and for a control theoretic perspective, see [2, 15, 18].

In this thesis, time-optimal control of the bi-steerable robot, a wheeled mobile robot with two independently steerable axles, is covered. The kinematics of the robot corresponds to that of a bicycle where both wheels have handlebars. Based on the nonholonomic constraint from the assumption of ideal rolling of the wheels, the nonholonomic kinematic system of the robot is obtained. From this system, the so-called reduced kinematic model is derived. For this model, time-optimal solutions from an initial configuration $q_0$ to a desired configuration $q_d$ are searched. Necessary optimality conditions of the Maximum Principle define the extremals which give candidates for optimal solutions. Based on the extremals, path planning is performed to find solutions from $q_0$ to $q_d$. The path planning is iterated over a decreasing time horizon to approximate time-optimal solutions. The optimality of the solutions is analyzed depending on the number of reversals of the driving direction of the robot.

## 1.1 Historical perspective

Optimal control of nonholonomic systems has a long history which originates from problems in classical differential geometry. Initially, curves in $\mathbb{R}^n$ were considered which minimize a cost function $J$ on the curvature or length of the curve. One of the first studies in this direction is the elastic problem of Euler from 1744. For this problem addressed in [49], two points $x_1, x_2 \in \mathbb{R}^2$,

two tangent vectors $\dot{x}_1$ and $\dot{x}_2$ at $x_1$ and $x_2$ satisfying $\|\dot{x}_1\| = \|\dot{x}_2\| = 1$, and an end time $T > 0$ are given. A curve $x(t)$ is searched which meets $x(0) = x_1$, $\dot{x}(0) = \dot{x}_1$, $x(T) = x_2$, and $\dot{x}(T) = \dot{x}_2$ and minimizes

$$J = \frac{1}{2} \int_0^T k^2(t) \, \mathrm{d}t$$

among all such curves. Here, $k(t)$ is the geodesic curvature along the curve $x(t)$. Solutions to the elastic problem called Euler elastica can be given by elliptic functions.

In 1957, L. E. Dubins published in [37] his famous work on curves between fixed initial and terminal points with given initial and terminal direction, bounded curvature, and minimal length in the plane. He called them $R$-geodesics, with $R$ being the minimal admissible radius of curvature. Dubins showed that $R$-geodesics are concatenations of a finite number of pieces, each of which is either a straight line segment $S$ or an arc of a circle $C$ of radius $R$. Moreover, he proved that every $R$-geodesic consists of at most three pieces and is of type $CSC$ (an arc of a circle, a line segment, one more arc of a circle) or $CCC$ (three arcs of circles in series), where one or more pieces can vanish. For this purpose, he showed that curves with more than three pieces or of other type than $CSC$ or $CCC$ cannot have minimal length. To obtain his result, Dubins used only elementary calculus and geometric reasoning. He did not apply techniques of the calculus of variations or optimal control theory.

Regarding optimal control of nonholonomic systems, the $R$-geodesics, called Dubins paths today, are the shortest paths of a simplified model of the car-like robot. The car-like robot is a mobile robot with a steerable front axle. To obtain Dubins paths, the robot drives forward at constant velocity and has fixed positive minimal turning radius. Figure 1.1 shows Dubins paths from $q_0$ to $q_d$. The circles have the minimal turning radius $R$. The pentagons represent the robot and their arrowheads give the forward direction. The control system of the car-like robot with configuration $q = (\theta, x, y)$ consisting of the orientation $\theta$ and the position $(x, y)$ is

$$\dot{q} = \begin{bmatrix} \dot{\theta} \\ \dot{x} \\ \dot{y} \end{bmatrix} = \begin{bmatrix} 1 \\ 0 \\ 0 \end{bmatrix} u_1 + \begin{bmatrix} 0 \\ \cos(\theta) \\ \sin(\theta) \end{bmatrix} u_2. \tag{1.3}$$

Here, $u_1$ is the steering input, $u_2$ the driving input, and $U_D = [-1, 1] \times \{1\}$ the input space. Due to $u_2 \equiv 1$, the robot drives at constant velocity. System (1.3) is addressed in Section 3.4.2.

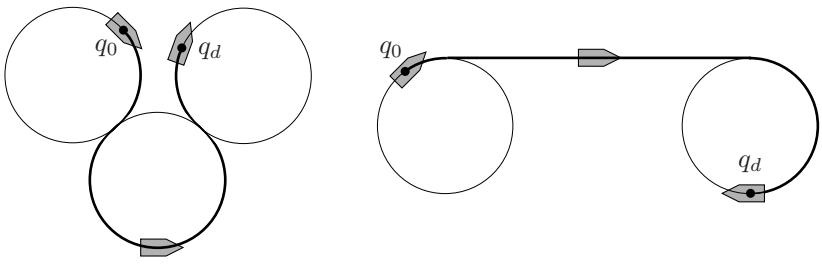


Figure 1.1: Dubins paths of type $CCC$ (left) and $CSC$ (right).

In their seminal paper [94] from 1990, J. A. Reeds and L. A. Shepp described the shortest paths of a car-like robot with fixed positive minimal turning radius that can drive forward and backward at constant absolute velocity, i. e., $u_2 = \pm 1$ holds. The control system is given by (1.3) for the input space $U_{RS} = [-1, 1] \times \{-1, 1\}$. In contrast to Dubins paths of a robot only driving forward, Reeds-Shepp paths can have cusps, i. e., reversals of the driving direction, which are indicated by the line $|$. That is, $X|Y$ represents a path consisting of one piece $X \in \{C, S\}$, a cusp, and one more piece $Y \in \{C, S\}$. Reeds and Shepp showed that every shortest path has at most two cusps and is of type $C|CSC|C$ or $CC|CC$, where one or several pieces or cusps

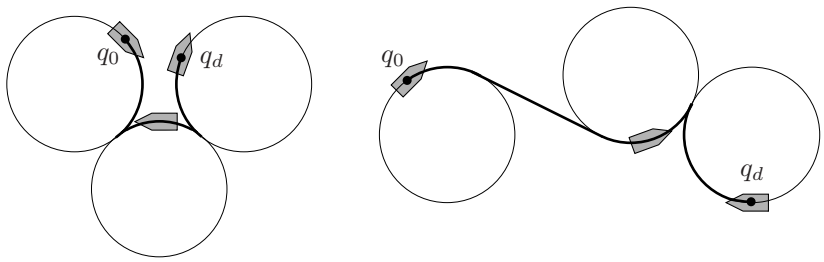


Figure 1.2: Reeds-Shepp paths of type $C|C|C$ (left) and $CSC|C$ (right).

may be missing. By considering arcs of circles $C$ turning left and right as well as arcs of circles $C$ and straight line segments $S$ traversed forward and backward, they constructed a sufficient family of 48 paths to connect each initial and desired configuration with minimal path length. Like Dubins, they did not resort to the calculus of variations or optimal control theory, but applied the results of Dubins and differential calculus to find critical points of the path length and analyzed whether they are minima or saddle points. Moreover, [94] provides closed-form solutions for the 48 paths of the sufficient family of the car-like robot. This allows to implement an optimal control by testing which of these paths connect the initial and desired configuration and then choosing the shortest one. Two Reeds-Shepp paths with the same initial and desired configurations as the Dubins paths in Figure 1.1 are depicted in Figure 1.2. According to the figures, Reeds-Shepp paths are in general shorter than Dubins paths.

In 1991, H. J. Sussmann and G. Tang sharpened and extended the results of [37, 94] by extensive application of geometric and optimal control theory in [120]. They used the Maximum Principle to obtain necessary optimality conditions to characterize candidates for shortest paths. Sussmann and Tang considered the Lie algebra of the input vectors fields of the car-like robot and computed the time derivatives of their switching functions using iterated Lie brackets. Based on this study, they analyzed the candidates for optimal paths and singled out non-optimal solutions. Moreover, they applied the theory of envelopes discussed in Section 4.5.3 to show that paths consisting of too many pieces cannot be optimal. They improved the findings of Reeds and Shepp by reducing the sufficient family from 48 to 46 paths. Besides, they extended the results of Dubins by imposing new conditions on the duration of the pieces $C$ and $S$ for the Dubins paths $CCC$ and $CSC$.

In 1996, P. Souères and J.-P. Laumond presented in [108] a complete characterization of the shortest paths for the car-like robot which can go forward and backward with bounded velocity and fixed positive minimal turning radius. Based on [94, 120], they constructed a finite partition of the configuration space into connected domains which are the regions of activity for the different paths. For each initial point in one of these domains, the optimal path to the origin is given by one or several of the 46 paths of the sufficient family. In combination with symmetry properties of the paths, this allows to select shortest paths from any initial to any desired point.

While the results in [37, 94, 108, 120] apply to the car-like robot (1.3), there are essential findings for optimal control of other nonholonomic systems as well. Optimal control of specific nonholonomic kinematic systems $\dot{q} = g_1(q)\,u_1 + \cdots + g_m(q)\,u_m$ with minimal control energy

$$J = \int_0^T \|u\|^2 \,\mathrm{d}t$$

is originally addressed in [18] and further analyzed in [12, 80, 81]. For nonholonomic kinematic systems which are first-order controllable, i. e., the accessibility distribution $\Delta_A$ defined in Section 3.1.4 is generated by the input vector fields $g_i$ and first-order Lie brackets $[g_i, g_j]$, optimal inputs for minimal control energy are sinusoids at integrally related frequencies. They are determined by a linear differential equation $\dot{u} = \Omega\,u$ with skew-symmetric $\Omega$. An example of

a first-order controllable system with sinusoids as optimal inputs is the Heisenberg system (1.2). Figure 1.3 shows the geodesic sphere of the Heisenberg system. It consists of the end points $(q_1, q_2, q_3) \in \mathbb{R}^3$ of geodesics which start from $(0, 0, 0)$ and have the same minimal control energy $J = \int_0^T \left(u_1^2 + u_2^2\right) \mathrm{d}t$. In Riemannian geometry, geodesic spheres are smooth manifolds, whereas in sub-Riemannian geometry, they are nonsmooth. Correspondingly, the geodesic sphere of the Heisenberg system is not smooth at the north and south pole.

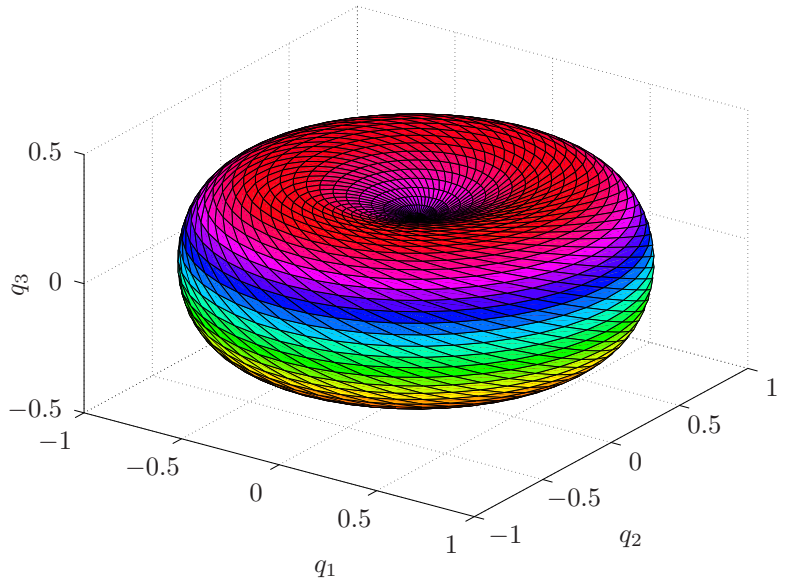


Figure 1.3: Geodesic sphere of the Heisenberg system.

## 1.2 Problem formulation and motivation

In this thesis, time-optimal control of the bi-steerable robot (BSR), a wheeled mobile robot with two independently steerable axles, is addressed. The BSR plays an important role in many applications of land-based robotics like reconnaissance, transportation, and disaster relief. The mobile soldier assistance system Mustang MK I and the automated straddle carrier AutoStrad in Figure 1.4 are applications of the BSR which are discussed in Chapter 5.

To obtain a control system of the BSR for optimal control, the bicycle model of the BSR depicted in Figure 1.5 is used, which consists of front axle, rear axle, and chassis. Its configuration $q = (\theta, x, y, \varphi_f, \varphi_r)$ includes of the orientation $\theta$ of the robot, the position $(x, y)$ of its center of mass, and the steering angles $(\varphi_f, \varphi_r)$ of the front and rear axle. The steering angles are restricted to $|\varphi_f| < \frac{\pi}{2}$ and $|\varphi_r| < \frac{\pi}{2}$, which is relevant for the controllability analysis in Section 3.1.4. The distances between the center of mass and the front and rear axle are $L_f$ and $L_r$, respectively. The nonholonomic kinematic system of the BSR is

$$\begin{aligned}
\dot{\theta} &= \tfrac{1}{L_f+L_r} \sin(\varphi_f - \varphi_r)\, u_1, \\
\dot{x} &= \tfrac{1}{L_f+L_r} \Big( L_f \cos(\varphi_f) \cos(\theta + \varphi_r) + L_r \cos(\varphi_r) \cos(\theta + \varphi_f) \Big) u_1, \\
\dot{y} &= \tfrac{1}{L_f+L_r} \Big( L_f \cos(\varphi_f) \sin(\theta + \varphi_r) + L_r \cos(\varphi_r) \sin(\theta + \varphi_f) \Big) u_1, \\
\dot{\varphi}_f &= u_2, \\
\dot{\varphi}_r &= u_3.
\end{aligned} \tag{1.4}$$

The inputs are the driving velocity $u_1$ and the steering rates $u_2$ and $u_3$. The driving velocity $u_1$ is the longitudinal velocity of the robot, i. e., the projection of the instantaneous velocity of the center of mass on the longitudinal axis of the BSR. The control system (1.4) is called full kinematic model (FKM) of the BSR to distinguish it from the reduced kinematic model described next. The derivation of the FKM is covered in Section 5.2.

Figure 1.4: Mustang MK I (left, photo by the author) and AutoStrad (right, photo courtesy of Kalmar Industries).

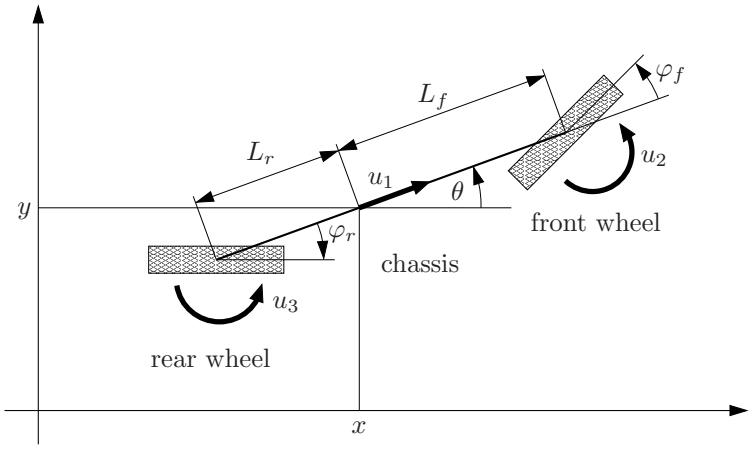


Figure 1.5: Model of the bi-steerable robot with steering angles $\varphi_f > 0$ and $\varphi_r < 0$.

The model of the BSR for which time-optimal control is considered in this thesis is the reduced kinematic model (RKM). This model obtained from the FKM has the reduced configuration $q_r = (\theta, x, y)$ as system state. The RKM is

$$\begin{aligned} \dot{\theta} &= \tfrac{1}{L_f+L_r} \sin(\varphi_f - \varphi_r)\, u_1, \\ \dot{x} &= \tfrac{1}{L_f+L_r} \Big( L_f \cos(\varphi_f) \cos(\theta + \varphi_r) + L_r \cos(\varphi_r) \cos(\theta + \varphi_f) \Big) u_1, \\ \dot{y} &= \tfrac{1}{L_f+L_r} \Big( L_f \cos(\varphi_f) \sin(\theta + \varphi_r) + L_r \cos(\varphi_r) \sin(\theta + \varphi_f) \Big) u_1. \end{aligned} \tag{1.5}$$

Here, the bounded steering angles $(\varphi_f, \varphi_r)$ are the steering inputs and the velocity $u_1$ is the driving input. The velocity enters the system linearly, whereas the steering inputs enter nonlinearly by trigonometric functions. Thus, the RKM is a control system with both affine and non-affine inputs. The steering angles can be set independently from each other. In particular, the rear steering angle $\varphi_r$ is no function of the front steering $\varphi_f$ angle, as it is often assumed to simplify the path planning for the BSR, see [11, 44, 78, 97, 101, 102, 125]. The goal of the time-optimal control covered here is to steer the RKM from a given initial configuration $(\theta_0, x_0, y_0)$ to a given desired configuration $(\theta_d, x_d, y_d)$ in minimal time.

The motivation to study the time-optimal control problem for the bi-steerable robot and to consider the reduced kinematic model for the analysis is as follows:

- **Bi-steerable robot.** Due to the merits of the BSR over other wheeled mobile robots, there are many applications of the BSR in land-based robotics. The advantages of the BSR include its high maneuverability, uniform steering characteristics, and redundant steering capability. Compared to vehicles with just one steerable axle, the BSR has an improved maneuverability, as it can do sharper turns and perform diagonal motions. The BSR has the same steering characteristics for driving forward and backward, which is advantageous for autonomous driving and teleoperation. Because of its two independently steerable axles, the BSR offers redundant steering capability, i. e., steering is possible even if the steering actuation of one axle fails. In spite of the many applications of the BSR, only very few results on path planning and optimal control are available, see Section 5.1. In addition, for most of them, the rear steering angle is a function of the front steering angle. However, only for independent steering angles $(\varphi_f, \varphi_r)$ as assumed in the following, one can take full advantage of the two steerable axles.

- **Time-optimal control problem.** At first, time-optimal control is inherently important, as solutions of minimal time duration are required for time-critical missions. Besides, such solutions are beneficial for many tasks as they are efficient with respect to other performance criteria like short path length or small sweep volume which has to be checked with respect to collisions. According to [46], time-optimal paths in the plane can be used as initial guesses for optimal solutions in rough terrain. Moreover, time-optimal solutions give motion primitives which have properties like small-time local controllability that are relevant for specific path planning methods, see [59, 60]. The author of this thesis is not aware of any published work on time-optimal control of the BSR. Only general methods for optimal control of wheeled mobile robots can be applied. These approaches are based on discretization and purely numerical methods to solve the resultant large-scale optimization problem like in [46]. As they do not directly take the special kinematics of the BSR into account, it is questionable whether such methods can find optimal solutions. Hence, time-optimal control of the BSR is an open problem.

- **Reduced kinematic model.** For time-optimal control of the BSR, the RKM with configuration $q_r = (\theta, x, y)$ is considered instead of the FKM with configuration $q = (\theta, x, y, \varphi_f, \varphi_r)$. The configuration $q_r$ contains all variables relevant for time-optimal control of the BSR, as transitions between two orientations and positions require time-consuming driving and steering maneuvers in general. Compared to this, the steering angles $(\varphi_f, \varphi_r)$ can be set in short time and are thus treated as inputs. The lower dimension of the RKM compared to the FKM reduces the complexity of the control problem. In particular, the analysis of the extremals from the Maximum Principle in Chapter 6 is less involved. In addition, singular extremals play a less important role for the RKM as discussed in Section 9.6. This makes the control problem simpler, as singular extremals are more difficult to handle than regular ones. In contrast, for the FKM, singular extremals are essential for time-optimal control, as only these extremals admit steering rates $(\dot{\varphi}_f, \dot{\varphi}_r)$ which do not have maximal modulus at all times. Because of these simplifications, the RKM is considered for time-optimal control of the BSR.

Several aspects make the time-optimal control problem for the BSR even more interesting. For other wheeled mobile robots like the car-like robot, only the bounded curvature of the paths has to be taken into account. For the BSR, in addition to bounded curvature, the freedom offered by diagonal motion has to be considered. This is why the extremals for time-optimal control of the BSR are more complex. Standard methods for path planning for nonholonomic systems like those described in Section 3.5 often rely on a transformation of the system to a normal form like the chain form in Section 3.3.2. As discussed in Section 5.1, the BSR can only be transformed to chain form if the steering angles satisfy $\varphi_f \neq \varphi_r$, which is a strong restriction on the feasible paths. The RKM is in some way special, as it has both affine and non-affine inputs. This is the case as the steering angles $(\varphi_f, \varphi_r)$ instead of their time derivatives $(\dot{\varphi}_f, \dot{\varphi}_r)$ are used as inputs. For control systems with affine and non-affine inputs, most standard methods for optimal control like switching time optimization addressed in Section 2.3 and most of the optimality conditions in Chapter 4 do not apply. Besides, extremals of wheeled mobile robots like the car-like robot are concatenations of elementary pieces like arcs of circles and straight line segments. Thus, the time derivative $\dot{\theta}$ of the orientation of the robots is piecewise constant and closed-form representations of the optimal solutions are available. Such closed-form solutions facilitate the path planning and the analysis of the optimality of the solutions. In contrast to this, for the RKM, no closed-form solutions can be derived, as $\dot{\theta}$ is not piecewise constant but varies continuously for most extremals, see Section 6.6. Without closed-form representations, one has to resort to numerical methods and approximations, making time-optimal control of the BSR more challenging.

## 1.3 Main results

The original results of this thesis include aspects of modeling, analysis, path planning, time-optimal control, and optimality of solutions of the BSR. The main contributions are as follows:

- **Modeling and analysis of the BSR with independently steerable axles.** The FKM (1.4) and RKM (1.5) of the BSR are derived and studied in detail in Chapter 5. The RKM is used in Chapter 6, 8, and 9 for time-optimal control of the BSR. Based on the kinematics of the bicycle model of the BSR, the velocity constraint and the constraint distribution of the robot are established, from which the FKM and RKM result. Controllability of the two models is proved and it is shown that the velocity constraint is completely nonholonomic. For the RKM, properties relevant for time-optimal control are analyzed, including its absolute translational velocity, minimal turning radius, and representation as left-invariant control system on $SE(2)$. The RKM of the BSR is also considered in [11, 78, 97, 125]. However, in these references, the rear steering angle $\varphi_r$ is a function of the front steering $\varphi_f$. In contrast, all findings in this thesis apply to the RKM with independently steerable axles.

- **Extremals for time-optimal control.** In Chapter 6, the extremals for time-optimal control of the RKM are studied, and the existence of time-optimal solutions is shown. The maximization of the Hamiltonian function is solved analytically, which reveals essential properties of the extremals. Moreover, the analytical maximization allows to simulate the extremals at low computational cost, compared to extremal inputs determined by numerical methods. The extremals of the RKM are classified into normal, abnormal, regular, and singular extremals. The relevant normal regular and normal singular extremals are analyzed in detail. Here, both analytical and simulation results are given. These findings are original contributions, as to the best of the author's knowledge, there are no published results on extremals for time-optimal control of the BSR.

- **Optimality of the extremals.** In Chapter 9, optimality results on normal regular and normal singular extremals for time-optimal control of the RKM are presented, including analytical and simulation results. In particular, a necessary optimality condition on the

number of cusps is stated. For most desired configurations $q_d$, normal regular extremals can only be time-optimal if they have the minimal number of cusps. In fact, normal regular extremals which satisfy the necessary optimality condition provide time-optimal solutions for most desired configurations. Besides, simulation data on time-optimal normal regular and time-optimal normal singular extremals is given and compared. All of these results are new contributions for the BSR, as the author is not aware of any published work on time-optimal solutions for this robot.

Further contributions of this thesis comprise a literature review for the BSR in Section 5.1 and a new approach for time-optimal control introduced in Chapter 7. In the literature review, published work on modeling, analysis, and control of the BSR is discussed, including findings for other wheeled mobile robots which also hold for the BSR. Our approach for time-optimal control from Chapter 7 was applied to the RKM to obtain the simulation results on time-optimal solutions presented in Chapter 8 and 9. Most standard methods for path planning and optimal control apply to fixed end time problems. Thus, a time transformation is required to convert a time-optimal control problem with free end time to a fixed end time problem. Our approach directly handles free end time problems. Hence, no time transformation has to be done. Moreover, the standard methods need a good initial guess of the solution. In contrast to this, our algorithm implementing the approach uses random values for initialization.

## 1.4 Outline of work

- Chapter 2 contains known definitions and results on time-optimal control. The considered class of control systems is given and solutions of such control systems are defined. Based on this, different optimal control problems like time-optimal and near time-optimal control problems are introduced. Finally, an overview of direct and indirect methods to solve time-optimal control problems is provided.

- Chapter 3 gives an introduction to nonholonomic systems. At first, basics of nonlinear control systems are discussed. Then, holonomic and nonholonomic constraints are defined, and nonholonomic systems, i. e., control systems subject to nonholonomic constraints, are addressed. As examples of nonholonomic systems, the unicycle, the car-like robot, and the snakeboard are described. At the end, an overview of methods for open-loop control of nonholonomic systems is presented.

- In Chapter 4, optimality conditions for time-optimal control problems are addressed. The existence of optimal solutions is discussed first. Then, the Pontryagin Maximum Principle is stated and its necessary optimality conditions are given which define the extremals. The boundary value problems resulting from time-optimal control problems are discussed. Afterwards, overviews of further necessary optimality conditions and of sufficient optimality conditions are provided. As an example, time-optimal control of the unicycle is studied.

- In Chapter 5, the bi-steerable robot (BSR) is covered, starting with a review of the literature on this system. Then, two models of the BSR, the full kinematic model (FKM) and the reduced kinematic model (RKM), are given and analyzed. Based on the bicycle model of the BSR, the nonholonomic constraint of the robot is established, and the two models are derived. Controllability, integrability of the nonholonomic constraint, and further system properties of the RKM are shown. Finally, the two models of the BSR are discussed with respect to their suitability for path planning and optimal control.

- In Chapter 6, the necessary optimality conditions of the Maximum Principle from Chapter 4 are applied to the RKM from Chapter 5 to define the extremals for time-optimal control. For this, the appropriate optimality conditions are derived and the maximization of the Hamiltonian function is performed analytically to determine the extremal inputs. Based

on knowledge of the extremal inputs, the existence of time-optimal solutions is shown. For time-optimal control of the RKM, normal regular and normal singular extremals are relevant. These extremals are discussed, and simulation results are presented.

- Chapter 7 introduces our approach for time-optimal control. The approach performs path planning based on normal regular extremals iteratively over a decreasing time horizon. At first, simplifications of the path planning problem are addressed. Then, the path planning problem is formulated as an optimization problem. An algorithm to solve the optimization problem is presented, and the convergence is analyzed. The time-optimal control by iterated path planning is introduced and an algorithm for time-optimal control is given, followed by an analysis of the convergence. At the end, modifications for practical application are discussed.

- In Chapter 8, the approach for time-optimal control from Chapter 7 is applied to the RKM, using the extremals of the RKM from Chapter 6. At first, the path planning problem is simplified. Then, implementation aspects of the approach are discussed. The conditions required for convergence of the time-optimal control are verified, and simulation data on time-optimal normal regular extremals of the RKM is presented. The time-optimal extremals are compared to shortest paths of the car-like robot. The approach for time-optimal control and the resultant solutions are discussed.

- In Chapter 9, the optimality of the normal regular extremals of the RKM is covered. For this, the necessary and sufficient optimality conditions from Chapter 4 are analyzed to find optimality conditions which apply to the extremals of the RKM. Then, simulation results on time-optimal normal regular extremals of the RKM are presented. Based on this, the optimality of the extremals is studied depending on the number of cusps. This leads to a necessary optimality condition for the normal regular extremals. Finally, simulation data on time-optimal normal singular extremals is given, and the optimality results obtained for the RKM are discussed.

- In Chapter 10, a summary of the original contributions of this thesis is given, and an overview of future work is provided.

- Appendix A contains listings of the algorithms for path planning and time-optimal control from Chapter 7.

# Part I

# Preliminaries

# 2 Time-optimal control

This chapter contains known definitions and results on time-optimal control. The considered class of control systems is given and solutions of such control systems are defined. Based on this, different optimal control problems including time-optimal and near time-optimal control problems are addressed. Finally, an overview of direct and indirect methods to solve time-optimal control problems is provided.

## 2.1 Control system

The following definitions of control system and its solution are required to define the control problems in Section 2.2. The nonholonomic systems in Chapter 3 are a specific class of the control systems addressed here. For an introduction to control systems, see [83, 98, 104]. The following assumption holds for the state space of all control systems in this thesis.

**Assumption 2.1.1** *(State space) The state space $M$ is an open subset of $\mathbb{R}^n$.*

**Definition 2.1.2** *(Control system) Let $M$ be an open subset of $\mathbb{R}^n$ and $U$ a compact subset of $\mathbb{R}^m$. Let $f\colon M \times U \to TM$, $(x,u) \mapsto f(x,u) \in T_xM$ be a map which is real analytic in $x$ for all $u$ and continuous in $u$. A system*

$$\dot{x} = f(x,u) \tag{2.1}$$

*with state $x = (x_1,\dots,x_n) \in M$, state space $M$, input $u = (u_1,\dots,u_m) \in U$, and input space $U$ is called control system.*

Here, $TM$ denotes the tangent bundle $TM = \bigcup_{x\in M} T_xM$ of $M$, and $T_xM$ the tangent space to $M$ at $x \in M$. As $M$ is an open subset of $\mathbb{R}^n$, the tangent space $T_xM$ can be identified with $\mathbb{R}^n$ at each $x \in M$, and $TM$ can be identified with $M \times \mathbb{R}^n$. Nevertheless, $\dot{x} \in T_xM$ is sometimes used in the following instead of $\dot{x} \in \mathbb{R}^n$ to stress that $\dot{x}$ lies in the tangent space to $M$ at $x$. The map $f = (f_1,\dots,f_n)$ of the system equation $\dot{x} = f(x,u)$ gives the dynamics of the system. A control system with $m = 1$ is called single-input system and with $m > 1$ multi-input system. For some of the optimality conditions in Chapter 4, further differentiability properties of $f$ with respect to $u$ are required. According to [22, 104], systems studied in classical mechanics are real analytic. Such systems are beneficial for integrability and controllability addressed in Section 3.1 and for regularity properties of time-optimal solutions discussed in Section 4.5.2. For a general discussion on the importance of real analyticity for control theory, in particular with respect to reachable sets and optimal solutions, see [114].

**Definition 2.1.3** *(Solution of a control system) A control system 2.1.2, an initial state $x_0 \in M$, a compact proper time interval $I = [0,T]$, and a bounded measurable input map $u\colon I \to U$, $t \mapsto u(t)$ are considered. A solution of the control system is an absolutely continuous state trajectory $x\colon I \to M, t \mapsto x(t)$ satisfying $x(0) = x_0$ and $\dot{x} = f(x,u)$ almost everywhere in $I$.*

Regarding the existence of solutions 2.1.3, the following assumption holds.

**Assumption 2.1.4** *(Existence of solutions) The solutions of a control system exist for all $t \in I$.*

As the control system (2.1) is autonomous, it is not restrictive to set the initial time of the interval $I$ to 0. The set of measurable bounded functions $u\colon I \to U$ is denoted by $\mathcal{L}_U(I)$ in the following. Assumption 2.1.4 is made since in general, solutions of a control system do not have to exist for all $t$. However, even if a solution $x(\cdot)$ does not exist for all $t$, there is always a sufficiently small final time $T > 0$ such that $x(\cdot)$ exists for all $t \in I$. Conditions for the existence of solutions are given e. g. in [1, 33, 98, 104]. These conditions involve properties of the right-hand side $f(x, u)$ of the control system like Lipschitz continuity and boundedness.

Solutions $x(\cdot)$ obtained for the addressed system and input class are called solutions in the sense of Carathéodory. They satisfy the differential equation of the control system almost everywhere in $I$ and are unique. For details on measurable and absolutely continuous functions and Carathéodory solutions, see [22, 26, 33, 104]. In this thesis, bounded measurable input maps $u(\cdot)$ are considered, since for some optimal control problems, less general classes of inputs like piecewise constant inputs give no optimal solutions as discussed in [77, 93].

**Definition 2.1.5** *(End-point map) A control system 2.1.2 with initial state $x_0 \in M$ is considered. For $I = [0, T]$, the map $E^T_{x_0}\colon \mathcal{L}_U(I) \to M, u \mapsto x(T)$ which gives the terminal state $x(T)$ of the solution $x(\cdot)$ is called end-point map.*

The notation $E^T_{x_0}$ is used to stress the dependence on the initial state $x_0$ and the final time $T$. If a closed-form representation of $E^T_{x_0}$ can be given, the end-point map is a valuable tool for analysis and control. For details and applications of end-point maps, see [2, 15, 104, 120].

For constant input values $\hat{u} \in U$, the right-hand side of control system (2.1) defines a family of real analytic vector fields $X_{\hat{u}}\colon M \to TM$ on the state space $M$ parameterized by $\hat{u}$. The control system is then written as

$$\dot{x} = f(x, \hat{u}) =: X_{\hat{u}}(x)\,. \tag{2.2}$$

This point of view is useful to analyze controllability and perform motion planning for control systems with piecewise constant inputs. Solutions of control systems under constant inputs can be described by the flow defined next. For details on vector fields, see [1, 22, 49].

**Definition 2.1.6** *(Flow under a constant input) For the vector field $X_{\hat{u}}$ (2.2), the map $\phi^{\hat{u}}\colon I \times M \to M, (t, x_0) \mapsto \phi^{\hat{u}}_t(x_0)$ which gives the state $x(t) = \phi^{\hat{u}}_t(x_0)$ of the solution $x(\cdot)$ at time $t$ is called flow under the constant input $\hat{u}$.*

The notation $\phi^{\hat{u}}_t$ shows the dependence on the constant input $\hat{u}$ and the time $t$. The flow meets the initial condition $\phi^{\hat{u}}_0(x_0) = x_0$, and, as the solution $x(\cdot)$ is assumed to exist for all $t \in I$, the ordinary differential equation $\dot{x} = X_{\hat{u}}(x)$ on $M$. That is, for all $t \in I$,

$$\frac{\mathrm{d}}{\mathrm{d}t}\phi^{\hat{u}}_t(x_0) = X_{\hat{u}}\big(\phi^{\hat{u}}_t(x_0)\big)$$

holds. Solutions from piecewise constant inputs can be represented by the concatenation of flows. Piecewise constant input on the boundary $\mathrm{bd}\,U$ of the input space are called bang-bang inputs. For details on flows, see [2, 22, 49, 80, 104].

## 2.2 Time-optimal control problems

Different time-optimal control problems and their solutions are defined next. In preparation for this, control problems with free end time and general optimal control problems are introduced.

**Definition 2.2.1** *(Control problem with free end time) A control system 2.1.2, an initial state $x_0 \in M$, and a desired state $x_d \in M$, $x_0 \neq x_d$, are given. The problem to find a bounded end time $\tau > 0$ and a bounded measurable input map $u(\cdot)$ such that a solution 2.1.3 results which satisfies $x(\tau) = x_d$ is called control problem with free end time. Any solution $(\tau, x(\cdot), u(\cdot))$ to this problem is called admissible solution denoted by $S(x_0, x_d)$.*

The initial state $x_0$ is also called starting state and the desired state $x_d$ is also called target state. More general control problems can be studied, for which no initial and desired states are fixed, but $x(0) \in M_0$ and $x(\tau) \in M_d$ has to hold for given subsets $M_0$ and $M_d$ of $M$. As $x_0 \neq x_d$ is assumed in Definition 2.2.1 to exclude trivial control problems, the end time satisfies $\tau > 0$, and the interval $I = [0, \tau]$ is proper. Since $\tau$ is unspecified as it is not part of the problem data but of the solution, problem 2.2.1 is a free end time problem. The existence of solutions to such problems depends on the controllability properties of the control system.

A control problem can be solved by open-loop control, closed-loop control, or a combination of both. For open-loop control, a steering law $u\colon I \to U$ generates the input without evaluation the current state. The corresponding problem is called steering problem or trajectory planning problem. In robotics, it is frequently called motion planning problem, and for kinematic systems, i. e., first-order control systems with velocity inputs, path planning problem. For closed-loop control also called feedback control, a feedback law $u\colon M \to U$ computes the input $u$ based on the current state $x$ of the system. Besides, combinations of closed-loop and open-loop control $u\colon I \times M \to U$ exist. In the following, only open-loop control is considered.

**Definition 2.2.2** *(Optimal control problem) Let $L(x, u)$ be a real-valued continuous function which is continuously differentiable with respect to $x$ for all $x \in M$. A control problem with free end time is considered. The problem to find an admissible solution $S(x_0, x_d)$ which gives the minimal value of the cost function*

$$J(\tau, x, u) = \int_0^\tau L(x, u)\ dt \tag{2.3}$$

*is called optimal control problem. Any solution $(\tau^o, x^o(\cdot), u^o(\cdot))$ to this problem is called optimal solution.*

Problem 2.2.2 results from problem 2.2.1 by the requirement that the solution should be optimal, i. e., the cost function $J$ should have minimal value among all admissible solutions $S(x_0, x_d)$. The cost function is also called objective function or performance criterion. It quantifies the total cost of the solution, e. g. with respect to time duration, path length, or control energy. The Lagrangian $L$ gives the change of $J$ over time, i. e., the instantaneous running cost along the solution. For some of the optimality conditions in Chapter 4, $L$ has to satisfy additional differentiability properties with respect to $x$ and $u$. If the initial and desired state of an optimal control problem is not fixed, more general cost functions than (2.3) are considered which take the resultant states $x(0)$ and $x(\tau)$ into account.

**Definition 2.2.3** *(Time-optimal control problem) The problem to find an optimal solution for the Lagrangian $L(x, u) = 1$ is called time-optimal control problem. Any solution $(\tau^{to}, x^{to}(\cdot), u^{to}(\cdot))$ to this problem is called time-optimal solution.*

The Lagrangian $L(x, u) = 1$ gives

$$J(\tau, x, u) = \int_0^\tau L(x, u)\ \mathrm{d}t = \tau.$$

Equivalently, a time-optimal solution $(\tau^{to}, x^{to}(\cdot), u^{to}(\cdot))$ is an admissible solution $S(x_0, x_d)$ which minimizes the end time $\tau^{to}$, i. e., $\tau^{to} \leq \tau$ holds for all admissible solutions. The existence of solutions to time-optimal control problems is addressed in Section 4.1. There, besides controllability, the system has to satisfy conditions on the convexity and boundedness of $f(x, u)$ for all $(x, u) \in M \times U$. Time-optimal solutions are in general not unique. For uniqueness, additional conditions like those in Section 4.6.1 have to hold.

The control problems considered so far are free end time problems, as the end time $\tau$ of the interval $I = [0, \tau]$ is unspecified. By the time transformation $s = \frac{1}{\tau}\, t$ for constant $\tau > 0$, such problems are converted to problems over the fixed interval $\check{I} = [0, 1]$. The transformed problems are called fixed end time problems. The unknown end time $\tau$ is represented by an addition state variable $z$, for which $z' = \mathrm{d}z/\mathrm{d}s = 0$ and $z(0) = \tau$ is assumed.

**Definition 2.2.4** *(Transformed time-optimal control problem with fixed end time) A time-optimal control problem is considered. Let $\check{X} = (\check{x}, z)$ be the extended state, $\check{M} = M \times \mathbb{R}_{>0}$ the extended state space, and*

$$\check{X}' = \begin{bmatrix} \check{x}' \\ z' \end{bmatrix} = \begin{bmatrix} z\, f\big(\check{x}, \check{u}\big) \\ 0 \end{bmatrix} =: \check{f}\big(\check{X}, \check{u}\big) \tag{2.4}$$

*the extended control system. The problem to find an initial condition $z(0) = \tau$ and an input map $\check{u}(\cdot)$ such that a solution $\check{X}(\cdot)$ results which satisfies $\check{X}(0) = (x_0, \tau)$ and $\check{X}(1) = (x_d, \tau)$ and gives the minimal value of the cost function $\check{J}\big(\check{X}, \check{u}\big) = \tau$ is called transformed time-optimal control problem with fixed end time. Any solution $\big(\check{X}^{to}(\cdot),\, \check{u}^{to}(\cdot)\big)$ to this problem is called transformed time-optimal solution.*

The extended state $\check{X} = (\check{x}, z)$ of dimension $\check{n} = n + 1$ arises from the extension of the state $\check{x}$ by the variable $z$ for the end time of problem 2.2.3. The time derivative $\check{X}' = (\check{x}', z')$ consists of the derivative of $\check{x}$ with respect to $s$ and $z' = 0$. The cost function $\check{J}\big(\check{X}, \check{u}\big) = \tau$ results from

$$\check{J}\big(\check{X}, \check{u}\big) = \int_0^1 \check{L}\big(\check{X}, \check{u}\big)\, \mathrm{d}s$$

for the Lagrangian $\check{L}\big(\check{X}, \check{u}\big) = z$. By $\check{x}(s) := x\big(\tau\, s\big) = x(t)$ and $\check{u}(s) := u\big(\tau\, s\big) = u(t)$, solutions $\big(\check{X}^{to}(\cdot)\,, \check{u}^{to}(\cdot)\big)$ to problem 2.2.4 and solutions $(\tau^{to}, x^{to}(\cdot), u^{to}(\cdot))$ to problem 2.2.3 are equivalent via $\check{X}^{to}(s) := \big(x^{to}\big(\tau\, s\big), \tau^{to}\big) = \big(x^{to}(t)\,, \tau^{to}\big)$ and $\check{u}^{to}(s) := u^{to}\big(\tau\, s\big) = u^{to}(t)$. In this thesis, the time-optimal control problem 2.2.3 with free end time is studied, except for some sections in Chapter 4 and 9. There, optimality conditions are addressed which are usually applied to the transformed time-optimal control problem 2.2.4.

**Definition 2.2.5** *(Near time-optimal control problem) A time-optimal control problem and the end time $\tau^{to}$ of a time-optimal solution to this problem are considered. Fix a constant $k \geq 1$. The problem to find an admissible solution $S(x_0, x_d)$ with end time $\tilde{\tau}^{to}$ satisfying*

$$\tilde{\tau}^{to} \leq k\, \tau^{to}$$

*is called near time-optimal control problem. Any solution $(\tilde{\tau}^{to}, \tilde{x}^{to}(\cdot), \tilde{u}^{to}(\cdot))$ to this problem is called near time-optimal solution. The constant $k$ is called quality factor.*

For near time-optimal control, other terms like almost or approximate time-optimal control are used as well. The factor $k$ is called quality factor as it quantifies how good a near time-optimal solution approximates a time-optimal one with respect to the end time. If $k = 1$ holds, the solution is time-optimal. For $k > 1$, a smaller value of $k$ indicates a better approximation.

If for a specific control problem, the end time $\tau^{to}$ is known or can be estimated, $k$ can be set depending on the required approximation quality. Then, a method for optimal control can be terminated when a solution with end time $\tilde{\tau}^{to}$ satisfying $\tilde{\tau}^{to} \leq k\, \tau^{to}$ is found. Besides, simulation results on time-optimal solutions with end time $\tau^{to}$ can be compared to solutions which meet specific optimality conditions. If these solutions give good approximations of time-optimal solutions, they can be defined to be near time-optimal solutions with end time $\tilde{\tau}^{to}$. In this case, the mean value of the resultant quality factor $k := \tilde{\tau}^{to}/\tau^{to}$ over many solutions rates the approximation of optimal solutions by solutions which satisfy the optimality conditions. This is done in Chapter 9 for time-optimal and near time-optimal solutions for the BSR.

Near time-optimality is a generalization of time-optimality, as time-optimality is obtained for $k = 1$. Thus, the conditions for the existence of time-optimal solutions from Section 4.1 are sufficient for the existence of near time-optimal solutions. Like time-optimal solutions, near time-optimal solutions are in general not unique. There are several reasons to use near time-optimal solutions instead of time-optimal ones. Their computation may be less costly, the structure of their inputs may be simpler, or it may be the only way to obtain satisfying solutions.

Even if time-optimal inputs can be computed, their implementation may be impossible due to poor robustness, high frequency inputs causing oscillations, or jumps increasing wear and tear. In contrast to this, near time-optimal solutions can take these limitations into account. They are addressed e. g. in the following references:

- Near time-optimal control of robotic manipulators using bang-bang inputs is studied in [82]. For near time-optimal control, the inputs are restricted to a subset of the input space. Then, inputs taking values in the full input space can be applied to compensate for disturbances. The bang-bang inputs are smoothed to avoid the excitation of high-frequency dynamics. The restriction of the input space and the smoothing of the inputs can be adjusted for steady transition between time-optimal and near time-optimal control.
- In [6], near time-optimal path planning for ground vehicles is considered. The Lagrangian $L(x,u)=1$ for time-optimal control is augmented by additional terms to take the driving and steering inputs into account. The solutions for the augmented Lagrangian give rise to additional flexibility and better robustness compared to time-optimal solutions.
- In [30, 31], time-optimal solutions for underwater vehicles with usually a high number of switchings between constant inputs are adapted to obtain inputs suitable for practical application. For these inputs, the number of switchings is restricted, which gives near time-optimal solutions, called time efficient solutions in the references.
- Trajectory planning for the snakeboard described in Section 3.4.3 is considered in [48]. The planning yields near time-optimal solutions, called subtime-optimal solutions there, which have the minimal number of switchings between motion primitives.

In this thesis, near time-optimal solutions for the BSR are studied, since only normal regular extremals from the Maximum Principle are considered as candidates for optimal solutions. Besides, the search for a solution with minimal time is terminated when a normal regular extremal with minimal number of cusps is found. Using only normal regular extremals and terminating the search depending on the number of cusps facilitates path planning, but makes it impossible to find time-optimal solutions for some desired states $x_d$. However, as discussed in Section 9.6, for most states $x_d$, normal regular extremals give time-optimal solutions.

The solutions considered so far are globally optimal, i. e., optimal among all solutions $x(\cdot)\in M$ from $x_0$ to $x_d$. Besides, strong and weak local optimality can be studied as defined next.

**Definition 2.2.6** *(Strongly locally time-optimal solution, weakly locally time-optimal solution) A time-optimal control problem, the interval $I=\left[0,\tau^{lo}\right]$, and some $\varepsilon>0$ are considered. An admissible solution $\left(\tau^{lo},x^{lo}(\cdot),u^{lo}(\cdot)\right)$ is called strongly locally time-optimal if it gives the minimal end time $\tau^{lo}$ among all admissible solutions $\left(\tau,x(\cdot),u(\cdot)\right)$ satisfying*

$$\max\left\{\left|\tau^{lo}-\tau\right|,\left\|x^{lo}-x\right\|_{\infty}\right\}<\varepsilon. \tag{2.5}$$

*An admissible solution $\left(\tau^{lo},x^{lo}(\cdot),u^{lo}(\cdot)\right)$ is called weakly locally time-optimal if it gives the minimal end time $\tau^{lo}$ among all admissible solutions $\left(\tau,x(\cdot),u(\cdot)\right)$ satisfying*

$$\max\left\{\left|\tau^{lo}-\tau\right|,\left\|x^{lo}-x\right\|_{\infty},\left\|u^{lo}-u\right\|_{\infty}\right\}<\varepsilon. \tag{2.6}$$

Here, $\|y\|_{\infty}=\max_{t\in I}\|y(t)\|$ is the infinity norm. A solution $\left(\tau^{lo},x^{lo}(\cdot),u^{lo}(\cdot)\right)$ is strongly locally time-optimal if it is optimal among all solutions $(\tau,x(\cdot),u(\cdot))$ in the $\varepsilon$-neighborhood (2.5) with respect to $\tau$ and $x$. A solution is weakly locally time-optimal if it is optimal among all solutions in the $\varepsilon$-neighborhood (2.6) with respect to $\tau$, $x$, and $u$. For the transformed time-optimal control problem 2.2.4, strong local optimality holds for $\left\|\check{X}^{lo}-\check{X}\right\|_{\infty}<\check{\varepsilon}$ instead of (2.5) for some $\check{\varepsilon}>0$, and weak local optimality for $\max\left\{\left\|\check{X}^{lo}-\check{X}\right\|_{\infty},\left\|\check{u}^{lo}-\check{u}\right\|_{\infty}\right\}<\check{\varepsilon}$ instead of (2.6). In this thesis, strong and weak local time-optimality are considered for some of the sufficient optimality conditions in Section 4.6. Besides the given ones, other definitions of local optimality are used based on different norms or topologies. For references to strong and weak local optimality, see [26, 49, 76, 85, 86, 89].

## 2.3 Methods for time-optimal control

Two types of methods to solve time-optimal control problems exist, direct and indirect methods. They differ in the way the optimal inputs are computed. For a comparison, see [24, 30, 60].

Direct methods rely on the direct computation of optimal inputs to solve an optimal control problem. Two different approaches are used. The first approach is based on a discretization of the time domain to obtain a finite dimensional optimization problem. Either the input is discretized and a direct sequential method is applied, or both the input and the state are discretized and a direct simultaneous method is used. The resultant optimization problem may be high-dimensional, depending on the dimension of the system and the resolution of the discretization. An optimization is executed to minimize the cost function over the discretized input and state, respectively. Constraints of the optimization arise from the system dynamics, initial and target conditions, and maybe additional state and input constraints. Thus, methods for constrained nonlinear optimization like sequential quadratic programming (SQP) are applied. For further details and applications, see [24, 29, 30, 60, 92]. For the second approach, the structure of the optimal solution must be known a priori, e. g. from the Maximum Principle. This allows a finite parameterization of the inputs. Based on the parameterization, optimal inputs are computed. For example, switching time optimization is applied to determine bang-bang inputs which give optimal solutions for some control systems with affine inputs. Among others, such inputs are parameterized by the times of the switchings between points on $\operatorname{bd} U$. Switching time optimization is addressed in [51, 71] for single-input systems and in [30, 31, 32, 73] for multi-input systems. Combinations of both approaches are used as well. Here, optimal inputs are computed by switching time optimization if they are bang-bang and by discretization otherwise.

In contrast to direct methods, indirect methods are based on optimality conditions from optimal control theory like the Maximum Principle covered in Chapter 4. The Maximum Principle gives necessary optimality conditions to characterize candidates for optimal solutions called extremals. The extremals are generated by the inputs obtained from the maximization of the Hamiltonian function, which depends on the state of the control system and the adjoint state. Among the extremals, optimal solutions have to be determined. The necessary optimality conditions for time-optimal control problems lead to a boundary value problem with fixed initial and target state, unknown initial condition of the adjoint state, and free end time. For applications of indirect methods to optimal control problems, see [5, 6, 60, 92].

Both methods have advantages and disadvantages: Direct methods do not require the sometimes difficult application of the Maximum Principle. Methods based on discretization are robust with respect to initialization, i. e., no detailed knowledge of the optimal solutions is required. Nevertheless, a fine discretization of the input and state space leads to a high-dimensional optimization problem which is computationally costly to solve. Without fine discretization, only crude approximations of the optimal results are achieved. Besides, the solutions are in general not optimal due to the discretization and since most of the solutions are only locally optimal, see [22, 29]. Parameterizations of optimal inputs usually lead to optimization problems of moderate dimension, but require detailed knowledge of the structure of the optimal solutions. Indirect methods depend heavily on the Maximum Principle, which gives deep mathematical insight into the control problem. However, it may be difficult to extract all information about the optimal solutions. Although computationally less costly than direct methods, solving an optimal control problem with an indirect method may be hard as a good initial guess of the solution is required to solve the emerging boundary value problem successfully. Without good initial guesses, standard solvers for boundary value problems like shooting methods may give poor results. Besides, solutions of the boundary value problems are only candidates for optimal solutions. Among them, optimal solutions have to be identified by other means like geometrical reasoning or higher-order optimality conditions.

In this thesis, near time-optimal solutions for the BSR are computed by an indirect method. The Maximum Principle is applied and the boundary value problem is solved by optimization. Near time-optimal solutions are obtained by an iterative approach which is terminated when a solution with minimal number of cusps is found.

# 3 Nonholonomic systems

This chapter gives an introduction to nonholonomic systems. In the following, nonholonomic systems are nonlinear control systems subject to nonholonomic constraints. A more comprehensive definition of nonholonomic system is given in Section 3.3. Nonholonomic constraints and nonholonomic systems were first addressed in classical mechanics. Nowadays, mechanical as well as other physical or non-physical systems are modeled as control systems with nonholonomic constraints. For the study of nonholonomic mechanical systems, the configuration and the configuration space are fundamental, which are defined next.

**Definition 3.0.1** *(Configuration, configuration space) For a mechanical system of $m$ rigid bodies, $m \geq 1$, let $q = (q_1, \ldots, q_p)$ be coordinates which uniquely define the free position and orientation of body 1 with respect to a fixed reference frame as well as the free relative positions and orientations of the remaining bodies, if any, with respect to a frame fixed to body 1. Let $Q$ be an open subset of $\mathbb{R}^p$ which is the set of all possible coordinates $q$. Then, $q$ is called configuration, and $Q$ is called configuration space.*

In Definition 3.0.1, a rigid body is an idealized model of a solid body which cannot be deformed, i. e., the relative position of any two points to one another is fixed. Free positions and orientations means that the positions and orientations can change independently from each other. A system with $\dim Q = p$ has $p$ degrees of freedom. The relative positions and orientations give the internal shape of the system. For more details on the configuration and the configuration space, see [22]. In classical mechanics, the configuration $q$ is called generalized position, the configuration variables $q_i$ are called generalized coordinates, and their time derivatives $\dot{q}_i$ generalized velocities. An introduction to classical mechanics is provided in [7].

For kinematic systems, i. e., first-order control systems with velocity inputs, the configuration space $Q$ gives the state space $M$ from Definition 2.1.2. In contrast, for dynamic systems which are second-order control systems with force inputs, $Q$ is a subspace of $M$, as $M$ is a subset of the tangent bundle $TQ$. The configuration space of the control systems considered in this chapter are open subsets of $\mathbb{R}^p$, except for Section 3.1.2, where systems on Lie groups are addressed. The configuration space of these systems are matrix Lie groups.

A nonholonomic constraint of a mechanical system with configuration $q$ is a velocity constraint $A(q)\,\dot{q} = c$ for constant $c$. For more general nonholonomic constraints, see [22, 79]. A constraint $A(q)\,\dot{q} = c$ defines the feasible velocities $\dot{q}$ of a system. These velocities specify how the configuration $q$ of the system can change over time. The feasible velocities $\dot{q}$ have to lie in the constraint distribution $D$ which results from the nonholonomic constraint and depends on the underlying configuration $q$. A holonomic constraint $h(q) = c$ only affects the configuration $q$ of a system. In contrast, a nonholonomic constraint $A(q)\,\dot{q} = c$ includes both $q$ and $\dot{q}$ and cannot be transformed to a constraint $h(q) = c$. Holonomic and nonholonomic constraints, constraint distributions, and nonholonomic systems are discussed in Section 3.2 and 3.3.

For mechanical systems, nonholonomic constraints appear e. g. in the following settings:

- Systems whose motions are restricted to specific directions are subject to nonholonomic constraints. Because of these constraints which are homogeneous velocity constraints $A(q)\,\dot{q} = 0$, no lateral velocities orthogonal to these directions are possible. An example of such a system is the rolling disk. Its constraint arises from the assumption of ideal rolling of the disk over the ground without sliding. Due to this assumption, the disk can turn around its vertical axis and roll in its heading direction, but it cannot slide orthogonally to this direction. Another example is a blade sliding on the ground. Under the

assumption of ideal sliding, the blade can change its heading direction and move forward or backward with respect to this direction, but no sliding orthogonally to the heading direction is possible. In both examples, the configuration $q$ includes the orientation $\theta$ and position $(x, y)$ of the system. The nonholonomic constraint $A(q)\,\dot{q} = 0$ restricts the feasible translational velocities $(\dot{x}, \dot{y})$ and depends on the orientation $\theta$ which gives the heading direction of the system. It cannot be transformed to a holonomic constraint on the position. For details and examples of such nonholonomic constraints, see [12, 22, 35, 79, 80]

- Free-flying multi-body systems like satellites with reaction wheels or hopping robots in flight phase have nonholonomic constraints due to the conservation of angular momentum. The configuration $q$ of such systems consists of the position, attitude, and the relative angles between the individual bodies. For nonzero angular momentum, inhomogeneous velocity constraints $A(q)\,\dot{q} = c$ result for constant $c \neq 0$. These velocity constraints are nonholonomic as they cannot be written as constraints on the configuration variables for the attitude and the relative angles. For details, see [12, 35, 80].

## 3.1 Basics of nonlinear control systems

The nonholonomic systems considered in the following are a specific class of control systems 2.1.2. At first, elementary properties of nonlinear control systems are given. Then, control systems on Lie groups are addressed. Finally, integrability and controllability are discussed.

### 3.1.1 Fundamental properties of nonlinear control systems

In the following, basic properties of nonlinear control systems are defined. These properties are required for the controllability conditions in Section 3.1.4, the definition of nonholonomic system in Section 3.3, and the optimality conditions in Chapter 4.

**Definition 3.1.1** *(Symmetric control system, driftless control system, affine control system) A control system $\dot{x} = f(x, u)$ is symmetric if for each $(x, u) \in M \times U$, there is an input $\tilde{u} \in U$ with $f(x, \tilde{u}) = -f(x, u)$. A control system $\dot{x} = f(x, u)$ with $f(x, 0) \equiv 0$ is called driftless system. A control system*

$$\dot{x} = f_0(x) + \sum_{i=1}^{m} g_i(x)\, u_i \tag{3.1}$$

*with a real analytic vector field $f_0$ and $m$ linearly independent real analytic vector fields $g_i$ is called affine control system.*

An affine control system (3.1) can also be written as $\dot{x} = f_0(x) + G(x)\,u$ for the $n \times m$ matrix $G(x) = [g_1(x), \ldots, g_m(x)]$. In (3.1), $f_0$ is the drift vector field, and $g_i$ are the input vector fields. The system class has its name from the fact that the inputs $u_i$ enter the system affinely. If $f_0$ vanishes identically, a driftless control system is obtained.

**Definition 3.1.2** *(Proper input space, symmetric input space) An input space $U \subset \mathbb{R}^m$ satisfying $0 \in \operatorname{int}(\operatorname{conv}(U))$ is called proper input space. An input space*

$$U = [-\hat{u}_1, \hat{u}_1] \times \cdots \times [-\hat{u}_m, \hat{u}_m]$$

*with $\hat{u}_i > 0$ is called symmetric input space.*

An input space $U$ is proper if the origin is an interior point of its convex hull $\operatorname{conv}(U)$. Here, $\operatorname{conv}(U)$ is the smallest convex set containing $U$. Proper input spaces are considered e. g. in [22, 49, 60]. They are required for the controllability properties in Section 3.1.4. Each symmetric input space is proper. A driftless affine system $\dot{x} = G(x)\,u$ with symmetric input space is symmetric. The symmetric input space is the standard input space in this thesis. It can be represented by $U = \{u \in \mathbb{R}^m \mid c(u) \leq 0\}$ using an input constraint defined next.

**Definition 3.1.3** *(Input constraint, active input constraint, modified input vector) For an symmetric input space 3.1.2, the inequality*

$$c(u) = \begin{pmatrix} c_1^-(u) \\ c_1^+(u) \\ \vdots \\ c_m^-(u) \\ c_m^+(u) \end{pmatrix} = \begin{pmatrix} -u_1 & - & \hat{u}_1 \\ u_1 & - & \hat{u}_1 \\ & \vdots & \\ -u_m & - & \hat{u}_m \\ u_m & - & \hat{u}_m \end{pmatrix} \leq 0$$

*is called input constraint. If at time $t$, the condition $c_i^-(u(t)) = 0$ or $c_i^+(u(t)) = 0$ holds for some $i \in \{1, \ldots, m\}$, then $c_i^-(u)$ and $c_i^+(u)$ is called active input constraint, respectively. The index set of active input constraints is*

$$I(t) := \left\{ i \in \{1, \ldots, m\} \,\middle|\, c_i^-(u(t)) = 0 \vee c_i^+(u(t)) = 0 \right\}. \tag{3.2}$$

*The number of active input constraints is $n_a(t) = |I(t)|$ and satisfies $0 \leq n_a(t) \leq m$.*

*The index set of input variables $u_j$ which are not affected by active input constraints is*

$$J(t) := \{ j \in \{1, \ldots, m\} \mid j \notin I(t) \}.$$

*The number of input variables not affected by active input constraints is $n_u(t) = |J(t)|$ and satisfies $0 \leq n_u(t) \leq m$. Besides, $n_a(t) + n_u(t) = m$ holds. The vector*

$$w := (u_j)_{j \in J(t)} \tag{3.3}$$

*of dimension $n_u(t)$ is called modified input vector.*

If there are active input constraints at time $t$, i. e., if $n_a(t) > 0$ holds, then $u(t) \in \operatorname{bd} U$ is true. The modified input vector $w$ (3.3) consists of all input variables $u_j$ which are not affected by active input constraints, i. e., which do not lie on $\operatorname{bd} U$. If there are no active input constraints at time $t$, then $n_u(t) = m$ and $w = u$ holds. Input constraints and modified input vectors are required for the optimality conditions in Section 4.5.1 and 4.6.2.

### 3.1.2 Control systems on Lie groups

In contrast to the remaining chapter, the configuration space $Q$ of the systems addressed here are $n$-dimensional Lie groups. To represent the configuration space of specific classes of control systems, matrix Lie groups like the special orthogonal group $SO(n)$ or the special Euclidean group $SE(n)$ are used. Satellites and spacecraft can be modeled as systems on the special orthogonal group $SO(3)$ to describe their attitude. Regarding the configuration space of wheeled mobile robots, the special Euclidean group $SE(2)$ gives the orientation and position of the robot in the plane. For the attitude and position of underwater and aerial vehicles in three-dimensional space, the special Euclidean group $SE(3)$ is applied. Nonholonomic systems transformable to the chain form described in Section 3.3.2 can be modeled as systems on the group $UT(n)$ of unipotent matrices, i. e., upper triangular matrices with ones on the diagonal. For references to matrix Lie groups, see [22, 80, 98], and to systems on Lie groups, see [2, 12, 22, 36, 49, 80, 84].

The configurations of the nonholonomic systems in Section 3.4 and Chapter 5 include the orientation angle $\theta$ and the coordinates $(x, y)$ of the center of mass. If a configuration is $q = (\theta, x, y)$ and $\theta \in \mathbb{R}$, $(x, y) \in \mathbb{R}^2$ is assumed, then the configuration space is $Q = \mathbb{R} \times \mathbb{R}^2$. For the orientation, angles $\theta$ and $\theta \pm 2\pi$ can be identified, as they result in equivalent rotations. Hence, the configuration space can actually be identified with $SO(2) \times \mathbb{R}^2 \simeq SE(2)$ and the configuration $q \in Q$ with a group element $g \in SE(2)$. A representation of $g \in SE(2)$ is

$$g = \begin{bmatrix} \cos(\theta) & -\sin(\theta) & x \\ \sin(\theta) & \cos(\theta) & y \\ 0 & 0 & 1 \end{bmatrix}. \tag{3.4}$$

The open interval $\mathbb{S} := (-\pi, \pi)$ gives a chart for the unit circle $S^1$ minus one point. Locally, $SE(2)$ can be identified with $Q = \mathbb{S} \times \mathbb{R}^2$. Thus, a system on $SE(2)$ induces a system on $\mathbb{S} \times \mathbb{R}^2$. To simplify computations, the configuration space $\mathbb{S} \times \mathbb{R}^2$ is sometimes used instead of $SE(2)$.

To describe the tangent space of a Lie group, the associated Lie algebra is considered. The Lie algebra $\mathfrak{g}$ of a Lie group $G$ is isomorphic to the tangent space $T_E G$ at the identity element $E$. For a general definition of Lie algebra, see Section 3.1.3. Each Lie algebra element $v \in T_E G$ can be shifted from $E$ to any group element $g$ in a specific way, resulting in a tangent vector $v_g \in T_g G$ at $g$. For a Lie group with identity element $E$, $v_g \in T_g G$ is obtained from $v \in T_E G$ by the tangent map of the left translation $T_E L_g \colon T_E G \to T_g G$, so that $v_g = T_E L_g v$ holds.

For matrix Lie groups, left translation is left matrix multiplication and the tangent map of left matrix multiplication is left matrix multiplication as well. Thus, for fixed $v$, $T_E L_g$ is given by left matrix multiplication by $g$ as in $f(g) = g\,v$. Any vector field $v_g = f(g)$ which results for some fixed $v$ and all $g \in G$ is called left-invariant vector field on $G$. For $SE(2)$, the standard basis vectors of the associated Lie algebra $\mathfrak{se}(2)$ are

$$e_1 = \begin{bmatrix} 0 & -1 & 0 \\ 1 & 0 & 0 \\ 0 & 0 & 0 \end{bmatrix}, \quad e_2 = \begin{bmatrix} 0 & 0 & 1 \\ 0 & 0 & 0 \\ 0 & 0 & 0 \end{bmatrix}, \quad e_3 = \begin{bmatrix} 0 & 0 & 0 \\ 0 & 0 & 1 \\ 0 & 0 & 0 \end{bmatrix}.$$

Each Lie algebra element $v \in \mathfrak{se}(2)$ can be written as $v = \alpha_1\, e_1 + \alpha_2\, e_2 + \alpha_3\, e_3$ for $\alpha_i \in \mathbb{R}$. For $g$ as in (3.4), any left-invariant vector field can be written in the form

$$f(g) = \begin{bmatrix} \cos(\theta) & -\sin(\theta) & x \\ \sin(\theta) & \cos(\theta) & y \\ 0 & 0 & 1 \end{bmatrix} \begin{bmatrix} 0 & -\alpha_1 & \alpha_2 \\ \alpha_1 & 0 & \alpha_3 \\ 0 & 0 & 0 \end{bmatrix}.$$

**Definition 3.1.4** *(Left-invariant control system on a matrix Lie group $G$) A control system*

$$\dot{g} = g \sum_{i=1}^{r} w_i(u)\, e_i = g\, V(u) \tag{3.5}$$

*on an $n$-dimensional matrix Lie group $G$, real analytic functions $w_i \colon U \to \mathbb{R}$, and $r$ linearly independent vectors $e_i \in T_E G$ of the Lie algebra, $r \leq n$, are considered. Any system (3.5) is called left-invariant control system on $G$.*

Equation (3.5) can be used to represent a kinematic control system with the configuration $q$ given by a Lie group element $g$ and the configuration space $Q$ given by $G$. The tangent vector $g\,V(u) \in T_g G$ at $g$ results from the Lie algebra element $V(u) = \sum_{i=1}^{r} w_i(u)\, e_i \in T_E G$. For $G = SO(n)$, the set of trajectories of a left-invariant control system is invariant under rotation. For $G = SE(n)$, it is invariant under translation and rotation. For references and examples of left-invariant systems, see [2, 22, 68, 84]. For invariant control systems, path planning problems can be simplified as in Section 7.1.

### 3.1.3 Integrability of distributions

In this section, the integrability of distributions is discussed which is required below to analyze controllability and to determine whether a velocity constraint $A(q)\,\dot{q} = 0$ is holonomic or nonholonomic. For this purpose, distributions, regular distributions, and Lie brackets are defined, and involutive distributions, the involutive closure, Lie algebras, and complete integrability of distributions are addressed, followed by the Theorems of Frobenius and Nagano-Sussmann. In this section, the state space $M$ is an open subset of $\mathbb{R}^n$ according to Assumption 2.1.1. All functions, vector fields, and distributions are assumed to be real analytic, since all control systems addressed in this thesis are real analytic systems, see Section 2.1. Details on distributions and their properties are given e. g. in [1, 16, 22, 49, 80, 98, 104].

**Definition 3.1.5** *(Distribution, distribution defined by vector fields, regular distribution) A map $\Delta\colon M \to TM$ which assigns to each $x \in M$ a linear subspace of the tangent space $T_xM$ is called a distribution.*

*Let $X_1, \ldots, X_m\colon M \to TM$ be a set of vector fields on $M$. The map $\Delta\colon M \to TM, x \mapsto \Delta(x)$ given by*

$$\Delta(x) := \operatorname{span}\{X_1(x), \ldots, X_m(x)\} \subseteq T_xM$$

*is called distribution defined by the vector fields $X_1, \ldots, X_m$.*

*A distribution $\Delta$ with constant rank $r = \dim \Delta(x)$ for all $x \in M$ is called regular.*

As $M$ is an open subset of $\mathbb{R}^n$, the tangent space $T_xM$ can be identified with $\mathbb{R}^n$ at each $x \in M$, and the tangent bundle $TM = \bigcup_{x\in M} T_xM$ of $M$ can be identified with $M \times \mathbb{R}^n$.

**Definition 3.1.6** *(Lie derivative, Lie bracket) Let $X\colon M \to TM$ be a vector field and $h\colon M \to \mathbb{R}$ a function on $M$. The function*

$$L_X h(x) = dh(x)\, X(x)$$

*is called Lie derivative of $h$ along $X$.*

*Let $X_1, X_2\colon M \to TM$ be vector fields on $M$. The operation $[\cdot,\cdot] : TM \times TM \to TM$ which is uniquely defined by*

$$L_{[X_1,X_2]}h = L_{X_1}L_{X_2}h - L_{X_2}L_{X_1}h \tag{3.6}$$

*for all functions $h\colon M \to \mathbb{R}$ is called Lie bracket of $X_1$ and $X_2$.*

The Lie derivative $L_X h$ gives the rate of change of $h$ along the flow of vector field $X$. For any vector fields $X_1$ and $X_2$, the vector field $[X_1, X_2]$ is uniquely defined by the way it acts as differential operator on a function $h$ according to (3.6). For details on the Lie derivative and the Lie bracket, see [1, 22, 49].

**Lemma 3.1.7** *(Properties of the Lie bracket) Let $X_1, X_2, X_3\colon M \to TM$ be vector fields and $h_1, h_2\colon M \to \mathbb{R}$ functions on $M$. The Lie bracket 3.1.6 satisfies skew-symmetry*

$$[X_1, X_2] = -[X_2, X_1],$$

*the Jacobi identity*

$$[X_1, [X_2, X_3]] + [X_3, [X_1, X_2]] + [X_2, [X_3, X_1]] = 0,$$

*and the chain rule*

$$[h_1X_1, h_2X_2] = h_1h_2\,[X_1, X_2] + h_1\,(L_{X_1}h_2)\,X_2 - h_2\,(L_{X_2}h_1)\,X_1.$$

Terms like $[X_1, [X_2, X_3]]$ are called repeated or iterated Lie brackets. An iterated Lie bracket is of degree $d$ if it consists of $d$ vector fields $X_i$ counting multiplicity. For example, the Lie bracket $[X_1, [X_1, X_2]]$ is of degree $d = 3$.

**Definition 3.1.8** *(Involutive distribution, involutive closure) A distribution $\Delta$ such that there holds $[X_i, X_j](x) \in \Delta(x)$ for all $x \in M$ and all $X_i, X_j \in \Delta$ is called involutive. The smallest distribution $\bar{\Delta}$ which contains $\Delta$ such that $[X_i, X_j] \in \bar{\Delta}$ holds for all $X_i, X_j \in \Delta$ is called involutive closure of $\Delta$.*

A distribution $\Delta$ is involutive if it is closed under the Lie bracket, i. e., any vector field $[X_i, X_j](x)$ resulting from Lie brackets of vector fields $X_i(x), X_j(x) \in \Delta(x)$ can be written as linear combination of vector fields of $\Delta(x)$ for all $x \in M$. It should be noted that for real analytic vector fields and distributions, the involutivity of a set of vector fields and of the

distribution defined by these vector fields is equivalent, see [22, 49]. Without real analyticity, this equivalence holds only under additional conditions concerning e. g. regularity.

If the distribution $\Delta$ is not involutive, new vector fields $[X_i, X_j]$ are generated for which $[X_i, X_j](x) \in \Delta(x)$ does not hold for all $x \in M$. If the new vector fields are added to the distribution $\Delta(x)$, this gives the new distribution

$$\Delta'(x) = \Delta(x) + \operatorname{span}\left\{[X_i, X_j](x) \mid X_i(x), X_j(x) \in \Delta(x)\right\}.$$

Its rank $r'(x) = \dim \Delta'(x)$ satisfies $r' \geq r$ for all $x \in M$ and $r' > r$ at least for some $x \in M$.

**Definition 3.1.9** *(Lie algebra) A vector space $V$ over $\mathbb{R}$ such that there is a bilinear operation $[\cdot,\cdot] : V \times V \to V$ which satisfies skew-symmetry and the Jacobi identity is called Lie algebra.*

In the following, Lie algebras of a set of vector fields are considered.

**Definition 3.1.10** *(Lie algebra of vector fields) Let $V(M)$ be the space of vector fields on $M$ and $X_1, \ldots, X_m \in V(M)$ a set of vector fields. The smallest linear subspace of $V(M)$ which contains $X_1, \ldots, X_m$ and is closed under the Lie bracket is called Lie algebra of the vector fields $X_1, \ldots, X_m$. It is denoted by $\mathcal{L}(X_1, \ldots, X_m)$.*

In Section 3.1.4, the accessibility algebra of an affine control system $\dot{x} = f_0(x) + \sum_{i=1}^{m} g_i(x)\, u_i$ is defined as the smallest Lie algebra of the vector fields $f_0, g_1, \ldots, g_m$. A Lie algebra is nilpotent if for some maximal degree $\hat{d}$, all iterated Lie brackets of degree $d > \hat{d}$ vanish.

**Definition 3.1.11** *(Completely integrable distribution) A distribution $\Delta$ such that for any $x \in M$, there is a local submanifold $N$ of $M$ which contains $x$ und satisfies $T_y N = \Delta(y)$ for each $y \in N$ is called completely integrable.*

The local submanifold $N$ is called local integral manifold of the distribution $\Delta$ at $x$. For regular distributions, the following definition of complete integrability holds.

**Definition 3.1.12** *(Completely integrable regular distribution) A distribution $\Delta$ of constant rank $r$ such that a map $h\colon M \to \mathbb{R}^l$, $l = n - r$, with pointwise linearly independent $dh_i(x)$ exists for which*

$$L_{X_j} h_i(x) = 0$$

*holds for all $x \in M$ and all $X_j \in \Delta$ is called completely integrable.*

For the map $h$ from Definition 3.1.12, the hypersurface defined by

$$\{x \in M \mid h(x) = c\}$$

for some specific $c \in \mathbb{R}^l$ is called integral manifold of the distribution $\Delta$. The map $h$ is used for the definition of nonholonomic constraint in Section 3.2.1.

**Theorem 3.1.13** *(Frobenius) A regular distribution is completely integrable if and only if it is involutive.*

For details on Theorem 3.1.13 and proofs, see [1, 15, 16, 22, 49, 80, 84, 104]. According to the theorem, for a regular distribution to be completely integrable, it is necessary and sufficient that the distribution is involutive, i. e., closed under the Lie bracket. The Theorem of Frobenius holds for regular distribution which are just smooth. In contrast, the following theorem applies to real analytic distributions which need not be regular.

**Theorem 3.1.14** *(Nagano-Sussmann) A real analytic distribution is completely integrable if and only if it is involutive.*

For details and proofs of Theorem 3.1.14, which is also called Theorem of Hermann-Nagano, see [15, 22, 49]. The Theorem of Frobenius is the basis for Theorem 3.2.6 below, which allows to classify constraints into holonomic and nonholonomic depending on the rank of the involutive closure of the constraint distribution.

### 3.1.4 Controllability

In this section, controllability of nonlinear control systems is addressed. For literature on controllability, see [22, 35, 49, 80, 83, 98, 104]. In the following, controllability, reachable sets, and accessibility are defined. Based on the accessibility distribution, the Theorem of Chow is given, providing necessary and sufficient conditions for accessibility of real analytic control systems. Afterward, controllability conditions are stated for driftless affine control systems and driftless control systems with non-affine inputs. The state space $M$ of the control systems are open subsets of $\mathbb{R}^n$. All vector fields, distributions, and control systems are real analytic.

**Definition 3.1.15** *(Controllability) A control system is controllable if there is an admissible solution $S(x_0, x_d)$ to control problem 2.2.1 for each pair $(x_0, x_d) \in M \times M$.*

According to Definition 2.2.1, an admissible solution $S(x_0, x_d)$ satisfies $x(0) = x_0$, $\dot{x} = f(x, u)$ for almost all $t$, and $x(\tau) = x_d$ for a bounded end time $\tau$. Controllability is required to solve the control problems defined in Section 2.2. Local controllability analysis via linearization about a fixed state does not apply to some nonlinear control systems like nonholonomic systems as discussed in [53, 98], since the linearization of such systems is not controllable.

**Definition 3.1.16** *(Reachable set) The reachable set at time $\tau$ denoted by $R(x_0, \tau)$ is the set of all states $x(\tau) \in M$ such that there is an admissible solution $S(x_0, x(\tau))$. The reachable set up to time $T$ is $R_T(x_0) = \bigcup_{\tau \leq T} R(x_0, \tau)$. The reachable set is $R(x_0) = \bigcup_{\tau > 0} R(x_0, \tau)$.*

If a control system is controllable, then $R(x_0) = M$ holds for all $x_0 \in M$.

**Definition 3.1.17** *(Accessibility) A control system is accessible at $x_0$ if $R_T(x_0)$ contains a non-empty open set for all times $T > 0$. A control system is accessible if it is accessible for all $x \in M$.*

For general control systems, accessibility does not imply controllability, and controllability does not imply accessibility.

**Definition 3.1.18** *(Accessibility distribution, accessibility algebra) For an affine control system $\dot{x} = f_0(x) + \sum_{i=1}^{m} g_i(x)\, u_i$, the accessibility distribution $\Delta_A$ is the involutive closure of the distribution of the vector fields $f_0, g_1, \ldots, g_m$. The accessibility algebra is the smallest Lie algebra containing $f_0, g_1, \ldots, g_m$.*

The accessibility algebra is the Lie algebra 3.1.10 of the vector fields $f_0, g_1, \ldots, g_m$.

**Theorem 3.1.19** *(Chow) Let $\Delta_A$ be the accessibility distribution 3.1.18. If the Lie algebra rank condition $\dim \Delta_A(x_0) = n$ holds, the control system is accessible at $x_0$. If the Lie algebra rank condition $\dim \Delta_A(x) = n$ holds for all $x \in M$, the control system is accessible.*

For proofs of Theorem 3.1.19, see [15, 22, 83, 98]. If $\dim \Delta_A(x) = n$ holds for all $x \in M$, the vector fields $f_0, g_1, \ldots, g_m$ of the system and their iterated Lie brackets span the whole tangent space $T_x M$ at every $x \in M$. For real analytic control systems, the Lie algebra rank condition is necessary and sufficient for accessibility, whereas for smooth systems, it is only sufficient, see [12, 15, 22, 35, 104].

**Theorem 3.1.20** *(Controllability of driftless affine control systems) Let $U$ be a proper input space 3.1.2. A driftless affine control system $\dot{x} = \sum_{i=1}^{m} g_i(x)\, u_i$ is controllable if and only if it is accessible at every $x \in M$.*

As addressed in [12, 49], without additional conditions, Theorem 3.1.20 is true only for control systems which are real analytic. For proofs and details on the theorem, see [15, 80, 83, 98, 104]. In contrast to Theorem 3.1.20 which applies only to driftless affine control systems, the following theorem holds for general driftless systems which may have non-affine inputs.

**Theorem 3.1.21** *(Controllability of driftless control systems) A driftless control system* $\dot{x} = f(x,u)$ *is controllable if it is symmetric and if for all* $x \in M$*, there are inputs* $u_i \in U$ *resulting in* $n$ *vector fields* $f(x,u_i)$ *such that* $\dim \operatorname{span}\{f(x,u_1),\ldots,f(x,u_n)\} = n$ *holds for all* $x \in M$*.*

For details on controllability of systems with non-affine inputs, see [15, 49, 103, 118]. Theorem 3.1.21 is similar to Theorem 3.1.20. Here, accessibility is replaced by the condition that $n$ vector fields $f_i(x)$ with $\dim \operatorname{span}\{f(x,u_1),\ldots,f(x,u_n)\} = n$ are generated by suitable inputs, and the proper input space $U$ is replaced by the requirement that the system is symmetric.

## 3.2 Holonomic and nonholonomic constraints

Holonomic and nonholonomic constraints originate from classical mechanics. Holonomic constraints affect the configuration $q$ of a system as in Definition 3.0.1, whereas nonholonomic constraints restrict the feasible velocities $\dot{q}$. Nonholonomic constraints are not equivalent to holonomic constraints, i. e., they cannot be expressed as constraints on the configuration $q$.

In the following, holonomic and nonholonomic constraints are addressed in Section 3.2.1 and 3.2.2, respectively. Besides holonomic and nonholonomic constraints, scleronomic and rheonomic constraints are distinguished in classical mechanics. A scleronomic constraint is time-independent, whereas a rheonomic constraint is time-dependent. All constraints considered in the following are scleronomic constraints.

### 3.2.1 Holonomic constraints

**Definition 3.2.1** *(Holonomic constraint) Let* $h\colon Q \to \mathbb{R}^l$ *be a real analytic map,* $\dim Q = p$*,* $1 \leq l < p$*, and* $c \in \mathbb{R}^l$ *a constant. A constraint*

$$h(q) = c \tag{3.7}$$

*with linearly independent* $\mathrm{d}h_i(q)$ *for all* $q \in Q$ *is called holonomic constraint.*

Holonomic constraints are constraints on the configuration $q$. In Definition 3.2.1, the differentials $\mathrm{d}h_i(q)$ are assumed to be linearly independent for all $q \in Q$. Otherwise, the $l$ scalar constraints $h_i(q) = c_i$ are not independent.

Holonomic constraints result e. g. from mechanical interconnections. For example, if a point mass with coordinates $q = (q_1, q_2, q_3)$ is attached to a fixed point $p = (p_1, p_2, p_3)$ by a rigid rod of constant length $L > 0$, the scalar holonomic constraint

$$h(q) = \sqrt{(q_1 - p_1)^2 + (q_2 - p_2)^2 + (q_3 - p_3)^2} = L$$

holds. The configuration of a mechanical system with a configuration space $Q$ of dimension $p$ and a holonomic constraint of dimension $l$ is restricted to evolve on a submanifold of the form $\{q \in Q \mid h(q) = c\}$ of dimension $p - l$. Thus, the system cannot reach configurations which do not satisfy $h(q) = c$. For details on holonomic constraints, see [12, 35, 80].

### 3.2.2 Nonholonomic constraints

In contrast to holonomic constraints which can be represented as configuration constraints (3.7), nonholonomic constraints are velocity constraints defined next.

**Definition 3.2.2** *(Velocity constraint, regular velocity constraint) Let* $A(q)$ *be a* $k \times p$ *matrix,* $\dim Q = p$*,* $1 \leq k < p$*, with real analytic elements* $a_{ij}(q)$*, and* $\dot{q} \in T_q Q$*. The constraint*

$$A(q)\,\dot{q} = 0$$

*is called velocity constraint. If* $A(q)$ *has full rank for all* $q \in Q$*, the velocity constraint is regular.*

A regular velocity constraint $A(q)\,\dot{q} = 0$ gives a set of $k$ scalar linear constraints $a_i^\top(q)\,\dot{q} = 0$ for $a_i(q) = (a_{i1}(q), \ldots, a_{ip}(q))$ and $i = 1,...,k$. Here, $k$ has to satisfy $1 \leq k < p$, as for $k = 0$, no constraint exists, and for $k \geq p$, only the trivial solution $\dot{q} \equiv 0$ satisfies $A(q)\,\dot{q} = 0$. In the following, $A(q)\,\dot{q} = 0$ is both referred to as one constraint of dimension $k$, to stress that it is one vector-valued constraint, and as $k$ constraints, considering the $k$ separate constraints.

By differentiation, each holonomic constraint $h(q) = c$ gives a velocity constraint $\mathrm{d}h(q)\,\dot{q} = 0$. As the differentials $\mathrm{d}h_i(q)$ are linearly independent for all $q \in Q$ according to Definition 3.2.1, $A(q) := \mathrm{d}h(q)$ has full rank for all $q$, and the velocity constraint $\mathrm{d}h(q)\,\dot{q} = 0$ is regular.

**Definition 3.2.3** *(Nonholonomic constraint) A regular velocity constraint is called completely nonholonomic if there is no real analytic map $h\colon Q \to \mathbb{R}^l$, $1 \leq l \leq k$, with linearly independent $dh_i(q)$ such that $dh(q)\,\dot{q} = 0$ holds for all $q \in Q$ and all $\dot{q} \in T_qQ$ which satisfy $A(q)\,\dot{q} = 0$.*

A regular velocity constraint $A(q)\,\dot{q} = 0$ can be holonomic, partially nonholonomic, or completely nonholonomic. It is holonomic if there is a real analytic map $h\colon Q \to \mathbb{R}^k$ with linearly independent $\mathrm{d}h_i(q)$ which satisfies $\mathrm{d}h(q)\,\dot{q} = 0$ for all $\dot{q} \in T_qQ$ for which $A(q)\,\dot{q} = 0$ is true. Then, $A(q)\,\dot{q} = 0$ can be transformed to a holonomic constraint (3.7) of dimension $k$, and the configuration is restricted to evolve on a submanifold $\{q \in Q \mid h(q) = c\}$ of dimension $p - k$. A constraint is partially nonholonomic if there is an $l$, $1 \leq l < k$, and a map $h\colon Q \to \mathbb{R}^l$ with linearly independent $\mathrm{d}h_i(q)$ satisfying $\mathrm{d}h(q)\,\dot{q} = 0$ for all $\dot{q} \in T_qQ$ with $A(q)\,\dot{q} = 0$. This means that $l$ independent linear combinations of the $k$ scalar constraints $a_i^\top(q)\,\dot{q} = 0$ are equivalent to holonomic constraints $h_j(q) = c_j$. The configuration evolves on a submanifold of dimension $p - l$. A constraint is completely nonholonomic if it is neither holonomic nor partially nonholonomic. Under a completely nonholonomic constraint, the configuration is not restricted to evolve on any submanifold of $Q$. Thus, every configuration $q \in Q$ can be reached. In the remainder of the thesis, nonholonomic means completely nonholonomic.

Nonholonomic constraints of mechanical systems are usually homogenous linear velocity constraints $A(q)\,\dot{q} = 0$. Details and examples of such constraints are given in [12, 22, 35, 53, 79, 80]. Moreover, there are more general nonholonomic constraints which are inhomogeneous or nonlinear in $\dot{q}$. Inhomogeneous constraints $A(q)\,\dot{q} = c$ for constant $c \neq 0$ result e. g. from the conservation of nonzero angular momentum, see [12, 35, 80]. Nonlinear constraints $h(q, \dot{q}) = 0$ are addressed in [22, 79]. If the matrix $A(q)$ of a velocity constraint drop ranks at specific configurations, then the constraint cannot be a nonholonomic constraint as in Definition 3.2.3 anymore. According to [22], at singular configurations of $A(q)$, it is not clear how to extend the definition of nonholonomic constraint. Usually, singular configurations of $A(q)$ are omitted from the analysis, as it is done in [22] for the snakeboard and in Section 5.2 for the BSR by restricting the steering angles.

Equivalently to Definition 3.2.3, a regular velocity constraint $A(q)\,\dot{q} = 0$ is completely nonholonomic if and only if for all full rank $l \times k$ matrices $Z(q)$, $1 \leq l \leq k$, there is no real analytic map $h\colon Q \to \mathbb{R}^l$ with $\mathrm{d}h(q) = Z(q)\,A(q)$ for all $q \in Q$. For details, see [35, 80]. The matrix $Z(q)$ serves as integrating factor. It is not easy to determine the type of a regular velocity constraint $A(q)\,\dot{q} = 0$, i. e., whether it is holonomic, partially nonholonomic, or completely nonholonomic, by constructing a suitable map $h$. This is true as not only the set of $k$ constraints $a_i^\top(q)\,\dot{q} = 0$, but also their linear combinations over real analytic functions have to be considered. Hence, the constraint distribution $D$ for a regular velocity constraint is defined next, and the dimension of the involutive closure $\bar{D}$ is analyzed to determine the type of the constraint.

**Definition 3.2.4** *(Constraint distribution) Let $A(q)$ be the matrix of a regular velocity constraint 3.2.2. The distribution $D$ of constant rank $m = p - k$ which satisfies*

$$\ker A(q) = D(q) \tag{3.8}$$

*for all $q \in Q$ is called constraint distribution.*

As the velocity constraint is regular and real analytic, the constraint distribution $D$ is regular, i. e., of constant rank $m$, and real analytic as well. Since $1 \leq k < p$ was assumed in Definition

3.2.2, $1 \leq m < p$ holds for $m = p - k$ in Definition 3.2.4. If the matrix $A(q)$ of a velocity constraint drops rank at singular configurations, i. e., the constraint is no regular constraint anymore, the dimension of the distribution $D$ satisfying (3.8) must change.

**Assumption 3.2.5** *(Global generators of the constraint distribution) There are $m$ real analytic global generators $X_1, \ldots, X_m$ of the constraint distribution $D$ such that*

$$D = \operatorname{span}\{X_1, \ldots, X_m\}$$

*holds for all $q \in Q$.*

The global generators $X_i$ are globally defined real analytic vector fields. As the constraint distribution $D$ is regular, they are linearly independent for all $q \in Q$. Conditions for the existence of global generators of a distribution are given in [1, 22]. The constraint distribution $D$ is a subbundle of the tangent bundle $TQ$. It gives a pointwise assignment of the subspace $D(q)$ of $T_qQ$ at each configuration $q \in Q$ such that every vector field $Y(q) = \sum_{i=1}^{m} \alpha_i X_i(q)$ for arbitrary $\alpha_i \in \mathbb{R}$ satisfies $A(q)\,Y(q) = 0$. The distribution $D$ is called annihilating distribution of the velocity constraint, as $A(q)\,\dot{q} = 0$ holds for all $q \in Q$ and all

$$\dot{q} = \sum_{i=1}^{m} \alpha_i X_i(q)\,.$$

**Theorem 3.2.6** *(Holonomic, partially nonholonomic, completely nonholonomic constraint) Let $Q$ be a configuration space 3.0.1 with $\dim Q = p$, $D$ be a constraint distribution 3.2.4 of rank $m$ of a regular velocity constraint 3.2.2, and $\bar{D}$ its involutive closure. Assume that $\bar{D}$ is of constant rank $r$. Then, if $r = m$ holds, the constraint is holonomic, if $m < r < p$ holds, it is partially nonholonomic, and if $r = p$ holds, it is completely nonholonomic.*

By Theorem 3.2.6, it is possible to check whether a regular velocity constraint is holonomic, partially nonholonomic, or completely nonholonomic by studying the integrability of the constraint distribution $D$. Hence, no explicit construction of the map $h$ from Definition 3.2.3 is required. Due to the connection between the integrability of $D$ and the type of the constraint, a constraint is called completely integrable, partially integrable, and nonintegrable if it is holonomic, partially nonholonomic, and completely nonholonomic, respectively. The proof of Theorem 3.2.6 is based on the Theorems of Frobenius and Chow. For details, see [35, 49, 60, 80].

## 3.3 Nonholonomic systems

In this section, nonholonomic systems are addressed, i. e., systems subject to nonholonomic constraints 3.2.3. All nonholonomic systems considered here are control systems, i. e., they have inputs to control their behavior. Apart from that, dynamical systems with nonholonomic constraints and no inputs can be studied as well.

**Definition 3.3.1** *(Nonholonomic system) Let $\dot{x} = f(x, u)$ be a control system 2.1.2 with state space $M$, $\dim M = n$, and input space $U$. Define the distribution*

$$D(x) := \operatorname{span}\{f(x, u) \mid u \in U\}\,. \tag{3.9}$$

*If the involutive closure $\bar{D}$ has rank $n$ for all $x \in M$, the control system is called nonholonomic system.*

Definition 3.3.1, which can be found e. g. in [2, 49], is a rather general definition of nonholonomic system. If the distribution $D$ obtained from (3.9) is regular, Definition 3.3.1 is related to Section 3.2.2 by considering $D$ as the constraint distribution 3.2.4 of a velocity constraint

$A(x)\,\dot{x} = 0$. According to Theorem 3.2.6, this constraint is a nonholonomic constraint if the involutive closure of $D$ has full rank $n = \dim M$ for all $x \in M$.

In the following, a specific class of nonholonomic systems is addressed, called nonholonomic kinematic systems. These systems are kinematic systems, i. e., first-order control systems with velocity inputs. Their state space is the configuration space $Q$ from Definition 3.0.1. Nonholonomic systems can also be modeled as dynamic systems, i. e., second-order control systems with force inputs. Such systems are briefly discussed in Section 3.4.3.

Besides nonholonomic systems, there are holonomic systems, i. e., systems subject to holonomic constraints. In contrast to nonholonomic systems, the constraints of holonomic systems can be eliminated by a change of coordinates, see [12, 35, 80]. For a system with a holonomic constraint $h(q) = c$ with $h\colon Q \to \mathbb{R}^l$ and $\dim Q = p$, new coordinates $\tilde{q} = (\tilde{q}_1, \dots, \tilde{q}_{p-l})$ can be chosen for a parameterization of the submanifold $\{q \in Q \mid h(q) = c\}$. Then, a new system with configuration $\tilde{q}$ can be studied which has the same trajectories as the original system with configuration $q$. For the new system, the holonomic constraint $h(q) = c$ is always satisfied.

### 3.3.1 Nonholonomic kinematic systems

The global generators $X_i$ of the constraint distribution of a nonholonomic constraint can be used as input vector fields $g_i$ of a driftless control system and the coefficients $\alpha_i$ in $\dot{q} = \sum_{i=1}^{m} \alpha_i\, X_i(q)$ as inputs. Then, the nonholonomic kinematic system results which is defined next.

**Definition 3.3.2** *(Nonholonomic kinematic system) Let $Q$ be a configuration space 3.0.1 and $X_1, \dots, X_m$ global generators of the constraint distribution 3.2.4 of a nonholonomic constraint 3.2.3. Define the input vector fields $g_i := X_i$. The driftless affine control system*

$$\dot{q} = \sum_{i=1}^{m} g_i(q)\, u_i \tag{3.10}$$

*with state space $Q$ is called nonholonomic kinematic system.*

A nonholonomic kinematic system 3.3.2 is a special case of a nonholonomic system 3.3.1, since the involutive closure $\bar{D}$ of the distribution

$$D := \operatorname{span}\{g_1, \dots, g_m\} \tag{3.11}$$

has rank $p = \dim Q$ for all $q \in Q$. System 3.3.2 is also called full kinematic model of a nonholonomic system in the following. It specifies the kinematics of a nonholonomic system, i. e., it describes the motion of the system in a differential-geometric way. The input variables $u_i$ have the physical meaning of velocities, although in general, they do not directly give the generalized velocities $\dot{q}_j$, but are related to $\dot{q}$ via (3.10). In contrast to dynamic systems, for kinematic systems, discontinuous changes of the velocities $u_i$ and thus of $\dot{q}$ are possible.

System (3.10) can also be written as $\dot{q} = G(q)\, u$. Here, the full rank $p \times m$ matrix $G(q) = [g_1(q), \dots, g_m(q)]$ has real analytic elements $g_{ij}(q)$. In Definition 3.3.2, $m < p$ holds, since $k \geq 1$ is assumed in Definition 3.2.2 and $m = p - k$ in Definition 3.2.4. Considered as first-order control system with $\dim Q = p$, $\dim U = m$, and $m < p$, system 3.3.2 is underactuated, as it has fewer input variables than degrees of freedom. However, because of the full rank of the involutive closure $\bar{D}$, it is controllable as stated next.

**Corollary 3.3.3** *(Controllability of nonholonomic kinematic systems) A nonholonomic kinematic system 3.3.2 with proper input space $U$ is controllable.*

Corollary 3.3.3 results from Theorem 3.1.20, as a nonholonomic kinematic system is a driftless affine control system which is real analytic and accessible at every $q \in Q$ by the Theorem of Chow. Accessibility holds since the involutive closure $\bar{D}$ of the distribution (3.11) has full rank $p$ for all $q \in Q$. Moreover, for real analytic systems, $\bar{D}$ can be identified with the accessibility distribution 3.1.18 for $f_0 \equiv 0$. Thus, a kinematic system $\dot{q} = \sum_{i=1}^{m} g_i(q)\, u_i$ with $m < p$ is controllable if the corresponding velocity constraint $A(q)\,\dot{q} = 0$ is completely nonholonomic and the input space $U$ is proper. For details on Corollary 3.3.3, see [80, 98].

### 3.3.2 Normal forms of nonholonomic kinematic systems

Normal forms of nonholonomic kinematic systems 3.3.2 are used to analyze system properties like controllability and to design open-loop and closed-loop controls. Most nonholonomic kinematic systems can be locally or globally converted to a normal form by a state transformation $z = \Phi(q)$ and an input transformation $v = \Theta(q)\,u$. Examples of normal forms for kinematic systems are the chain form and the power form, which are equivalent by a state transformation. For details on normal forms for nonholonomic systems, see [12, 35, 80, 81, 98].

The most widely used normal form is the chain form. For a system with $p$-dimensional configuration $q = (q_1, \ldots, q_p)$ and two-dimensional input $u = (u_1, u_2)$, the one-chain form is

$$\begin{aligned} \dot{\xi} &= v_1, \\ \dot{\zeta}_1 &= v_2, \\ \dot{\zeta}_2 &= \zeta_1\, v_1, \\ &\vdots \\ \dot{\zeta}_{p_2} &= \zeta_{p_2-1}\, v_1 \end{aligned}$$

with state variables $z = (\xi, \zeta)$, $\zeta = (\zeta_1, \ldots, \zeta_{p_2})$, $1 + p_2 = p$, and input variables $v = (v_1, v_2)$.

The transformation of the unicycle and the car-like robot to chain form is addressed below. Necessary and sufficient conditions for the local transformation of nonholonomic kinematic systems with two-dimensional input to one-chain form are given in [35]. A constructive algorithm based on a sufficient condition for local conversion to chain form is described in [12, 35, 80, 98]. For this, two functions $h_1(q)$ and $h_2(q)$ are determined by solving a system of partial differential equations. Then, the state transformation $z = \Phi(q)$ and the input transformation $v = \Theta(q)\,u$ are obtained from iterated Lie derivatives of $h_1(q)$ and $h_2(q)$ along the input vector fields $g_i$ of the nonholonomic kinematic system.

If a nonholonomic kinematic system with $p$-dimensional configuration and $m$-dimensional input $u = (u_1, \ldots, u_m)$ for $m \geq 3$ is transformed to chain form, the resultant multi-chain form consisting of $m - 1$ chains is

$$\begin{array}{lllllllllll} \dot{z}^1 &=& v_1, & & & & & & & & \\ \dot{z}^2_1 &=& v_2, & \dot{z}^3_1 &=& v_3, & \cdots & \dot{z}^m_1 &=& v_m, & \\ \dot{z}^2_2 &=& z^2_1\, v_1, & \dot{z}^3_2 &=& z^3_1\, v_1, & \cdots & \dot{z}^m_2 &=& z^m_1\, v_1, & \\ & \vdots & & & \vdots & & & & \vdots & & \\ \dot{z}^2_{p_2} &=& z^2_{p_2-1}\, v_1, & \dot{z}^3_{p_3} &=& z^3_{p_3-1}\, v_1, & \cdots & \dot{z}^m_{p_m} &=& z^m_{p_m-1}\, v_1. & \end{array} \tag{3.12}$$

It has the new state variables $z = \left(z^1, z^2, \ldots, z^m\right)$, $z^i = \left(z^i_1, \ldots, z^i_{p_i}\right)$ for $i = 2,...,m$, $1 + p_2 + \cdots + p_m = p$, and the new input variables $v = (v_1, \ldots, v_m)$.

In [61], a transformation of the FKM (1.4) of the BSR with $p = 5$ and $m = 3$ to two-chain form is given. As discussed in Section 5.1, for this transformation to be defined, steering angle configurations with $\varphi_f = \varphi_r$ have to be excluded, which is a strong restriction on the feasible paths. Another example of a nonholonomic system transformed to two-chain form is the fire truck with $p = 6$ and $m = 3$ in [23, 122]. Sufficient conditions for the local conversion of nonholonomic kinematic systems with $m \geq 3$ to chain form are given [23, 81].

Chain form systems, i. e., kinematic systems transformed to chain form, are triangular control systems. They become linear systems for constant input $v_1$ and behave like chains of integrators then. Kinematic systems transformable to chain form are controllable as shown in [35, 80, 81, 98]. There are several methods for open-loop and closed-loop control of nonholonomic kinematic systems which apply exclusively to chain form systems. Some of these methods are discussed in Section 3.5.

## 3.4 Examples

In this section, well-known examples of nonholonomic systems are given. The systems are used to exemplify the definitions and properties of nonholonomic systems of this chapter and to evaluate the results obtained for the BSR. In Section 3.4.1 and 3.4.2, the unicycle and the car-like robot are described which are wheeled mobile robots modeled as nonholonomic kinematic systems. The nonholonomic constraints and the kinematic models of these robots can be derived the same way as it is done for the BSR in Section 5.2. In Section 3.4.3, the snakeboard is considered as nonholonomic dynamic system.

Other known nonholonomic systems are the differential drive, the car with $n$ trailers, the roller racer, and the Chaplygin sleigh. The differential drive is a wheeled mobile robot with two independently driven coaxial wheels. Depending on the rotational velocity of the wheels, the robot drives a straight or curved path or turns on the spot. For the differential drive, both the nonholonomic kinematic and dynamic system is studied, in particular with respect to motion planning and optimal control. Time-optimal control of the kinematic system of the differential drive is covered in [9, 10, 60, 106]. In [27, 60], the closely related problem of steering the differential drive with minimal wheel rotation is analyzed. The car with $n$ trailers is addressed as nonholonomic kinematic system which is transformable to chain form. For this wheeled mobile robot, path planning is performed based on finite parameterizations of the inputs and differential flatness discussed in Section 3.5. For references to the car with $n$ trailers, see [35, 40, 53, 59, 60, 80]. The roller racer, a nonholonomic system consisting of two coupled rigid bodies propelled by cyclic motions of the first body, is considered as nonholonomic dynamic system. For this system, controllability properties and motion planning is addressed in [12, 20, 22]. The Chaplygin sleigh is a rigid body sliding on a horizontal plane on two sliding posts and one knife edge, i. e., a blade which imposes a nonholonomic constraint. For the Chaplygin sleigh modeled as nonholonomic dynamic system, the computation of closed-form solutions and the control of the sliding direction is studied in [12].

### 3.4.1 Unicycle

The unicycle is one of the most basic nonholonomic systems. It is considered both as kinematic and dynamic system in the literature and serves as benchmark system for path planning and feedback control of nonholonomic systems. For references, see [12, 22, 35, 45, 53, 60, 80].

Figure 3.1 shows a model of the unicycle in the plane consisting of one rigid body. The unicycle can change its heading direction by turning around the vertical axis, called steering, and move in this direction, called driving. The rotation of the unicycle around its rotation axis is neglected, i. e., the unicycle is not treated as a wheel, but as a blade which defines the heading direction. In Figure 3.1, $(x, y)$ are the coordinates of the center of mass with respect to a fixed reference frame. The angle $\theta$ gives the orientation relative to the $x$-axis. The configuration is $q = (\theta, x, y)$ and the configuration space is $Q = SE(2)$.

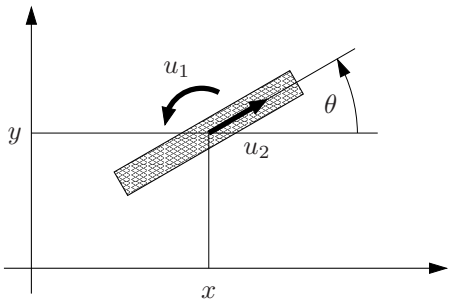


Figure 3.1: Model of the unicycle.

The nonholonomic constraint follows from the assumption that the unicycle cannot slide

orthogonally to its heading direction. The resultant velocity constraint is

$$\begin{bmatrix} 0 & \sin(\theta) & -\cos(\theta) \end{bmatrix} \begin{bmatrix} \dot{\theta} \\ \dot{x} \\ \dot{y} \end{bmatrix} = 0. \tag{3.13}$$

The constraint distribution $D$ is generated by the globally defined vector fields

$$X_1 = \begin{bmatrix} 1 \\ 0 \\ 0 \end{bmatrix}, \quad X_2(q) = \begin{bmatrix} 0 \\ \cos(\theta) \\ \sin(\theta) \end{bmatrix}.$$

For $g_1 := X_1$ and $g_2(q) := X_2(q)$, the corresponding nonholonomic kinematic system is

$$\dot{q} = \begin{bmatrix} \dot{\theta} \\ \dot{x} \\ \dot{y} \end{bmatrix} = \begin{bmatrix} 1 \\ 0 \\ 0 \end{bmatrix} u_1 + \begin{bmatrix} 0 \\ \cos(\theta) \\ \sin(\theta) \end{bmatrix} u_2. \tag{3.14}$$

The velocities $u_1$ and $u_2$ are the steering and driving velocity. For $\hat{u}_i > 0$, the symmetric input space is $U = [-\hat{u}_1, \hat{u}_1] \times [-\hat{u}_2, \hat{u}_2]$.

The accessibility distribution $\Delta_A$ of the unicycle is $\Delta_A = \operatorname{span}\{g_1, g_2, [g_1, g_2]\}$ with

$$[g_1, g_2](q) = \begin{bmatrix} 0 \\ -\sin(\theta) \\ \cos(\theta) \end{bmatrix}.$$

The vector field $[g_1, g_2](q)$ corresponds to a lateral motion orthogonal to the heading direction of the unicycle. The matrix $[g_1, g_2(q), [g_1, g_2](q)]$ has constant rank 3 for all $q \in Q$, since $\det[g_1, g_2(q), [g_1, g_2](q)] = 1$ holds. Hence, the Lie algebra rank condition is satisfied for all $q \in Q$, and the unicycle is accessible by the Theorem of Chow. As the input space $U$ is proper, the unicycle is controllable by Theorem 3.1.20. The constraint (3.13) is completely nonholonomic according to Theorem 3.2.6, since system (3.14) is real analytic and for such systems, the involutive closure $\bar{D}$ of the constraint distribution $D = \operatorname{span}\{X_1, X_2\}$ can be identified with the accessibility distribution $\Delta_A$.

The nonholonomic kinematic system of the unicycle in one-chain form is

$$\begin{aligned} \dot{\xi} &= v_1, \\ \dot{\zeta}_1 &= v_2, \\ \dot{\zeta}_2 &= \zeta_1 v_1. \end{aligned}$$

It is obtained from system (3.14) by the globally defined state and input transformations

$$\begin{aligned} \xi &= \theta, \\ \zeta_1 &= x\cos(\theta) + y\sin(\theta), \\ \zeta_2 &= x\sin(\theta) - y\cos(\theta), \\ v_1 &= u_1, \\ v_2 &= (y\cos(\theta) - x\sin(\theta))u_1 + u_2. \end{aligned}$$

In Section 4.7, time-optimal control of the unicycle is addressed to exemplify the necessary optimality conditions of the Maximum Principle.

### 3.4.2 Car-like robot

The car-like robot is a nonholonomic system of great importance for applications. It is mostly studied as kinematic system with respect to path planning, optimal control, and feedback control. Results on time-optimal control of the car-like robot are given in [13, 19, 37, 94, 106, 108, 120]. For more references to the car-like robot, see [6, 35, 45, 59, 60, 80, 81].

Figure 3.2 shows the bicycle model of the car-like robot. It has a steerable front axle and a fixed rear axle like a car. The model is called bicycle model, as a single wheel in the midpoint of each axle represents the pair of wheels of this axle. As for the unicycle, the rotation of the wheels is neglected, i. e., they are considered as blades. With respect to a fixed reference frame, $(x, y)$ gives the coordinates of the midpoint of the rear axle. The angle $\theta$ describes the orientation of the longitudinal axis relative to the $x$-axis. The steering angle of the front axle relative to the longitudinal axis is $\varphi_f$. It satisfies $|\varphi_f| < \hat{\varphi}$ for $0 < \hat{\varphi} < \frac{\pi}{2}$. The configuration is $q = (\theta, x, y, \varphi_f)$ and the configuration space is $Q = SE(2) \times (-\hat{\varphi}, \hat{\varphi})$. The distance between front and rear axle is $L > 0$.

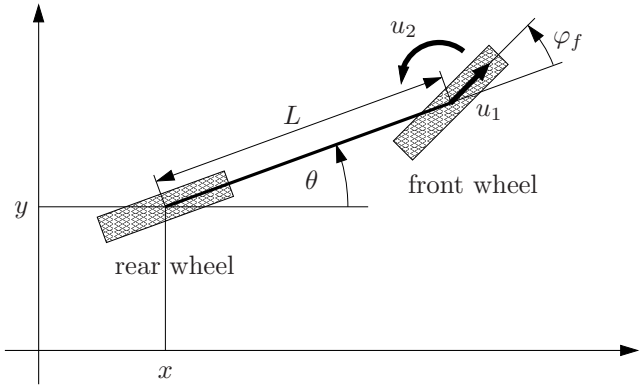


Figure 3.2: Model of the car-like robot.

The nonholonomic constraint results from the assumption that the two wheels do not slide laterally. The corresponding velocity constraint is

$$\begin{bmatrix} -L\cos(\varphi_f) & \sin(\theta+\varphi_f) & -\cos(\theta+\varphi_f) & 0 \\ 0 & \sin(\theta) & -\cos(\theta) & 0 \end{bmatrix} \begin{bmatrix} \dot{\theta} \\ \dot{x} \\ \dot{y} \\ \dot{\varphi}_f \end{bmatrix} = \begin{bmatrix} 0 \\ 0 \end{bmatrix}.$$

The global generators of the constraint distribution $D$ are

$$X_1(q) = \begin{bmatrix} \frac{1}{L}\sin(\varphi_f) \\ \cos(\theta)\cos(\varphi_f) \\ \sin(\theta)\cos(\varphi_f) \\ 0 \end{bmatrix}, \quad X_2 = \begin{bmatrix} 0 \\ 0 \\ 0 \\ 1 \end{bmatrix}.$$

For $g_1(q) := X_1(q)$ and $g_2 := X_2$, the nonholonomic kinematic system of the car-like robot is

$$\dot{q} = \begin{bmatrix} \dot{\theta} \\ \dot{x} \\ \dot{y} \\ \dot{\varphi}_f \end{bmatrix} = \begin{bmatrix} \frac{1}{L}\sin(\varphi_f) \\ \cos(\theta)\cos(\varphi_f) \\ \sin(\theta)\cos(\varphi_f) \\ 0 \end{bmatrix} u_1 + \begin{bmatrix} 0 \\ 0 \\ 0 \\ 1 \end{bmatrix} u_2. \tag{3.15}$$

Its inputs are the driving velocity $u_1$ at the front wheel and the steering velocity $u_2$. For $\hat{u}_i > 0$, the symmetric input space is $U = [-\hat{u}_1, \hat{u}_1] \times [-\hat{u}_2, \hat{u}_2]$.

The accessibility distribution is $\Delta_A = \operatorname{span}\{g_1, g_2, [g_1, g_2], [g_1, [g_1, g_2]]\}$ with

$$[g_1, g_2](q) = \begin{bmatrix} -\frac{1}{L}\cos(\varphi_f) \\ \cos(\theta)\sin(\varphi_f) \\ \sin(\theta)\sin(\varphi_f) \\ 0 \end{bmatrix}, \quad [g_1, [g_1, g_2]](q) = \begin{bmatrix} 0 \\ -\frac{1}{L}\sin(\theta) \\ \frac{1}{L}\cos(\theta) \\ 0 \end{bmatrix}.$$

The new vector field $[g_1, [g_1, g_2]](q)$ corresponds to a pure translation of the car-like robot. The matrix $[g_1(q), g_2, [g_1, g_2](q), [g_1, [g_1, g_2]](q)]$ has constant rank 4 for all $q \in Q$ because of $\det[g_1(q), g_2, [g_1, g_2](q), [g_1, [g_1, g_2]](q)] = 1/L^2$. Thus, the Lie algebra rank condition is satisfied for all $q \in Q$, and the car-like robot is accessible by the Theorem of Chow. For the proper input space $U$, it is controllable according to Theorem 3.1.20. Since system (3.15) is real analytic and the involutive closure $\bar{D}$ of the constraint distribution $D = \operatorname{span}\{X_1, X_2\}$ can thus be identified with the accessibility distribution $\Delta_A$, the constraint of the car-like robot is completely nonholonomic by Theorem 3.2.6.

The nonholonomic kinematic system of the car-like robot in one-chain form is

$$\begin{aligned} \dot{\xi} &= v_1, \\ \dot{\zeta}_1 &= v_2, \\ \dot{\zeta}_2 &= \zeta_1 v_1, \\ \dot{\zeta}_3 &= \zeta_2 v_1. \end{aligned}$$

It is derived from system (3.15) using the state and input transformations

$$\begin{aligned} \xi &= x, \\ \zeta_1 &= \tfrac{1}{L}\sec^3(\theta)\tan(\varphi_f), \\ \zeta_2 &= \tan(\theta), \\ \zeta_3 &= y, \\ v_1 &= \cos(\theta)\cos(\varphi_f)\, u_1, \\ v_2 &= \tfrac{1}{L^2}\sec^3(\theta)\left(3\tan(\theta)\sin(\varphi_f)\tan(\varphi_f)\, u_1 + L\sec^2(\varphi_f)\, u_2\right). \end{aligned}$$

These transformations are only local transformations, as $\sec(\theta)$ is not defined at $\theta = \pm\frac{\pi}{2}$.

In [13, 59, 60, 106, 108, 120, 124], a simplified model of the car-like robot is studied. It is obtained from (3.15) by neglecting the dynamics of $\varphi_f$, fixing $\hat{\varphi} = \frac{\pi}{4}$ and $L = 1$, and using the new inputs $(v_1, v_2) = (\sin(\varphi_f)\, u_1, \cos(\varphi_f)\, u_1)$. This model already given in Section 1.1 is

$$\dot{q} = \begin{bmatrix} \dot{\theta} \\ \dot{x} \\ \dot{y} \end{bmatrix} = \begin{bmatrix} 1 \\ 0 \\ 0 \end{bmatrix} v_1 + \begin{bmatrix} 0 \\ \cos(\theta) \\ \sin(\theta) \end{bmatrix} v_2. \tag{3.16}$$

The system looks like the nonholonomic kinematic system (3.14) of the unicycle, but the input space is different. This is true as the inputs $(v_1, v_2)$ cannot take values independently from each other, but have to satisfy $(v_1, v_2) = (\sin(\varphi_f)\, u_1, \cos(\varphi_f)\, u_1)$. To obtain Dubins paths of a robot which drives forward at constant velocity, the input space is $U_D = [-1, 1] \times \{1\}$. For Reeds-Shepp paths of a robot that can drive forward and backward at constant absolute velocity, $U_{RS} = [-1, 1] \times \{-1, 1\}$ is used. The results on time-optimal control of the car-like robot in Section 1.1 apply to system (3.16). In Section 6.6, extremals for time-optimal control of the car-like robot are compared to those of the BSR. Time-optimal normal regular extremals of the RKM and shortest paths of the car-like robot are compared in Section 8.5.

### 3.4.3 Snakeboard

The snakeboard, a variant of the skateboard, is a nonholonomic system of great theoretical interest. It is a complex system due to its underactuation, drift, nonholonomic constraints, and symmetries. Its snake-like locomotion results from angular momentum generated by motions of the rider. It is studied as nonholonomic dynamic system with torques as inputs and serves as benchmark system for path planning for nonholonomic systems. For this system, controllability is addressed in [21, 22, 62], motion planning in [21, 22, 63], and optimal control in [48, 54, 87].

Figure 3.3 shows the snakeboard consisting of two pairs of wheels, called front and rear wheels, the coupler connecting the pairs of wheels, and the rotor. The front and rear wheels can rotate about vertical axes through their pivotal points, controlled by foot movements of the rider. The rider generates motion by twisting his torso and turning the wheels appropriately. This way, a snake-like locomotion is generated without the rider touching the ground. The motion of the human torso is simulated by the rotation of the rotor about a vertical axis through the center of mass of the snakeboard. The rotor acts as a momentum wheel. Spinning this momentum wheel causes a counter torque which acts on the coupler and wheels. If the wheels are turned simultaneously with proper phase to the rotor, a combined translational and rotational motion arises. This motion comes from the conservation of angular momentum about the instantaneous center of rotation. Depending on the phase between rotor and wheels, different motions result which propel the snakeboard in forward, lateral, or rotational direction.

For modeling, each pair of wheels is considered as one wheel. The rotation of the wheels around their rotation axes is neglected. Relative to a fixed reference frame, $(x, y)$ are the coordinates of the center of mass. The angle $\theta$ gives the orientation of the snakeboard with respect to the $x$-axis. The steering angles of the front and rear wheel are $\varphi$ and $-\varphi$ for $|\varphi| < \frac{\pi}{2}$. The rotation angle of the rotor around the center of mass is given by $\psi$ relative to the longitudinal axis. The configuration is $q = (\theta, x, y, \varphi, \psi)$ and the configuration space $Q = SE(2) \times (-\pi/2, \pi/2) \times SO(2)$. The distance between the center of mass and the front and rear wheels is $L > 0$. As discussed in [22, 87], configurations with $\varphi = \pm\frac{\pi}{2}$ are omitted from the analysis, as the matrix $A(q)$ of the nonholonomic constraint drops rank there.

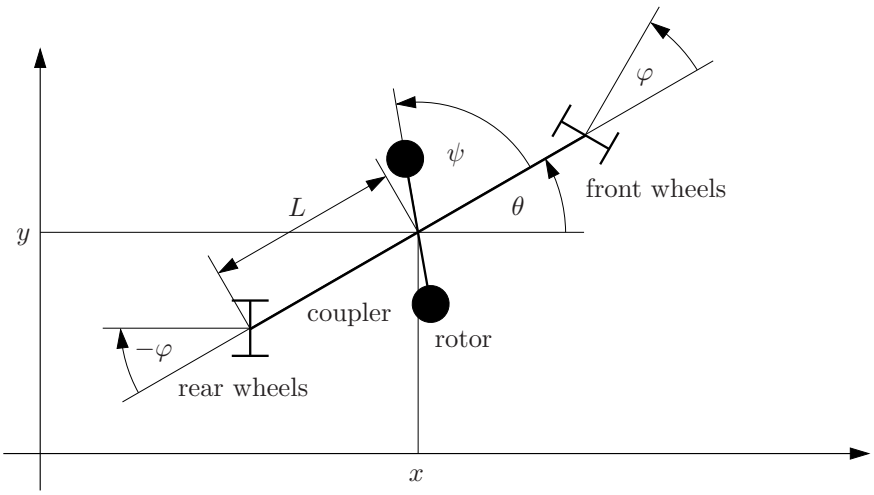


Figure 3.3: Model of the snakeboard.

The constraint resulting from the assumption that the wheels do not slide laterally is

$$\underbrace{\begin{bmatrix} -L\cos(\varphi) & \sin(\theta+\varphi) & -\cos(\theta+\varphi) & 0 & 0 \\ L\cos(\varphi) & \sin(\theta-\varphi) & -\cos(\theta-\varphi) & 0 & 0 \end{bmatrix}}_{A(q)} \begin{bmatrix} \dot{\theta} \\ \dot{x} \\ \dot{y} \\ \dot{\varphi} \\ \dot{\psi} \end{bmatrix} = \begin{bmatrix} 0 \\ 0 \end{bmatrix}. \tag{3.17}$$

This constraint can be derived from the constraint of the BSR, which is discussed Section 5.2.3. The velocity constraint (3.17) is completely nonholonomic, which can be shown the same way as it is done for the BSR in Section 5.3.2.

For the snakeboard, no nonholonomic kinematic system like for the unicycle and the car-like robot is given here, as the snakeboard is studied as nonholonomic dynamic system, i. e., a second-order control system with torques as inputs. Such a system can be represented as affine control system

$$\begin{aligned} \dot{q} &= G(q)\, v, \\ \dot{v} &= -\tilde{M}(q)\, G^{\top}(q) \Big( M(q) \sum_{i=1}^{m} \big( \mathrm{d}g_i\, G(q)\, v\, e_i^{\top} \big) + C(q, G(q)\, v)\, G(q) \Big) v + \tilde{M}(q)\, G^{\top}(q)\, B(q)\, u. \end{aligned} \tag{3.18}$$

The state $(q, v)$ of the system includes the configuration $q \in Q$ and the vector of velocities $v$, which is denoted by $u$ in Section 3.3.1. The input variables $u_i$ in (3.18) have the physical meaning of forces and torques. The $p \times m$ matrix $G(q) = [g_1(q), \ldots, g_m(q)]$ consists of the input vector fields of the nonholonomic kinematic system, meaning that if $A(q)\, \dot{q} = 0$ is the nonholonomic constraint of the system, $A(q)\, g_i(q) = 0$ holds for all $q \in Q$ and all vector fields $g_i$. The vector $e_i$ is the $i$-th standard basis vector of $\mathbb{R}^m$, i. e., the vector $e_i = (e_{i1}, \ldots, e_{im})$ with $e_{ii} = 1$ and $e_{ij} = 0$ for $i \neq j$. The row vector $e_i^{\top}$ is used to represent $\dot{G}(q)$ as addressed below. The $p \times m$ matrix $B(q)$ is the input matrix. The inertia matrix $M(q)$ is a symmetric positive definite $p \times p$ matrix. From $G(q)$ and $M(q)$, the matrix $\tilde{M}(q) = \big[ G^{\top}(q)\, M(q)\, G(q) \big]^{-1}$ results. The elements of the $p \times p$ matrix of the Coriolis forces $C(q, G(q)\, v) = C(q, \dot{q})$ are

$$c_{ij}(q, \dot{q}) = \frac{1}{2} \sum_{k=1}^{p} \left( \frac{\partial m_{ij}(q)}{\partial q_k} + \frac{\partial m_{ik}(q)}{\partial q_j} - \frac{\partial m_{kj}(q)}{\partial q_i} \right) \dot{q}_k.$$

System (3.18) consists of two subsystems, the kinematic subsystem for $\dot{q}$ and the dynamic subsystem for $\dot{v}$. The kinematic subsystem corresponds to the nonholonomic kinematic system except that the velocities $v_i$ of (3.18) are state variables and no input variables. Thus, the velocities $\dot{q} = G(q)\, v$ satisfy the nonholonomic constraint $A(q)\, \dot{q} = 0$ for all $v \in \mathbb{R}^m$. Both subsystems together specify the dynamics of a nonholonomic system. That is, they describe how the state $(q, v)$ evolves over time driven by the input $u$ and subject to the nonholonomic constraints and dynamic effects represented by the drift vector field. System (3.18) can be derived from the equations of motion of a nonholonomic mechanical system which are

$$\begin{aligned} M(q)\, \ddot{q} + C(q, \dot{q})\, \dot{q} &= A^{\top}(q)\, \lambda + B(q)\, u, \\ A(q)\, \dot{q} &= 0. \end{aligned} \tag{3.19}$$

The first equation comes from the Lagrange-d'Alembert equations, a generalization of the Euler-Lagrange equations to systems with constraints and the kinetic energy Lagrangian $L = \frac{1}{2} \dot{q}^{\top} M(q)\, \dot{q}$. The second equation $A(q)\, \dot{q} = 0$ is the nonholonomic constraint. The $k$ unknown time-varying constraint forces $\lambda$ act as Lagrange multiplier which takes values so that the motions of the system satisfy the constraint. The Lagrange-d'Alembert equations are based on the Lagrange-d'Alembert principle, see [12, 79, 80]. According to this principle, the constraint

forces $\lambda$ do no virtual work. System (3.18) is obtained from (3.19) by elimination of the unknown constraint forces $\lambda$, substitution of $\ddot{q}$ by

$$\ddot{q} = \frac{\mathrm{d}}{\mathrm{d}t}\dot{q} = \frac{\mathrm{d}}{\mathrm{d}t}\left(G(q)\,v\right) = \dot{G}(q)\,v + G(q)\,\dot{v} = \sum_{i=1}^{m}\left(\mathrm{d}g_i\,G(q)\,v\,e_i^{\top}\right)v + G(q)\,\dot{v},$$

and solving for $\dot{v}$. System (3.19) is a second-order system, as the acceleration $\ddot{q}$ of the system appears. Likewise, (3.18) is a second-order system, as $\dot{v}$ is the time derivative of the velocity $v$ and thus an acceleration as well. The systems (3.18) and (3.19) are discussed in [12, 35, 80].

The nonholonomic dynamic system of the snakeboard results from (3.18) for $A(q)$ as in (3.17) and the inertia and input matrices

$$M = \begin{bmatrix} J + J_r + 2\,J_w & 0 & 0 & 0 & J_r \\ 0 & m & 0 & 0 & 0 \\ 0 & 0 & m & 0 & 0 \\ 0 & 0 & 0 & 2\,J_w & 0 \\ J_r & 0 & 0 & 0 & J_r \end{bmatrix}, \quad B(q) = \begin{bmatrix} 0 & 0 \\ 0 & 0 \\ 0 & 0 \\ 1 & 0 \\ 0 & 1 \end{bmatrix}.$$

Here, $m$ is the mass of the snakeboard, $J$ is the inertia of the coupler and the two wheels around the center of mass, $J_r$ is the inertia of the rotor around the center of mass, and $J_w$ is the inertia of each wheel around its pivotal point. The total mass and the inertias are positive, resulting in a positive definite matrix $M$. As $M$ is constant, $C(q, \dot{q}) = 0$ holds for the matrix of the Coriolis forces. The inputs $u = (u_\varphi, u_\psi)$ are torques which set the steering angle of the front and rear wheels and actuate the rotor. The nonholonomic dynamic system (3.18) of the snakeboard can be found e. g. in [21, 22, 62]. It is not given here, as the equations are very long. In this thesis, the snakeboard serves as example of a system modeled as nonholonomic dynamic system. Results on optimal control of the snakeboard are reviewed with respect to applicability to the BSR in Section 5.1. In Section 5.2.3, the nonholonomic constraint of the snakeboard and its singular configurations at $\varphi = \pm\frac{\pi}{2}$ are compared to those of the BSR.

## 3.5 Open-loop control of nonholonomic systems

This section gives an overview of methods for open-loop control of nonholonomic kinematic and dynamic systems which solve the control problem 2.2.1. For this, a steering law $u\colon I \mapsto U$ over a compact time interval $I = [0, T]$ is used. This problem is called steering problem or trajectory planning problem. In robotics, it is frequently called motion planning problem, and, in particular for kinematic systems like system 3.3.2, path planning problem, as for kinematic systems with the state being the configuration $q$, a solution $q(\cdot)$ from $q_0$ to $q_d$ over the interval $I$ is called a path. Some of the described steering methods are specific to nonholonomic systems, while others are general trajectory planning methods. For further examples and details on steering methods for nonholonomic systems, see [22, 35, 59, 60, 80, 98].

For nonholonomic kinematic systems transformable to chain form, path planning can be done based on finite parameterizations of the inputs, as the chain form allows to successively integrate the equations of the transformed system due to its triangular structure. Using the integrated system, the parameters for a specific input which steers the transformed system from $q_0$ to $q_d$ over a fixed interval $I$ can be computed analytically. Then, the corresponding input for the original system is derived from the input for the transformed system. There are different types of parameterizable inputs for nonholonomic kinematic systems in chain form. In [23, 35, 59, 60, 80, 81], sinusoidal inputs with integrally related frequencies are addressed. Piecewise constant inputs inspired by multi-rate digital control which result in piecewise linear systems are discussed in [35, 80, 98, 122]. For polynomial inputs which expand the features of piecewise constant inputs by additional differentiability properties, see [23, 35, 59].

A path planning method for nonholonomic kinematic systems $\dot{q} = g_1(q)\,u_1 + \cdots + g_m(q)\,u_m$ using an extended system is described in [57, 59, 60, 80]. Piecewise constant inputs generate motions in the direction of iterated Lie brackets of the input vector fields $g_1, \ldots, g_m$. These Lie brackets give new fictitious input vector fields. The extended system

$$\dot{q} = g_1(q)\,u_1 + \cdots + g_m(q)\,u_m + g_{m+1}(q)\,u_{m+1} + \cdots + g_r(q)\,u_r$$

is considered. It has additional input vector fields $g_{m+1}, \ldots, g_r$ obtained from iterated Lie brackets and additional input variables $u_{m+1}, \ldots, u_r$. Path planning is performed for the extended system, which is straightforward if enough input vector fields are added. Based on a path for the extended system from an initial configuration $q_0$ to a desired configuration $q_d$, a path of the original system from $q_0$ to $q_d$ is determined. If the original system is nilpotent, i. e., if there is a maximal degree $\hat{d}$ such that all iterated Lie brackets of the input vector fields of degree $d > \hat{d}$ vanish, the method allows exact steering from any $q_0$ to any $q_d$, as every path planned for the extended system can be realized exactly by the original system. For systems which are not nilpotent, the method can be applied iteratively to move arbitrarily close to $q_d$.

For the implementation to real-world nonholonomic systems and for constructive controllability analysis, it is desirable to obtain solutions with a simple structure. Such solutions can be constructed from a finite set of motion primitives. Motion primitives addressed in [41, 60] are segments of solutions which are generated e. g. by constant inputs. Solutions from an initial to a desired state result from suitable sequences of motion primitives which are applied over appropriate durations. The straight line segments and arcs of circles discussed in Section 1.1 are motion primitives for the car-like robot. In [48], motion planning is performed for the snakeboard, and solutions with minimal number of motion primitives are determined.

A general steering method for nonholonomic kinematic and dynamic systems is based on averaging theory and oscillatory inputs, i. e., high-amplitude, high-frequency or small-amplitude, low-frequency periodic inputs. Oscillatory inputs generate motions in the direction of iterated Lie brackets of the input vector fields $g_1, \ldots, g_m$. These motions facilitate exact steering of the averaged system and approximate steering of the original system. For details on averaging and oscillatory inputs, see [12, 20, 22].

Another method for steering of nonholonomic systems is flatness based control arising from the property of differential flatness originally given in [39]. A system is differentially flat if there is a fictitious flat output $z = \Phi\big(x, u, \dot{u}, \ldots, \overset{(\alpha)}{u}\big)$, $\dim z = \dim u$, which depends on the state $x$, the input $u$, and a finite number $\alpha$ of time derivatives of $u$. If there is a flat output $z$, then $x$ and $u$ can be expressed in terms of $z$ and a finite number of its time derivatives, i. e., $x = \Theta\big(z, \dot{z}, \ldots, \overset{(\beta)}{z}\big)$ and $u = \Psi\big(z, \dot{z}, \ldots, \overset{(\beta+1)}{z}\big)$ holds for finite $\beta$, and the resultant $x$ and $u$ are unique. A flat output may be locally or globally defined. If such an output $z$ can be determined, path planning reduces to the problem to find a sufficiently often differentiable trajectory $z(\cdot)$ satisfying conditions imposed by the initial and desired state and input constraints. The input trajectory $u(\cdot)$ required to steer a system from an initial state $x_0$ to a desired state $x_d$ can be computed directly from the trajectory $z(\cdot)$. There is a close connection between the transformability to chain form and the existence of a flat output. For details on flatness based control and its application to nonholonomic systems, see [40, 44, 59, 64, 67, 96, 101].

A fundamental approach to generate inputs for nonholonomic systems is optimal control. Different cost functions are considered. For nonholonomic kinematic systems, shortest paths and time-optimal solutions are studied most often, which are equivalent for specific systems, see [108, 120, 124]. Shortest paths of the kinematic system of the car-like robot are covered in [37, 94, 108, 120]. For additional references, see [2, 6, 13, 49, 106, 124]. For the kinematic system of the differential drive mentioned in Section 3.4, time-optimal control is addressed in [9, 10, 60, 106]. The related problem of steering with minimal wheel rotation is discussed in [27, 60]. For nonholonomic dynamic systems, solutions with minimal control energy are mostly studied. This is done for the snakeboard in [87]. Optimal control problems for nonholonomic systems can be solved by direct and indirect methods described in Section 2.3. For more results on optimal control of nonholonomic systems, see [12, 60, 80, 98].

# 4 Optimality conditions for time-optimal control problems

This chapter addresses optimality conditions to characterize solutions to time-optimal control problems. Optimality conditions comprise necessary and sufficient conditions. Necessary optimality conditions specify candidates for optimal solutions. Such conditions are addressed in Section 4.2 and 4.5. In contrast, sufficient optimality conditions discussed in Section 4.6 guarantee that solutions are optimal. For additional information on necessary and sufficient optimality conditions, see [2, 15, 26, 43, 75, 104, 106].

Regarding necessary optimality conditions, the most basic result of optimal control theory is the Maximum Principle introduced in 1962 by L. S. Pontryagin and his co-workers in the landmark book [93]. According to [116], the Maximum Principle is a generalization of the Euler-Lagrange equations, the Legendre condition, and the Weierstrass condition from the classical calculus of variations. It gives necessary optimality conditions for solutions which minimize a specific cost function subject to initial and final conditions, constraints obtained from the differential equations of the control system, and maybe additional constraints on the state and input. For this, the Maximum Principle makes use of the adjoint state which acts as Lagrange multiplier. Trajectories satisfying the necessary conditions of the Maximum Principle are called extremals. They are a superset of the optimal solutions. The Maximum Principle gives first-order optimality conditions. For optimal motion planning, it reduces the problem to find input trajectories $u(\cdot)$ in the infinite space of bounded measurable input functions to the finite dimensional problem to find initial conditions of the adjoint state. The Maximum Principle for time-optimal control problems with free end time and with fixed end time is stated in Section 4.2. Besides [93], for literature on the Maximum Principle in the context of classical control theory, see [26, 43, 104], and in the context of geometric control theory, see [2, 15, 22, 49, 117].

## 4.1 Existence of time-optimal solutions

If candidates for time-optimal solutions from an initial state $x_0$ to a desired state $x_d$ should be characterized by the necessary optimality conditions of the Maximum Principle, it makes sense to verify that such solutions exist at all. Otherwise, there may be trajectories which satisfy the necessary optimality conditions, but cannot give time-optimal or any other solutions from $x_0$ to $x_d$, rendering the information from the optimality conditions useless. At first, the existence of solutions depends on the controllability 3.1.15 of the control system. Only if a system is controllable, i. e., if there is a solution from $x_0$ to $x_d$, a time-optimal solution from $x_0$ to $x_d$ can exist. Besides, for the existence of optimal solutions, conditions on the boundedness and convexity of $f(x, u)$ for all $(x, u) \in M \times U$ have to be satisfied.

**Theorem 4.1.1** *(Filippov Existence Theorem) Let $\dot{x} = f(x, u)$ be a control system 2.1.2 with compact input space $U$. Time-optimal solutions exist if the control system is controllable, $f(x, u)$ satisfies the linear growth condition $\|f(x, u)\| \leq c\,(1 + \|x\|)$ for some constant $c > 0$ and all $(x, u) \in M \times U$, and the velocity sets $F_U(x) := \{f(x, u) \mid u \in U\}$ are convex for all $x \in M$.*

Theorem 4.1.1 is the standard existence theorem for time-optimal control. For details, see [2, 15, 26, 43]. Without additional assumptions, the linear growth condition rules out the existence of time-optimal solutions for most systems with unbounded inputs. For such systems, time-optimal solutions in general do not exist. By the principle of time-optimal evolution given

in [106], the state $x(T)$ of an optimal trajectory has to lie on the boundary bd $R_T(x_0)$ of the reachable set $R_T(x_0)$ for each $T > 0$. For unbounded inputs, bd $R_T(x_0)$ may be empty.

Under additional assumptions, the convexity condition on $F_U(x)$ can be replaced by less restrictive conditions. For systems satisfying the linear growth condition but not the convexity condition, the existence of time-optimal solutions can be shown by the following corollary.

**Corollary 4.1.2** *(Existence for systems with non-convex velocity sets) Let $\dot{x} = f(x,u)$ be a control system with compact input space $U$ which satisfies the conditions of Theorem 4.1.1 except for the convexity of the velocity sets $F_U(x)$. If the velocity sets $F_{\widehat{U}}(x) = \{f(x,u) \mid u \in \widehat{U}\}$ obtained for a modified input space $\widehat{U} \supset U$ are convex, and if the optimal inputs of the control system with input space $\widehat{U}$ lie in the original input space $U$ for almost all $t$, time-optimal solutions exist for the control system with input space $U$.*

Corollary 4.1.2 is discussed in [120], where it is applied to the model (3.16) of the car-like robot with compact non-convex input space $U_{RS} = [-1,1] \times \{-1,1\}$. The modified input space $\widehat{U}_{RS} = \operatorname{conv}(U_{RS}) = [-1,1] \times [-1,1]$ is used to prove the existence of shortest paths, as it is done in [13, 106, 108, 124]. In [15], the existence of optimal solutions is shown for nonholonomic kinematic systems with $U = \{u \in \mathbb{R}^m \mid \|u\|^2 = 1\}$ by considering $\widehat{U} = \{u \in \mathbb{R}^m \mid \|u\|^2 \leq 1\}$. More results on the existence for systems with non-convex velocity sets are given in [26] using generalized solutions and in [2] based on relaxed systems, for which $\operatorname{conv}(F_U(x))$ is studied.

## 4.2 The Maximum Principle for time-optimal control problems

This section gives the necessary optimality conditions of the Maximum Principle for the time-optimal control problems 2.2.3 and 2.2.4. To formulate these conditions, the Hamiltonian function is introduced first.

### 4.2.1 Hamiltonian function

To define the Hamiltonian function for an optimal control problem, the adjoint state $\lambda$ is used, which is also called adjoint vector, costate, or covector. For a control system $\dot{x} = f(x,u)$ with state space $M$ which is an open subset of $\mathbb{R}^n$, the adjoint state is a vector $\lambda = (\lambda_1, \ldots, \lambda_n) \in \mathbb{R}^n$. Its elements $\lambda_i$ are called adjoint variables. According to the Maximum Principle for the time-optimal control problem given below, there is an absolutely continuous trajectory $\lambda\colon I \to \mathbb{R}^n$, $t \mapsto \lambda(t)$ which satisfies an ordinary differential equation, the adjoint equation (4.2), for almost all $t \in I$. The initial condition $\lambda(0)$ of the adjoint state is denoted by $\lambda_0$.

As discussed in Section 2.1, for $M$ being an open subset of $\mathbb{R}^n$, the tangent space $T_xM$ can be identified with $\mathbb{R}^n$ at each $x \in M$. Thus, $f(x,u) \in \mathbb{R}^n$ holds, and the scalar product $\lambda^\top f(x,u)$ gives a real number. This way, the adjoint state $\lambda$ acts as Lagrange multiplier to include the right-hand side $f(x,u)$ of the control system into the Hamiltonian function defined next.

**Definition 4.2.1** *(Hamiltonian function) Let $\dot{x} = f(x,u)$ be a control system 2.1.2 with state space $M$, $\lambda \in \mathbb{R}^n$ the adjoint state, and $\mu \in \{0,1\}$ a constant. The function $H\colon M \times \{0,1\} \times \mathbb{R}^n \times U \to \mathbb{R}, (x,\mu,\lambda,u) \mapsto H(x,\mu,\lambda,u)$,*

$$H(x,\mu,\lambda,u) := -\mu + \lambda^\top f(x,u) \tag{4.1}$$

*is called Hamiltonian function of the time-optimal control problem.*

The scalar Lagrange multiplier $\mu$ is called abnormal multiplier or cost function multiplier. It incorporates the Lagrangian $L$ which defines the running cost of the solution into the Hamiltonian function. For a general Lagrangian, the Hamiltonian function is

$$H(x,\mu,\lambda,u) = -\mu\, L(x,u) + \lambda^\top f(x,u)\,.$$

For time-optimal control, $L(x,u) = 1$ holds, and the Hamiltonian function (4.1) results. According to [26, 104], it is sufficient to consider $\mu \in \{0,1\}$ for the abnormal multiplier instead of all values $\mu \geq 0$.

### 4.2.2 Necessary optimality conditions

In the following, necessary optimality conditions for the time-optimal control problems 2.2.3 and 2.2.4 are given. Trajectories of the state $x$, the adjoint state $\lambda$, and the input $u$ which satisfy these conditions are called extremals. They are denoted by $x^*(\cdot)$, $\lambda^*(\cdot)$, and $u^*(\cdot)$.

**Theorem 4.2.2** *(Maximum Principle for the time-optimal control problem with free end time) A time-optimal control problem 2.2.3 for a control system with compact input space $U$ is considered. Let $\lambda \in \mathbb{R}^n$ be the adjoint state, $H$ the Hamiltonian function 4.2.1, $(x^*(\cdot)\,,\,\lambda^*(\cdot)\,,\,u^*(\cdot))$ an extremal, and $H^*(\cdot) := H(x^*(\cdot)\,,\mu,\lambda^*(\cdot)\,,u^*(\cdot))$ the extremal Hamiltonian function over the time interval $I = [0,T]$. Then, the following conditions hold:*

**N1:** *For all $t \in I$, $(\mu, \lambda^*(t)) \neq 0$ is true.*

**N2:** *For almost all $t \in I$, there holds the adjoint equation*

$$\dot{\lambda}^* = -\frac{\partial H}{\partial x^*}(x^*, \mu, \lambda^*, u^*)\,. \tag{4.2}$$

**N3:** *For almost all $t \in I$, $u^*$ satisfies*

$$H(x^*, \mu, \lambda^*, u^*) = \max_{u \in U} H(x^*, \mu, \lambda^*, u)\,. \tag{4.3}$$

**N4:** *For almost all $t \in I$, $H^*(t) = 0$ holds.*

In Theorem 4.2.2, the nontriviality condition N1 requires that the vector consisting of the Lagrange multiplier $\mu$ and the extremal adjoint state $\lambda^*$ does not vanish for any $t \in I$. The adjoint equation of condition N2 is a differential equation for the extremal adjoint state $\lambda^*$. Starting from an initial condition $\lambda(0) = \lambda_0$, the trajectory $\lambda^*(\cdot)$ is determined by this differential equation. According to the maximization condition N3, the extremal input $u^*$ solves the maximization problem (4.3) over the compact input space $U$ almost everywhere in $I$. For control systems and Lagrangians which are autonomous, the extremal Hamiltonian function $H^*$ is constant. Besides, $H^*(T) = 0$ is obtained from the transversality condition of the Maximum Principle for free end time problems. The resultant null-maximizing condition N4 is characteristic for free time problems. For general fixed end time problems, a constant extremal Hamiltonian function unequal to zero results. For proofs of the Maximum Principle 4.2.2, see [2, 15, 22, 26, 93].

In Section 2.2, the transformed time-optimal control problem 2.2.4 with fixed end time was defined. This problem arises from the time-optimal control problem 2.2.3 with free end time by the time transformation $s = \frac{1}{\tau}\,t$ for constant $\tau > 0$ which corresponds to the unknown end time of problem 2.2.3. For the transformed problem, solutions $\big(\check{X}^{to}(\cdot), \check{u}^{to}(\cdot)\big)$ of the extended control system $\check{X}' = \check{f}\big(\check{X}, \check{u}\big)$ as in (2.4) are considered over the time interval $\check{I} = [0,1]$. Using the additional state variable $z$ with $z' = \mathrm{d}z/\mathrm{d}s = 0$ and $z(0) = \tau$ to represent $\tau$, the extended state $\check{X} = (\check{x}, z)$ of dimension $\check{n} = n + 1$ results. Besides, $\check{x}(s) := x\big(\tau\, s\big) = x(t)$ and $\check{u}(s) := u\big(\tau\, s\big) = u(t)$ applies. To give the necessary optimality conditions of the Maximum Principle for the transformed problem, the extended adjoint state $\check{\Lambda} = \big(\check{\lambda}, \check{\lambda}_{\check{n}}\big) \in \mathbb{R}^{\check{n}}$ is used. It results from the extension of $\check{\lambda}$ by the adjoint state variable $\check{\lambda}_{\check{n}}$ related to $z$. Here, $\check{\lambda}(s) := \lambda\big(\tau\, s\big) = \lambda(t)$ applies. For the extended adjoint state $\check{\Lambda}$, the Lagrangian $\check{L}\big(\check{X}, \check{u}\big) = z$, and the extended control system $\check{X}' = \check{f}\big(\check{X}, \check{u}\big)$, the Hamiltonian function is

$$\check{H}\big(\check{X}, \mu, \check{\Lambda}, \check{u}\big) = -\mu\, z + \check{\Lambda}^{\top} \check{f}\big(\check{X}, \check{u}\big). \tag{4.4}$$

**Theorem 4.2.3** *(Maximum Principle for the transformed time-optimal control problem with fixed end time) A transformed time-optimal control problem 2.2.4 for an extended control system with compact input space $U$ in considered. Let $\check{\Lambda} = \left(\check{\lambda}, \check{\lambda}_{\check{n}}\right) \in \mathbb{R}^{\check{n}}$ be the extended adjoint state, $\check{H}$ the Hamiltonian function (4.4), $\left(\check{X}^*(\cdot), \check{\Lambda}^*(\cdot), \check{u}^*(\cdot)\right)$ an extremal, and $\check{H}^*(\cdot) := \check{H}\left(\check{X}^*(\cdot), \mu, \check{\Lambda}^*(\cdot), \check{u}^*(\cdot)\right)$ the extremal Hamiltonian function over the time interval $\check{I} = [0,1]$. Then, the following conditions hold:*

**N1′:** *For all $s \in \check{I}$, $\left(\mu, \check{\Lambda}^*(s)\right) \neq 0$ is true.*

**N2′:** *For almost all $s \in \check{I}$, there holds the adjoint equation*

$$\check{\Lambda}'^* = -\frac{\partial \check{H}}{\partial \check{X}^*}\left(\check{X}^*, \mu, \check{\Lambda}^*, \check{u}^*\right).$$

**N3′:** *For almost all $s \in \check{I}$, $\check{u}^*$ satisfies*

$$\check{H}\left(\check{X}^*, \mu, \check{\Lambda}^*, \check{u}^*\right) = \max_{\check{u} \in U} \check{H}\left(\check{X}^*, \mu, \check{\Lambda}^*, \check{u}\right).$$

**N4′:** *For almost all $s \in \check{I}$, $\check{H}^*(s) = 0$ holds.*

**N5′:** *There holds $\check{\lambda}_{\check{n}}(0) = \check{\lambda}_{\check{n}}(1) = 0$.*

The conditions N1′ to N4′ correspond to the conditions N1 to N4 of Theorem 4.2.2. Condition N5′ comes from the transversality conditions of the Pontryagin Maximum Principle adapted to problem 2.2.4. The transversality conditions are relevant if the initial state $x_0$ and desired state $x_d$ of a solution over an interval $I = [0, \tau]$ are not fixed, but $x(0) \in M_0$ and $x(\tau) \in M_d$ has to hold for given subsets $M_0$ and $M_d$ of $M$. Then, the transversality conditions are $\lambda^*(0) \perp T_{x^*(0)} M_0$ and $\lambda^*(\tau) \perp T_{x^*(\tau)} M_d$. At time 0, the extremal adjoint state $\lambda^*(0)$ has to be orthogonal to the tangent space to $M_0$ at the resultant state $x^*(0)$, and at time $\tau$, $x^*(\tau)$ has to be orthogonal to the tangent space to $M_d$ at $x^*(\tau)$. For the transformed problem with state space $\check{M} = M \times \mathbb{R}_{>0}$, the corresponding subsets $\check{M}_0$ and $\check{M}_d$ of $\check{M}$ are

$$\check{M}_0 = \left\{(x,z) \in \check{M} \mid x = x_0, z > 0\right\}, \quad \check{M}_d = \left\{(x,z) \in \check{M} \mid x = x_d, z > 0\right\}.$$

Thus, $x$ is fixed, but $z$ is not specified. Hence, at time 0 and $\tau = 1$, the transversality conditions give $\check{\lambda}_{\check{n}}(0) = \check{\lambda}_{\check{n}}(1) = 0$. For details on transversality conditions, see [2, 15, 26, 93].

For the Hamiltonian functions $\check{H}$ and $H$ given by (4.4) and (4.1), the extended state $\check{X} = (\check{x}, z)$, and the extended adjoint state $\check{\Lambda} = \left(\check{\lambda}, \check{\lambda}_{\check{n}}\right)$,

$$\check{H}\left(\check{X}, \mu, \check{\Lambda}, \check{u}\right) = z\, H\left(\check{x}, \mu, \check{\lambda}, \check{u}\right) \tag{4.5}$$

holds. From condition N2′, $\check{\lambda}'^*_{\check{n}} = -\frac{1}{z^*} H^*$ is obtained. Using condition N4′, $\check{\lambda}'^*_{\check{n}} = 0$ results, and $\check{\lambda}_{\check{n}}(s) = 0$ is true for all $s \in \check{I}$ due to condition N5′. Since $\check{H}$ as in (4.4) does not depend on $\check{\lambda}_{\check{n}}$ due to $z' = 0$, the adjoint variable $\check{\lambda}_{\check{n}}$ is not relevant for the control problem. Just like for free end time problems, the extremal Hamiltonian function $\check{H}^*$ is equal to zero.

### 4.2.3 Discussion of the Maximum Principle

The Maximum Principle in Theorem 4.2.2 and 4.2.3 gives necessary optimality conditions for time-optimal control problems with free and fixed end time. The resulting extremals, which are candidates for time-optimal solutions, are discussed in Section 4.3. In Section 4.4, boundary value problems are formulated which have to be solved to find solutions from $x_0$ to $x_d$ based on the extremals. Moreover, the Maximum Principle is the basis for several optimality conditions in Section 4.5 and 4.6. If the conditions of the Maximum Principle are completed by additional conditions as in Section 4.6.1 and 4.6.4, sufficient optimality conditions are obtained.

As discussed in [106, 108, 124], for optimal control of nonholonomic systems, the conditions of the Maximum Principle have to be complemented by global conditions like geometric arguments to find optimal solutions. This is the case as the Maximum Principle is a purely local principle based on the comparison of solutions from infinitesimal perturbations of the input trajectory. Thus, the conditions are inherently local. For control problems with fixed end time $\tau$, the extremals $(x^*(\cdot), u^*(\cdot))$ from the Maximum Principle are optimal among all admissible solutions $(x(\cdot), u(\cdot))$ satisfying

$$\|x^* - x\|_\infty^{[0,\tau]} < \varepsilon, \quad \int_0^\tau \|u^*(t) - u(t)\|_1 \, \mathrm{d}t < \varepsilon$$

for some $\varepsilon > 0$. This local optimality called Pontryagin optimality is addressed in [85, 89]. It is similar to weak local optimality 2.2.6, since both types of local optimality take the trajectories of $x$ and $u$ into account. However, for weak local optimality, the input trajectory has to lie in an $\varepsilon$-neighborhood with respect to the infinity norm, whereas for Pontryagin optimality, the $L_1$-norm of the input is considered.

## 4.3 Extremals

In the following, properties of extremals $(x^*(\cdot), \lambda^*(\cdot), u^*(\cdot))$ obtained from the Maximum Principle 4.2.2 for the time-optimal control problem with free end time are discussed. All properties also apply to extremals $\left(\check{X}^*(\cdot), \check{\Lambda}^*(\cdot), \check{u}^*(\cdot)\right)$ from the Maximum Principle 4.2.3 for the transformed time-optimal control problem with fixed end time.

**Definition 4.3.1** *(Extremal) Any triple $(x^*(\cdot), \lambda^*(\cdot), u^*(\cdot))$ satisfying the necessary optimality conditions of the Maximum Principle 4.2.2 is called extremal.*

The trajectories $x^*(\cdot)$, $\lambda^*(\cdot)$, and $u^*(\cdot)$ are the extremal state, extremal adjoint state, and extremal input. The Hamiltonian function $H^*(\cdot) = H(x^*(\cdot), \mu, \lambda^*(\cdot), u^*(\cdot))$ is the extremal Hamiltonian function. Extremals are candidates for solutions to the time-optimal control problem 2.2.3. If $x^*(\tau) = x_d$ holds for some $\tau$, the solution has not to be optimal, as $\tau > \tau^{to}$ can be true. Thus, time-optimal solutions are a subset of the extremals.

**Definition 4.3.2** *(Normal extremal, abnormal extremal) Any extremal 4.3.1 satisfying the necessary optimality conditions of the Maximum Principle for $\mu = 1$ is called normal extremal. Any extremal satisfying the necessary optimality conditions for $\mu = 0$ is called abnormal extremal.*

If an extremal is abnormal, the Lagrangian $L$ does not affect the Hamiltonian function due to $\mu = 0$. Thus, the cost function $J(\tau, x, u) = \int_0^\tau L(x, u) \, \mathrm{d}t$ is not taken into account when candidates for solutions are determined. For most nonholonomic kinematic systems, non-constant abnormal extremals do not exist due to properties of their Lie algebras, see [117, 120].

**Definition 4.3.3** *(Regular extremal, singular extremal) Any extremal 4.3.1 for which the input $u^*(\cdot)$ is uniquely determined for almost all $t \in I$ by the maximization (4.3) of the Hamiltonian function is called regular extremal. Any extremal for which the input $u^*(\cdot)$ is not uniquely determined by this maximization over a proper time interval is called singular extremal.*

For specific classes of control systems like affine systems, singular inputs can be determined from successive time derivatives of the Hamiltonian function, see [2, 15, 56]. Besides extremals which are either regular and singular, for some optimal control problems, there are extremals which consist of regular and singular subarcs, i. e., segments where the extremal is regular and segments where it is singular.

By the null-maximizing condition N4 of the Maximum Principle 4.2.2, $-1+\lambda_0^\top f(x_0,u^*(0))=0$ holds for $\mu=1$ at time $t=0$. Then,

$$\hat{\Lambda}_{x_0} := \left\{\lambda_0 \in \mathbb{R}^n \;\middle|\; -1+\lambda_0^\top f(x_0,u^*(0))=0\right\} \tag{4.6}$$

is the set of all initial conditions $\lambda_0$ of the adjoint state for which there are normal extremals $(x^*(\cdot),\lambda^*(\cdot),u^*(\cdot))$ which satisfy the necessary optimality conditions of the Maximum Principle for $x^*(0)=x_0$ and $\lambda^*(0)=\lambda_0$. The set $\hat{\Lambda}_{x_0}$ satisfies $\dim\hat{\Lambda}_{x_0}\leq n-1$ for $\dim M=n$, see [104]. If all initial conditions $\lambda_0\in\hat{\Lambda}_{x_0}$ which result in normal singular extremals are removed from $\hat{\Lambda}_{x_0}$, the search space $\Lambda_{x_0}\subset\hat{\Lambda}_{x_0}$ is obtained, which is defined next.

**Definition 4.3.4** *(Search space) A time-optimal control problem 2.2.3 with initial state $x_0$ is considered. The set $\Lambda_{x_0}\subset\hat{\Lambda}_{x_0}$ of initial conditions $\lambda_0$ for which there are normal regular extremals $(x^*(\cdot),\lambda^*(\cdot),u^*(\cdot))$ which satisfy the necessary optimality conditions of the Maximum Principle for $x^*(0)=x_0$ and $\lambda^*(0)=\lambda_0$ is called search space.*

The set $\Lambda_{x_0}$ is called search space since for the path planning in Section 7.2, initial conditions $\lambda_0\in\Lambda_{x_0}$ are searched such that normal regular extremals $x^*(\cdot)$ result which go from $x_0$ to the desired state $x_d$. The search space depends on the initial state $x_0$ of the control problem. If no normal regular extremal exists for an initial state $x_0$, $\Lambda_{x_0}$ is empty.

**Definition 4.3.5** *(Switching function, switching time, arc duration, bang-bang input, bang-bang extremal) For an affine control system $\dot{x}=f_0(x)+\sum_{i=1}^m g_i(x)\,u_i$, the Hamiltonian function (4.1) is written as*

$$H(x,\mu,\lambda,u)=-\mu+\lambda^\top f_0(x)+\sum_{i=1}^m s_i(x,\lambda)\,u_i. \tag{4.7}$$

*The real-valued functions $s_i(x,\lambda):=\lambda^\top g_i(x)$ are called switching functions.*

*Let the switching functions have discrete sets of zeros and $n_s\in\mathbb{N}$ be finite. If $s_i(x(t_j),\lambda(t_j))=0$ holds for at least one switching function $s_i$ at time $t=t_j$, then $t_j$ is called switching time. For $n_s$ switchings taking place in the interval $I=[0,T]$ at the switching times $\{t_1,\ldots,t_{n_s}\}$ with $0\leq t_1<\cdots<t_{n_s}\leq T$, the finite partition*

$$I=I_1\cup I_2\cup\cdots\cup I_{n_s}\cup I_{n_s+1}=[0,t_1)\cup[t_1,t_2)\cup\cdots\cup[t_{n_s-1},t_{n_s})\cup[t_{n_s},T]$$

*of $I$ results. The periods $\triangle t_1=t_1$, $\triangle t_j=t_j-t_{j-1}$, $\triangle t_{n_s+1}=T-t_{n_s}$ are called arc durations.*

*To implement the maximization of the Hamiltonian function (4.7) for the symmetric input space $U=[-\hat{u}_1,\hat{u}_1]\times\cdots\times[-\hat{u}_m,\hat{u}_m]$, the extremal input variables $u_i^*$ have to satisfy*

$$u_i^*=\operatorname{sgn}(s_i^*)\,\hat{u}_i$$

*for $s_i^*(\cdot):=s_i(x^*(\cdot),\lambda^*(\cdot))$. The extremal input $u^*(\cdot)$ called bang-bang input is constant over each arc duration $\triangle t_j$ for $j=1,\ldots,n_s+1$ and satisfies $u^*(t)\in bdU$ for almost all $t\in I$. The resultant extremal called bang-bang extremal is regular.*

If an extremal switching function $s_i^*$ has a zero-crossing at the switching time $t_j$, the extremal input $u_i^*$ switches from $\pm\hat{u}_i$ to $\mp\hat{u}_i$ according to $u_i^*=\operatorname{sgn}(s_i^*)\,\hat{u}_i$. Here, sgn is the sign function. As the switching functions $s_i^*$ are assumed to have discrete sets of zeros in Definition 4.3.5, the extremal inputs are uniquely determined by $u_i^*=\operatorname{sgn}(s_i^*)\,\hat{u}_i$ for almost all $t\in I$. Thus, the bang-bang extremals are regular. Otherwise, if $s_i^*(t)=0$ holds over a proper time interval, a singular extremal is obtained, as $u_i^*$ is not defined by the maximization of the Hamiltonian function. If at a switching time $t_j$, there holds $s_i(x(t_j),\lambda(t_j))=0$ for one switching function $s_i$, then $t_j$ is called simple switching time. If $s_i(x(t_j),\lambda(t_j))=0$ holds for several switching functions, $t_j$ is called multiple switching time. In Definition 4.3.5, the number of switchings $n_s$ is finite, which is the relevant case for most optimal control problems. In general, extremals with

infinitely many switchings can occur. This situation called Fuller phenomenon was originally described in [42]. In [2, 31, 32, 88, 99, 100, 106], optimal control problems for nonholonomic and other systems are discussed which exhibit the Fuller phenomenon.

As the input $u^*(\cdot)$ is constant over each arc duration $\triangle t_j$ for a finite number of arcs, $u^*(\cdot)$ is piecewise constant over the interval $I$. Bang-bang inputs are piecewise constant inputs which take values on $\operatorname{bd} U$ for almost all $t$. Trajectories obtained from bang-bang inputs are called bang-bang solutions. Optimal bang-bang solutions can be computed by switching time optimization addressed in [30, 31, 32, 51, 71, 73]. For references to switching functions, bang-bang inputs, and bang-bang extremals, see [2, 3, 15, 26, 76, 104, 120].

For optimal control of affine control systems like the car-like robot, the study of switching functions, their time derivatives, and the switching structure equations of the coupled dynamics of the switching functions is a key step to understand the optimal control problem. For details on the analysis of optimal control problems by means of switching functions, see [28, 106, 108, 120, 124]. A bang-bang extremal for time-optimal control of the unicycle is given in Section 4.7. In Chapter 6, extremals for time-optimal control of the BSR are considered which are similar to bang-bang extremals.

## 4.4 Boundary value problems

In this section, the boundary value problems which result from the application of the Maximum Principle to the time-optimal control problems 2.2.3 and 2.2.4 are defined, and an overview of standard solvers for boundary value problems is given. Only regular extremals are considered as solutions to these problems, as the solutions should be potentially optimal and uniquely determined by the initial state, the initial condition of the adjoint state, and the interval $I$. Thus, regular extremals are applied, for which the extremal input $u^*(\cdot)$ is uniquely given by the maximization of the Hamiltonian function for almost all $t \in I$. In contrast, for singular extremals, $u^*(\cdot)$ is not uniquely determined by the maximization for almost all $t \in I$.

**Definition 4.4.1** *(Boundary value problem of the time-optimal control problem) For a time-optimal control problem 2.2.3, let $(x^*(\cdot), \lambda^*(\cdot), u^*(\cdot))$ be regular extremals which satisfy the necessary optimality conditions of the Maximum Principle 4.2.2. The problem to find an end time $\tau > 0$ and an initial condition $\lambda_0$ such that for an extremal satisfying $x^*(0) = x_0$ and $\lambda^*(0) = \lambda_0$, there holds $x^*(\tau) = x_d$ is called boundary value problem of the time-optimal control problem with free end time. Any solution $(\lambda_0, \tau)$ is called solution to the boundary value problem.*

In Definition 4.4.1, no minimal end time $\tau^{to}$ for a time-optimal solution 2.2.3 is required, but any end time $\tau$ satisfying $x^*(\tau) = x_d$. Problem 4.4.1 is a problem with free end time, as the end time $\tau$ is not specified. The value of the extremal adjoint state $\lambda^*(\tau)$ at $\tau$ is arbitrary.

**Definition 4.4.2** *(Boundary value problem of the transformed time-optimal control problem) For a transformed time-optimal control problem 2.2.4, let $\left(\check{X}^*(\cdot), \check{\Lambda}^*(\cdot), \check{u}^*(\cdot)\right)$ be regular extremals which satisfy the necessary optimality conditions of the Maximum Principle 4.2.3. The problem to find an initial condition $z(0) = \tau$ and an initial condition $\check{\lambda}_0$ such that for an extremal satisfying $\check{X}^*(0) = (x_0, \tau)$ and $\check{\Lambda}^*(0) = \left(\check{\lambda}_0, 0\right)$, there holds $\check{X}^*(1) = (x_d, \tau)$ is called boundary value problem of the transformed time-optimal control problem with fixed end time. Any solution $\left(\check{\lambda}_0, \tau\right)$ is called solution to the boundary value problem.*

For the initial condition $\check{\Lambda}^*(0) = \left(\check{\lambda}_0, \check{\lambda}_{\tilde{n}}(0)\right)$, there holds $\check{\lambda}_{\tilde{n}}(0) = 0$ due to condition N5′. Problem 4.4.2 is a problem with fixed end because of $\tau = 1$. Boundary value problems with fixed end time can be solved by standard solvers, as these solvers require a fixed time interval. In contrast, our approach for path planning in Chapter 7 directly tackles the boundary value problem with free end time. Most standard solvers for boundary value problems are based on the shooting method, the collocation method, or continuation. Compared to initial value problems, boundary value problems are harder to solve. Depending on the boundary conditions,

there may exist no solution or a finite or infinite number. The solvers discussed here need a good guess of the solution for initialization. Otherwise, they give poor results, as they cannot find solutions which are not close to the initial guess.

Shooting methods solve a boundary value problem by transforming it to an initial value problem and a root-finding problem for the shooting function which gives the deviation from the desired state at time $\tau$. The root-finding problem is usually solved by an iterative method like SQP. Starting from an initial guess of the solution $(\lambda_0, \tau)$, the values of $\lambda_0$ and $\tau$ are iteratively updated until the shooting function falls below a given tolerance. For details on shooting methods, see [6, 30, 60], and for applications to boundary value problems which result from optimal control problems, see [6, 8, 65, 72, 75, 76]. Shooting methods give poor convergence if no good initial guess is available or if the initial value problem becomes unstable.

To handle boundary value problems which give unstable initial value problems, collocation methods as discussed in [60] are applied. A frequently used implementation of a collocation method is the solver **bvp4c** provided by MATLAB. For the approximation of the solution of the boundary value problem, **bvp4c** uses cubic polynomials. To initialize the solver, an initial mesh and a guess of the solution at the mesh points are required. The mesh is adapted to obtain the specified accuracy of the solution for an almost minimal number of mesh points. For highly accurate results, many mesh points are needed, slowing down the computation. Details on **bvp4c** are given in [52]. In [47], **bvp4c** is used to solve an optimal control problem for spacecraft formations.

To facilitate the initialization of the solutions, boundary value problems can be solved by continuation. Starting from a simplified boundary value problem for which a closed-form solution exists, the boundary value problem is solved iteratively. Here, the solution of the previous run is the initialization of the next. A continuation parameter $\varepsilon \in [0, 1]$ is increased from iteration to iteration, starting from $\varepsilon = 0$. For $\varepsilon = 0$, the simplified boundary value problem with the closed-form solution arises, and for $\varepsilon = 1$, the original problem. In general, there is no guarantee that a solution to the original boundary value problem is found this way, as it may have a completely different structure than the solution to the simplified problem. Besides, the iterative approach may be computationally costly, since at each iteration, the resultant boundary value problem has to be solved. In [5], continuation is used to compute shortest paths for a wheeled mobile robot. For the simplified boundary value problem, the orientation of the robot is neglected, and the initial and desired configuration are connected by a straight line. In [47], an optimal control problem for spacecraft formations is solved by continuation.

## 4.5 Overview of further necessary optimality conditions

Besides the necessary optimality conditions of the Maximum Principle, there are other necessary optimality conditions which specify candidates for optimal solutions. The necessary conditions addressed here comprise the Legendre-Clebsch conditions in Section 4.5.1, bounds on the number of switchings in Section 4.5.2, and the theory of envelopes in Section 4.5.3. These necessary optimality conditions are applicable to time-optimal control problems with free end time. All optimality conditions of this section are used to analyze the optimality of extremals $(x^*(\cdot), \lambda^*(\cdot), u^*(\cdot))$ from the Maximum Principle. Hence, the superscript $^*$ is omitted for the extremals in the following, and $(x(\cdot), \lambda(\cdot), u(\cdot))$ is written to simplify the notation. Other necessary conditions not discussed here are higher-order Maximum Principles addressed in [15, 17, 56]. Based on the ordinary Maximum Principle which provides first-order conditions, the higher-order Maximum Principles give second- and third-order conditions.

### 4.5.1 Legendre-Clebsch conditions

For systems with compact input space $U$, the maximization condition N3 is a necessary optimality condition. In this section, systems with non-compact input space $U$ are considered, i. e., $U$ is either an open subset of $\mathbb{R}^m$ or $\mathbb{R}^m$ itself. Moreover, the Hamiltonian function $H$ is

assumed to be twice differentiable with respect to $u$. Then, the condition $H_u = \partial H/\partial u = 0$ is used instead of condition N3. The condition $H_u = 0$ is true if $u$ gives a minimum, a maximum, or a saddle point of $H$. If in addition to $H_u = 0$, the Legendre-Clebsch condition

$$H_{uu} = \frac{\partial^2 H}{\partial u^2}(x, \mu, \lambda, u) \leq 0 \tag{4.8}$$

holds, then the Hessian $H_{uu}$ is negative semidefinite and $H$ is concave in $u$. If the strict Legendre-Clebsch condition $H_{uu} < 0$ is true, then $H_{uu}$ is negative definite, $H$ is strictly concave in $u$, and $u$ gives a local maximum of $H$. The condition $H_{uu} < 0$ is a second-order necessary optimality condition for systems with non-compact input space. It is a sufficient condition for an input $u$ satisfying $H_u = 0$ to give a local maximum of $H$. However, it is no sufficient optimality condition, as $H_u = 0$ and $H_{uu} < 0$ only guarantee that the maximization condition N3 holds for systems with non-compact $U$. The strengthened Legendre-Clebsch condition

$$u^\top H_{uu} u \leq -\alpha \|u\|^2 \tag{4.9}$$

for $\alpha > 0$ is a prerequisite for the local second-order sufficient conditions in Section 4.6.2. For details on Legendre-Clebsch conditions, see [15, 26, 56, 95].

While the conditions (4.8) and (4.9) apply to systems with non-compact input space $U$, there are other conditions related to the Legendre-Clebsch conditions for systems with compact input space. In [65, 75, 86], modified Legendre-Clebsch conditions are stated for systems with compact input space $U = \{u \in \mathbb{R}^m \mid c(u) \leq 0\}$ specified by an input constraint 3.1.3. Recall that the modified input vector $w$ (3.3) consists of all input variables $u_i$ which are not affected by active input constraints, i. e., the input variables $w_i$ are those which do not lie on $\operatorname{bd} U$. The input vector $v$ contains all input variables $u_i$ which are not in $w$, i. e., which do lie on $\operatorname{bd} U$. Using $v$ and $w$, the modified Legendre-Clebsch condition is

$$H_{ww} = \frac{\partial^2 H}{\partial w^2}(x, \mu, \lambda, v, w) \leq 0. \tag{4.10}$$

The strengthened modified Legendre-Clebsch condition for $\alpha > 0$ is

$$w^\top H_{ww} w \leq -\alpha \|w\|^2 . \tag{4.11}$$

For singular extremals, generalized Legendre-Clebsch conditions are given in [2, 15, 56, 77, 95].

### 4.5.2 Bounds on the number of switchings

For bang-bang extremals 4.3.5, necessary optimality conditions for time-optimal control problems can be given based on the number of switchings $n_s$, i. e., the number the inputs change between values on $\operatorname{bd} U$. General results on upper bounds on $n_s$ exist for linear time-invariant systems and single-input affine systems of low dimension. The theory of envelopes which may also give bounds on $n_s$ is discussed separately in Section 4.5.3.

For time-optimal control of linear time-invariant systems $\dot{x} = A\,x + B\,u$ with compact convex input space $U$, bounds on $n_s$ are addressed in [2, 15, 26, 93, 104, 117]. If $A$ has only real eigenvalues, a basic result for optimal bang-bang extremals of controllable single-input systems $\dot{x} = A\,x + b\,u$ with $\dim M = n$ and symmetric input space $U = [-\hat{u}, \hat{u}]$ is that $n_s \leq n - 1$ holds.

For time-optimal control of single-input affine systems $\dot{x} = f(x) + g(x)\,u$ with symmetric input space $U$, results on bounds on $n_s$ exist for $n \in \{2, 3\}$. For the bounds to hold, the Lie algebra of the vector fields $f$ and $g$ has to satisfy specific conditions. For $n = 2$ and $C^\infty$ vector fields, bounds on $n_s$ are given in [15, 111, 117] which require additional nondegeneracy conditions. For $n = 2$ and real analytic vector fields, results can be found in [112, 113]. They do not rely on additional nondegeneracy conditions, as these conditions are satisfied for all real analytic systems. In the most basic setting, for $n = 2$, bang-bang extremals with more than one switching cannot be time-optimal. For systems $\dot{x} = f(x) + g(x)\,u$ with $C^\infty$ vector fields

and $n = 3$, bounds on $n_s$ are discussed in [17, 99, 100]. Here, time-optimal solutions have at most two switchings in the most elementary case.

Besides time-optimal control of linear time-invariant and single-input affine systems, bounds on $n_s$ exist for other specific systems. Most of these findings are derived based on closed-form solutions. In [28, 32], time-optimal solutions for underwater vehicles modeled as multi-input dynamic systems are considered and bounds on $n_s$ are stated. For paths of the snakeboard with minimal number of switchings between motion primitives, bounds on $n_s$ are provided in [48]. For paths of underactuated left-invariant systems on matrix Lie groups with minimal number of switchings between left-invariant vector fields, bounds on $n_s$ are given in [68]. For the Dubins and Reeds-Shepp paths covered in [37, 94, 108, 120], $n_s \leq 2$ and $n_s \leq 4$ holds, respectively. Besides, the number of cusps of the Reeds-Shepp paths satisfies $n_c \leq 2$.

### 4.5.3 Theory of envelopes

In [110, 115, 120], necessary optimality conditions are derived based on a generalization of the theory of envelopes from the classical calculus of variations. Among others, the necessary conditions apply to bang-bang extremals 4.3.5. To obtain the conditions, exponential notation is used to represent the flow under bang-bang inputs. For details on exponential notation, see [80, 104]. By this notation, it is possible to give end-point maps 2.1.5 of the extremals for specific systems. If such end-point maps are available, they can be differentiated with respect to the arc durations. Using the resultant differentials, envelopes are constructed, and the generalized envelope condition is applied to exclude bang-bang extremals with too many switchings.

In [110, 115], systems $\dot{x} = f(x) + g(x)\ u$ with symmetric input space $U$ are considered. Under conditions on $f$, $g$, and $[f, g]$, it is shown by the generalized envelope condition that bang-bang extremals with more than one and two switchings cannot be time-optimal for $n = 2$ and $n = 3$, respectively. In [120], the generalization of the theory of envelopes is used to prove that specific Reeds-Shepp paths of type $C|CC|C$ are not optimal. Likewise, it is shown that some Dubins paths of type $CCC$ and all paths of type $CCCC$ cannot be optimal.

## 4.6 Overview of sufficient optimality conditions

Sufficient optimality conditions guarantee that a solution is optimal. The conditions addressed here are the Arrow and Mangasarian sufficient conditions in Section 4.6.1, local second-order sufficient conditions with Riccati equation in Section 4.6.2, local second-order sufficient conditions for bang-bang extremals in Section 4.6.3, and Boltyanskii's sufficient condition in Section 4.6.4. The Arrow and Mangasarian sufficient conditions and Boltyanskii's sufficient condition lead to global optimality, whereas the other conditions give local optimality. The sufficient conditions of Section 4.6.1 and 4.6.2 are usually applied to transformed time-optimal control problems 2.2.4 with fixed end time. The other conditions are also used for time-optimal control problems 2.2.3 with free end time. Like in Section 4.5, the optimality conditions are applied only to extremals from the Maximum Principle and the superscript $^*$ is omitted. Further results of optimal control theory regarding sufficiency are based on the Hamilton Jacobi Bellman theory not discussed here. For references, see [2, 15, 26, 88, 104, 119].

### 4.6.1 Arrow and Mangasarian sufficient conditions

For the transformed time-optimal control problem 2.2.4 with fixed end time, a normal extremal $\big(\check{X}(\cdot)\,, \check{\Lambda}(\cdot)\,, \check{u}(\cdot)\big)$ is considered, i. e., an extremal which satisfies the conditions of the Maximum Principle 4.2.3 for $\mu = 1$. If the extremal Hamiltonian function $\check{H} = \check{H}\big(\check{X}, \mu, \check{\Lambda}, \check{u}\big)$ is concave in $\check{X}$ on the whole state space, the extremal is globally optimal. This condition called Arrow sufficient condition is addressed in [43, 50]. In general, concavity of the Hamiltonian function $\check{H}$ in $\check{X}$ is very restrictive and not satisfied for most control problems. An even more restrictive condition for global optimality discussed in [43, 66] is the Mangasarian sufficient condition

which requires that $\check{H}$ is concave in $\check{X}$ and $\check{u}$. If the Arrow or Mangasarian sufficient condition holds for strict concavity instead of simple concavity, the solution is optimal and unique.

In [74, 86], the Arrow sufficient condition is applied to a control problem of optimal production and maintenance. As $\check{H}$ is not concave in $\check{X}$, no optimality can be shown. In [47], optimality and uniqueness of solutions for spacecraft formations with minimal fuel consumption are proved by the Mangasarian sufficient condition.

### 4.6.2 Local second-order sufficient conditions with Riccati equation

Local second-order sufficient optimality conditions for systems with non-compact input space which satisfy the strengthened Legendre-Clebsch condition $u^\top H_{uu} u \leq -\alpha \|u\|^2$ as in (4.9) are covered in [8, 65, 70, 72, 75]. These conditions result from a study of the second variation along an extremal. The solvability of a matrix Riccati differential equation is analyzed to check positive definiteness of the quadratic form of the second variation. Provided that additional regularity conditions hold, for an extremal to be locally optimal, a bounded solution $Q(\cdot)$ to the Riccati equation has to exist which meets specific boundary conditions. To check strong local optimality 2.2.6 of extremals of time-optimal control problems, the transformed time-optimal control problem 2.2.4 is considered. The dimension of the extended state $\check{X} = (\check{x}, \tau)$ is $\check{n} = n+1$. For the symmetric $\check{n} \times \check{n}$ matrix $Q$, the Riccati equation

$$Q' = -Q\,\check{f}_{\check{X}} - \check{f}_{\check{X}}^\top Q - \check{H}_{\check{X}\check{X}} + \left(\check{H}_{\check{X}\check{u}} + Q\,\check{f}_{\check{u}}\right) \check{H}_{\check{u}\check{u}}^{-1} \left(\check{H}_{\check{X}\check{u}} + Q\,\check{f}_{\check{u}}\right)^\top \tag{4.12}$$

is studied for the partial derivatives

$$\check{f}_{\check{X}} = \frac{\partial \check{f}}{\partial \check{X}}, \quad \check{f}_{\check{u}} = \frac{\partial \check{f}}{\partial \check{u}}, \quad \check{H}_{\check{X}\check{X}} = \frac{\partial^2 \check{H}}{\partial \check{X}^2}, \quad \check{H}_{\check{X}\check{u}} = \frac{\partial^2 \check{H}}{\partial \check{X}\partial \check{u}}, \quad \check{H}_{\check{u}\check{u}} = \frac{\partial^2 \check{H}}{\partial \check{u}^2}. \tag{4.13}$$

Here $\check{f}$ and $\check{H}$ are assumed to be such that the derivatives (4.13) exist. The derivatives are evaluated along the extremal trajectories of $\check{X}$ and $\check{u}$. For time-optimal control problems with fixed initial and desired state, an extremal is strongly locally optimal if a bounded solution $Q(\cdot)$ can be found whose element $q_{\check{n}\check{n}}$ satisfies the boundary conditions $q_{\check{n}\check{n}}(0) > 0$ and $q_{\check{n}\check{n}}(1) < 0$.

For control systems with compact input space $U = \{u \in \mathbb{R}^m \mid c(u) \leq 0\}$ specified by an input constraint 3.1.3, a modified local second-order sufficient optimality condition addressed in [65, 72, 75] gives weak local optimality 2.2.6. For this condition to apply, the strengthened modified Legendre-Clebsch condition $w^\top H_{ww} w \leq -\alpha \|w\|^2$ as in (4.11) has to hold. Depending on the active input constraints, the right-hand side of the Riccati equation switches, i. e., changes discontinuously. The relevant Riccati equation is

$$Q' = -Q\,\check{f}_{\check{X}} - \check{f}_{\check{X}}^\top Q - \check{H}_{\check{X}\check{X}} + \left(\check{H}_{\check{X}\check{u}} + Q\,\check{f}_{\check{u}}\right) P \left(P^\top \check{H}_{\check{u}\check{u}} P\right)^{-1} P^\top \left(\check{H}_{\check{X}\check{u}} + Q\,\check{f}_{\check{u}}\right)^\top. \tag{4.14}$$

Recall the index set $I(s)$ as in (3.2) of active input constraints at time $s$ and the number of active input constraints $n_a(s) = |I(s)|$ which satisfies $0 \leq n_a(s) \leq m$. The matrix $P$ in (4.14) is a full rank $m \times (m - n_a(s))$ matrix which has to satisfy $C_{\check{u}} P = 0$ for the $n_a(s) \times m$ matrix $C_{\check{u}}$. Based on the vector $c = (c_1^-, c_1^+, \ldots, c_m^-, c_m^+)$ of the functions of the input constraint $c(\check{u}) \leq 0$, the vector $C$ consists of the functions $c_i^-$ and $c_i^+$ of the active input constraints $c_i^-(\check{u}) = 0$ and $c_i^+(\check{u}) = 0$. From $C$, the matrix

$$C_{\check{u}} = \frac{\partial C}{\partial \check{u}} \tag{4.15}$$

is obtained. If no input constraint is active, i. e., if $n_a(s) = 0$ holds at time $s$, the Riccati equation (4.14) results in (4.12). If $n_a(s) = m$ input constraints are active, the Riccati equation (4.14) gives the linear matrix differential equation

$$Q' = -Q\,\check{f}_{\check{X}} - \check{f}_{\check{X}}^\top Q - \check{H}_{\check{X}\check{X}}. \tag{4.16}$$

If a bounded solution $Q(\cdot)$ to equation (4.14) exists which satisfies $q_{\check{n}\check{n}}(0) > 0$ and $q_{\check{n}\check{n}}(1) < 0$, the extremal is weakly locally optimal.

For control systems

$$\dot{x} = f(x, v, w) = f_0(x, w) + \sum_{i=1}^{m_1} g_i(x, w)\, v_i \tag{4.17}$$

with affine input $v \in V$ and non-affine input $w \in W$, compact input space $V \subset \mathbb{R}^{m_1}$, and $W = \mathbb{R}^{m_2}$, a local second-order sufficient optimality condition is stated in [86]. This condition can be applied if the input $w$ meets the strengthened modified Legendre-Clebsch condition (4.11). Then, it gives strong local optimality.

For applications of local second-order sufficient conditions with Riccati equation to time-optimal control problems of the Earth-Mars orbit transfer, see [75], the Zermelo problem with non-constant velocity field, see [70], and the Rayleigh problem, see [75]. For applications to other than time-optimal control problems, see [8, 65, 72, 86].

### 4.6.3 Local second-order sufficient conditions for bang-bang extremals

Local second-order sufficient conditions for bang-bang extremals 4.3.5 are addressed in [3, 32, 73, 76, 85, 90, 91]. These conditions differ in the principles they are derived from, the required assumptions, and the resultant local optimality. The conditions in [73, 76, 90] can be used for the time-optimal control problem 2.2.3, whereas the conditions in [3, 91] apply to the transformed time-optimal control problem 2.2.4. The optimality conditions for bang-bang extremals are not given here in detail, as this would require to introduce much notation. In particular, the conditions are not applicable to normal regular extremals of the BSR, as these extremals are no bang-bang extremals, see Section 6.4.

One common precondition for all second-order sufficient conditions for bang-bang extremals is the strict bang-bang property $\dot{s}_i(x(t_j), \lambda(t_j)) \neq 0$, which has to hold for all switching functions with $s_i(x(t_j), \lambda(t_j)) = 0$ at each switching time $t_j$. Most conditions require more restrictive versions of this property which rule out multiple switching times, i. e., switchings of several inputs at the same time. Only the conditions in [32, 91] allow multiple switching times.

According to [85], most second-order sufficient conditions for bang-bang extremals arise from two basic approaches, the study of a quadratic form on a finite dimensional critical cone and the transformation to a finite dimensional optimization problem. The optimality conditions derived from these two principles are equivalent and give strong local time-optimality.

The first approach presented in [76, 85] provides local second-order sufficient conditions which require that a quadratic form $\Omega$ on a finite dimensional critical cone is positive definite. The elements of this critical cone are first-order variations of an extremal with respect to the switching times. To show positive definiteness, a transformation of $\Omega$ to perfect squares is applied which is based on the solution of a Riccati equation similar to (4.16).

For the second approach described in [3, 73, 85, 90, 91], the control problem is transformed to a finite dimensional optimization problem, the induced optimization problem. It arises from perturbations of the switching times $t_j$ and the free end time $\tau$. Local second-order sufficient conditions for optimization problems with equality conditions are analyzed for this problem. If these conditions and the strict bang-bang property hold, strong local time-optimality results.

Local second-order sufficient conditions for bang-bang extremals are applied to the time-optimal control problem for the Van der Pol Oscillator in [76, 90], the Rayleigh problem in [73, 76], an underwater vehicle in [32], a nuclear reactor in [76], and a two-link manipulator in [73]. For applications to other than time-optimal control problems, see [73, 74].

### 4.6.4 Boltyanskii's sufficient condition

Boltyanskii's sufficient condition, also called Boltyanskii's regular synthesis, is originally given in [14] and discussed in [26, 88, 105, 106, 119]. Regular synthesis means to find a piecewise

smooth feedback $u\colon I\times M \to U, (t,x) \mapsto u(t,x)$ to generate solutions which satisfy the necessary optimality conditions of the Maximum Principle. Solutions obtained this way are globally optimal if they meet additional regularity conditions.

For Boltyanskii's sufficient condition, the additional regularity conditions are analyzed based on a partition of the state space $M$ of dimension $n$ into cells $P_i$ which are submanifolds of dimension $\dim P_i \leq n$. The following conditions have to hold for optimality: The feedback $u(t,x)$ has to be smooth in each cell. The resultant solution has to enter each cell at a nonzero angle. If a solution passes from cell $P_i$ to cell $P_j$, $\dim P_i$ and $\dim P_j$ have to fit. The minimal cost function $J$ has to depend continuously on $x_0$. For details, see [14, 26, 88, 106].

In [105, 106], Boltyanskii's sufficient condition is applied to show optimality of the Reeds-Shepp paths. For this, closed-form representations of the Reeds-Shepp paths are used. The 46 paths required to connect each initial and desired configuration are divided into seven path types. For each path type, the cells implementing the partition of the configuration space are given. As discussed in [88, 105, 106], Boltyanskii's sufficient condition requires very strong assumptions. According to [106], it does not apply to solutions with infinitely many switchings resembling the Fuller phenomenon from Section 4.3. Besides, optimality of the Dubins paths cannot be proved by Boltyanskii's sufficient condition as the minimal path length does not depend continuously on the initial state. Based on other definitions of regular synthesis, sufficient conditions are given in [88, 119] under less strict assumptions.

## 4.7 Example: Time-optimal control of the unicycle

To exemplify the definitions and theorems of this chapter, time-optimal control of the unicycle is addressed. For this, the kinematic model (3.14) of the unicycle, an affine control system with symmetric input space $U = [-\hat{u}_1, \hat{u}_1] \times [-\hat{u}_2, \hat{u}_2]$, should be steered from an initial configuration $q_0$ to a desired configuration $q_d$ in minimal time. By the Filippov Existence Theorem, time-optimal solutions exist for this control problem. This is true as the unicycle is controllable, see Section 3.4.1, and it satisfies the linear growth condition, as $\|G(q)\,u\| = \sqrt{u_1^2 + u_2^2} \leq \sqrt{\hat{u}_1^2 + \hat{u}_2^2} \leq c\,(1 + \|q\|)$ holds for $c \geq \sqrt{\hat{u}_1^2 + \hat{u}_2^2}$. The velocity sets $F_U(q) = \{G(q)\,u \mid u \in U\}$ are convex for all $q \in Q$, as $U$ is convex and convexity is preserved under $G(q)$.

To formulate the necessary optimality conditions of the Maximum Principle, the Hamiltonian function is required. For system (3.14) and the adjoint state $\lambda = (\lambda_1, \lambda_2, \lambda_3)$, it is

$$H(q, \mu, \lambda, u) = -\mu + \lambda_1 u_1 + (\lambda_2 \cos(\theta) + \lambda_3 \sin(\theta))\, u_2. \tag{4.18}$$

The Maximum Principle gives necessary optimality conditions which have to be satisfied by extremals $(q^*(\cdot)\,, \lambda^*(\cdot)\,, u^*(\cdot))$ and $H^* = H(q^*, \mu, \lambda^*, u^*)$. Because of condition N1, $(\mu, \lambda^*) \neq 0$ must hold for all $t \in I$. The adjoint equation

$$\begin{aligned} \dot{\lambda}_1^* &= (\lambda_2^* \sin(\theta^*) - \lambda_3^* \cos(\theta^*))\, u_2^*, \\ \dot{\lambda}_2^* &= 0, \\ \dot{\lambda}_3^* &= 0 \end{aligned}$$

from condition N2 has to be true for almost all $t \in I$. Hence, $\lambda_2^*(t) = \lambda_2(0)$ and $\lambda_3^*(t) = \lambda_3(0)$ applies for all $t \in I$. By condition N3, $u^*$ has to maximize the Hamiltonian function (4.18) such that $H(q^*, \mu, \lambda^*, u^*) = \max_{u \in U} H(q^*, \mu, \lambda^*, u)$ holds for almost all $t \in I$. Condition N4 requires $H^* = 0$ for almost all $t \in I$. There are no abnormal extremals for time-optimal control of the unicycle, since for these extremals, the conditions N1 and N4 cannot be true simultaneously.

As the kinematic model of the unicycle is an affine control system, the Hamiltonian function (4.18) can be written in the form (4.7) as $H(q, \mu, \lambda, u) = -\mu + s_1(q, \lambda)\; u_1 + s_2(q, \lambda)\; u_2$ with the switching functions $s_1(q, \lambda) = \lambda_1$ and $s_2(q, \lambda) = \lambda_2 \cos(\theta) + \lambda_3 \sin(\theta)$. For $s_1^* = s_1(q^*, \lambda^*)$ and $s_2^* = s_2(q^*, \lambda^*)$, the extremal inputs $u_1^* = \operatorname{sgn}(s_1^*)\, \hat{u}_1$ and $u_2^* = \operatorname{sgn}(s_2^*)\, \hat{u}_2$ results.

For $\mu = 1$, $\hat{u}_1 = \hat{u}_2 = 1$, and $I = [0, 4]$, a bang-bang extremal of the unicycle is shown in Figure 4.1. The figure consists of a time plot of the orientation angle $\theta^*$, an $(x^*, y^*)$ plot of the position of the unicycle, a time plot of the elements $(\lambda_1^*, \lambda_2^*, \lambda_3^*)$ of the adjoint state, and time plots of the switching functions $s_i^*$ and inputs $u_i^*$ for $i = 1, 2$. The extremal starts from $q_0 = (0, 0, 0)$ and has $n_s = 3$ switchings. Table 4.1 gives the switching times $t_j$, arc durations $\triangle t_j$, and extremal inputs $\hat{u}_j$. The switching of $u_1$ at $t_2 = 2.173$ changes the steering from right to left. The switchings of $u_2$ at $t_1 = 1.004$ and $t_3 = 3.342$ cause cusps, i. e., reversals of the driving direction. The bang-bang extremal in Figure 4.1 is a normal regular extremal.

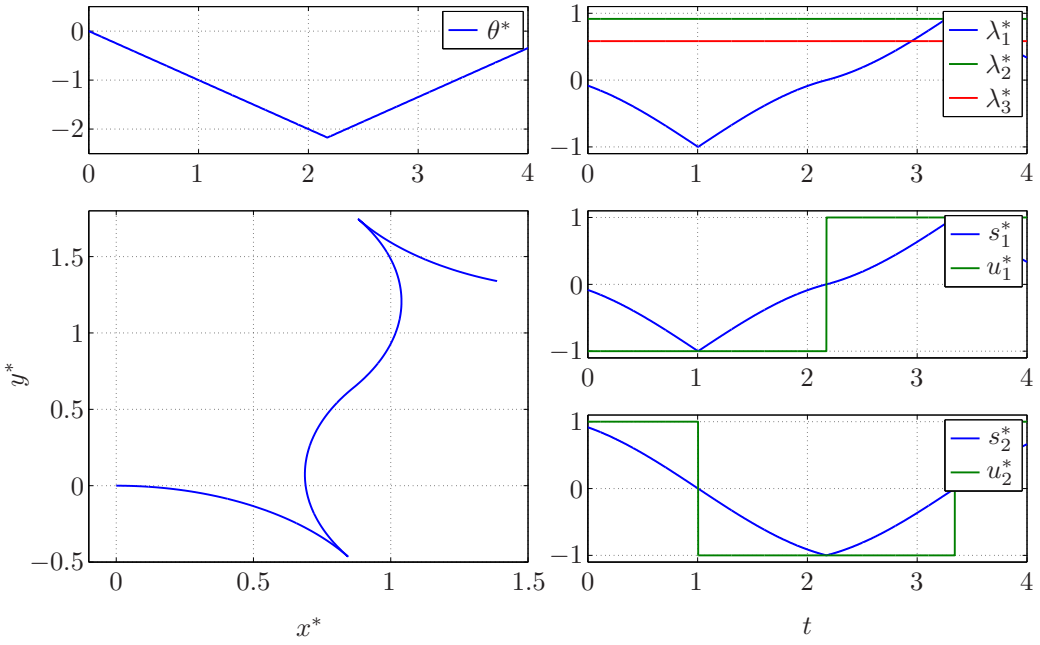


Figure 4.1: Bang-bang extremal of the unicycle.

| switching/final time | arc duration | extremal input |
|---|---|---|
| $t_1 = 1.004$ | $\triangle t_1 = 1.004$ | $\hat{u}_1 = (-\hat{u}_1, \hat{u}_2)$ |
| $t_2 = 2.173$ | $\triangle t_2 = 1.169$ | $\hat{u}_2 = (-\hat{u}_1, -\hat{u}_2)$ |
| $t_3 = 3.342$ | $\triangle t_3 = 1.169$ | $\hat{u}_3 = (\hat{u}_1, -\hat{u}_2)$ |
| $T = 4.000$ | $\triangle t_4 = 0.658$ | $\hat{u}_4 = (\hat{u}_1, \hat{u}_2)$ |

Table 4.1: Switching times, arc durations, and extremal inputs of the bang-bang extremal of the unicycle.

To solve the boundary value problem of the time-optimal control problem, an end time $\tau$ and an initial condition $\lambda(0)$ are required such that an extremal $q^*(\cdot)$ with $q^*(0) = q_0$ results which satisfies $q^*(\tau) = q_d$. Extremals meeting this boundary value problem may give time-optimal solutions. To single out optimal solutions of the unicycle with minimal end time $\tau^{to}$, optimality conditions like those from Section 4.5 and 4.6 can be applied.

# Part II

# Modeling and extremals

# 5 The bi-steerable robot

In this chapter, models of the bi-steerable robot (BSR) are developed and analyzed. The BSR is a wheeled mobile robot with two independently steerable axles. There are many applications of the BSR in land-based robotics. Examples of the BSR are Mustang MK I, CyCab, and AutoStrad. Figure 5.1 shows Mustang MK I, a technology demonstrator of a mobile soldier assistance system. This robot, co-developed by Diehl BGT Defence of Germany, is designed for force protection, reconnaissance, and transportation. For details on Mustang MK I and its capabilities regarding path planning and autonomous convoy driving in rough terrain, see [55]. In Figure 5.2, two CyCab robots are depicted. The CyCab is a driverless automated electric vehicle for passenger transport from Robosoft, a France-based company. It is addressed in [11, 44, 78, 101, 102]. Another example of a wheeled mobile robot which can be modeled to have the kinematics of the BSR is the automated straddle carrier AutoStrad in Figure 5.3. This vehicle from Kalmar Industries of Finland is used for driverless container handling. At the port of Brisbane, Australia, 18 automated straddle carriers are in operation since 2005. For references to this robot, see [38, 125].

Figure 5.1: Mustang MK I from Diehl BGT Defence, Germany (photo by the author).

Compared to vehicles with just one steerable axle, the BSR has improved maneuverability, as it can do sharper turns and perform diagonal motions. If both axles are steered in the same direction, i. e., if $\varphi_f \, \varphi_r > 0$ holds for the front and rear steering angles $\varphi_f$ and $\varphi_r$, the BSR moves diagonally. If the axles are rotated in opposite directions, i. e., if $\varphi_f \, \varphi_r < 0$ is true, the BSR goes through curves of smaller turning radius than a robot with only one steerable axle rotated at $\varphi_f$ or $\varphi_r$. Due to its improved maneuverability, the BSR can maneuver in narrower spaces than robots with just one steerable axle, see [101]. This is beneficial for operations in unstructured environments like disaster areas. Compared to other ground vehicles, the BSR provides a highly maneuverable locomotion platform without resorting to tracks or skid steering which are less suitable for high speed driving. Besides, the BSR can drive from one position to another in maybe shorter time and with shorter path length than wheeled mobile robots with one

Figure 5.2: CyCab robots from Robosoft, France (photo courtesy of Robosoft).

steerable axle. This is addressed in Section 8.5, where time-optimal normal regular extremals of the RKM and shortest paths of the car-like robot are compared. Moreover, the BSR can be controlled to have the same steering characteristics for driving forward or backward, which is advantageous for autonomous driving and teleoperation. Finally, the BSR offers redundancy as a limited steering capability remains if the steering actuation of one axle fails.

Figure 5.4 shows the bicycle model of the BSR used for modeling. This model, consisting of front axle, rear axle, and chassis, is discussed in Section 5.2. The configuration $q = (\theta, x, y, \varphi_f, \varphi_r)$ of the BSR includes the orientation angle $\theta$ also called heading angle, the position $(x, y)$ of the center of mass, and the front and rear steering angles $\varphi = (\varphi_f, \varphi_r)$. In Figure 5.4, $\varphi_f > 0$ and $\varphi_r < 0$ holds. The distances between the center of mass and the front and rear axle are $L_f$ and $L_r$. The nonholonomic kinematic system 3.3.2 of the BSR, called full kinematic model (FKM) of the BSR here, is defined next.

**Definition 5.0.1** *(Full kinematic model (FKM) of the BSR) Let $Q = SE(2) \times (-\hat{\varphi}, \hat{\varphi}) \times (-\hat{\varphi}, \hat{\varphi})$, $0 < \hat{\varphi} < \frac{\pi}{2}$, be the configuration space, $q = (\theta, x, y, \varphi_f, \varphi_r) \in Q$ the configuration, and $g_{11}$, $g_{12}$, and $g_{13}$ the real-valued functions*

$$\begin{aligned} g_{11}(q) &= \tfrac{1}{L_f+L_r} \sin(\varphi_f - \varphi_r)\,, \\ g_{12}(q) &= \tfrac{1}{L_f+L_r} \Big( L_f \cos(\varphi_f)\cos(\theta+\varphi_r) + L_r \cos(\varphi_r)\cos(\theta+\varphi_f) \Big), \\ g_{13}(q) &= \tfrac{1}{L_f+L_r} \Big( L_f \cos(\varphi_f)\sin(\theta+\varphi_r) + L_r \cos(\varphi_r)\sin(\theta+\varphi_f) \Big) \end{aligned} \tag{5.1}$$

*with $L_f > 0$ and $L_r > 0$. The nonholonomic kinematic system 3.3.2 given by*

$$\dot{q} = \begin{bmatrix} \dot{\theta} \\ \dot{x} \\ \dot{y} \\ \dot{\varphi}_f \\ \dot{\varphi}_r \end{bmatrix} = \begin{bmatrix} g_{11}(q) \\ g_{12}(q) \\ g_{13}(q) \\ 0 \\ 0 \end{bmatrix} u_1 + \begin{bmatrix} 0 \\ 0 \\ 0 \\ 1 \\ 0 \end{bmatrix} u_2 + \begin{bmatrix} 0 \\ 0 \\ 0 \\ 0 \\ 1 \end{bmatrix} u_3 = g_1(q)\,u_1 + g_2\,u_2 + g_3\,u_3 \tag{5.2}$$

*with input space $U = [-\hat{u}_1, \hat{u}_1] \times [-\hat{u}_2, \hat{u}_2] \times [-\hat{u}_3, \hat{u}_3]$, $\hat{u}_i > 0$, and input $u = (u_1, u_2, u_3) \in U$ is called FKM of the BSR.*

The input $u$ of system (5.2) consists of the driving velocity $u_1$ and the steering velocities $u_2 = \dot{\varphi}_f$ and $u_3 = \dot{\varphi}_r$ of the front and rear axle. Model 5.0.1 is called full kinematic model to


Figure 5.3: Automated straddle carrier AutoStrad from Kalmar Industries, Finland (photo courtesy of Kalmar Industries).

distinguish it from the reduced kinematic model (RKM) of the BSR. The RKM is introduced next to simplify the subsequent analysis, in particular the study of the extremals for time-optimal control in Chapter 6. For the RKM, the steering angles $\varphi = (\varphi_f, \varphi_r)$ are no longer state but input variables. This is justified as the configuration variables $(\theta, x, y)$ for the position and heading of the robot are the essential configuration variables for path planning and time-optimal control. In general, transitions between two positions and headings can only be achieved by time-consuming driving and steering maneuvers due to the nonholonomic constraint. Compared to this, the steering angles $\varphi$ can be changed in short time. Thus, they are considered as inputs.

**Definition 5.0.2** *(Reduced kinematic model (RKM) of the BSR) Let $Q_r = SE(2)$ be the configuration space, $q_r = (\theta, x, y) \in Q_r$ the configuration, and $g_1$, $g_2$, and $g_3$ the real-valued functions*

$$\begin{aligned} g_1(\theta,\varphi) &= \sin(\varphi_f - \varphi_r)\,, \\ g_2(\theta,\varphi) &= \tfrac{1}{2}\Big(\cos(\varphi_f)\cos(\theta+\varphi_r) + \cos(\varphi_r)\cos(\theta+\varphi_f)\Big), \\ g_3(\theta,\varphi) &= \tfrac{1}{2}\Big(\cos(\varphi_f)\sin(\theta+\varphi_r) + \cos(\varphi_r)\sin(\theta+\varphi_f)\Big). \end{aligned} \tag{5.3}$$

*The driftless control system*

$$\dot{q}_r = \begin{bmatrix} \dot\theta \\ \dot x \\ \dot y \end{bmatrix} = \begin{bmatrix} g_1(\theta,\varphi) \\ g_2(\theta,\varphi) \\ g_3(\theta,\varphi) \end{bmatrix} v = g(\theta,\varphi)\, v \tag{5.4}$$

*with input space $U_r = [-\hat v, \hat v] \times [-\hat\varphi, \hat\varphi] \times [-\hat\varphi, \hat\varphi]$, $\hat v > 0$, $0 < \hat\varphi < \frac{\pi}{2}$, and input $u_r = (v, \varphi_f, \varphi_r) \in U_r$ is called RKM of the BSR.*

The configuration space $Q_r$ of the RKM is a subspace of the configuration space $Q$ of the FKM. In the following, $Q_r$ is called reduced configuration space and $q_r$ reduced configuration.

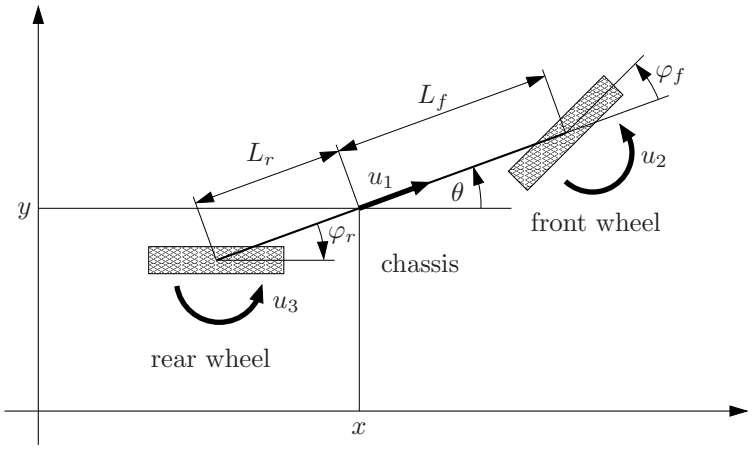


Figure 5.4: Model of the bi-steerable robot with steering angles $\varphi_f > 0$ and $\varphi_r < 0$.

For path planning for the RKM, $(\theta_0, x_0, y_0)$ is the initial configuration and $(\theta_d, x_d, y_d)$ the desired configuration. The functions (5.3) result from the functions (5.1) for a normalized model of the BSR with $L_f = L_r = \frac{1}{2}$. This normalized model is used in the following to simplify the subsequent studies, in particular in Chapter 6. Using $L_f = L_r$ does neither affect the controllability nor the integrability of the constraint distribution of the BSR. System (5.4) is no nonholonomic kinematic system 3.3.2, as the steering angles $\varphi$ are no configuration variables but input variables which enter the system by trigonometric functions. The driving velocity of the RKM is denoted by $v$ instead of $u_1$, since it is the only remaining velocity input. As $\dot{q}_r \equiv 0$ holds for $u_r = (0, 0, 0)$, the RKM is driftless.

## 5.1 Literature review

Compared to the vast literature on other wheeled mobile robots like the unicycle, the car-like robot, or the differential drive, there is little literature on the BSR. In the following references, related work concerning modeling, analysis, and control of the BSR as well as results for other wheeled mobile robots applicable to the BSR are discussed.

In [25], wheeled mobile robots with fixed and steerable conventional wheels as well as omnidirectional wheels are analyzed and classified into five classes. The BSR is a representative of one of these classes. Generic models for robots of each class are given, and structural properties like controllability and feedback equivalence are analyzed. In [34], tracking control of the five classes of wheeled mobile robots by static and dynamic state feedback is addressed. For the feedback law of the BSR to be defined, $\sin(\varphi_f)\sin(\varphi_r)\,u_1 \neq 0$ is required, i. e., configurations with $\varphi_f = 0$ or $\varphi_r = 0$ are not feasible.

In [123], modeling, tracking control, and stabilization of wheeled mobile robots with several steerable wheels or axles is discussed. One of the example systems is the BSR. For the considered kinematic systems, tracking of non-constant reference trajectories by linearizing feedback and stabilization of constant configurations by time-variant feedback is studied.

Tracking control of a reduced kinematic model of the BSR is addressed in [11]. The controller is based on fuzzy logic and consists of a path tracking controller for steering and a velocity planner. The velocity planner takes dynamic properties into account to compute the maximal admissible velocity depending on the turning radius. For the steering of the BSR in [11], $\varphi_r = \pm\varphi_f$ is always applied, i. e., $\varphi_r$ is not set independently of $\varphi_f$. In [78], the tracking controller is extended by a reactive component for collision avoidance and applied to the CyCab.

In [69], the author of this thesis presents a robust tracking controller for nonholonomic dynamic systems. The tracking control is based on inverse kinematic models and sliding-mode

control. The controller allows global tracking of arbitrary reference trajectories with bounded first and second time derivatives. It makes the closed-loop system robust with respect to bounded disturbances. The tracking is applied in [69] to the FKM 5.0.1 of the BSR.

In [61], the transformation of wheeled mobile robots including the BSR to the chain form from Section 3.3.2 is addressed. For the FKM of the BSR with $q = (\theta, x, y, \varphi_f, \varphi_r)$ and $u = (u_1, u_2, u_3)$, there holds $p = 5$ and $m = 3$. Thus, in multi-chain form (3.12), the system is

$$\begin{aligned} \dot{z}^1 &= v_1, \\ \dot{z}_1^2 &= v_2, \qquad \dot{z}_1^3 = v_3, \\ \dot{z}_2^2 &= z_1^2\, v_1, \qquad \dot{z}_2^3 = z_1^3\, v_1. \end{aligned} \tag{5.5}$$

In [61], a state and input transformation for the BSR with $L_f = L_r$ to (5.5) is given. Based on this, a transformation for $L_f \neq L_r$ can be derived. It consists of the state transformation

$$\begin{aligned} z^1 &= \theta, \\ z_1^2 &= -x\,\sin(\theta) + y\,\cos(\theta) + \tfrac{(L_f+L_r)\cos(\varphi_f)\cos(\varphi_r)}{\sin(\varphi_f-\varphi_r)}, \\ z_2^2 &= x\,\cos(\theta) + y\,\sin(\theta)\,, \\ z_1^3 &= x\,\cos(\theta) + y\,\sin(\theta) - \tfrac{L_f\cos(\varphi_f)\sin(\varphi_r)+L_r\cos(\varphi_r)\sin(\varphi_f)}{\sin(\varphi_f-\varphi_r)}, \\ z_2^3 &= x\,\sin(\theta) - y\,\cos(\theta) \end{aligned}$$

and the input transformation $v = \Theta(q)\,u$ with

$$\Theta(q) = \begin{bmatrix} \frac{\sin(\varphi_f-\varphi_r)}{L} & 0 & 0 \\ \frac{L_f\cos(\varphi_f)\sin(\varphi_r)+L_r\cos(\varphi_r)\sin(\varphi_f)-\sin(\varphi_f-\varphi_r)(x\cos(\theta)+y\sin(\theta))}{L} & \frac{-L\cos^2(\varphi_r)}{\sin^2(\varphi_f-\varphi_r)} & \frac{L\cos^2(\varphi_f)}{\sin^2(\varphi_f-\varphi_r)} \\ \frac{L\cos(\varphi_f)\cos(\varphi_r)+\sin(\varphi_f-\varphi_r)(y\cos(\theta)-x\sin(\theta))}{L} & \frac{L\sin(2\,\varphi_r)}{2\,\sin^2(\varphi_f-\varphi_r)} & \frac{-L\cos(\varphi_f)\sin(\varphi_f)}{\sin^2(\varphi_f-\varphi_r)} \end{bmatrix}$$

for $L = L_f + L_r$. As discussed in [61] for $L_f = L_r$, both transformations are not defined at configurations with $\varphi_f = \varphi_r$. This is true for $L_f \neq L_r$ as well. Thus, to apply the transformation to chain form, configurations with $\varphi_f = \varphi_r$ have to be excluded. This is a strong restriction on the feasible paths, as such configurations are essential for the BSR to go straight on or perform diagonal motions at constant heading angle. To the best of the author's knowledge, no globally defined transformation of the FKM to chain form is available.

In [101, 102], a flat output of the kinematic system of the CyCab is presented based on the results in [67]. For this, the rear steering angle of the CyCab is given as function of the front steering angle. Configurations with $\varphi_f = \varphi_r$ are excluded, as the flat output is not defined there. This exemplifies the close connection between the transformability to chain form and the existence of flat outputs, see [64]. A flatness based tracking controller for the CyCab can be found in [44]. Here, $\varphi_r := -k\,\varphi_f$ is used with constant $k$ satisfying $0 < k \leq 1$.

Under additional assumptions on the dimensions and steering angles of the BSR discussed in Section 5.2.3, the nonholonomic constraint of the snakeboard equals that of the BSR. As discussed in Section 3.4.3, the snakeboard is considered as nonholonomic dynamic system. This is justified by the snake-like locomotion of the snakeboard resulting from angular momentum generated by motions of the rider. Several references address optimal control of the snakeboard. In [48], optimal trajectory planning for solutions with minimal number of switchings between motion primitives is addressed. In [54], optimal trajectories between two configurations with fixed end time $\tau$ are studied which minimize the cost function

$$J = \int_0^\tau \left(\dot{\varphi}^2 + \dot{\psi}^2\right) \mathrm{d}t.$$

Here, $\dot{\varphi}$ is the derivative of the steering angle and $\dot{\psi}$ the derivative of the rotation angle of the rotor. Optimal motions of the snakeboard which minimize the control energy are addressed in [87]. For time-optimal control of a kinematic model of the BSR, these results are not relevant.

Trajectory planning for an automated straddle carrier modeled as BSR is addressed in [125]. The trajectory planner consists of a steering planner and a velocity planner. For a reduced kinematic model of the BSR, the steering planner implements the turning of the vehicle, while the velocity planner determines the driving velocity along the path, taking dynamic effects and bounded driving forces into account. Two maneuvers of the BSR are considered, the zero-side-slip and the parallel-parking maneuver. For both maneuvers, $\varphi_r$ is a function of $\varphi_f$, i. e., $\varphi_f$ and $\varphi_r$ are not set independently from each other.

In [97], Reeds-Shepp paths of the car-like robot are extended for a reduced kinematic model of the BSR. For this, steering angles with $\varphi_r = \pm\varphi_f$ are applied, resulting in straight line segments for $\varphi_f = \varphi_r = 0$, arcs of circles for $\varphi_r = -\varphi_f \neq 0$, and new path segments called parallel steer paths for $\varphi_f = \varphi_r \neq 0$. In the latter two cases, $\varphi_r$ is set depending on $\varphi_f$. The new segments give paths for the BSR which are shorter than Reeds-Shepp paths. In addition, different paths for the BSR between fixed initial and desired configurations are considered which have the same path length and allow to avoid obstacles by using the parallel steer paths.

In the reviewed references, there are no results on path planning or optimal control of the BSR with independent steering angles $\varphi_f$ and $\varphi_r$. For the transformation to chain form in [61] and the flatness based control in [44, 101, 102], steering angles $\varphi_f = \varphi_r$ have to be excluded, which restricts the admissible paths. The findings on optimal control of the nonholonomic dynamic system of the snakeboard from [48, 54, 87] are not relevant for path planning and optimal control of the BSR, which is considered as kinematic system with velocity inputs. The studies in [97, 125] are most close in spirit to this thesis, as path planning for a reduced kinematic model of the BSR similar to (5.4) is addressed. However, in both references, $\varphi_r$ is set depending on $\varphi_f$, and the optimality of the paths is not regarded.

## 5.2 Modeling

In this section, the modeling of the BSR is covered which results in the FKM 5.0.1. The bicycle model of the BSR is described, and the configuration space of the BSR is discussed, along with the configuration space of an idealized BSR with unrestricted steering angles. Then, the kinematics of the bicycle model is specified, the velocity constraint is derived, and the constraint distribution is given. The generators of this distribution provide the basis for the FKM.

### 5.2.1 Bicycle model and configuration space

Like in Section 3.4.2 where the kinematic model of the car-like robot is addressed, the bicycle model is used here to obtain the FKM 5.0.1 of the BSR. For further applications of the bicycle model to the BSR, see [44, 97, 125]. The bicycle model has its name from the two wheels in the midpoint of the front and rear axle which represent the two pairs of wheels of the axles. Instead of considering two wheels per axle with slightly different steering angles to implement Ackermann steering, one wheel per axle is sufficient to determine the path of the robot. The wheels for the front and rear axle have the front steering angle $\varphi_f$ and rear steering angle $\varphi_r$, respectively. Both angles are given with respect to the longitudinal axis of the robot. The angles $(\varphi_f, \varphi_r)$ are uniquely related to the angles of the two wheels of the front and rear axle of the original BSR.

For the car-like robot driving a curve, Figure 5.5 shows the four dark wheels of the vehicle with the front wheels performing Ackermann steering and the resultant two light gray wheels of the bicycle model. The distance between the center of rotation $C$ and the reference point $P$ at the midpoint of the fixed rear axle is $R$, the distance between front and rear axle is $L$, and the length of both axles is $d$. For the angles $\left(\varphi_f^l, \varphi_f^r\right)$ of the left and right front wheel and the

angle $\varphi_f$ of the front wheel of the bicycle model,

$$\tan\left(\varphi_f^l\right) = \frac{L}{R - \frac{d}{2}}, \quad \tan\left(\varphi_f^r\right) = \frac{L}{R + \frac{d}{2}}, \quad \tan(\varphi_f) = \frac{L}{R}$$

holds. Thus, for $\varphi_f$ obtained from path planning, $\varphi_f^l$ and $\varphi_f^r$ have to satisfy

$$\varphi_f^l = \arctan\left(\frac{L}{L\cot(\varphi_f) - \frac{d}{2}}\right), \quad \varphi_f^r = \arctan\left(\frac{L}{L\cot(\varphi_f) + \frac{d}{2}}\right).$$

Corresponding equations hold for the BSR. For details on steering angles of several wheels on one steerable axle and the related steering angle in the midpoint of the axle, see [4].

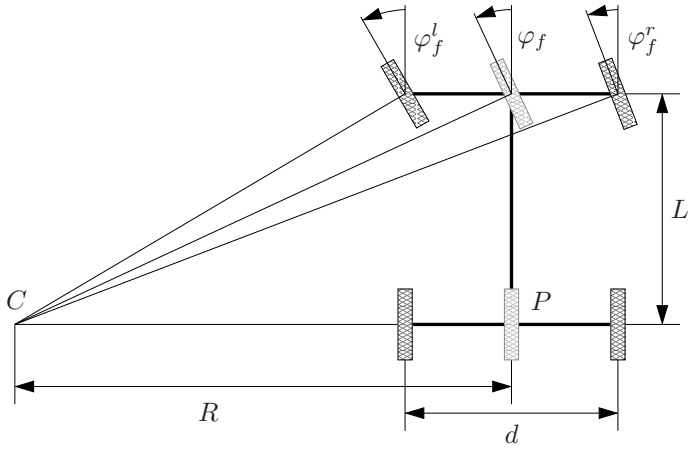


Figure 5.5: Ackermann steering of the car-like robot.

The bicycle model of the BSR is shown in Figure 5.6 with a fixed reference frame. With respect to this frame, $(x, y)$ are the coordinates of the center of mass, and $\theta$ is the orientation relative to the $x$-axis. The robot moves in a horizontal plane. The model of the BSR consist of three rigid bodies: the front and rear axle each represented by a single wheel, and the chassis connecting the axles. As for the unicycle and car-like robot, the rotation of the wheels is neglected. The steering angles $(\varphi_f, \varphi_r)$ are given relative to the longitudinal axis of the robot. In Figure 5.6, $\varphi_f > 0$ and $\varphi_r < 0$ holds. The center of mass of the BSR lies on its longitudinal axis and is used as reference point for modeling. The distances between the center of mass and the pivotal points of the front and rear axle are $L_f > 0$ and $L_r > 0$.

**Definition 5.2.1** *(Configuration and configuration space of the BSR) The configuration*

$$q = (\theta, x, y, \varphi_f, \varphi_r)$$

*of the BSR has dimension $p = 5$ and consists of the heading angle $\theta$ for the orientation of the vehicle, the coordinates $(x, y)$ of the center of mass, and the steering angles $\varphi = (\varphi_f, \varphi_r)$. The configuration space of the BSR is*

$$Q = SE(2) \times (-\hat{\varphi}, \hat{\varphi}) \times (-\hat{\varphi}, \hat{\varphi}) \tag{5.6}$$

*with $(\theta, x, y) \in SE(2)$, $\varphi_f \in (-\hat{\varphi}, \hat{\varphi})$, and $\varphi_r \in (-\hat{\varphi}, \hat{\varphi})$. The steering limit of the front and rear axle satisfies $0 < \hat{\varphi} < \frac{\pi}{2}$.*

The configuration $q$ and the configuration space $Q$ of the BSR are the same as in Definition 5.0.1 of the FKM. The steering limit $\hat{\varphi} < \frac{\pi}{2}$ is required since otherwise, the constraint distribution of the BSR is not regular as shown in Section 5.3.2. For real-world robots, considerably smaller values of $\hat{\varphi}$ result from the restricted displacement of the steerable wheels due to the mechanical setup of the robots.

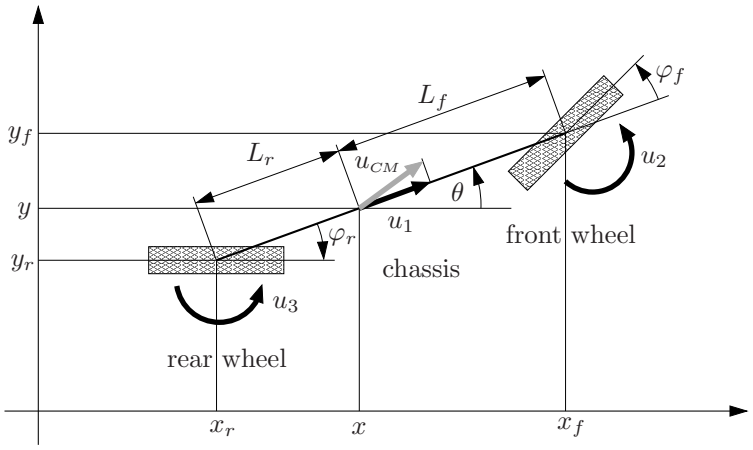


Figure 5.6: Detailed model of the bi-steerable robot.

**Definition 5.2.2** *(Configuration space of the idealized BSR) The configuration space of the idealized BSR is*

$$Q^* = SE(2) \times SO(2) \times SO(2)\,. \tag{5.7}$$

The idealized BSR has the same configuration $q = (\theta, x, y, \varphi_f, \varphi_r)$ as the BSR, but the configuration space $Q^*$ (5.7) instead of $Q$ (5.6). The steering angles $(\varphi_f, \varphi_r)$ of the idealized BSR are unrestricted, i. e., the steerable axles can make complete rotations. The idealized BSR is of theoretical interest for the analysis of the BSR, as it shows the effects of unrestricted steering angles. In [5], a car-like robot with unrestricted steering angle $\varphi_f$ is considered.

### 5.2.2 Kinematics of the bicycle model

For the kinematics of the bicycle model, the following assumption holds.

**Assumption 5.2.3** *(Kinematics of the bicycle model of the BSR) The front and rear wheel of the bicycle model of the BSR act as blades which can change their heading directions and move forward or backward with respect to these directions.*

Considering the wheels as blades makes sense as the rotation of the wheels around their rotation axes is neglected. The heading directions of the wheels relative to the $x$-axis are $\theta+\varphi_f$ and $\theta + \varphi_r$. The blades cannot slide laterally, i. e., no motions orthogonal to their heading directions can occur.

**Lemma 5.2.4** *(Velocities of the wheels of the bicycle model) Under Assumption 5.2.3, the velocities $v_f$ and $v_r$ of the front and rear wheel of the bicycle model are*

$$v_f = \begin{bmatrix} \dot{x}_f \\ \dot{y}_f \end{bmatrix} = \begin{bmatrix} \dot{x} - L_f\,\dot{\theta}\,\sin(\theta) \\ \dot{y} + L_f\,\dot{\theta}\,\cos(\theta) \end{bmatrix}, \quad v_r = \begin{bmatrix} \dot{x}_r \\ \dot{y}_r \end{bmatrix} = \begin{bmatrix} \dot{x} + L_r\,\dot{\theta}\,\sin(\theta) \\ \dot{y} - L_r\,\dot{\theta}\,\cos(\theta) \end{bmatrix} \tag{5.8}$$

*and satisfy*

$$\begin{aligned} \dot{x}_f \sin(\theta+\varphi_f) - \dot{y}_f \cos(\theta+\varphi_f) &= 0, \\ \dot{x}_r \sin(\theta+\varphi_r) - \dot{y}_r \cos(\theta+\varphi_r) &= 0. \end{aligned} \tag{5.9}$$

**Proof** According to Figure 5.6, the positions of the front and rear wheel are

$$r_f = \begin{bmatrix} x_f \\ y_f \end{bmatrix} = \begin{bmatrix} x + L_f\cos(\theta) \\ y + L_f\sin(\theta) \end{bmatrix}, \quad r_r = \begin{bmatrix} x_r \\ y_r \end{bmatrix} = \begin{bmatrix} x - L_r\cos(\theta) \\ y - L_r\sin(\theta) \end{bmatrix}.$$

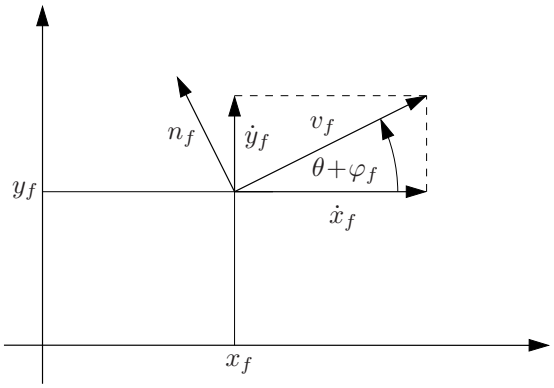


Figure 5.7: Velocity of the front wheel of the bi-steerable robot.

Differentiating these positions with respect to time gives the velocities $v_f$ and $v_r$ as in (5.8).

Because of Assumption 5.2.3, the velocities of the wheels orthogonal to their heading directions vanish. Figure 5.7 shows the velocity $v_f$ with direction $\theta + \varphi_f$ and a unit vector $n_f$ orthogonal to $v_f$. As $v_f$ can be written as

$$v_f = \begin{bmatrix} \dot{x}_f \\ \dot{y}_f \end{bmatrix} = \sqrt{\dot{x}_f^2 + \dot{y}_f^2} \begin{bmatrix} \cos(\theta + \varphi_f) \\ \sin(\theta + \varphi_f) \end{bmatrix},$$

the unit vector $n_f$ orthogonal to $v_f$ is

$$n_f = \begin{bmatrix} -\sin(\theta + \varphi_f) \\ \cos(\theta + \varphi_f) \end{bmatrix}.$$

The scalar product

$$v_f^\top n_f = \begin{bmatrix} \dot{x}_f & \dot{y}_f \end{bmatrix} \begin{bmatrix} -\sin(\theta + \varphi_f) \\ \cos(\theta + \varphi_f) \end{bmatrix} = -\dot{x}_f \sin(\theta + \varphi_f) + \dot{y}_f \cos(\theta + \varphi_f)$$

equals zero because of the orthogonality of $v_f$ and $n_f$. This gives the upper equation of (5.9). The lower equation is obtained from the scalar product of the velocity $v_r$ of the rear wheel with direction $\theta + \varphi_r$ represented by

$$v_r = \begin{bmatrix} \dot{x}_r \\ \dot{y}_r \end{bmatrix} = \sqrt{\dot{x}_r^2 + \dot{y}_r^2} \begin{bmatrix} \cos(\theta + \varphi_r) \\ \sin(\theta + \varphi_r) \end{bmatrix}$$

and the unit vector

$$n_r = \begin{bmatrix} -\sin(\theta + \varphi_r) \\ \cos(\theta + \varphi_r) \end{bmatrix}$$

orthogonal to $v_r$. ■

### 5.2.3 Velocity constraint and constraint distribution

**Theorem 5.2.5** *(Velocity constraint and constraint distribution of the BSR) For the BSR with configuration space $Q$ (5.6) and velocities (5.8) of the front and rear wheel,*

$$\underbrace{\begin{bmatrix} -L_f\cos(\varphi_f) & \sin(\theta+\varphi_f) & -\cos(\theta+\varphi_f) & 0 & 0 \\ L_r\cos(\varphi_r) & \sin(\theta+\varphi_r) & -\cos(\theta+\varphi_r) & 0 & 0 \end{bmatrix}}_{A(q)} \begin{bmatrix} \dot\theta \\ \dot x \\ \dot y \\ \dot\varphi_f \\ \dot\varphi_r \end{bmatrix} = \begin{bmatrix} 0 \\ 0 \end{bmatrix} \tag{5.10}$$

*is a regular velocity constraint 3.2.2 of dimension $k = 2$ for all $q \in Q$. The distribution*

$$D = \operatorname{span}\{X_1, X_2, X_3\}$$

*generated by the globally defined vector fields*

$$X_1(q) = \begin{bmatrix} \frac{1}{L_f+L_r}\sin(\varphi_f-\varphi_r) \\ \frac{1}{L_f+L_r}\Big(L_f\cos(\varphi_f)\cos(\theta+\varphi_r) + L_r\cos(\varphi_r)\cos(\theta+\varphi_f)\Big) \\ \frac{1}{L_f+L_r}\Big(L_f\cos(\varphi_f)\sin(\theta+\varphi_r) + L_r\cos(\varphi_r)\sin(\theta+\varphi_f)\Big) \\ 0 \\ 0 \end{bmatrix}, X_2 = \begin{bmatrix} 0 \\ 0 \\ 0 \\ 1 \\ 0 \end{bmatrix}, X_3 = \begin{bmatrix} 0 \\ 0 \\ 0 \\ 0 \\ 1 \end{bmatrix}$$

*is a constraint distribution 3.2.4 of the constraint (5.10) of rank $m = 3$ for all $q \in Q$.*

**Proof** Evaluating the velocities $v_f$ and $v_r$ as in (5.8) with the equations (5.9) gives

$$\begin{aligned} -L_f\,\dot\theta\,\cos(\varphi_f) + \dot x\,\sin(\theta+\varphi_f) - \dot y\,\cos(\theta+\varphi_f) &= 0, \\ L_r\,\dot\theta\,\cos(\varphi_r) + \dot x\,\sin(\theta+\varphi_r) - \dot y\,\cos(\theta+\varphi_r) &= 0. \end{aligned}$$

This is equivalent to (5.10), which is a velocity constraint of the form $A(q)\,\dot q = 0$.

To prove that the velocity constraint is regular, it is shown that there are no singular configurations in $Q$ at which $A(q)$ drops rank, i. e., $\operatorname{rk} A(q) = 2$ holds for all $q \in Q$. By inspection, $A(q) \neq 0$ is true for all $q \in Q$, leading to $\operatorname{rk} A(q) \geq 1$ for all $q \in Q$. For $\operatorname{rk} A(q) = 1$,

$$\begin{aligned} \det\begin{bmatrix} \sin(\theta+\varphi_f) & -\cos(\theta+\varphi_f) \\ \sin(\theta+\varphi_r) & -\cos(\theta+\varphi_r) \end{bmatrix} &= -\cos(\theta+\varphi_r)\sin(\theta+\varphi_f) + \cos(\theta+\varphi_f)\sin(\theta+\varphi_r) \\ &= -\sin(\varphi_f-\varphi_r) \\ &= 0 \end{aligned} \tag{5.11}$$

has to hold. For the configuration space $Q$ (5.6), $(\varphi_f, \varphi_r) \in (-\hat\varphi, \hat\varphi) \times (-\hat\varphi, \hat\varphi)$ for $0 < \hat\varphi < \frac{\pi}{2}$ is true. Thus, the steering angles $(\varphi_f, \varphi_r)$ satisfy $|\varphi_f| < \frac{\pi}{2}$ and $|\varphi_r| < \frac{\pi}{2}$. Then, condition (5.11) holds only for $\varphi_f - \varphi_r = 0$, from which $\varphi_f = \varphi_r$ results. Plugging $\varphi_f = \varphi_r$ in $A(q)$ gives

$$A(q) = \begin{bmatrix} -L_f\cos(\varphi_r) & \sin(\theta+\varphi_r) & -\cos(\theta+\varphi_r) & 0 & 0 \\ L_r\cos(\varphi_r) & \sin(\theta+\varphi_r) & -\cos(\theta+\varphi_r) & 0 & 0 \end{bmatrix}.$$

As $\sin(\theta+\varphi_r)$ and $\cos(\theta+\varphi_r)$ cannot be zero simultaneously, $\operatorname{rk} A(q) = 1$ is satisfied only if

$$-L_f\cos(\varphi_r) = L_r\cos(\varphi_r) \tag{5.12}$$

holds. However, $\cos(\varphi_r) > 0$ is always true for $|\varphi_r| < \frac{\pi}{2}$, and $L_f > 0$ and $L_r > 0$ applies. Thus, there is no $\varphi_r$ which satisfies (5.12), and $\operatorname{rk} A(q) = 2$ holds for all $|\varphi_r| < \frac{\pi}{2}$. Consequently, there are no singular configurations of $A(q)$ in $Q$, and the velocity constraint (5.10) is regular.

For $\varphi_f \neq \varphi_r$, the first element of $X_1(q)$ satisfies $\frac{1}{L_f+L_r}\sin(\varphi_f - \varphi_r) \neq 0$ due to $|\varphi_f - \varphi_r| < \pi$ for $|\varphi_f| < \frac{\pi}{2}$ and $|\varphi_r| < \frac{\pi}{2}$. For $\varphi_f = \varphi_r$, there holds $\|X_1(q)\| = \cos^2(\varphi_f) > 0$ for $|\varphi_f| < \frac{\pi}{2}$. Thus, the vector field $X_1(q)$ is defined and satisfies $X_1(q) \neq 0$ for all $q \in Q$. The vector fields $X_2$ and $X_3$ are defined for all $q \in Q$ and satisfy $X_i \neq 0$. Hence, $D = \operatorname{span}\{X_1, X_2, X_3\}$ is a distribution of constant rank $m = 3$ for all $q \in Q$. By inspection, $\ker A(q) = D(q)$ holds, and $D$ is a constraint distribution 3.2.4. ■

In Section 5.3.2, it is shown that the velocity constraint (5.10) is completely nonholonomic. For $g_1(q) := X_1(q)$, $q_2 := X_2$, and $g_3 := X_3$, the FKM 5.0.1 of the BSR results. The inputs $(u_1, u_2, u_3)$ of the FKM are depicted in Figure 5.6. The velocity $u_1$ is the driving input. It is the longitudinal velocity of the robot, i. e., the projection of the instantaneous velocity $u_{CM}$ of the center of mass on the longitudinal axis of the BSR. To obtain $u_1$, the velocity $u_{CM}$ of the robot is projected on its longitudinal axis with orientation angle $\theta$. Using the input $u_1$ instead of $u_{CM}$ allows to set $g_1(q) = X_1(q)$. Otherwise, for the input $u_{CM}$, the input vector field $\tilde{g}_1$ satisfying $\dot{q} = \tilde{g}_1(q)\, u_{CM} + g_2\, u_2 + g_3\, u_3$ has to be used, which has more complicated elements than $g_1$. The inputs $u_2$ and $u_3$ give the steering rates $\dot{\varphi}_f$ and $\dot{\varphi}_r$ of the front and rear axle. If the steering angles $\varphi_f$ and $\varphi_r$ are treated as inputs and the distances $L_f$ and $L_r$ are set to $L_f = L_r = \frac{1}{2}$, the RKM 5.0.2 of the BSR is obtained.

For the idealized BSR with configuration space $Q^*$ (5.7), steering angles $\varphi_f = \pm\frac{\pi}{2}$ and $\varphi_r = \pm\frac{\pi}{2}$ are permitted. For theses steering angles, the matrix $A(q)$ gives

$$A(q) = \begin{bmatrix} 0 & \operatorname{sgn}(\varphi_f)\cos(\theta) & \operatorname{sgn}(\varphi_f)\sin(\theta) & 0 & 0 \\ 0 & \operatorname{sgn}(\varphi_r)\cos(\theta) & \operatorname{sgn}(\varphi_r)\sin(\theta) & 0 & 0 \end{bmatrix},$$

and $\operatorname{rk} A(q) = 1$ holds. Thus, configurations with $\varphi_f = \pm\frac{\pi}{2}$ and $\varphi_r = \pm\frac{\pi}{2}$ are singular. Hence, for the idealized BSR, the constraint (5.10) is no regular velocity constraint 3.2.2.

Using $L_f = L_r$ or $L_f \neq L_r$ does not affect Theorem 5.2.5. Setting $L_f = L_r = L$ and $\varphi_f = -\varphi_r = \varphi$ gives the matrix $A(q)$ of the nonholonomic constraint (3.17) of the snakeboard. Regarding the velocity variables $(\dot{\theta}, \dot{x}, \dot{y})$ affected by $A(q)$, the snakeboard and the BSR have the same constraint. As discussed in [22], configurations with $\varphi = \pm\frac{\pi}{2}$ are omitted from the analysis of the snakeboard, as the matrix $A(q)$ drops rank there. These singular configurations correspond to the singular configurations of the matrix $A(q)$ of the BSR.

## 5.3 Model analysis

In this section, the FKM and RKM of the BSR are analyzed. Regarding controllability of the BSR in Section 5.3.1 and integrability of the constraint distribution in Section 5.3.2, the idealized BSR is considered as well to compare the results obtained for the configuration spaces $Q$ and $Q^*$. In Section 5.3.3, properties of the RKM relevant for time-optimal control are given.

### 5.3.1 Controllability

**Theorem 5.3.1** *(Controllability of the FKM of the BSR) The FKM 5.0.1 is controllable.*

**Proof** According to Theorem 3.1.20, a driftless affine control system with proper input space is controllable if and only if it is accessible at every $q \in Q$. The FKM 5.0.1 is a driftless affine control system. Its input space $U = [-\hat{u}_1, \hat{u}_1] \times [-\hat{u}_2, \hat{u}_2] \times [-\hat{u}_3, \hat{u}_3]$ is proper.

To show that the FKM is accessible at every $q \in Q$, its accessibility distribution $\Delta_A$ is considered, which is the involutive closure of the distribution of the vector fields $g_1$, $g_2$, and $g_3$.

Using the Lie brackets

$$[g_1, g_2](q) = \begin{bmatrix} -\frac{1}{L_f+L_r}\cos(\varphi_f - \varphi_r) \\ \frac{1}{L_f+L_r}\Big(L_f \sin(\varphi_f)\cos(\theta+\varphi_r) + L_r \cos(\varphi_r)\sin(\theta+\varphi_f)\Big) \\ \frac{1}{L_f+L_r}\Big(L_f \sin(\varphi_f)\sin(\theta+\varphi_r) - L_r \cos(\varphi_r)\cos(\theta+\varphi_f)\Big) \\ 0 \\ 0 \end{bmatrix}$$

and

$$[g_1, g_3](q) = \begin{bmatrix} \frac{1}{L_f+L_r}\cos(\varphi_f - \varphi_r) \\ \frac{1}{L_f+L_r}\Big(L_f \cos(\varphi_f)\sin(\theta+\varphi_r) + L_r \sin(\varphi_r)\cos(\theta+\varphi_f)\Big) \\ \frac{1}{L_f+L_r}\Big(-L_f \cos(\varphi_f)\cos(\theta+\varphi_r) + L_r \sin(\varphi_r)\sin(\theta+\varphi_f)\Big) \\ 0 \\ 0 \end{bmatrix},$$

the accessibility distribution is

$$\Delta_A = \operatorname{span}\left\{g_1, g_2, g_3, [g_1, g_2], [g_1, g_3]\right\}. \tag{5.13}$$

According to the Theorem of Chow, a control system is accessible if the Lie algebra rank condition $\dim \Delta_A(q) = p$ holds for all $q \in Q$. The matrix $[g_1(q), g_2, g_3, [g_1, g_2](q), [g_1, g_3](q)]$ has constant rank $p = 5$ for all $q \in Q$, as

$$\det\left[g_1(q), g_2, g_3, [g_1, g_2](q), [g_1, g_3](q)\right] = -\frac{1}{L_f + L_r}\cos(\varphi_f)\cos(\varphi_r) \neq 0 \tag{5.14}$$

holds for $|\varphi_f| < \frac{\pi}{2}$ and $|\varphi_r| < \frac{\pi}{2}$. Hence, the Lie algebra rank condition is satisfied for all $q \in Q$, and the FKM is accessible by the Theorem of Chow and controllable by Theorem 3.1.20. ■

Like Theorem 5.2.5, Theorem 5.3.1 does not depend on $L_f = L_r$ or $L_f \neq L_r$.

To analyze the accessibility of the FKM of the idealized BSR with configuration space $Q^*$ (5.7), steering angles $\varphi_f \in [-\pi, \pi)$ and $\varphi_r \in [-\pi, \pi)$ have to be considered, as the trigonometric functions in the elements of $g_1$ are periodic with period $2\,\pi$. Then, condition (5.14) does not hold at specific configurations which do not satisfy $|\varphi_f| < \frac{\pi}{2}$ and $|\varphi_r| < \frac{\pi}{2}$. Instead of the single accessibility distribution (5.13), the Lie algebra rank condition has to be checked for several accessibility distributions. For configurations with $\varphi_f \neq \pm\frac{\pi}{2}$ and $\varphi_r \neq \pm\frac{\pi}{2}$, distribution (5.13) satisfies the Lie algebra rank condition. For configurations with $\varphi_f \notin \{-\pi, 0\}$ and $\varphi_r \neq \pm\frac{\pi}{2}$, the accessibility distribution

$$\Delta_A = \operatorname{span}\left\{g_1, g_2, g_3, [g_1, g_2], [g_2, [g_1, g_3]]\right\} \tag{5.15}$$

meets the Lie algebra rank condition for the Lie bracket

$$[g_2, [g_1, g_3]](q) = \begin{bmatrix} -\frac{1}{L_f+L_r}\sin(\varphi_f - \varphi_r) \\ -\frac{1}{L_f+L_r}\Big(L_f \sin(\varphi_f)\sin(\theta+\varphi_r) - L_r \sin(\varphi_r)\sin(\theta+\varphi_f)\Big) \\ \frac{1}{L_f+L_r}\Big(L_f \sin(\varphi_f)\cos(\theta+\varphi_r) + L_r \sin(\varphi_r)\cos(\theta+\varphi_f)\Big) \\ 0 \\ 0 \end{bmatrix},$$

since

$$\det\left[g_1(q)\,,g_2,g_3,[g_1,g_2](q)\,,[g_2,[g_1,g_3]](q)\right]=\frac{1}{L_f+L_r}\sin(\varphi_f)\cos(\varphi_r)\neq 0$$

holds. For configurations with $\varphi_f \neq \pm\frac{\pi}{2}$ and $\varphi_r \notin \{-\pi, 0\}$, the accessibility distribution

$$\Delta_A=\operatorname{span}\left\{g_1,g_2,g_3,[g_1,g_3]\,,[g_2,[g_1,g_3]]\right\} \tag{5.16}$$

satisfies the Lie algebra rank condition due to

$$\det\left[g_1(q)\,,g_2,g_3,[g_1,g_3](q)\,,[g_2,[g_1,g_3]](q)\right]=-\frac{1}{L_f+L_r}\cos(\varphi_f)\sin(\varphi_r)\neq 0.$$

Finally, for configurations with $\varphi_f \notin \{-\pi, 0\}$ and $\varphi_r \notin \{-\pi, 0\}$, the accessibility distribution

$$\Delta_A=\operatorname{span}\left\{g_2,g_3,[g_1,g_2]\,,[g_1,g_3]\,,[g_2,[g_1,g_3]]\right\} \tag{5.17}$$

meets the Lie algebra rank condition because of

$$\det\left[g_2,g_3,[g_1,g_2](q)\,,[g_1,g_3](q)\,,[g_2,[g_1,g_3]](q)\right]=-\frac{1}{L_f+L_r}\sin(\varphi_f)\sin(\varphi_r)\neq 0.$$

By choosing the right distribution from (5.13), (5.15), (5.16), and (5.17) depending on $q$, accessibility of the FKM of the idealized BSR results from the Theorem of Chow. Thus, controllability follows from Theorem 3.1.20.

It is more complex to show controllability for the idealized BSR with configuration space $Q^*$ (5.7) than for the BSR with configuration space $Q$ (5.6), since for specific configurations, iterated Lie brackets of degree $d = 3$ instead of degree $d = 2$ are required for accessibility. Thus, path planning for the idealized BSR is more complex in general.

**Theorem 5.3.2** *(Controllability of the RKM of the BSR) The RKM 5.0.2 is controllable.*

**Proof** According to Theorem 3.1.21, a driftless control system is controllable if it is symmetric and if for all $q \in Q$, there are inputs $u_i \in U$ resulting in $p$ vector fields $f(q, u_i)$ such that $\dim\operatorname{span}\{f(q,u_1),\ldots,f(q,u_p)\} = p$ holds for all $q \in Q$. The RKM 5.0.2 is a driftless control system which is symmetric, since for every $\dot{q}_r = g(\theta,\varphi)\,v$ obtained for some input $u_r = (v, \varphi_f, \varphi_r)$, the input $\tilde{u}_r = (-v, \varphi_f, \varphi_r)$ gives $-g(\theta,\varphi)\,v$. As the input space $U_r = [-\hat{v}, \hat{v}] \times [-\hat{\varphi}, \hat{\varphi}] \times [-\hat{\varphi}, \hat{\varphi}]$ is symmetric, $\tilde{u}_r \in U_r$ holds for each $u_r \in U_r$.

The constant inputs $u_{r1} = (v, 0, 0)$, $u_{r2} = (v, \varphi, \varphi)$, $u_{r3} = (v, \varphi, -\varphi)$ give the vector fields

$$f(q,u_1)=\begin{bmatrix}0\\ \cos(\theta)\\ \sin(\theta)\end{bmatrix}v,\; f(q,u_2)=\begin{bmatrix}0\\ \cos(\varphi)\cos(\theta+\varphi)\\ \sin(\varphi)\sin(\theta+\varphi)\end{bmatrix}v,\; f(q,u_3)=\begin{bmatrix}\sin(2\varphi)\\ \cos^2(\varphi)\cos(\theta)\\ \cos^2(\varphi)\sin(\theta)\end{bmatrix}v.$$

For $v \neq 0$ and $0 < |\varphi| < \frac{\pi}{2}$,

$$\det\left[f(q,u_1)\,,f(q,u_2)\,,f(q,u_3)\right]=2\,v^3\cos^2(\varphi)\sin^2(\varphi)\neq 0$$

results. Thus, $\dim\operatorname{span}\{f(q,u_1)\,,f(q,u_2)\,,f(q,u_3)\} = 3$ holds for all $q_r \in Q_r$, and the RKM is controllable. ■

## 5.3.2 Integrability of the constraint distribution

**Corollary 5.3.3** *(Nonholonomic constraint of the BSR) The velocity constraint (5.10) of the BSR is a nonholonomic constraint 3.2.3.*

**Proof** According to Theorem 5.2.5, the constraint (5.10) is a regular velocity constraint 3.2.2. To prove that it is a nonholonomic constraint 3.2.3, it has to be shown that the constraint is completely nonholonomic, for which Theorem 3.2.6 is applied.

As the RKM is a real analytic system, the involutive closure $\bar{D}$ of the constraint distribution $D = \operatorname{span}\{X_1, X_2, X_3\}$ can be identified with the accessibility distribution $\Delta_A = \operatorname{span}\{g_1, g_2, g_3, [g_1, g_2], [g_1, g_3]\}$ of the RKM given by (5.13). The accessibility distribution has full rank $\dim \Delta_A(q) = p$ for all $q \in Q$ as shown in the proof of Theorem 5.3.1. Thus, the involutive closure $\bar{D}$ of the constraint distribution has full rank $p$ for all $q \in Q$ as well, and the velocity constraint (5.10) is completely nonholonomic. ■

As before, Corollary 5.3.3 does not dependent on $L_f = L_r$ or $L_f \neq L_r$.

For the idealized BSR with configuration space $Q^*$, the constraint (5.10) is no regular velocity constraint at configurations with $\varphi_f = \pm\frac{\pi}{2}$ and $\varphi_r = \pm\frac{\pi}{2}$, see Section 5.2.3. According to Definition 3.2.3, a velocity constraint $A(q)\,\dot{q} = 0$ has to be regular to be qualified for a nonholonomic constraint. Thus, for the idealized BSR with configuration space $Q^*$, the constraint (5.10) cannot be a nonholonomic constraint 3.2.3. Nevertheless, the idealized BSR is controllable as shown in Section 5.3.1. This is true as the Lie algebra rank condition holds if the right accessibility distribution is chosen depending on the configuration $q$.

### 5.3.3 System properties of the reduced kinematic model

In the following, several properties of the RKM 5.0.2 including the absolute translational velocity, the norm of the right-hand side of system (5.4), the minimal turning radius, and the representation of the RKM as left-invariant control system on $SE(2)$ are discussed. The properties are used in the subsequent chapters, where time-optimal control of the RKM is addressed.

**Lemma 5.3.4** *(Absolute translational velocity of the RKM) The absolute translational velocity* $|v_t| := \sqrt{\dot{x}^2 + \dot{y}^2}$ *of the RKM is*

$$|v_t| = \sqrt{\frac{1}{8}\Big(3 + 2\cos(2\,\varphi_f) + \cos(2\,(\varphi_f - \varphi_r)) + 2\cos(2\,\varphi_r)\Big)}\,|v|\,. \tag{5.18}$$

*For* $|v| = \hat{v}$ *and* $\hat{\varphi} = \frac{\pi}{4}$*, the absolute translational velocity satisfies*

$$|v_t| \leq \hat{v}. \tag{5.19}$$

*The maximal value* $|v_t| = \hat{v}$ *is obtained at* $\varphi = (0, 0)$*.*

**Proof** For $\dot{x} = g_2(\theta, \varphi)\,v$ and $\dot{y} = g_3(\theta, \varphi)\,v$ given by (5.4),

$$\begin{aligned}
\dot{x}^2 + \dot{y}^2 \;=\; & \tfrac{v^2}{4}\Big(\cos^2(\varphi_f)\big(\cos^2(\theta+\varphi_r)+\sin^2(\theta+\varphi_r)\big)+\cos^2(\varphi_r)\big(\cos^2(\theta+\varphi_f)+\sin^2(\theta+\varphi_f)\big)\\
& +2\,\cos(\varphi_f)\,\cos(\varphi_r)\,(\cos(\theta+\varphi_f)\,\cos(\theta+\varphi_r)+\sin(\theta+\varphi_f)\,\sin(\theta+\varphi_r))\Big)\\
\overset{(1)}{=}\; & \tfrac{v^2}{4}\Big(\cos^2(\varphi_f)+\cos^2(\varphi_r)+2\,\cos(\varphi_f)\,\cos(\varphi_r)\,\cos(\varphi_f-\varphi_r)\Big)\\
\overset{(2)}{=}\; & \tfrac{v^2}{4}\Big(\tfrac{1}{2}\,(1+\cos(2\,\varphi_f))+\tfrac{1}{2}\,(1+\cos(2\,\varphi_r))\\
& +\tfrac{1}{2}\,(1+\cos(2\,\varphi_f)+\cos(2\,(\varphi_f-\varphi_r))+\cos(2\,\varphi_r))\Big)\\
=\; & \tfrac{v^2}{8}\Big(3+2\cos(2\,\varphi_f)+\cos(2\,(\varphi_f-\varphi_r))+2\cos(2\,\varphi_r)\Big)
\end{aligned}$$

holds. Here, for (1),

$$\cos^2(\alpha) + \sin^2(\alpha) = 1$$

and

$$\cos(\alpha)\cos(\beta) + \sin(\alpha)\sin(\beta) = \cos(\alpha - \beta)$$

is applied, and for (2),

$$\cos^2(\alpha) = \frac{1}{2}\left(1 + \cos(2\,\alpha)\right)$$

and

$$\cos(\alpha)\cos(\beta)\cos(\gamma) = \frac{1}{4}\left(\cos(\alpha+\beta-\gamma) + \cos(\beta+\gamma-\alpha) + \cos(\gamma+\alpha-\beta) + \cos(\alpha+\beta+\gamma)\right)$$

is used. Then, for $|v_t| = \sqrt{\dot{x}^2 + \dot{y}^2}$, (5.18) follows from

$$\dot{x}^2 + \dot{y}^2 = \frac{v^2}{8}\left(3 + 2\cos(2\,\varphi_f) + \cos(2\,(\varphi_f - \varphi_r)) + 2\cos(2\,\varphi_r)\right).$$

To show that $|v_t| \leq \hat{v}$ holds for $|v| = \hat{v}$ and $\hat{\varphi} = \frac{\pi}{4}$ and that $|v_t| = \hat{v}$ is true for $\varphi = (0,0)$,

$$\sigma(\varphi_f, \varphi_r) := \frac{1}{v^2}\left(\dot{x}^2 + \dot{y}^2\right) = \frac{1}{8}\left(3 + 2\cos(2\,\varphi_f) + \cos(2\,(\varphi_f - \varphi_r)) + 2\cos(2\,\varphi_r)\right)$$

is considered for $|\varphi_f| \leq \hat{\varphi} = \frac{\pi}{4}$ and $|\varphi_r| \leq \hat{\varphi} = \frac{\pi}{4}$. Then, $|v_t| = \sqrt{\sigma}\,\hat{v}$ holds. The derivatives of $\sigma$ with respect to $\varphi_f$ and $\varphi_r$ are

$$\begin{aligned}
\frac{\partial \sigma}{\partial \varphi_f} &= \tfrac{1}{4}\left(-2\sin(2\,\varphi_f) - \sin(2\,(\varphi_f - \varphi_r))\right), \\
\frac{\partial \sigma}{\partial \varphi_r} &= \tfrac{1}{4}\left(\sin(2\,(\varphi_f - \varphi_r)) - 2\sin(2\,\varphi_f)\right).
\end{aligned}$$

If $\sigma$ has an extremum, $\partial\sigma/\partial\varphi_f = \partial\sigma/\partial\varphi_r = 0$ holds, and

$$\frac{\partial \sigma}{\partial \varphi_f} + \frac{\partial \sigma}{\partial \varphi_r} = -\tfrac{1}{2}\left(\sin(2\,\varphi_f) + \sin(2\,\varphi_r)\right) = 0 \tag{5.20}$$

holds as well. For $|\varphi_f| \leq \frac{\pi}{4}$ and $|\varphi_r| \leq \frac{\pi}{4}$, (5.20) implies $\varphi_r = -\varphi_f$. Then,

$$\tilde{\sigma}(\varphi_f) := \sigma(\varphi_f, -\varphi_f) = \cos^4(\varphi_f)$$

results. For $|\varphi_f| \leq \frac{\pi}{4}$, the maximal value of $\tilde{\sigma}(\varphi_f)$ is 1, which is obtained at $\varphi_f = 0$. If $\varphi_r = -\varphi_f$ is applied, $\sigma$ takes its maximal value 1 at $\varphi = (0,0)$. Then, $|v_t| \leq \hat{v}$ and $|v_t| = \hat{v}$ for $\varphi = (0,0)$ arises from $|v_t| = \sqrt{\sigma}\,\hat{v}$, and Lemma 5.3.4 is true. ■

The absolute translational velocity $|v_t|$ depends on $(\varphi_f, \varphi_r)$ and is not constant for constant $|v|$. Thus, time-optimal solutions of the RKM are in general no shortest paths, see Section 8.5.

**Lemma 5.3.5** *(Norm of the right-hand side of the RKM) The norm of the right-hand side of system (5.4) is*

$$\|g(\theta,\varphi)\ v\| = \sqrt{\frac{1}{8}\Big(7 + 2\,\cos(2\,\varphi_f) - 3\,\cos(2\,(\varphi_f - \varphi_r)) + 2\,\cos(2\,\varphi_r)\Big)}\,|v|\,. \tag{5.21}$$

*For $|v| = \hat{v}$ and $\hat{\varphi} = \frac{\pi}{4}$, the norm satisfies*

$$\hat{v} \leq \|g(\theta,\varphi)\ v\| \leq \frac{2}{\sqrt{3}}\,\hat{v}. \tag{5.22}$$

**Proof** The norm of the right-hand side of system (5.4) is $\|g(\theta,\varphi)\ v\| = \sqrt{\dot\theta^2+\dot x^2+\dot y^2}$. Using $\dot\theta = \sin(\varphi_f-\varphi_r)\,v$ according to (5.4) and $\dot x^2+\dot y^2 = |v_t|^2$ with $|v_t|$ given by (5.18),

$$\begin{aligned}\dot\theta^2+\dot x^2+\dot y^2 &= \sin^2(\varphi_f-\varphi_r)\,v^2 + \tfrac{v^2}{8}\left(3+2\cos(2\,\varphi_f)+\cos(2\,(\varphi_f-\varphi_r))+2\cos(2\,\varphi_r)\right)\\ &= \tfrac{v^2}{8}\Big(7+2\cos(2\,\varphi_f)-3\cos(2\,(\varphi_f-\varphi_r))+2\cos(2\,\varphi_r)\Big)\end{aligned}$$

results for

$$\sin^2(\alpha) = \frac{1}{2}\left(1-\cos(2\,\alpha)\right).$$

Thus, $\|g(\theta,\varphi)\ v\| = \sqrt{\dot\theta^2+\dot x^2+\dot y^2}$ gives (5.21).

To obtain the bounds (5.22) on $\|g(\theta,\varphi)\ v\|$ for $|v|=\hat v$ and $\hat\varphi=\frac{\pi}{4}$,

$$\omega(\varphi_f,\varphi_r) := \frac{1}{v^2}\left(\dot\theta^2+\dot x^2+\dot y^2\right) = \frac{1}{8}\Big(7+2\cos(2\,\varphi_f)-3\cos(2\,(\varphi_f-\varphi_r))+2\cos(2\,\varphi_r)\Big)$$

is considered for $|\varphi_f|\le\hat\varphi=\frac{\pi}{4}$ and $|\varphi_r|\le\hat\varphi=\frac{\pi}{4}$. Then, $\|g(\theta,\varphi)\ v\| = \sqrt{\omega}\,\hat v$ holds. The derivatives of $\omega$ with respect to $\varphi_f$ and $\varphi_r$ are

$$\begin{aligned}\frac{\partial\omega}{\partial\varphi_f} &= \tfrac{1}{4}\left(-2\sin(2\,\varphi_f)+3\sin(2\,(\varphi_f-\varphi_r))\right),\\ \frac{\partial\omega}{\partial\varphi_r} &= \tfrac{1}{4}\left(-3\sin(2\,(\varphi_f-\varphi_r))-2\sin(2\,\varphi_f)\right).\end{aligned}$$

If $\omega$ has an extremum, $\partial\omega/\partial\varphi_f = \partial\omega/\partial\varphi_r = 0$ holds. Then,

$$\frac{\partial\omega}{\partial\varphi_f}+\frac{\partial\omega}{\partial\varphi_r} = -\tfrac{1}{2}\left(\sin(2\,\varphi_f)+\sin(2\,\varphi_r)\right) = 0 \tag{5.23}$$

is true as well. Because of $|\varphi_f|\le\frac{\pi}{4}$ and $|\varphi_r|\le\frac{\pi}{4}$, (5.23) implies $\varphi_r=-\varphi_f$, and

$$\tilde\omega(\varphi_f) := \omega(\varphi_f,-\varphi_f) = \frac{1}{2}\cos^2(\varphi_f)\left(5-3\cos(2\,\varphi_f)\right) \tag{5.24}$$

results. To obtain an extremum of $\tilde\omega$,

$$\frac{\partial\tilde\omega}{\partial\varphi_f} = \cos(\varphi_f)\left(-5\sin(\varphi_f)+3\sin(3\,\varphi_f)\right) = 0 \tag{5.25}$$

has to hold. For $|\varphi_f|\le\frac{\pi}{4}$, (5.25) holds for $\varphi_f=0$ and $\varphi_f=\pm\arccos\left(\sqrt{2/3}\right)$, and (5.24) gives

$$\tilde\omega(0)=1,\quad \tilde\omega\left(\pm\arccos\left(\sqrt{2/3}\right)\right)=\tfrac{4}{3},\quad \tilde\omega\left(\pm\tfrac{\pi}{4}\right)=\tfrac{5}{4}.$$

Thus, the minimal value of $\tilde\omega$ and $\omega$ is 1, and the maximal value is $\frac{4}{3}$. Hence, $\|g(\theta,\varphi)\ v\| = \sqrt{\omega}\,\hat v$ satisfies $\hat v\le\|g(\theta,\varphi)\ v\|\le 2/\sqrt{3}\,\hat v$. ■

For the conditions (5.19) and (5.22), $\hat\varphi=\frac{\pi}{4}$ is assumed, as this steering limit is used for time-optimal control of the RKM in the subsequent chapters. Besides, $|v|=\hat v$ applies, as $v(t)=\pm\hat v$ holds for the extremals for time-optimal control of the RKM for almost all $t$, see Section 6.1.1.

**Definition 5.3.6** *(Minimal turning radius) The radius of the smallest circle a wheeled mobile robot can drive is called minimal turning radius $R$.*

The Dubins paths and Reeds-Shepp paths described in Section 1.1 give the shortest paths of a car-like robot which can drive forward and forward and backward, respectively. These shortest paths consist of straight line segments and arcs of circles of minimal turning radius $R$. The radius $r$ of the osculating circle to a curve $(x, y)$ called radius of curvature is

$$r = \left| \frac{\left(\dot{x}^2 + \dot{y}^2\right)^{\frac{3}{2}}}{\dot{x}\,\ddot{y} - \ddot{x}\,\dot{y}} \right|, \tag{5.26}$$

see e. g. [16]. If the position of a wheeled mobile robot is described by $(x, y)$, the minimal possible value of $r$ is the minimal turning radius $R$.

**Lemma 5.3.7** *(Minimal turning radius of the RKM) For $0 < \hat{\varphi} < \frac{\pi}{2}$, the minimal turning radius of the RKM is*

$$R = \frac{1}{2} \cot(\hat{\varphi}) .$$

*It is obtained at $\varphi = (\pm\hat{\varphi}, \mp\hat{\varphi})$.*

**Proof** To determine the minimal turning radius $R$, the radius $r$ (5.26) is considered for $\dot{x} = g_2(\theta, \varphi)\, v$ and $\dot{y} = g_3(\theta, \varphi)\, v$ given by (5.4). For constant inputs $(v, \varphi_f, \varphi_r)$, i. e., for $\dot{v} = \dot{\varphi}_f = \dot{\varphi}_r = 0$,

$$\begin{aligned} \ddot{x} &= \frac{\partial g_2}{\partial \theta}\, \dot{\theta}\, v &&= -g_3(\theta, \varphi) \sin(\varphi_f - \varphi_r)\, v^2, \\ \ddot{y} &= \frac{\partial g_3}{\partial \theta}\, \dot{\theta}\, v &&= g_2(\theta, \varphi) \sin(\varphi_f - \varphi_r)\, v^2 \end{aligned}$$

results from $\dot{x} = g_2(\theta, \varphi)\, v$ and $\dot{y} = g_3(\theta, \varphi)\, v$ using $\dot{\theta} = \sin(\varphi_f - \varphi_r)\, v$, $\partial g_2/\partial\theta = -g_3(\theta, \varphi)$, and $\partial g_3/\partial\theta = g_2(\theta, \varphi)$. Then, (5.26) yields

$$r = \left| \frac{\left(g_2^2(\theta, \varphi)\, v^2 + g_3^2(\theta, \varphi)\, v^2\right)^{\frac{3}{2}}}{\left(g_2^2(\theta, \varphi)\, v^2 + g_3^2(\theta, \varphi)\, v^2\right) \sin(\varphi_f - \varphi_r)\, v} \right| = \left| \frac{\sqrt{g_2^2(\theta, \varphi)\, v^2 + g_3^2(\theta, \varphi)\, v^2}}{\sin(\varphi_f - \varphi_r)\, v} \right| .$$

For $\sqrt{g_2^2(\theta, \varphi)\, v^2 + g_3^2(\theta, \varphi)\, v^2} = \sqrt{\dot{x}^2 + \dot{y}^2} = |v_t|$ according to (5.18),

$$r = \left| \frac{\sqrt{\frac{1}{8}\Big(3 + 2\cos(2\,\varphi_f) + \cos(2\,(\varphi_f - \varphi_r)) + 2\cos(2\,\varphi_r)\Big)}}{\sin(\varphi_f - \varphi_r)} \right| \tag{5.27}$$

follows, which gives

$$r = \frac{\sqrt{\frac{1}{8}\Big(3 + 2\cos(2\,\varphi_f) + \cos(2\,(\varphi_f - \varphi_r)) + 2\cos(2\,\varphi_r)\Big)}}{\sin(\varphi_f - \varphi_r)}$$

for $\sin(\varphi_f - \varphi_r) > 0$. To determine the minimal turning radius, the derivatives

$$\begin{aligned} \frac{\partial r}{\partial \varphi_f} &= \frac{-\left(3\,\cos(\varphi_f) + \cos(\varphi_f - 2\,\varphi_r)\right)\cos(\varphi_r)}{\sqrt{2\,(3 + 2\cos(2\,\varphi_f) + \cos(2\,(\varphi_f - \varphi_r)) + 2\cos(2\,\varphi_r))}\,\sin^2(\varphi_f - \varphi_r)}, \\ \frac{\partial r}{\partial \varphi_r} &= \frac{\left(\cos(2\,\varphi_f - \varphi_r) + 3\,\cos(\varphi_r)\right)\cos(\varphi_f)}{\sqrt{2\,(3 + 2\cos(2\,\varphi_f) + \cos(2\,(\varphi_f - \varphi_r)) + 2\cos(2\,\varphi_r))}\,\sin^2(\varphi_f - \varphi_r)} \end{aligned}$$

are considered. Then, $\partial r/\partial\varphi_f = \partial r/\partial\varphi_r = 0$ holds for minimal $r$. From this, $\partial r/\partial\varphi_f + \partial r/\partial\varphi_r = 0$ follows, which gives

$$\frac{\partial r}{\partial \varphi_f} + \frac{\partial r}{\partial \varphi_r} = \frac{-\left(\sin(2\,\varphi_f) + \sin(2\,\varphi_r)\right)}{\sqrt{2\left(3 + 2\cos(2\,\varphi_f) + \cos(2\,(\varphi_f - \varphi_r)) + 2\cos(2\,\varphi_r)\right)}\sin(\varphi_f - \varphi_r)}.$$

For $\partial r/\partial\varphi_f + \partial r/\partial\varphi_r = 0$ to hold, $\sin(2\,\varphi_f) + \sin(2\,\varphi_r) = 0$ has to be satisfied. Because of $|\varphi_f| \leq \hat{\varphi}$ and $|\varphi_r| \leq \hat{\varphi}$ for $0 < \hat{\varphi} < \frac{\pi}{2}$, there results $\varphi_r = -\varphi_f$. Then, (5.27) yields

$$r = \frac{1}{2}\left|\cot(\varphi_f)\right|.$$

The minimal turning radius $R$ is obtained at $\varphi_f = \pm\hat{\varphi}$. This gives $\varphi = (\varphi_f, \varphi_r) = (\pm\hat{\varphi}, \mp\hat{\varphi})$ and $R = \frac{1}{2}\cot(\hat{\varphi})$. ■

For $0 < \hat{\varphi} < \frac{\pi}{2}$, Figure 5.8 shows the minimal turning radius $R = \frac{1}{2}\cot(\hat{\varphi})$ of the RKM. The radius $R$ goes to zero for $\hat{\varphi} \to \frac{\pi}{2}$. For the idealized BSR with unrestricted steering angles $(\varphi_f, \varphi_r)$, $R = 0$ holds, i. e., the robot can turn on the spot.

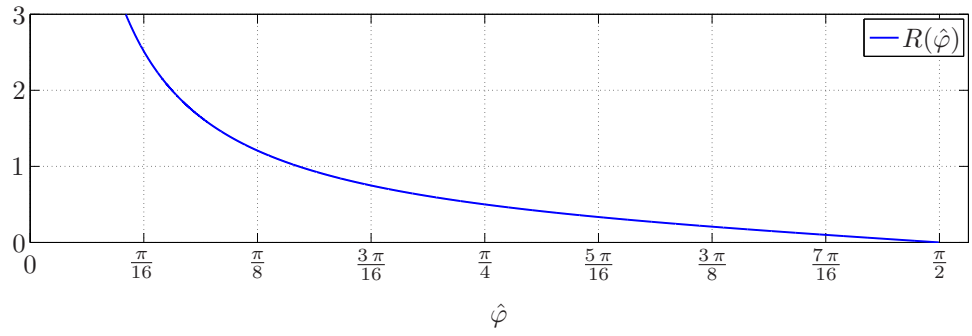


Figure 5.8: Minimal turning radius $R(\hat{\varphi})$ for $0 < \hat{\varphi} < \frac{\pi}{2}$.

Next, it is shown that the RKM can be written as left-invariant control system on $SE(2)$. For this, the configuration $q_r = (\theta, x, y)$ of the RKM is represented by the Lie group element

$$g = \begin{bmatrix} \cos(\theta) & -\sin(\theta) & x \\ \sin(\theta) & \cos(\theta) & y \\ 0 & 0 & 1 \end{bmatrix}. \tag{5.28}$$

As discussed in Section 3.1.2, the standard basis vectors of the associated Lie algebra $\mathfrak{se}(2)$ are

$$e_1 = \begin{bmatrix} 0 & -1 & 0 \\ 1 & 0 & 0 \\ 0 & 0 & 0 \end{bmatrix}, \quad e_2 = \begin{bmatrix} 0 & 0 & 1 \\ 0 & 0 & 0 \\ 0 & 0 & 0 \end{bmatrix}, \quad e_3 = \begin{bmatrix} 0 & 0 & 0 \\ 0 & 0 & 1 \\ 0 & 0 & 0 \end{bmatrix}. \tag{5.29}$$

**Lemma 5.3.8** *(Left-invariant control system on $SE(2)$) Let $g$ (5.28) be the group element of $SE(2)$ for the configuration $q_r$ of the RKM and $\{e_1, e_2, e_3\}$ given by (5.29) basis vectors of the Lie algebra $\mathfrak{se}(2)$. Then, the RKM can be represented as left-invariant control system*

$$\dot{g} = g\left(w_1(u)\,e_1 + w_2(u)\,e_2 + w_3(u)\,e_3\right) \tag{5.30}$$

*on $G = SE(2)$.*

**Proof** According to Definition 3.1.4, a left-invariant control system on a matrix Lie group $G$ has the form $\dot{g} = g \sum_{i=1}^{r} w_i(u)\, e_i$ for real analytic functions $w_i \colon U \to \mathbb{R}$ and linearly independent vectors $e_i \in T_E G$ of the Lie algebra. For the RKM 5.0.2 with configuration space $Q_r = SE(2)$, the Lie group element $g$ (5.28) is used to represent the configuration $q_r = (\theta, x, y)$. The time derivative of $g$ is

$$\dot{g} = \begin{bmatrix} -\dot{\theta}\sin(\theta) & -\dot{\theta}\cos(\theta) & \dot{x} \\ \dot{\theta}\cos(\theta) & -\dot{\theta}\sin(\theta) & \dot{y} \\ 0 & 0 & 0 \end{bmatrix}.$$

The derivatives $(\dot{\theta}, \dot{x}, \dot{y})$ are given by (5.4). Using the basis vectors (5.29) and the functions

$$w(u) = \begin{bmatrix} w_1(u) \\ w_2(u) \\ w_3(u) \end{bmatrix} = \begin{bmatrix} \sin(\varphi_f - \varphi_r)\, v \\ \cos(\varphi_f)\cos(\varphi_r)\, v \\ \frac{1}{2}\sin(\varphi_f + \varphi_r)\, v \end{bmatrix}, \tag{5.31}$$

system (5.30) results which is a left-invariant control system 3.1.4 on $G = SE(2)$. ■

The real analytic functions $w_i(u)$ in (5.31) can be considered as new input variables of the transformed input $w = w(u)$. Then, for the transformation matrix

$$T(\theta) = \begin{bmatrix} 1 & 0 & 0 \\ 0 & \cos(\theta) & -\sin(\theta) \\ 0 & \sin(\theta) & \cos(\theta) \end{bmatrix}, \tag{5.32}$$

the RKM (5.4) can be written as driftless affine control system $\dot{q}_r = T(\theta)\, w$. The transformed input $w$ takes values in the transformed input space

$$W = \{(w_1, w_2, w_3) \mid w_1 = w_1(u)\,, w_2 = w_2(u)\,, w_3 = w_3(u)\,, u \in U_r\}\,.$$

For $v = 1$, $W$ is shown in Figure 5.9 for $\hat{\varphi} \in \left\{\frac{3\,\pi}{16}, \frac{\pi}{4}, \frac{5\,\pi}{16}, \frac{7\,\pi}{16}\right\}$. For fixed $v$, the transformed input $w$ results from (5.31) depending on $\varphi_f$ and $\varphi_r$ with $|\varphi_f| \leq \hat{\varphi}$ and $|\varphi_r| \leq \hat{\varphi}$. According to the figure, there are no inputs $w \in W$ with $w_1 \neq 0$ or $w_3 \neq 0$ for $w_2 = 0$. This is true since only if the RKM drives forward or backward, i. e., $w_2 \neq 0$ holds, the BSR can change its orientation $\theta$ which requires $w_1 \neq 0$ or perform lateral motions which requires $w_3 \neq 0$. In Section 6.2, the transformed input space $W$ is analyzed to show the existence of time-optimal solutions.

## 5.4 Discussion of the models of the bi-steerable robot

The FKM 5.0.1 with configuration $q = (\theta, x, y, \varphi_f, \varphi_r)$ is the standard model of the BSR studied as kinematic nonholonomic system. Derived from the nonholonomic constraint (5.10), it describes the complete kinematics of the robot. The inputs of the FKM are the driving velocity $u_1$ and the steering rates $(u_2, u_3) = (\dot{\varphi}_f, \dot{\varphi}_r)$. The RKM 5.0.2 with configuration $q_r = (\theta, x, y)$ is obtained from the FKM by using the steering angles $(\varphi_f, \varphi_r)$ instead of the steering rates $(\dot{\varphi}_f, \dot{\varphi}_r)$ as inputs. This is justified, as the configuration $q_r$ consists of the position and orientation. Thus, it includes all essential configuration variables for path planning and time-optimal control, as transitions between two positions and orientations require time-consuming driving and steering maneuvers in general. Compared to this, the steering angles $(\varphi_f, \varphi_r)$ can be changed in short time. Hence, they are treated as inputs which can directly be set.

Trajectories of the RKM can be reproduced by the FKM only approximately, as bounded measurable inputs $u_2 = \dot{\varphi}_f$ and $u_3 = \dot{\varphi}_r$ of the FKM result in absolutely continuous trajectories of $\varphi_f$ and $\varphi_r$. Such trajectories do not permit discontinuous changes of the steering angles, which are feasible for the bounded measurable steering angle inputs of the RKM. For more

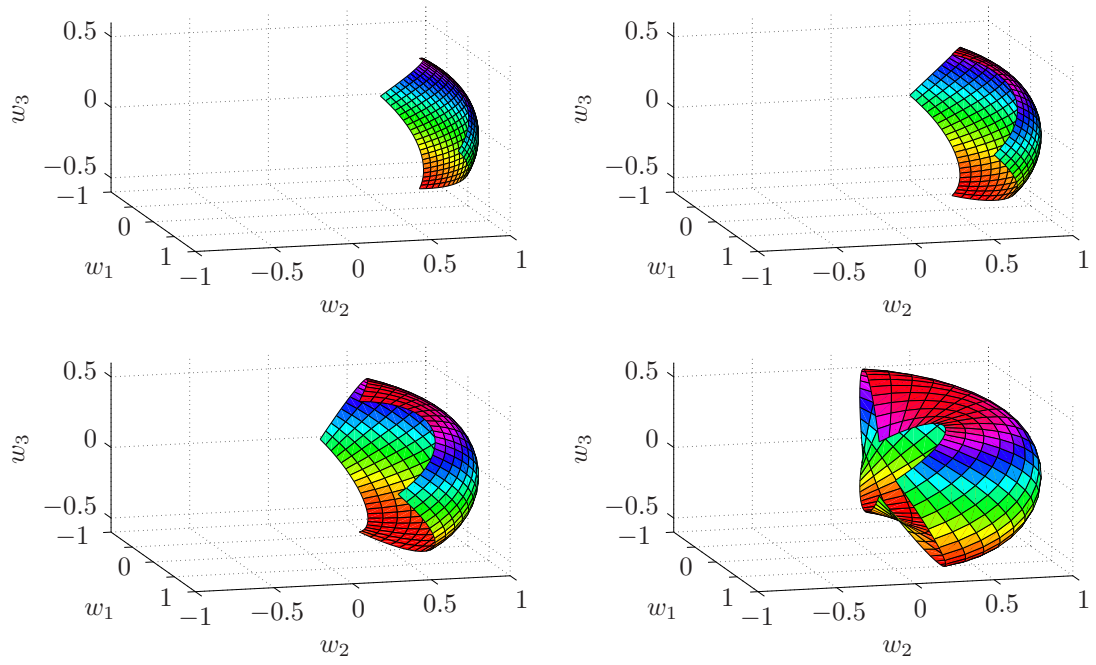


Figure 5.9: Transformed input space $W$ for $v = 1$ and $\hat{\varphi} = \frac{3\pi}{16}$ (top left), $\hat{\varphi} = \frac{\pi}{4}$ (top right), $\hat{\varphi} = \frac{5\pi}{16}$ (bottom left), and $\hat{\varphi} = \frac{7\pi}{16}$ (bottom right).

examples of reduced kinematic models with steering angle inputs, see [5, 45, 125]. Model (3.16) of the car-like robot is a different kind of reduced kinematic model. Here, the dynamics of $\varphi_f$ is also neglected, but $\varphi_f$ is no new input variable, but only affects the inputs $(v_1, v_2)$.

For motion planning and optimal control, both the FKM and RKM are suitable, since they are controllable, see Section 5.3.1. Although the FKM is the standard model of the BSR, standard methods like path planning for systems in chain form or flatness based control are not applicable to the FKM. This is the case as steering angles $\varphi_f = \varphi_r$ have to be excluded according to Section 5.1, which strongly restricts the feasible paths. For the RKM, $z = q_r$ is a globally defined flat output, and flatness based control can be applied. However, flatness is not used here, as for most $z_0$ and $z_r$, trajectories $z(\cdot)$ from $z_0$ to $z_d$ can only be determined iteratively. Moreover, bounded measurable input trajectories and absolutely continuous state trajectories are required for optimal solutions in general, see [77, 93]. For path planning based on flatness, the trajectory $z(\cdot)$ from $z_0$ to $z_d$ must be at least once differentiable, which may rule out optimal solutions. Thus, no time-optimal control for the flat output $z = q_r$ is considered.

The RKM has a lower dimensional configuration than the FKM. This decreases the complexity of the control problem and simplifies the analysis of the extremals from the Maximum Principle in the next chapter. In contrast to the FKM, the inputs enter the RKM both linearly and nonlinearly. Hence, the maximization of the Hamiltonian function of the RKM is more demanding. Due to the affine and non-affine inputs, most control methods like switching time optimization for bang-bang extremals and most optimality conditions from Section 4.5 and 4.6 are not applicable, making the control problem more interesting. On the other hand, singular extremals play a less important role for the RKM as shown in Chapter 9. This makes the control problem simpler, as singular extremals are difficult to handle. Besides, the RKM can be represented as left-invariant control system on $G = SE(2)$. For left-invariant systems, path planning problems can be simplified as addressed in Section 7.1.

# 6 Extremals for time-optimal control of the bi-steerable robot

In this chapter, the necessary optimality conditions of the Maximum Principle from Chapter 4 are applied to the RKM 5.0.2 to define the extremals for time-optimal control. For this, the appropriate optimality conditions are derived and the maximization of the Hamiltonian function is performed analytically to determine the extremal inputs. Based on knowledge of the extremal inputs, the existence of time-optimal solutions is shown. The resultant extremals are classified into normal, abnormal, regular, and singular. For time-optimal control of the RKM, only normal regular and normal singular extremals are relevant.

To simplify the structure of the extremals of the RKM, the following assumption holds.

**Assumption 6.0.1** *(Steering limit of the RKM) The steering limit of the front and rear axle of the RKM is* $\hat{\varphi} := \frac{\pi}{4}$.

In Chapter 5, $0 < \hat{\varphi} < \frac{\pi}{2}$ was assumed to achieve a regular velocity constraint (5.10) according to Theorem 5.2.5. In the following, the steering limit $\hat{\varphi} = \frac{\pi}{4}$ applies to obtain a less complex structure of normal regular and normal singular extremals. The additional complexity of the extremals which arise for steering limits $\hat{\varphi} \neq \frac{\pi}{4}$ with $0 < \hat{\varphi} < \frac{\pi}{2}$ is discussed in Section 6.3. The steering limit $\hat{\varphi} = \frac{\pi}{4}$ is also used for the BSR in [69, 101] and for the car-like robot in [13, 59, 60, 106, 108, 120, 124]. The space of the admissible steering angles $(\varphi_f, \varphi_r)$ is

$$\Phi := \left[-\frac{\pi}{4}, \frac{\pi}{4}\right] \times \left[-\frac{\pi}{4}, \frac{\pi}{4}\right]. \tag{6.1}$$

**Definition 6.0.2** *(Time-optimal control problem for the RKM) The time-optimal control problem 2.2.3 for the RKM 5.0.2 with initial configuration* $q_0$*, desired configuration* $q_d$*, and input space* $U = [-\hat{v}, \hat{v}] \times \Phi$*,* $\hat{v} > 0$*, is called time-optimal control problem for the RKM.*

In the remaining thesis, the configuration $q = (\theta, x, y)$, the configuration space $Q = SE(2)$, the input $u = (v, \varphi) = (v, \varphi_f, \varphi_r)$, and the input space $U = [-\hat{v}, \hat{v}] \times \Phi$ are considered. To simplify the notation, $q$, $Q$, $u$, and $U$ is used instead of $q_r$, $Q_r$, $u_r$, and $U_r$ as in Definition 5.0.2.

## 6.1 Necessary optimality conditions

This section addresses the necessary optimality conditions of the Maximum Principle and the maximization of the Hamiltonian function $H(q, \mu, \lambda, u) = -\mu + \lambda^\top f(q, u)$ for time-optimal control of the RKM. The optimality conditions define the extremals $(q^*(\cdot), \lambda^*(\cdot), u^*(\cdot))$ over the time interval $I = [0, T]$. The initial conditions of $q^*(\cdot)$ and $\lambda^*(\cdot)$ are denoted by $q(0) = q_0$ and $\lambda(0) = \lambda_0$. The necessary optimality conditions in Section 6.1.1 arise from the conditions of the Maximum Principle 4.2.2 applied to problem 6.0.2. The maximization of the Hamiltonian function is performed analytically, based on partial derivatives of the Hamiltonian function with respect to $\varphi$ in int $\Phi$ and a study of the Hamiltonian function on bd $\Phi$.

### 6.1.1 Application of the Maximum Principle

**Theorem 6.1.1** *(Necessary optimality conditions for time-optimal control of the RKM) The time-optimal control problem 6.0.2 is considered. Let* $\lambda = (\lambda_1, \lambda_2, \lambda_3)$ *be the adjoint state and*

$\mu \in \{0,1\}$ *a constant. Then, the Hamiltonian function*

$$H(q,\mu,\lambda,u) = -\mu + h(q,\lambda,\varphi)\; v \tag{6.2}$$

*results with*

$$\begin{aligned} h(q,\lambda,\varphi) \;:=\; & \lambda_1 \sin(\varphi_f - \varphi_r) + (\cos(\theta)\,\lambda_2 + \sin(\theta)\,\lambda_3)\cos(\varphi_f)\cos(\varphi_r) \\ & + \tfrac{1}{2}\,(-\sin(\theta)\,\lambda_2 + \cos(\theta)\,\lambda_3)\sin(\varphi_f + \varphi_r)\,. \end{aligned} \tag{6.3}$$

*Let* $(q^*(\cdot)\,,\,\lambda^*(\cdot)\,,\,u^*(\cdot))$ *be an extremal and* $H^*(\cdot) := H(q^*(\cdot)\,,\mu,\lambda^*(\cdot)\,,u^*(\cdot))$ *the extremal Hamiltonian function over the time interval* $I = [0,T]$*. Then, the following conditions hold:*

**N1:** *For all* $t \in I$*,* $(\mu,\lambda^*(t)) \neq (0,0)$ *is true.*

**N2:** *For almost all* $t \in I$*, there holds the adjoint equation*

$$\begin{aligned} \dot\lambda_1^* &= \Big(\tfrac{1}{2}\cos(\theta^*)\sin\big(\varphi_f^* + \varphi_r^*\big) + \sin(\theta^*)\cos\big(\varphi_f^*\big)\cos\big(\varphi_r^*\big)\Big)\lambda_2^*\, v^* \\ &\quad + \Big(\tfrac{1}{2}\sin(\theta^*)\sin\big(\varphi_f^* + \varphi_r^*\big) - \cos(\theta^*)\cos\big(\varphi_f^*\big)\cos\big(\varphi_r^*\big)\Big)\lambda_3^*\, v^*, \\ \dot\lambda_2^* &= 0, \\ \dot\lambda_3^* &= 0. \end{aligned} \tag{6.4}$$

**N3:** *For almost all* $t \in I$*,* $u^* = (v^*,\varphi^*)$ *satisfies*

$$|h(q^*,\lambda^*,\varphi^*)| = \max_{\varphi\in\Phi} |h(q^*,\lambda^*,\varphi)| \tag{6.5}$$

*and*

$$v^* = \operatorname{sgn}(h^*)\,\hat v. \tag{6.6}$$

**N4:** *For almost all* $t \in I$*,* $H^*(t) = 0$ *holds.*

**Proof** The Hamiltonian function $H$ (6.2) and the function $h$ (6.3) result from $H(q,\mu,\lambda,u) = -\mu + \lambda^\top f(q,u)$ for $\lambda = (\lambda_1,\lambda_2,\lambda_3)$ and the right-hand side $f(q,u) := g(\theta,\varphi)\,v$ of the RKM (5.4). The nontriviality condition N1 of Theorem 6.1.1 is obtained from condition N1 of the Maximum Principle 4.2.2. Condition N2 is the adjoint equation (4.2) applied to the Hamiltonian function (6.2). Regarding condition N3, the extremal inputs $u^* = (v^*,\varphi^*)$ maximize the Hamiltonian function over all $u \in U = [-\hat v,\hat v] \times \Phi$, as $H(q,\mu,\lambda,u) = -\mu + h(q,\lambda,\varphi)\; v$ is maximal for maximal $h(q,\lambda,\varphi)\,v$. This is achieved if both $h(q,\lambda,\varphi)$ and $v$ have maximal modulus and the same sign. Condition N4 is the null-maximizing condition. ■

Regarding the maximization condition N3, the extremal velocity arising from (6.6) satisfies $v^* = \pm\hat v$ for almost all $t \in I$. In contrast to this, the extremal steering angles $\varphi^* = \big(\varphi_f^*,\varphi_r^*\big)$ do not satisfy $\varphi_i^* = \pm\hat\varphi$ for almost all $t \in I$, as they enter the RKM and the function $h$ nonlinearly.

**Definition 6.1.2** *(Transformed adjoint state) For the adjoint state* $\lambda = (\lambda_1,\lambda_2,\lambda_3)$ *and*

$$R(\theta) = \begin{bmatrix} 1 & 0 & 0 \\ 0 & \cos(\theta) & \sin(\theta) \\ 0 & -\sin(\theta) & \cos(\theta) \end{bmatrix}, \tag{6.7}$$

*the vector* $\gamma = (\gamma_1,\gamma_2,\gamma_3)$ *given by*

$$\gamma := R(\theta)\,\lambda = (\lambda_1, \cos(\theta)\,\lambda_2 + \sin(\theta)\,\lambda_3, -\sin(\theta)\,\lambda_2 + \cos(\theta)\,\lambda_3)$$

*is called transformed adjoint state.*

In terms of the transformation matrix $T(\theta)$ as in (5.32), $R(\theta) = T(-\theta)$ holds. As $\det R(\theta) = 1$ is true for all $\theta$, $\lambda \neq 0$ implies $\gamma \neq 0$, and vice versa. The adjoint state $\lambda$ relates to the coordinates $(x, y)$ of the fixed reference frame in Figure 5.6. The transformed adjoint state $\gamma$ results from $\lambda$ via the rotation matrix $R(\theta)$. Thus, $\gamma$ relates to a body-fixed frame of the robot. In this thesis, $\gamma$ is used instead of $\lambda$ to shorten the notation and simplify the analysis of the extremals. The function $h$ written as function of the transformed adjoint state $\gamma$ gives

$$b(\gamma, \varphi) = \gamma_1 \sin(\varphi_f - \varphi_r) + \gamma_2 \cos(\varphi_f) \cos(\varphi_r) + \frac{1}{2}\gamma_3 \sin(\varphi_f + \varphi_r)\,. \tag{6.8}$$

Using the function $b$, the maximization $|h(q^*, \lambda^*, \varphi^*)| = \max_{\varphi\in\Phi} |h(q^*, \lambda^*, \varphi)|$ can be replaced by $|b(\gamma^*, \varphi^*)| = \max_{\varphi\in\Phi} |b(\gamma^*, \varphi)|$ and $v^* = \operatorname{sgn}(h^*)\, \hat{v}$ by

$$v^* = \operatorname{sgn}(b^*)\ \hat{v}. \tag{6.9}$$

The differential equation for $\gamma^*$ obtained from $\gamma^* = R(\theta^*)\,\lambda^*$ and $\dot{\gamma}^* = \dot{R}(\theta^*)\,\lambda^* + R(\theta^*)\,\dot{\lambda}^*$ is

$$\begin{aligned} \dot{\gamma}_1^* &= \left(\tfrac{1}{2}\,\gamma_2^*\,\sin\big(\varphi_f^* + \varphi_r^*\big) - \gamma_3^*\,\cos\big(\varphi_f^*\big)\cos\big(\varphi_r^*\big)\right) v^*, \\ \dot{\gamma}_2^* &= \gamma_3^*\,\sin\big(\varphi_f^* - \varphi_r^*\big) v^*, \\ \dot{\gamma}_3^* &= -\gamma_2^*\,\sin\big(\varphi_f^* - \varphi_r^*\big) v^*. \end{aligned} \tag{6.10}$$

### 6.1.2 Maximization of the Hamiltonian function

For the maximization of the Hamiltonian function, $|h|$ has to be maximized over $\varphi \in \Phi$ according to condition N3. With respect to $\varphi$, the maximization of $|h|$ is equivalent to the maximization of $|b|$. In the following, $|b|$ is considered to obtain more compact results. The maximization is not performed numerically but analytically, which reveals essential properties for the analysis of the extremals. Moreover, it allows to simulate the extremals at low computational cost.

**Theorem 6.1.3** *(Candidates for extremal points of $b$ for $\varphi \in \Phi$) There are nine possible candidates for extremal points of $b$. On* bd $\Phi$*, four candidates are $\varphi_1 = (-\hat{\varphi}, -\hat{\varphi})$, $\varphi_2 = (-\hat{\varphi}, \hat{\varphi})$, $\varphi_3 = (\hat{\varphi}, -\hat{\varphi})$, and $\varphi_4 = (\hat{\varphi}, \hat{\varphi})$, and four more candidates are $\varphi_5 = (-\hat{\varphi}, \varphi_{r_5})$ and $\varphi_6 = (\hat{\varphi}, \varphi_{r_6})$ with $|\varphi_{r_i}| < \hat{\varphi}$, and $\varphi_7 = (\varphi_{f_7}, -\hat{\varphi})$ and $\varphi_8 = (\varphi_{f_8}, \hat{\varphi})$ with $|\varphi_{f_i}| < \hat{\varphi}$. In* int $\Phi$*, there is one candidate $\varphi_9 = (\varphi_{f_9}, \varphi_{r_9})$.*

*For $2\,\gamma_2 \cos(\hat{\varphi}) - (2\,\gamma_1 + \gamma_3)\sin(\hat{\varphi}) \neq 0$, $\varphi_5 = (-\hat{\varphi}, \varphi_{r_5})$ is a candidate if $|\varphi_{r_5}| < \hat{\varphi}$ holds for*

$$\varphi_{r_5} = \arctan\left(\frac{(-2\,\gamma_1 + \gamma_3)\cos(\hat{\varphi})}{2\,\gamma_2\cos(\hat{\varphi}) - (2\,\gamma_1 + \gamma_3)\sin(\hat{\varphi})}\right). \tag{6.11}$$

*For $2\,\gamma_2 \cos(\hat{\varphi}) + (2\,\gamma_1 + \gamma_3)\sin(\hat{\varphi}) \neq 0$, $\varphi_6 = (\hat{\varphi}, \varphi_{r_6})$ is a candidate if $|\varphi_{r_6}| < \hat{\varphi}$ holds for*

$$\varphi_{r_6} = \arctan\left(\frac{(-2\,\gamma_1 + \gamma_3)\cos(\hat{\varphi})}{2\,\gamma_2\cos(\hat{\varphi}) + (2\,\gamma_1 + \gamma_3)\sin(\hat{\varphi})}\right). \tag{6.12}$$

*For $2\,\gamma_2 \cos(\hat{\varphi}) + (2\,\gamma_1 - \gamma_3)\sin(\hat{\varphi}) \neq 0$, $\varphi_7 = (\varphi_{f_7}, -\hat{\varphi})$ is a candidate if $|\varphi_{f_7}| < \hat{\varphi}$ holds for*

$$\varphi_{f_7} = \arctan\left(\frac{(2\,\gamma_1 + \gamma_3)\cos(\hat{\varphi})}{2\,\gamma_2\cos(\hat{\varphi}) + (2\,\gamma_1 - \gamma_3)\sin(\hat{\varphi})}\right). \tag{6.13}$$

*For $2\,\gamma_2 \cos(\hat{\varphi}) - (2\,\gamma_1 - \gamma_3)\sin(\hat{\varphi}) \neq 0$, $\varphi_8 = (\varphi_{f_8}, \hat{\varphi})$ is a candidate if $|\varphi_{f_8}| < \hat{\varphi}$ holds for*

$$\varphi_{f_8} = \arctan\left(\frac{(2\,\gamma_1 + \gamma_3)\cos(\hat{\varphi})}{2\,\gamma_2\cos(\hat{\varphi}) - (2\,\gamma_1 - \gamma_3)\sin(\hat{\varphi})}\right). \tag{6.14}$$

*For $\gamma_2 \neq 0$, $\varphi_9 = (\varphi_{f_9}, \varphi_{r_9})$ is a candidate if $|\varphi_{f_9}| < \hat{\varphi}$ and $|\varphi_{r_9}| < \hat{\varphi}$ holds for*

$$\begin{aligned} \varphi_{f_9} &= \tfrac{1}{2}\left(\ \arctan\left(\tfrac{2\,\gamma_1}{\gamma_2}\right) + \arctan\left(\tfrac{\gamma_3}{\gamma_2}\right)\right), \\ \varphi_{r_9} &= \tfrac{1}{2}\left(-\arctan\left(\tfrac{2\,\gamma_1}{\gamma_2}\right) + \arctan\left(\tfrac{\gamma_3}{\gamma_2}\right)\right). \end{aligned} \tag{6.15}$$

*Not all candidates $\varphi_i$, $i = 1,\ldots,9$ have to exist. All existing candidates are different.*

**Proof** Extremal points of the function $b$ can lie on bd $\Phi$ or in int $\Phi$. Candidates for extremal points on bd $\Phi$ are the vertices $(\pm\hat{\varphi}, \pm\hat{\varphi})$ which give the points $\varphi_i$, $i = 1,...,4$ and points on the line segments between these vertices which give $\varphi_i$, $i = 5,...,8$. The points $\varphi_i$, $i = 5,...,8$ represent candidates for extremal points if the solutions of (6.11) to (6.14) satisfy $|\varphi_{r_5}| < \hat{\varphi}$, $|\varphi_{r_6}| < \hat{\varphi}$, $|\varphi_{f_7}| < \hat{\varphi}$, and $|\varphi_{f_8}| < \hat{\varphi}$, respectively. The equations (6.11) to (6.14) result from

$$\begin{aligned}
\frac{\partial b}{\partial \varphi_r} &= \left(\tfrac{\gamma_3}{2} - \gamma_1\right)\cos(\varphi_f)\cos(\varphi_r) - \left(\gamma_2\cos(\varphi_f) + \left(\gamma_1 + \tfrac{\gamma_3}{2}\right)\sin(\varphi_f)\right)\sin(\varphi_r) &= 0,\\
\frac{\partial b}{\partial \varphi_f} &= \left(\gamma_1 + \tfrac{\gamma_3}{2}\right)\cos(\varphi_f)\cos(\varphi_r) - \left(\gamma_2\cos(\varphi_r) - \left(\gamma_1 - \tfrac{\gamma_3}{2}\right)\sin(\varphi_r)\right)\sin(\varphi_f) &= 0
\end{aligned}$$

for $\varphi_f = \pm\hat{\varphi}$ and $\varphi_r = \pm\hat{\varphi}$, respectively. Solutions with vanishing denominator of the argument of the arc tangent function of (6.11) to (6.14) are excluded, as they give no angles on bd $\Phi$.

The point $\varphi_9$ is a candidate if the solution of (6.15) lies in int $\Phi$, i. e., $|\varphi_{f_9}| < \hat{\varphi}$ and $|\varphi_{r_9}| < \hat{\varphi}$ holds. The equations (6.15) are obtained from $\partial b/\partial\varphi_f = 0$ and $\partial b/\partial\varphi_r = 0$ solved for $(\varphi_{f_9}, \varphi_{r_9})$. Here, $\gamma_2 = 0$ is excluded, as $\gamma_2 = 0$ gives a point $\varphi_9$ not located in int $\Phi$.

Not all candidates $\varphi_i$, $i = 1,...,9$ have to exist, as the solutions of (6.11) to (6.15) may not satisfy $|\varphi_{f_i}| < \hat{\varphi}$ and $|\varphi_{r_i}| < \hat{\varphi}$, respectively. The existing candidates are different due to their different domains. ■

The candidates $\varphi_i$, $i = 1,...,9$ and $\varphi_0 = (0, 0)$ are summarized in Table 6.1.

| extremal point | value | location |
|---|---|---|
| $\varphi_0$ | $(0, 0)$ | int $\Phi$ |
| $\varphi_1$ | $(-\hat{\varphi}, -\hat{\varphi})$ | bd $\Phi$ |
| $\varphi_2$ | $(-\hat{\varphi}, \hat{\varphi})$ | bd $\Phi$ |
| $\varphi_3$ | $(\hat{\varphi}, -\hat{\varphi})$ | bd $\Phi$ |
| $\varphi_4$ | $(\hat{\varphi}, \hat{\varphi})$ | bd $\Phi$ |
| $\varphi_5$ | $(-\hat{\varphi}, \varphi_{r_5})$ from (6.11) | bd $\Phi$ |
| $\varphi_6$ | $(\hat{\varphi}, \varphi_{r_6})$ from (6.12) | bd $\Phi$ |
| $\varphi_7$ | $(\varphi_{f_7}, -\hat{\varphi})$ from (6.13) | bd $\Phi$ |
| $\varphi_8$ | $(\varphi_{f_8}, \hat{\varphi})$ from (6.14) | bd $\Phi$ |
| $\varphi_9$ | $(\varphi_{f_9}, \varphi_{r_9})$ from (6.15) | int $\Phi$ |

Table 6.1: Candidates for extremal points of $b$.

In the following, the maximization of $|b|$ over $\varphi \in \Phi$ is considered. Depending on $\gamma = (\gamma_1, \gamma_2, \gamma_3)$, six different cases C1 to C6 are distinguished. If for some case C$i$, $|b|$ is maximized by one point, this point is denoted by $\varphi^{Ci} = \left(\varphi_f^{Ci}, \varphi_r^{Ci}\right)$. If $|b|$ is maximized by two points, they are denoted by $\varphi_I^{Ci} = \left(\varphi_{fI}^{Ci}, \varphi_{rI}^{Ci}\right)$ and $\varphi_{II}^{Ci} = \left(\varphi_{fII}^{Ci}, \varphi_{rII}^{Ci}\right)$. Here, $\varphi_I^{Ci} = -\varphi_{II}^{Ci}$ holds as discussed below, and $\varphi_{fI}^{Ci} \leq 0$ is assumed for a unique specification of $\varphi_I^{Ci}$ and $\varphi_{II}^{Ci}$.

**Theorem 6.1.4** *(Maximization of $|b|$ over $\varphi \in \Phi$) For a particular $\gamma$, let $J \subset \{1,\ldots,9\}$ be the index set of the existing candidates for extremal points $\varphi_i$ of $b$. For the maximization of $|b|$ over $\varphi \in \Phi$, the following cases are distinguished depending on $\gamma$:*

**C1:** $\gamma_1 = \gamma_2 = \gamma_3 = 0$: *This case is not relevant for time-optimal control of the RKM.*

**C2:** $\gamma_1 = \gamma_2 = 0$, $\gamma_3 \neq 0$: *$|b|$ is maximized by the points $\varphi_I^{C2} = \varphi_1$ and $\varphi_{II}^{C2} = \varphi_4$ on* bd $\Phi$.

**C3:** $\gamma_1 = 0$, $\gamma_2 \neq 0$, $\gamma_3 = 0$: *$|b|$ is maximized by the point $\varphi^{C3} = \varphi_0$ in* int $\Phi$.

**C4:** $\gamma_1 \neq 0$, $\gamma_2 = \gamma_3 = 0$: *$|b|$ is maximized by the points $\varphi_I^{C4} = \varphi_2$ and $\varphi_{II}^{C4} = \varphi_3$ on* bd $\Phi$.

**C5:** $\gamma_1 \neq 0$, $\gamma_2 = 0$, $\gamma_3 \neq 0$: *If* $\gamma_1\,\gamma_3 > 0$ *holds,* $|b|$ *is maximized by the points* $\varphi_I^{C5} = \varphi_5 = \left(-\hat{\varphi}, \varphi_{r_I}^{C5}\right)$ *and* $\varphi_{II}^{C5} = \varphi_6 = \left(\hat{\varphi}, -\varphi_{r_I}^{C5}\right)$ *with* $\varphi_{r_I}^{C5} = \varphi_{r_5} = -\varphi_{r_6}$ *and* $\left|\varphi_{r_I}^{C5}\right| < \hat{\varphi}$.

*If* $\gamma_1\,\gamma_3 < 0$ *and* $\varphi_{f_7} \leq 0$ *holds,* $|b|$ *is maximized by the points* $\varphi_I^{C5} = \varphi_7 = \left(\varphi_{f_I}^{C5}, -\hat{\varphi}\right)$ *and* $\varphi_{II}^{C5} = \varphi_8 = \left(-\varphi_{f_I}^{C5}, \hat{\varphi}\right)$ *with* $\varphi_{f_I}^{C5} = \varphi_{f_7} = -\varphi_{f_8}$ *and* $\left|\varphi_{f_I}^{C5}\right| < \hat{\varphi}$.

*If* $\gamma_1\,\gamma_3 < 0$ *and* $\varphi_{f_7} > 0$ *holds,* $|b|$ *is maximized by the points* $\varphi_I^{C5} = \varphi_8 = \left(\varphi_{f_I}^{C5}, \hat{\varphi}\right)$ *and* $\varphi_{II}^{C5} = \varphi_7 = \left(-\varphi_{f_I}^{C5}, -\hat{\varphi}\right)$ *with* $\varphi_{f_I}^{C5} = \varphi_{f_8} = -\varphi_{f_7}$ *and* $\left|\varphi_{f_I}^{C5}\right| < \hat{\varphi}$.

*The points* $\varphi_I^{C5}$ *and* $\varphi_{II}^{C5}$ *are located on* bd $\Phi$.

**C6:** $\gamma_2 \neq 0$, $\gamma_1^2 + \gamma_3^2 > 0$: $|b|$ *is maximized by the point* $\varphi^{C6}$ *on* bd $\Phi$ *or in* int $\Phi$ *with*

$$|b(\gamma, \varphi^{C6})| = \max_{j \in J} |b(\gamma, \varphi_j)| \,. \tag{6.16}$$

*In case C1, the maximized* $|b|$ *satisfies* $|b(\gamma, \varphi)| = 0$. *In all other cases, it satisfies* $|b(\gamma, \varphi)| > 0$.

**Proof**

**C1:** Case C1 is not relevant for time-optimal control, as the conditions of Theorem 6.1.1 can neither be satisfied for $\mu = 0$ nor for $\mu = 1$. For $\mu = 0$, the nontriviality condition N1 is not true, and for $\mu = 1$, the null-maximizing condition N4 does not hold, as for $b$ (6.8) and $\gamma = (0, 0, 0)$, always $b(\gamma, \varphi) = 0$ is true.

**C2:** In case C2, $|b^{C2}(\gamma, \varphi)| = \left|\frac{1}{2}\gamma_3 \sin(\varphi_f + \varphi_r)\right|$ applies. Then, $\sin(\varphi_f + \varphi_r)$ has to take its maximal absolute value over $\varphi \in \Phi$ to maximize $|b^{C2}|$. From this, $\varphi_I^{C2} = (-\hat{\varphi}, -\hat{\varphi}) = \varphi_1$ and $\varphi_{II}^{C2} = (\hat{\varphi}, \hat{\varphi}) = \varphi_4$ results.

**C3:** In case C3, $|b^{C3}(\gamma, \varphi)| = |\gamma_2 \cos(\varphi_f) \cos(\varphi_r)|$ is maximal for maximal $\cos(\varphi_f) \cos(\varphi_r)$. Thus, $\varphi^{C3} = (0, 0) = \varphi_0$ holds.

**C4:** In case C4, $|b^{C4}(\gamma, \varphi)| = |\gamma_1 \sin(\varphi_f - \varphi_r)|$ is maximized over $\varphi \in \Phi$. Hence, $\sin(\varphi_f - \varphi_r)$ has to take its maximal absolute value, which is achieved for $\varphi_I^{C4} = (-\hat{\varphi}, \hat{\varphi}) = \varphi_2$ and $\varphi_{II}^{C4} = (\hat{\varphi}, -\hat{\varphi}) = \varphi_3$.

**C5:** In case C5, $|b^{C5}(\gamma, \varphi)| = \left|\gamma_1 \sin(\varphi_f - \varphi_r) + \frac{1}{2}\gamma_3 \sin(\varphi_f + \varphi_r)\right|$ is maximized over $\varphi \in \Phi$. As $b^{C5}(\gamma, \varphi) = b^{C5}(\gamma, -\varphi)$ holds in this case, two points $\{\varphi_I^{C5}, \varphi_{II}^{C5}\}$ maximize $|b^{C5}|$ which satisfy $\varphi_I^{C5} = -\varphi_{II}^{C5}$. For extremal points of $b^{C5}$ in int $\Phi$,

$$\begin{aligned} \frac{\partial h^{C5}}{\partial \varphi_f} &= \gamma_1 \cos(\varphi_f - \varphi_r) + \tfrac{1}{2}\gamma_3 \cos(\varphi_f + \varphi_r) = 0, \\ \frac{\partial h^{C5}}{\partial \varphi_r} &= -\gamma_1 \cos(\varphi_f - \varphi_r) + \tfrac{1}{2}\gamma_3 \cos(\varphi_f + \varphi_r) = 0 \end{aligned} \tag{6.17}$$

has to apply with $\left|\varphi_{f_I}^{C5}\right| < \hat{\varphi}$, $\left|\varphi_{r_I}^{C5}\right| < \hat{\varphi}$, $\left|\varphi_{f_{II}}^{C5}\right| < \hat{\varphi}$, and $\left|\varphi_{r_{II}}^{C5}\right| < \hat{\varphi}$. As (6.17) is only true for the points $\varphi = \left(0, \pm\frac{\pi}{2}\right)$ and $\varphi = \left(\pm\frac{\pi}{2}, 0\right)$ which do not satisfy $\varphi \in \Phi$, no extremal points of $b^{C5}$ exist in int $\Phi$. Hence, the extremals points $\{\varphi_I^{C5}, \varphi_{II}^{C5}\}$ are located on bd $\Phi$, and $\left|\varphi_{f_I}^{C5}\right| = \left|\varphi_{f_{II}}^{C5}\right| = \hat{\varphi}$ or $\left|\varphi_{r_I}^{C5}\right| = \left|\varphi_{r_{II}}^{C5}\right| = \hat{\varphi}$ has to hold.

To show that $\left|\varphi_{f_I}^{C5}\right| = \left|\varphi_{f_{II}}^{C5}\right| = \hat{\varphi}$ or $\left|\varphi_{r_I}^{C5}\right| = \left|\varphi_{r_{II}}^{C5}\right| = \hat{\varphi}$ holds, but $\left|\varphi_{f_I}^{C5}\right| = \left|\varphi_{f_{II}}^{C5}\right| = \left|\varphi_{r_I}^{C5}\right| = \left|\varphi_{r_{II}}^{C5}\right| = \hat{\varphi}$ is not possible, the case $\varphi_f = \pm\hat{\varphi}$ is considered. Then, according to (6.17),

$$\frac{\partial h^{C5}}{\partial \varphi_r} = -\gamma_1 \cos(\pm\hat{\varphi} - \varphi_r) + \tfrac{1}{2}\gamma_3 \cos(\pm\hat{\varphi} + \varphi_r) = 0 \tag{6.18}$$

has to apply. Since for $\varphi \in \Phi$, always $\cos(\pm\hat{\varphi} - \varphi_r) \geq 0$ and $\cos(\pm\hat{\varphi} + \varphi_r) \geq 0$ is true, (6.18) can only be satisfied for $\gamma_1\,\gamma_3 > 0$. Solving (6.18) for $\varphi_r$ yields

$$\varphi_r = \arctan\left(\frac{-2\,\gamma_1 + \gamma_3}{2\,\gamma_1 + \gamma_3} \frac{1}{\tan(\pm\hat{\varphi})}\right).$$

For $\gamma_1\,\gamma_3 > 0$, $\left|\frac{-2\,\gamma_1+\gamma_3}{2\,\gamma_1+\gamma_3}\right| < 1$ holds. Besides, $\tan(\pm\hat{\varphi}) = \pm 1$ is true for $\hat{\varphi} = \frac{\pi}{4}$. Thus,

$$\left|\frac{-2\,\gamma_1+\gamma_3}{2\,\gamma_1+\gamma_3}\frac{1}{\tan(\pm\hat{\varphi})}\right| < 1$$

and $|\varphi_r| < \hat{\varphi}$ results. Likewise, if $\varphi_r = \pm\hat{\varphi}$ applies, $\gamma_1\,\gamma_3 < 0$ has to hold for $\varphi \in \Phi$, and $|\varphi_f| < \hat{\varphi}$ is satisfied. As $\gamma_1 \neq 0$ and $\gamma_3 \neq 0$ holds in case C5, $\gamma_1\,\gamma_3 = 0$ does not occur.

For $\gamma_1\,\gamma_3 > 0$, $|b|$ is maximized by two points $\varphi_I^{C5}$ and $\varphi_{II}^{C5}$ which satisfy $\left|\varphi_{f_I}^{C5}\right| = \left|\varphi_{f_{II}}^{C5}\right| = \hat{\varphi}$ and $\left|\varphi_{r_I}^{C5}\right| = \left|\varphi_{r_{II}}^{C5}\right| < \hat{\varphi}$. Thus, $\varphi_I^{C5} = \varphi_5$ and $\varphi_{II}^{C5} = \varphi_6$ holds. As $\gamma_2 = 0$ is true, $\varphi_{r_5}$ obtained from (6.11) and $\varphi_{r_6}$ from (6.12) satisfy $\varphi_{r_5} = -\varphi_{r_6}$. Hence, $\varphi_I^{C5} = \left(-\hat{\varphi}, \varphi_{r_I}^{C5}\right)$ and $\varphi_{II}^{C5} = \left(\hat{\varphi}, -\varphi_{r_I}^{C5}\right)$ results for $\varphi_{f_I}^{C5} = \varphi_{f_7}$.

For $\gamma_1\,\gamma_3 < 0$, the cases $\varphi_{f_7} \leq 0$ and $\varphi_{f_7} > 0$ are distinguished to obtain $\varphi_{f_I}^{C5} \leq 0$ for a unique specification of $\varphi_I^{C5}$ and $\varphi_{II}^{C5}$. If $\gamma_1\,\gamma_3 < 0$ holds, $|b|$ is maximized by two points $\varphi_I^{C5}$ and $\varphi_{II}^{C5}$ which satisfy $\left|\varphi_{r_I}^{C5}\right| = \left|\varphi_{r_{II}}^{C5}\right| = \hat{\varphi}$ and $\left|\varphi_{f_I}^{C5}\right| = \left|\varphi_{f_{II}}^{C5}\right| < \hat{\varphi}$. Thus, if $\varphi_{f_7} \leq 0$ holds, $\varphi_I^{C5} = \varphi_7$ and $\varphi_{II}^{C5} = \varphi_8$ is obtained. If $\varphi_{f_7} > 0$ is true, $\varphi_I^{C5} = \varphi_8$ and $\varphi_{II}^{C5} = \varphi_7$ applies. Due to $\gamma_2 = 0$, for $\varphi_{f_7}$ from (6.13) and $\varphi_{f_8}$ from (6.14), $\varphi_{f_7} = -\varphi_{f_8}$ holds. Hence, if $\varphi_{f_7} \leq 0$ is assumed, $\varphi_I^{C5} = \left(\varphi_{f_I}^{C5}, -\hat{\varphi}\right)$ and $\varphi_{II}^{C5} = \left(-\varphi_{f_I}^{C5}, \hat{\varphi}\right)$ results for $\varphi_{f_I}^{C5} = \varphi_{f_7}$. If $\varphi_{f_7} > 0$ is assumed, $\varphi_I^{C5} = \left(\varphi_{f_I}^{C5}, \hat{\varphi}\right)$ and $\varphi_{II}^{C5} = \left(-\varphi_{f_I}^{C5}, -\hat{\varphi}\right)$ is obtained for $\varphi_{f_I}^{C5} = \varphi_{f_8}$.

**C6:** In the generic case C6, one extremal point $\varphi^{C6}$ exists. This is true as $b(\gamma,\varphi) = -b(\gamma,-\varphi)$ does not hold for $\gamma_2 \neq 0$ due to $\gamma_2\cos(\varphi_f)\cos(\varphi_r) = \gamma_2\cos(-\varphi_f)\cos(-\varphi_r) \neq 0$. Hence, there are no extremal points $\{\varphi_I^{C6}, \varphi_{II}^{C6}\}$ with $b(\gamma,\varphi_I^{C6}) = -b(\gamma,\varphi_{II}^{C6})$. The index set $J \subset \{1,\ldots,9\}$ gives the candidates for extremal points $\varphi_i$, $i = 1,...,9$ which exist for the particular $\gamma$. Then, $\varphi^{C6}$ is the one extremal point which arises from (6.16) for the candidates $\varphi_j$, $j \in J$.

In case C1, i. e., for $\gamma = (0,0,0)$, there holds $b(\gamma,\varphi) = 0$ for all $\varphi \in \Phi$, resulting in $|b(\gamma,\varphi)| = 0$. In the cases C2 to C6, $b$ can take values unequal to zero. Thus, $|b(\gamma,\varphi^{Ci})| > 0$ is true, as $|b|$ is maximized in each case C$i$ by the corresponding $\varphi^{Ci}$. ■

In summary, for the maximization of $|b|$ over $\varphi \in \Phi$, five cases are considered, as case C1 is not relevant. Case C3 and C6 with $\gamma_2 \neq 0$ give one extremal point $\varphi^{C3}$ and $\varphi^{C6}$, respectively. Case C2, C4, and C5 with $\gamma_2 = 0$ result in two extremal points $\{\varphi_I^{C2}, \varphi_{II}^{C2}\}$, $\{\varphi_I^{C4}, \varphi_{II}^{C4}\}$, and $\{\varphi_I^{C5}, \varphi_{II}^{C5}\}$, respectively, which satisfy $\varphi_I^{Ci} = -\varphi_{II}^{Ci}$ and $\varphi_{f_I} \leq 0$. If there is one extremal point, it lies on bd $\Phi$ or in int $\Phi$, and if there are two extremal points, they lie on bd $\Phi$.

## 6.2 Existence of time-optimal solutions

As discussed in Section 4.1, before candidates for time-optimal solutions from an initial state $x_0$ to a desired state $x_d$ are defined by necessary optimality conditions, it makes sense to verify that such solutions exist. Otherwise, there may be trajectories which satisfy the necessary optimality conditions, but give no time-optimal solutions from $x_0$ to $x_d$. For the time-optimal control problem for the RKM, the existence of time-optimal solutions is shown next.

**Theorem 6.2.1** *(Existence of time-optimal solutions for the RKM) For the time-optimal control problem 6.0.2, time-optimal solutions exist.*

**Proof** To show the existence of time-optimal solutions for the RKM 5.0.2 by the Filippov Existence Theorem 4.1.1, controllability has to hold, the linear growth condition

$$\|g(\theta,\varphi)\;v\| \leq c\,(1+\|q\|) \tag{6.19}$$

has to apply for a constant $c > 0$ and all $(q,u) \in Q \times U$, and the velocity sets $F_U(q) = \{f(q,u) \mid u \in U\}$ have to be convex for $f(q,u) = g(\theta,\varphi)\,v$ and all $q \in Q$.

According to Theorem 5.3.2, the RKM is controllable. Regarding condition (6.19), the norm of the right-hand side of the RKM satisfies $\|g(\theta,\varphi)\, v\| \leq 2/\sqrt{3}\,\hat{v}$ for $|v| \leq \hat{v}$ and $\varphi \in \Phi$ by Lemma 5.3.5. Thus, condition (6.19) is satisfied for $c \geq 2/\sqrt{3}\,\hat{v}$.

To analyze the convexity of the velocity sets $F_U(q)$, the RKM $\dot{q} = g(\theta,\varphi)\, v$ is written as driftless affine control system $\dot{q} = T(\theta)\, w(u)$ using the transformation matrix $T(\theta)$ given by (5.32) and the transformed input (5.31) which is

$$w(u) = \begin{bmatrix} w_1(u) \\ w_2(u) \\ w_3(u) \end{bmatrix} = \begin{bmatrix} \sin(\varphi_f - \varphi_r)\, v \\ \cos(\varphi_f)\cos(\varphi_r)\, v \\ \frac{1}{2}\sin(\varphi_f + \varphi_r)\, v \end{bmatrix}. \tag{6.20}$$

For $U = [-\hat{v}, \hat{v}] \times \Phi$, the transformed input satisfies $w \in W$ for the transformed input space

$$W = \{(w_1, w_2, w_3) \mid w_1 = w_1(u)\,, w_2 = w_2(u)\,, w_3 = w_3(u)\,, u \in U\}\,.$$

For $\hat{v} = 1$, three views of $W$ are shown in the upper row of Figure 6.1. The input space $W$ has the shape of a solid double cone with elliptic profile and curved boundary surfaces similar to spherical caps. Obviously, $W$ is non-convex.

The velocity sets of the RKM can be represented by $F_U(\theta) = \{g(\theta,\varphi)\, v \mid (v,\varphi) \in U\}$ for $u = (v,\varphi) \in U$ and by $F_W(\theta) = \{T(\theta)\, w \mid w \in W\}$ for $w \in W$. As $F_W(\theta)$ results from the rotation of the non-convex input space $W$ by the matrix $T(\theta)$, the velocity sets $F_W(\theta)$ are non-convex. Thus, the velocity sets $F_U(\theta)$ generated by the original input space $U$ are non-convex, and the Filippov Existence Theorem does not apply.

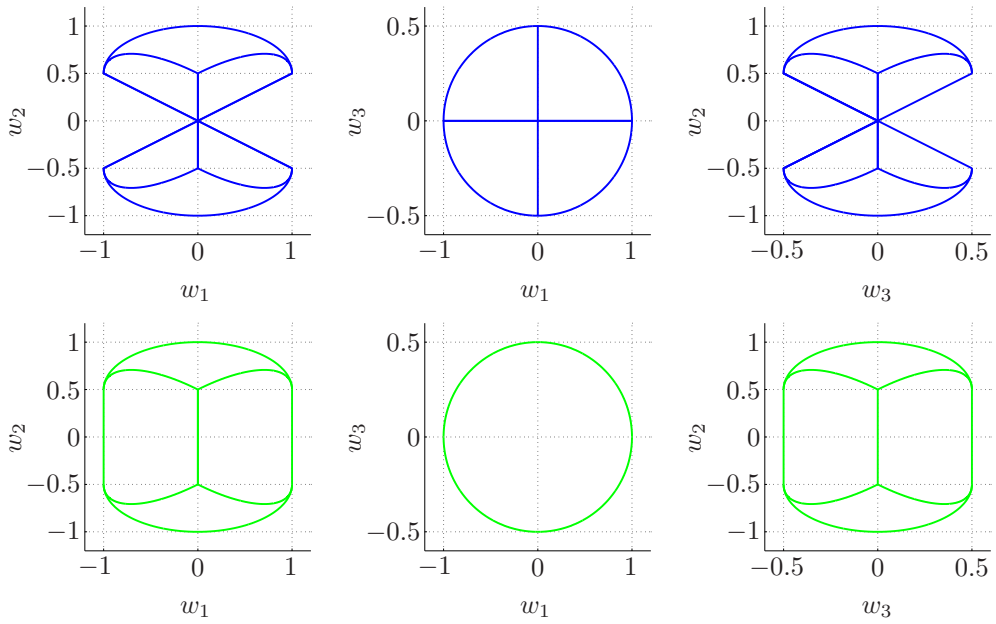


Figure 6.1: Non-convex input space $W$ (upper row) and convexified input space $\widehat{W}$ (lower row).

As the conditions of the Filippov Existence Theorem are true except for the convexity of the velocity sets, Corollary 4.1.2 is used to show existence. For this, the driftless affine control system $\dot{q} = T(\theta)\, w$ is studied for the convexified input space $\widehat{W} = \operatorname{conv}(W)$. The convexified input space $\widehat{W}$ is depicted in the lower row of Figure 6.1. As the map $w\colon U \to W$ given by (6.20) is continuous and $U$ is compact, $W$ and $\widehat{W}$ are compact as well.

By Theorem 6.1.4, for all $\gamma^* \neq (0,0,0)$, always $|b(\gamma^*, \varphi^*)| > 0$ holds, and $\gamma = (0,0,0)$ is not relevant for time-optimal control. Thus, $v^* = \pm\hat{v}$ given by (6.9) is true for almost all $t \in I$.

Hence, the extremal inputs $u^*$ satisfy $u^* \in \widetilde{U}$ for the modified input space $\widetilde{U} = \{-\hat{v}, \hat{v}\} \times \Phi$ for almost all $t \in I$. The modified transformed input space $\widetilde{W}$ which corresponds to $W$ is

$$\widetilde{W} = \left\{ (w_1, w_2, w_3) \;\middle|\; w_1 = w_1(u^*), w_2 = w_2(u^*), w_3 = w_3(u^*), u^* \in \widetilde{U} \right\}.$$

Because of $v^* = \pm\hat{v}$ for almost all $t$, the extremal inputs $w^* \in \widehat{W}$ satisfy $w^* \in \widetilde{W}$ for almost all $t$. Moreover, $\widetilde{W} \subset W$ holds for $\widetilde{U} \subset U$. Thus, the extremal inputs $w^*$ of the driftless affine control system $\dot{q} = T(\theta)\, w$ with convexified input space $\widehat{W}$ lie in the original input space $W \supset \widetilde{W}$ for almost all $t$, and time-optimal solutions exist according to Corollary 4.1.2. ■

## 6.3 Classification of the extremals

In preparation for the classification of the extremals of the RKM into normal, abnormal, regular, and singular, basic properties of the extremals are shown next.

**Lemma 6.3.1** *(Properties of the extremals of the RKM) Let the necessary optimality conditions of Theorem 6.1.1 be satisfied. Then, the following properties hold for the extremals:*

**E1:** *If $\gamma^*(t) \neq 0$ holds for some $t \in I$, it holds for all $t \in I$.*

**E2:** *The conditions of case C2 can be satisfied by $\gamma^*$ only at isolated times.*

**E3:** *If $\gamma^*(t)$ is of case C3 for some $t \in I$, it is of case C3 for all $t \in I$.*

**E4:** *If $\gamma^*(t)$ is of case C4 for some $t \in I$, it is of case C4 for all $t \in I$.*

**E5:** *The conditions of case C5 can be satisfied by $\gamma^*$ only at isolated times.*

**E6:** *If $\gamma^*(t)$ is of case C2, C5, or C6 for some $t \in I$, it is of one of these cases for all $t \in I$. For almost all $t \in I$, $\gamma^*(t)$ is of case C6 then.*

**E7:** *For $\gamma(0) \neq 0$, the extremal configuration $q^*(\cdot)$ is non-constant.*

**Proof**

**E1:** To show property E1, the time derivative of $\gamma^*$ is considered for positive and negative time. For positive time $t^+ := t$, the time derivative $\dot{\gamma}^{*+} = \mathrm{d}\gamma^*/\mathrm{d}t^+$ given by (6.10) is

$$\begin{aligned} \dot{\gamma}_1^{*+} &= \left( \tfrac{1}{2}\gamma_2^* \sin(\varphi_f^* + \varphi_r^*) - \gamma_3^* \cos(\varphi_f^*)\cos(\varphi_r^*) \right) v^*, \\ \dot{\gamma}_2^{*+} &= \gamma_3^* \sin(\varphi_f^* - \varphi_r^*) v^*, \\ \dot{\gamma}_3^{*+} &= -\gamma_2^* \sin(\varphi_f^* - \varphi_r^*) v^*. \end{aligned} \tag{6.21}$$

For negative time $t^- := -t$, the time derivative $\dot{\gamma}^{*-} = \mathrm{d}\gamma^*/\mathrm{d}t^-$ is

$$\begin{aligned} \dot{\gamma}_1^{*-} &= -\left( \tfrac{1}{2}\gamma_2^* \sin(\varphi_f^* + \varphi_r^*) - \gamma_3^* \cos(\varphi_f^*)\cos(\varphi_r^*) \right) v^*, \\ \dot{\gamma}_2^{*-} &= -\gamma_3^* \sin(\varphi_f^* - \varphi_r^*) v^*, \\ \dot{\gamma}_3^{*-} &= \gamma_2^* \sin(\varphi_f^* - \varphi_r^*) v^*. \end{aligned} \tag{6.22}$$

For $\gamma^*(t)$ of case C4, $\dot{\gamma}^{*+} = 0$ holds due to $\gamma_2^* = \gamma_3^* = 0$. Thus, $\gamma^*$ is constant in positive time, and $\gamma^*(t') \neq 0$ is true for all $t'$ satisfying $t \leq t' \leq T$. Likewise, for $\gamma_2^* = \gamma_3^* = 0$, $\dot{\gamma}^{*-} = 0$ holds, and $\gamma^*$ is constant in negative time. Thus, $\gamma^*(t') \neq 0$ is true for all $t'$ meeting $0 \leq t' \leq t$. Hence, $\gamma^*(t) \neq 0$ holds for all $t \in I$. For $\gamma^*$ of case C2, C3, C5, or

C6, $\bar{\gamma}_{23}^* = \frac{1}{2}\big((\gamma_2^*)^2 + (\gamma_3^*)^2\big)$ is considered, which satisfies $\bar{\gamma}_{23}^* > 0$ in these cases. Using (6.21) and (6.22) yields

$$\dot{\bar{\gamma}}_{23}^{*+} = \gamma_2^*\,\dot{\gamma}_2^{*+} + \gamma_3^*\,\dot{\gamma}_3^{*+} = \gamma_2^*\,\gamma_3^*\,\sin\big(\varphi_f^* - \varphi_r^*\big)v^* - \gamma_3^*\,\gamma_2^*\,\sin\big(\varphi_f^* - \varphi_r^*\big)v^* = 0,$$

$$\dot{\bar{\gamma}}_{23}^{*-} = \gamma_2^*\,\dot{\gamma}_2^{*-} + \gamma_3^*\,\dot{\gamma}_3^{*-} = -\gamma_2^*\,\gamma_3^*\,\sin\big(\varphi_f^* - \varphi_r^*\big)v^* + \gamma_3^*\,\gamma_2^*\,\sin\big(\varphi_f^* - \varphi_r^*\big)v^* = 0.$$

As the time derivative of $\bar{\gamma}_{23}^*$ in positive and negative time equals zero, $\bar{\gamma}_{23}^*$ is constant in positive and negative time. Thus, $\gamma^*(t) \neq 0$ holds for all $t \in I$, and property E1 is true.

**E2:** To show property E2, the time derivative (6.21) in positive time is considered for $\gamma^*(t)$ of case C2, i. e., for $\gamma_1^* = \gamma_2^* = 0$, $\gamma_3^* \neq 0$, and $\varphi_I^{C2} = \varphi_1 = (-\hat{\varphi}, -\hat{\varphi})$ or $\varphi_{II}^{C2} = \varphi_4 = (\hat{\varphi}, \hat{\varphi})$. Then, $\dot{\gamma}_1^{*+} \neq 0$ holds, and $\gamma^*(t+\varepsilon)$ is not of case C2 for sufficiently small $\varepsilon > 0$.

**E3:** To prove property E3, the time derivatives (6.21) and (6.22) in positive and negative time are analyzed for $\gamma^*(t)$ of case C3, i. e., for $\gamma_1^* = 0$, $\gamma_2^* \neq 0$, $\gamma_3^* = 0$, and $\varphi^{C3} = \varphi_0 = (0,0)$. As $\dot{\gamma}^{*+} = \dot{\gamma}^{*-} = 0$ holds, $\gamma^*(t)$ is of case C3 for all $t \in I$.

**E4:** Likewise, property E4 is shown for $\gamma^*(t)$ of case C4 with $\gamma_1^* \neq 0$, $\gamma_2^* = \gamma_3^* = 0$, and $\varphi_I^{C4} = \varphi_2 = (-\hat{\varphi}, \hat{\varphi})$ or $\varphi_{II}^{C4} = \varphi_3 = (\hat{\varphi}, -\hat{\varphi})$. For $\varphi_I^{C4}$ and $\varphi_{II}^{C4}$, there holds $\dot{\gamma}^{*+} = \dot{\gamma}^{*-} = 0$, and $\gamma^*(t)$ is of case C4 for all $t \in I$.

**E5:** Property E5 is shown like property E2. For $\gamma^*(t)$ of case C5, i. e., if $\gamma_1^* \neq 0$, $\gamma_2^* = 0$, $\gamma_3^* \neq 0$, and $\varphi^* = \varphi_I^{C5}$ or $\varphi^* = \varphi_{II}^{C5}$ holds, $\dot{\gamma}_2^{*+} \neq 0$ applies. This is true as $\gamma_3^* \neq 0$, $|\varphi_f^*| = \hat{\varphi}$, $|\varphi_r^*| < \hat{\varphi}$ or $\gamma_3^* \neq 0$, $|\varphi_f^*| < \hat{\varphi}$, $|\varphi_r^*| = \hat{\varphi}$ holds, resulting in $\dot{\gamma}_2^{*+} = \gamma_3^*\sin\big(\varphi_f^* - \varphi_r^*\big) \neq 0$. Thus, $\gamma^*(t+\varepsilon)$ is not of case C5 for sufficiently small $\varepsilon > 0$, and property E5 holds.

**E6:** To show property E6, it is utilized that $\gamma^*(t) \neq 0$ holds for all $t \in I$ by property E1, and, if $\gamma^*(t)$ is of case C3 or C4, then $\gamma^*(t)$ is of this case for all $t \in I$ due to property E3 and E4, respectively. Hence, if $\gamma^*(t)$ is of case C2, C5, or C6 at some $t \in I$, it satisfies $\gamma^*(t) \neq 0$ for all $t \in I$, i. e., it is of one of the cases C2 to C6 for all $t \in I$. As the cases C3 and C4 are excluded because of property E3 and E4, $\gamma^*(t)$ is of one of the cases C2, C5, or C6 for all $t$. Since $\gamma^*(t)$ can be of case C2 or C5 only at isolated times due to property E2 and E5, $\gamma^*(t)$ is of case C6 for almost all $t \in I$, and property E6 is true.

**E7:** The proof of property E7 is based on that $\gamma^*(t) \neq 0$ holds for $\gamma(0) \neq 0$ for all $t \in I$ due to property E1. Besides, for $\gamma^*(t) \neq 0$, always $|b(\gamma^*, \varphi^*)| > 0$ holds by Theorem 6.1.4. Thus, $v^* = \operatorname{sgn}(b^*)\,\hat{v}$ results in $v^* = \pm\hat{v}$ for $\hat{v} > 0$. Then $\dot{q}^*(t) \neq 0$ is true for all $t \in I$, as $\|\dot{q}^*\| = \|g(\theta^*, \varphi^*)\,v^*\|$ given by (5.21) meets $\|\dot{q}^*\| \geq \hat{v}$ for $v^* = \pm\hat{v}$ and $\varphi^* \in \Phi$ according to Lemma 5.3.5. Hence, the extremal configuration $q^*(\cdot)$ is always non-constant. ■

**Definition 6.3.2** *(Normalized initial condition of the transformed adjoint state) For any* $\gamma_0 = (\gamma_{10}, \gamma_{20}, \gamma_{30}) \neq 0$ *and* $\hat{v} > 0$,

$$\tilde{\gamma}_0 := \frac{1}{|b(\gamma_0, \varphi^*(0))|\;\hat{v}}\;\gamma_0 \tag{6.23}$$

*is called normalized initial condition of the transformed adjoint state.*

In (6.23), $b(\gamma_0, \varphi^*(0))$ is the function (6.8) evaluated at $\gamma = \gamma_0$ and $\varphi = \varphi^*(0)$. For any $\gamma_0 = (\gamma_{10}, \gamma_{20}, \gamma_{30}) \neq 0$, the normalized initial condition $\tilde{\gamma}_0 = \big(\tilde{\gamma}_{10}, \tilde{\gamma}_{20}, \tilde{\gamma}_{30}\big)$ of the transformed adjoint state $\gamma$ is obtained. It is normalized, as for $v^*(0) = \operatorname{sgn}(b(\gamma_0, \varphi^*(0)))\;\hat{v}$, there results

$$b(\tilde{\gamma}_0, \varphi^*(0))\;v^*(0) = 1. \tag{6.24}$$

**Theorem 6.3.3** *(Normal and abnormal extremals of the RKM) Let the necessary optimality conditions of Theorem 6.1.1 be satisfied. Then, there are no abnormal extremals for* $\mu = 0$. *For any* $\gamma_0 \neq 0$ *and* $\gamma(0) = \tilde{\gamma}_0$ *as in (6.23), a non-constant normal extremal results for* $\mu = 1$.

**Proof** By Theorem 6.2.1, time-optimal solutions exist for the RKM. To show that there are no abnormal extremals, but normal extremals for normalized initial conditions $\tilde{\gamma}_0$, the conditions N1 and N4 of Theorem 6.1.1 are considered. The conditions N2 and N3 are not relevant, as they do not take the value of $\mu$ into account. To satisfy condition N1 for $\mu = 0$, $\gamma^*(t) \neq 0$ has to be true for all $t \in I$. This implies $|b(\gamma^*, \varphi^*)| > 0$ by Theorem 6.1.4. Hence, $b^* \neq 0$ holds, and condition N4 cannot be true due to $b^* \neq 0$ and $v^* \neq 0$ for $v^* = \operatorname{sgn}(b^*)\, \hat{v}$. Thus, there are no abnormal extremals.

Since time-optimal solutions exist for the RKM, but there are no abnormal extremals, normal extremals have to exist. As condition N1 is trivially satisfied for $\mu = 1$, it only has to be shown that there are suitable initial conditions called $\tilde{\gamma}_0$ such that condition N4 holds. Since $H^*(t) = 0$ holds according to condition N4 for almost all $t \in I$, it is sufficient to consider $t = 0$. Initial conditions $\tilde{\gamma}_0$ which satisfy condition N4 result from (6.23) for $\gamma_0 \neq 0$. The normalization (6.23) is required since for $\varphi^*(0)$ obtained from condition N3 at $t = 0$, $|b(\gamma_0, \varphi^*(0))| > 0$ applies by Theorem 6.1.4, and $b(\gamma_0, \varphi^*(0))\, v^* > 0$ holds for $v^* = \operatorname{sgn}(b(\gamma_0, \varphi^*(0)))\, \hat{v}$. Hence, for $\tilde{\gamma}_0$ as in (6.23), (6.24) results. Then, for $\mu = 1$, condition N4 is true at $t = 0$, and, as $H^*$ is constant, for all $t$. Because of $\gamma_0 \neq 0$, the extremals are non-constant due to property E7. ■

**Theorem 6.3.4** *(Normal singular extremals of the RKM) Let the necessary optimality conditions of Theorem 6.1.1 be satisfied for $\mu = 1$. For a normalized initial condition $\tilde{\gamma}_0$ of case C4 and $\gamma(0) = \tilde{\gamma}_0$, a non-constant normal singular extremal results which is singular with respect to $\varphi^*$. There are no singular extremals with respect to $v^*$.*

**Proof** By Theorem 6.3.3, non-constant normal extremals exist for normalized initial conditions $\tilde{\gamma}_0$. Due to property E2, if a normalized initial condition $\tilde{\gamma}_0$ is of case C4, $\gamma^*(t)$ is of case C4 for all $t$. For $\gamma^*(t)$ of case C4, $|b|$ is maximized by the two points $\varphi_I^{C4} = \varphi_2$ and $\varphi_{II}^{C4} = \varphi_3$. Thus, the input $u^* = (v^*, \varphi^*)$ is not uniquely determined over the proper time interval $I$, leading to singular extremals with respect to $\varphi^*$.

No normal singular extremals with respect to $v^*$ exist, since for $\tilde{\gamma}_0 \neq 0$, there holds $\gamma^*(t) \neq 0$ for all $t$ by property E1. Thus, due to Theorem 6.1.4, $|b(\gamma^*, \varphi^*)| > 0$ and $b(\gamma^*, \varphi^*) \neq 0$ applies for all $t \in I$, and $v^*$ is uniquely determined by $v^* = \operatorname{sgn}(b^*)\, \hat{v}$. ■

**Theorem 6.3.5** *(Normal regular extremals of the RKM) Let the necessary optimality conditions of Theorem 6.1.1 be satisfied for $\mu = 1$. For a normalized initial condition $\tilde{\gamma}_0$ of case C2, C3, C5, or C6 and $\gamma(0) = \tilde{\gamma}_0$, a non-constant normal regular extremal results.*

**Proof** Non-constant normal extremals exist for normalized initial conditions $\tilde{\gamma}_0$ according to Theorem 6.3.3. For a normalized initial condition $\tilde{\gamma}_0$ of case C3, $\gamma^*(t)$ is of case C3 for all $t$ due to property E3. For $\gamma^*(t)$ of case C3, $|b|$ is maximized by $\varphi^{C3} = \varphi_0$. Thus, the extremal input $u^* = (v^*, \varphi^*)$ is uniquely determined for all $t \in I$, and a normal regular extremal arises.

For a normalized initial condition $\tilde{\gamma}_0$ of case C2, C5, or C6, $\gamma^*(t)$ is of one of these cases for all $t$ by property E6. Due to Theorem 6.1.4, in case C2, $|b|$ is maximized by the points $\{\varphi_I^{C2}, \varphi_{II}^{C2}\}$, in case C5, by the points $\{\varphi_I^{C5}, \varphi_{II}^{C5}\}$, and in the generic case C6, by the single point $\varphi^{C6}$. By property E2 and E5, $\gamma^*(t)$ can be of case C2 or C5 only at isolated times. Thus, the extremal inputs $u^*$ are not uniquely determined only at isolated times. Due to property E6, $\gamma^*(t)$ is of case C6 for almost all $t \in I$. As $u^*$ is uniquely determined then, a normal regular extremal results. ■

By Theorem 6.3.5 and 6.3.4, normal regular and normal singular extremals of the RKM are obtained for normalized initial conditions $\tilde{\gamma}_0$ of case C2, C3, C5, and C6, and of case C4, respectively. There are no extremals of the RKM which consist of regular and singular subarcs, i. e., segments where the extremal is regular and segments where it is singular.

At the beginning of this chapter, the steering limit $\hat{\varphi} = \frac{\pi}{4}$ was fixed by Assumption 6.0.1. This steering limit gives a simple structure of the extremals of the RKM. If instead of $\hat{\varphi} = \frac{\pi}{4}$, a steering limit $0 < \hat{\varphi} < \frac{\pi}{4}$ would be used and $\gamma^*$ would be of case C5, then the solutions $\varphi_I^{C5}$ and $\varphi_{II}^{C5}$ would not satisfy $\left|\varphi_f^{C5}\right| = \hat{\varphi}$ and $\left|\varphi_r^{C5}\right| < \hat{\varphi}$ or $\left|\varphi_f^{C5}\right| < \hat{\varphi}$ and $\left|\varphi_r^{C5}\right| = \hat{\varphi}$ for all $(\gamma_1^*, \gamma_3^*)$.

Instead, $\left|\varphi_f^{C5}\right| = \left|\varphi_r^{C5}\right| = \hat{\varphi}$ could be true. In this case, property E5 of Lemma 6.3.1 would not be guaranteed, but $\dot{\gamma}_2^* = 0$ could hold over a proper time interval. Then, $\gamma^*$ could be of case C5 over a proper time interval, leading to a singular extremal, as $\varphi$ could be chosen from $\varphi_I^{C5}$ and $\varphi_{II}^{C5}$ over this interval. The resultant extremal could be singular over the whole interval $I$ or consist of singular and regular arcs. That is, it could be singular at the beginning and become regular after a time when the maximization of $|b|$ gives solutions $\varphi_I^{C5}$ and $\varphi_{II}^{C5}$ with $\left|\varphi_f^{C5}\right| = \hat{\varphi}$ and $\left|\varphi_r^{C5}\right| < \hat{\varphi}$ or $\left|\varphi_f^{C5}\right| < \hat{\varphi}$ and $\left|\varphi_r^{C5}\right| = \hat{\varphi}$. Then, $\dot{\gamma}_2^* = 0$ would not hold any more, and $\gamma^*$ would not be of case C5 any longer. In contrast, for $\hat{\varphi} = \frac{\pi}{4}$, property E5 holds, i. e., the conditions of case C5 can be satisfied by $\gamma^*$ only at isolated times. Thus, $\varphi$ can be chosen from $\varphi_I^{C5}$ and $\varphi_{II}^{C5}$ only at isolates times, and the extremals are regular. In particular, there are no extremals with singular and regular arcs. This considerably simplifies the structure of the extremals for time-optimal control of the RKM.

If a steering limit $\frac{\pi}{4} < \hat{\varphi} < \frac{\pi}{2}$ would hold, then for $\gamma^*$ of case C4, the maximization of $|b|$ would not give two isolated solutions $\{\varphi_I^{C4}, \varphi_{II}^{C4}\}$. Instead, all steering angles satisfying

$$\varphi_f - \varphi_r = \pm\frac{\pi}{2} \tag{6.25}$$

would maximize $|b|$. For all steering angles meeting condition (6.25), property E4 holds, i. e., if $\gamma^*(t)$ is of case C4 for some $t \in I$, it is of case C4 for all $t \in I$. Since the steering angles are not uniquely determined by (6.25), singular extremals result. As discussed in Section 6.5, for singular extremals obtained for $\gamma^*$ of case C4 and $\hat{\varphi} = \frac{\pi}{4}$, the extremal steering angles can be chosen at each time from $\{\varphi_I^{C4}, \varphi_{II}^{C4}\}$. The corresponding singular extremals are arcs of circles of minimal turning radius. In contrast, for $\frac{\pi}{4} < \hat{\varphi} < \frac{\pi}{2}$, arbitrary steering angles satisfying (6.25) can be chosen at each time. Depending on the chosen $\varphi$, different derivatives $(\dot{x}, \dot{y})$ and different singular extremals result, which do not have to consist of arcs of circles of constant radius. Thus, singular extremals for $\hat{\varphi} = \frac{\pi}{4}$ have a less complex structure than for $\frac{\pi}{4} < \hat{\varphi} < \frac{\pi}{2}$.

Recall Definition 4.3.4 of the search space $\Lambda_{x_0}$. It includes all initial conditions $\lambda_0$ of the adjoint state for which there are normal regular extremals with $x^*(0) = x_0$ and $\lambda^*(0) = \lambda_0$. Based on Theorem 6.3.5, the search space for time-optimal control of the RKM is given next.

**Corollary 6.3.6** *(Search space $\Lambda_{q_0}$) The time-optimal control problem 6.0.2 is considered for an initial configuration $q_0 = (\theta_0, x_0, y_0)$ with $\theta_0 = 0$. Let $\gamma_0$ be of case C2, C3, C5, or C6. Then, $\lambda_0 = \gamma_0$ holds, and the search space $\Lambda_{q_0}$ consists of all normalized initial conditions*

$$\tilde{\lambda}_0 := \frac{1}{|b(\lambda_0, \varphi^*(0))|\ \hat{v}}\ \lambda_0. \tag{6.26}$$

**Proof** For $\theta_0 = 0$, the transformation (6.7) gives $R(\theta_0) = E_3$. Thus, $\lambda_0 = \gamma_0$ holds for the adjoint state $\lambda$ and the transformed adjoint state $\gamma$, and $\tilde{\lambda}_0 = \tilde{\gamma}_0$ for their normalized initial conditions. For $\lambda_0 = \gamma_0$, (6.26) results from (6.23). By Theorem 6.3.5, non-constant normal regular extremals arise from normalized initial conditions $\tilde{\gamma}_0$ of case C2, C3, C5, and C6. Hence, $\Lambda_{q_0}$ consists of all normalized initial conditions $\tilde{\lambda}_0$ which are of one of these cases. ■

For $\lambda_0 = (\lambda_{10}, \lambda_{20}, \lambda_{30}) \neq 0$, the normalized initial condition $\tilde{\lambda}_0 = \left(\tilde{\lambda}_{10}, \tilde{\lambda}_{20}, \tilde{\lambda}_{30}\right)$ of the adjoint state $\lambda$ results from (6.26).

## 6.4 Analysis of normal regular extremals

In this section, the normal regular extremals of the RKM are analyzed. They result from normalized initial conditions $\tilde{\gamma}_0$ of case C2, C3, C5, and C6. Depending on the trajectory $\theta^*(\cdot)$, the following types of normal regular extremals are distinguished.

**Definition 6.4.1** *(Types of normal regular extremals of the RKM) Depending on $\theta^*(\cdot)$, the normal regular extremals of the RKM are divided into the following types:*

***Type S:*** *$\theta^*(\cdot)$ is constant, i. e., $\dot{\theta}^*(t) = 0$ and $\theta^*(t) = \theta_0$ holds for all $t \in I$.*

***Type M:*** *$\theta^*(\cdot)$ is strictly monotone, i. e., $\dot{\theta}^*(t) < 0$ or $\dot{\theta}^*(t) > 0$ holds for all $t \in I$.*

***Type P:*** *$\theta^*(\cdot)$ is periodic, i. e., $\theta^*(t) = \theta^*(t + \triangle t)$ holds for some $\triangle t > 0$ and all $t \in I$.*

According to simulations, all normal regular extremals of the RKM are of type S, M, or P. The extremals with constant $\theta^*(\cdot)$ are denoted by type S, as they are straight line segments.

**Definition 6.4.2** *(Cusp, cusp time) A reversal of the driving direction of the RKM at time $t_c$ when $v^* = \operatorname{sgn}(h^*)\,\hat{v}$ switches from $\pm\hat{v}$ to $\mp\hat{v}$ is called cusp. The time $t_c$ is called cusp time.*

Definition 6.4.2 holds for $b^* = b(\gamma^*, \varphi^*)$ and $v^* = \operatorname{sgn}(b^*)\,\hat{v}$ as well. The cusps are a major feature of the extremals of type M and P. Moreover, normal singular extremals in Section 6.5 can have cusps. In the next section, properties of normal regular extremals are given, in Section 6.4.2, simulation results are presented, and in Section 6.4.3, the extremals are discussed. As only normal regular extremals are addressed here, they are simply referred to as extremals.

### 6.4.1 Properties

**Lemma 6.4.3** *(Properties of normal regular extremals of the RKM) For normal regular extremals of the RKM, the following properties hold:*

***NR1:*** *Extremals arising from normalized initial conditions $\tilde{\gamma}_0$ of case C3 are of type S.*

***NR2:*** *Extremals of type S have no cusps.*

***NR3:*** *Let $q_0 = (\theta_0, x_0, y_0)$ be the initial condition of an extremal of type S. There holds*

$$q^*(t) = \begin{bmatrix} \theta_0 \\ x_0 + \operatorname{sgn}(\tilde{\gamma}_{20}) \cos(\theta_0)\,\hat{v}\,t \\ y_0 + \operatorname{sgn}(\tilde{\gamma}_{20}) \sin(\theta_0)\,\hat{v}\,t \end{bmatrix}. \tag{6.27}$$

***NR4:*** *Extremals from initial conditions $\tilde{\gamma}_0$ of case C2, C5, and C6 are of type M or P.*

***NR5:*** *If $\gamma_2^*$ has a zero-crossing at time $t_c$, then $t_c$ is a cusp time.*

***NR6:*** *Extremals of type M and P can have cusps.*

***NR7:*** *If an extremal of type M has two consecutive cusps at the times $t_1$ and $t_2$, then $\theta^*(t_2) - \theta^*(t_1) = \pm\pi$ holds.*

**Proof**

**NR1:** According to property E3 of Lemma 6.3.1, if an initial condition $\tilde{\gamma}_0$ is of case C3, $\gamma^*(t)$ is of case C3 for all $t$. As $\varphi^* = \varphi_0 = (0, 0)$ is obtained from the maximization of $|b|$ for $\gamma^*$ of case C3, $\dot{\theta}^* = \sin\left(\varphi_f^* - \varphi_r^*\right) v^* = 0$ holds for all $t$. Thus, $\theta^*(t) = \theta_0$ is constant for all $t$, and an extremal of type S results.

**NR2:** For extremals of type S, the right-hand side of the differential equation for $\gamma^*$ given by (6.10) vanishes due to $\varphi^* = \varphi_0 = (0, 0)$ and $\gamma_3^* = 0$. Thus, $\gamma^*$ and $b^*$ are constant. Hence, $b^*$ has no zero-crossings, $v^* = \operatorname{sgn}(b^*)\,\hat{v}$ is constant, and there are no cusps.

**NR3:** For $\varphi^* = \varphi_0 = (0, 0)$ and constant $v^* = \operatorname{sgn}(\tilde{\gamma}_{20})\,\hat{v}$, the RKM (5.4) gives

$$\begin{aligned} \dot{\theta}^* &= 0, \\ \dot{x}^* &= \operatorname{sgn}(\tilde{\gamma}_{20}) \cos(\theta_0)\,\hat{v}, \\ \dot{y}^* &= \operatorname{sgn}(\tilde{\gamma}_{20}) \sin(\theta_0)\,\hat{v}. \end{aligned} \tag{6.28}$$

Here, $v^* = \operatorname{sgn}(b^*)\,\hat{v}$ gives $v^* = \operatorname{sgn}(\tilde{\gamma}_{20})\,\hat{v}$, as for $\gamma_1^* = 0$, $\gamma_2^* = \tilde{\gamma}_{20} \neq 0$, $\gamma_3^* = 0$, and $\cos(\varphi_f^*)\cos(\varphi_r^*) > 0$, there holds $\operatorname{sgn}(b^*) = \operatorname{sgn}(\tilde{\gamma}_{20})$. By analytical integration of (6.28) starting from $q_0 = (\theta_0, x_0, y_0)$ at $t = 0$, (6.27) results.

**NR4:** According to Definition 6.4.1, normal regular extremals of the RKM are of type S, M, or P. By property NR1, extremals of type S result from initial conditions $\tilde{\gamma}_0$ of case C3. By property E3 of Lemma 6.3.1, for $\tilde{\gamma}_0$ of case C3, $\gamma^*(t)$ is of case C3 for all $t$. By Theorem 6.3.5, normal regular extremals arise from initial conditions $\tilde{\gamma}_0$ of one of these cases. By property E6, for $\tilde{\gamma}_0$ of case C2, C5, or C6, $\gamma^*(t)$ is of case C2, C5, or C6 for all $t \in I$. Hence, disregarding $\tilde{\gamma}_0$ of case C3 leading to extremals of type S, initial conditions $\tilde{\gamma}_0$ of case C2, C5, and C6 give normal regular extremals which are not of type S. Thus, they are of type M or P.

**NR5:** If $b^*$ has a zero-crossing, $v^* = \operatorname{sgn}(b^*)\,\hat{v}$ switches from $\pm\hat{v}$ to $\mp\hat{v}$, and a cusp occurs. In the following, it is assumed that $\gamma_2^*$ has a zero-crossing at time $t_c$ such that $\gamma_2^*(t_c - \varepsilon) < 0$, $\gamma_2^*(t_c) = 0$, $\gamma_2^*(t_c + \varepsilon) > 0$ holds for small $\varepsilon > 0$. At time $t_c$, $\gamma^*(t_c)$ is of case C$j$ for $j \in \{2, 5\}$, and $|b|$ is maximized by two points $\{\varphi_I^*(t_c), \varphi_{II}^*(t_c)\}$ with $\varphi_{II}^*(t_c) = -\varphi_I^*(t_c)$, as for $\gamma_2^* = 0$, there holds $b(\gamma^*, \varphi^*) = -b(\gamma^*, -\varphi^*)$.

For $\gamma_2^* \neq 0$, $b(\gamma^*, \varphi^*) = -b(\gamma^*, -\varphi^*)$ does not hold. At time $t_c - \varepsilon$ before the zero-crossing of $\gamma_2^*$, the maximization of $|b|$ results in $|b(\gamma^*, \varphi^*)| = -b(\gamma^*, \varphi^*)$, as $\gamma_2^* \cos(\varphi_f^*)\cos(\varphi_r^*) < 0$ holds for $\gamma_2^* < 0$ and all $\varphi^* \in \Phi$. At time $t_c + \varepsilon$ after the zero-crossing, $|b(\gamma^*, \varphi^*)| = b(\gamma^*, \varphi^*)$ results from the maximization of $|b|$, as $\gamma_2^* \cos(\varphi_f^*)\cos(\varphi_r^*) > 0$ holds for $\gamma_2^* > 0$ and all $\varphi^* \in \Phi$. Thus, if $\gamma_2^*$ has a zero-crossing at time $t_c$, then $b^*$ has a zero-crossing at time $t_c$, and a cusp occurs.

**NR6:** By property NR4, extremals of type M and P arise from initial conditions $\tilde{\gamma}_0$ of case C2, C5, and C6. According to Definition 6.1.2 of the transformed adjoint state,

$$\gamma_2^*(t) = \cos(\theta^*(t))\,\lambda_2^*(t) + \sin(\theta^*(t))\,\lambda_3^*(t)$$

holds, and due to the adjoint equation (6.4), $\lambda_2^* = \tilde{\lambda}_{20}$ and $\lambda_3^* = \tilde{\lambda}_{30}$ is true. If $\tilde{\gamma}_0$ is of case C2, C5, or C6, then $\gamma_2^*$ is not constant, as $\lambda_2^2(0) + \lambda_3^2(0) > 0$ holds for these initial conditions, and $\theta^*$ is not constant for extremals of type M and P. Here, $\lambda_2^2(0) + \lambda_3^2(0) > 0$ is true for $\tilde{\gamma}_0$ of case C2, C5, and C6, since for these initial conditions, always $\tilde{\gamma}_2^2(0) + \tilde{\gamma}_3^2(0) > 0$ holds, and from $\gamma = R(\theta)\,\lambda$,

$$\lambda = R^{-1}(\theta)\,\gamma = R(-\theta)\,\gamma = (\gamma_1, \cos(\theta)\,\gamma_2 - \sin(\theta)\,\gamma_3, \sin(\theta)\,\gamma_2 + \cos(\theta)\,\gamma_3)$$

follows. As $\gamma_2^*$ is not constant, it may have zero-crossings, which give rise to cusps.

**NR7:** If $\gamma_2^*(t_c) = 0$ holds for an extremal of type M, $\gamma_2^*$ has a zero-crossing and does not touch zero, i. e., $\gamma_2^*(t_c - \varepsilon) < 0$, $\gamma_2^*(t_c) = 0$, $\gamma_2^*(t_c + \varepsilon) < 0$ cannot hold. To see this,

$$\gamma_2^*(t_c) = \cos(\theta^*(t_c))\,\tilde{\lambda}_{20} + \sin(\theta^*(t_c))\,\tilde{\lambda}_{30} = 0 \tag{6.29}$$

is assumed, resulting in

$$\frac{\sin(\theta^*(t_c))}{\cos(\theta^*(t_c))} = -\frac{\tilde{\lambda}_{20}}{\tilde{\lambda}_{30}} \tag{6.30}$$

for $\cos(\theta^*(t_c)) \neq 0$. For constant $\tilde{\lambda}_{20}$ and $\tilde{\lambda}_{30}$, the time derivative of (6.29) gives

$$\dot{\gamma}_2^*(t_c) = -\dot{\theta}^*(t_c)\sin(\theta^*(t_c))\,\tilde{\lambda}_{20} + \dot{\theta}^*(t_c)\cos(\theta^*(t_c))\,\tilde{\lambda}_{30} = 0. \tag{6.31}$$

Because of $\dot{\theta}^*(\cdot) \neq 0$ for an extremal of type M, (6.31) yields

$$\frac{\sin(\theta^*(t_c))}{\cos(\theta^*(t_c))} = \frac{\tilde{\lambda}_{30}}{\tilde{\lambda}_{20}} \tag{6.32}$$

for $\cos(\theta^*(t_c)) \neq 0$. For (6.30) and (6.32) to hold simultaneously, $\tilde{\lambda}_{20} = \tilde{\lambda}_{30} = 0$ must be true. However, according to property NR4, extremals of type M arise from initial conditions $\tilde{\gamma}_0$ of case C2, C5, and C6, for which $\tilde{\gamma}_2^2(0) + \tilde{\gamma}_3^2(0) > 0$ and thus $\lambda_2^2(0) + \lambda_3^2(0) > 0$ holds. Hence, if $\gamma_2^*(t_c) = 0$ holds, $\gamma_2^*$ cannot just touch zero at $t_c$.

If $\gamma_2^*$ has a zero-crossing at time $t_1$,

$$\gamma_2^*(t_1) = \cos(\theta^*(t_1))\,\tilde{\lambda}_{20} + \sin(\theta^*(t_1))\,\tilde{\lambda}_{30} = 0$$

holds. Then, $\gamma_2^*(t_2) = 0$ applies if

$$\theta^*(t_2) - \theta^*(t_1) = \pm n\,\pi \tag{6.33}$$

is true for $n \in \mathbb{N}$, since

$$\begin{aligned}
\gamma_2^*(t_2) &= \cos(\theta^*(t_2))\,\tilde{\lambda}_{20} + \sin(\theta^*(t_2))\,\tilde{\lambda}_{30} \\
&= \cos(\theta^*(t_1) \pm k\,\pi)\,\tilde{\lambda}_{20} + \sin(\theta^*(t_1) \pm k\,\pi)\,\tilde{\lambda}_{30} \\
&= (-1)^n \left(\cos(\theta^*(t_1))\,\tilde{\lambda}_{20} + \sin(\theta^*(t_1))\,\tilde{\lambda}_{30}\right) \\
&= 0
\end{aligned}$$

follows then. Here, $n = 0$ resulting in $\theta^*(t_2) - \theta^*(t_1) = 0$ is excluded, as $\theta^*(\cdot)$ is strictly monotone for an extremal of type M according to Definition 6.4.1. If (6.33) is true, the extremal has cusps at $t_1$ and $t_2$. Then, only $n = 1$ can hold, since otherwise for $n > 1$, there would be additional zero-crossings of $\gamma_2^*$ and thus additional cusps between $t_1$ and $t_2$. Then, the cusps at $t_1$ and $t_2$ would be no consecutive cusps as assumed. Hence, $n = 1$ holds, and (6.33) gives $\theta^*(t_2) - \theta^*(t_1) = \pm\pi$. ■

Normalized initial conditions of case C3 which lead to extremals of type S by property NR1 are $\tilde{\gamma}_0 = (0, \pm 1/\hat{v}, 0)$. The closed-form representation (6.27) for extremals of type S exists due to the constant orientation $\theta^*$. For fixed $q_0$ and $t = T$, it gives an end-point map 2.1.5. For extremals of type M and P with non-constant $\theta^*$, no closed-form representations and no end-point maps can be derived, see Section 6.6. Regarding property NR5, the sign of $b^*$ from the maximization of $|b|$ equals the sign of $\gamma_2^*$. Hence, cusps occur at the zero-crossings of $\gamma_2^*$.

### 6.4.2 Simulation results

For the simulation data given here, the differential equations (5.4) of the RKM and the adjoint equation (6.4) were integrated numerically. The equations were driven by the extremal inputs $u^* = (v^*, \varphi^*)$ obtained from $|b(\gamma^*, \varphi^*)| = \max_{\varphi \in \Phi} |b(\gamma^*, \varphi)|$ and $v^* = \operatorname{sgn}(b^*)\,\hat{v}$. For numerical integration, the MATLAB function **ode45** was used which implements a Runge-Kutta solver of fifth order. All simulations were generated for $q_0 = (0, 0, 0)$, $I = [0, 10]$, and $\hat{v} = 1$.

Figure 6.2 shows an extremal of type S obtained from the initial condition $\tilde{\gamma}_0 = (0, 1, 0)$ which is of case C3. The figure consists of time plots of the orientation angle $\theta^*$ and the adjoint state $(\lambda_1^*, \lambda_2^*, \lambda_3^*)$, an $(x^*, y^*)$ plot, and time plots of the transformed adjoint state $(\gamma_1^*, \gamma_2^*, \gamma_3^*)$, the input $\left(v^*, \varphi_f^*, \varphi_r^*\right)$, the Hamiltonian function $H^*$ (6.2), and the function $h^*$ (6.3). Extremals of type S are straight line segments with constant velocity $v^* = \operatorname{sgn}(\tilde{\gamma}_{20})\,\hat{v}$, constant steering angles $\varphi^* = \varphi_0$, and no cusps.

The extremals of type M and P in Figure 6.3 and 6.4 arise from initial conditions $\tilde{\gamma}_0$ of case C6. For Figure 6.3, $\tilde{\gamma}_0 = (0.5, 0.6, 0.6)$ is used, and for Figure 6.4, $\tilde{\gamma}_0 = (0.18, 0.8, 0.8)$. The figures consist of the same plots as Figure 6.2. In Figure 6.3, $\theta^*$ is plotted once as real number $\theta^* \in \mathbb{R}$ and once as angle $\theta^* \in [-\pi, \pi)$, for which values $\theta^*$ and $\theta^* + 2\,n\,\pi$ are identified. In Figure 6.3, $\theta^* \in \mathbb{R}$ is strictly increasing, i. e., $\dot{\theta}^*(t) > 0$ holds for all $t \in I$. In Figure 6.4, $\theta^*$ is periodic and satisfies $\theta^*(t) = \theta^*(t + \triangle t)$. The cusps of extremals of type M are located on one side of an imaginary line in the gross direction of the extremal, and the cusps of extremals of type P lie alternately on both sides. According to simulations, extremals of type M or P can arise from initial conditions $\tilde{\gamma}_0$ of case C2, C5, and C6. The type depends on the specific $\tilde{\gamma}_0$.

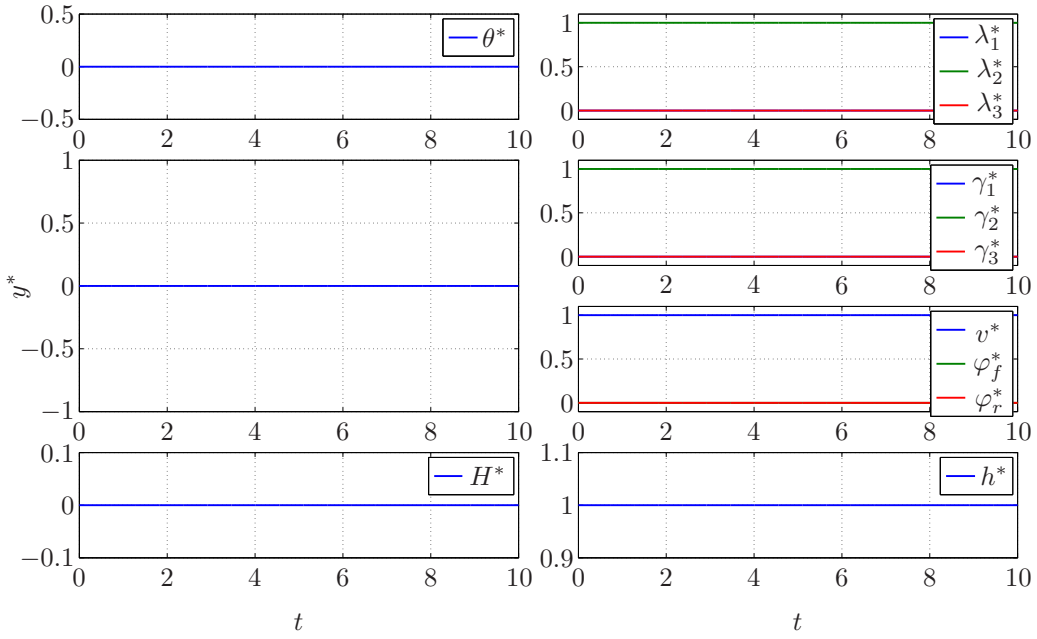


Figure 6.2: Normal regular extremal of the RKM of type S.

### 6.4.3 Discussion

Due to $v^* = \operatorname{sgn}(h^*)\,\hat{v}$ as in (6.6) and $v^* = \operatorname{sgn}(b^*)\,\hat{v}$ as in (6.9), the functions $h^*$ and $b^*$ resemble switching functions 4.3.5. However, extremals of type M and P are no bang-bang solutions, as the RKM is no affine control system. Between consecutive cusps, the extremal velocity $v^*$ is constant, and at cusps, it is discontinuous. The extremal steering angles $\varphi^*$ from the maximization of $|b|$ are piecewise differentiable. As long as $\varphi^* = \varphi_i$ holds for fixed $i = 1,...,9$, the steering angles are differentiable, as they are either constant or result from the differentiable functions (6.11) to (6.15). When the steering angles enter or leave bd $\Phi$, they are continuous, since at this instant of time, they change from $\varphi^* = \varphi_i$ to $\varphi^* = \varphi_j$ for $i \neq j$ and $\varphi_i = \varphi_j$. At a cusp time $t_c$, the steering angles $\varphi^*(t_c)$ can be discontinuous, as $\gamma^*(t_c)$ is of case C$i$ for $i \in \{2, 5\}$, and the steering angles change from $\varphi^* = \varphi_I^{Ci}$ to $\varphi^* = \varphi_{II}^{Ci}$, or vice versa.

Since $\theta^*$ is periodic for extremals of type P and $\theta^*(t + \triangle t) = \theta^*(t) \pm 2\,\pi$ holds for extremals of type M due to property NR7, $\gamma_2^*$ oscillates periodically and symmetrically around zero. As the cusps occur at the zero-crossings of $\gamma_2^*$ due to property NR5, the arc duration $\triangle t_c = \frac{1}{2}\triangle t$ between two cusps is constant for each extremal. Extremals of type M and P are uniquely determined by $\tilde{\gamma}_0$. They are independent of whether $\varphi_I^{Ci}$ or $\varphi_{II}^{Ci}$ is chosen at a cusp time $t_c$ with $\gamma^*(t_c)$ of case C$i$ for $i \in \{2, 5\}$. This is true as $\dot{\gamma}_2^*(t_c)$ is independent of the chosen extremal point $\varphi_I^{Ci}$ or $\varphi_{II}^{Ci}$. The time derivatives $\left(\dot{\theta}^*, \dot{x}^*, \dot{y}^*\right)$ as in (5.4) and $(\dot{\gamma}_1^*, \dot{\gamma}_3^*)$ given by (6.10) have different values at $t = t_c$ for $\varphi_I^{Ci}$ and $\varphi_{II}^{Ci}$, but are uniquely determined for almost all $t \in I$ due to property E2 and E5. Thus, extremals of type M and P are uniquely determined by $\tilde{\gamma}_0$.

For extremals of type M, $\theta^*(t + \triangle t_c) = \theta^*(t) \pm \pi$ holds due to property NR7. According to simulations, for extremals of type P, the total change of the orientation $\triangle\theta_c = \int_{t_1}^{t_2} \left|\dot{\theta}(t)\right| \mathrm{d}t$ between two cusps at time $t_1$ and $t_2$ satisfies $0 < \triangle\theta_c < \pi$. The value of $\triangle\theta_c$ depends on $\tilde{\gamma}_0$. Both types of extremals have periodic trajectories $\gamma_2^*$ and constant arc durations $\triangle t_c$ between cusps. Due to $\dot{\theta}^* = \sin\left(\varphi_f^* - \varphi_r^*\right) v^*$ and $v^* = \pm\hat{v}$, there holds $\left|\dot{\theta}^*(t)\right| \leq \hat{v}$ for all $t$. Thus, for extremals of type M and P, $\triangle t_c > \pi/\hat{v}$ and $\triangle t_c > \triangle\theta_c/\hat{v}$ holds, respectively. As both bounds on $\triangle t_c$ are positive, only a finite number of cusps can occur in each compact interval $I$. Hence, no Fuller phenomenon with an infinite number of switchings exists. Between two cusps, there

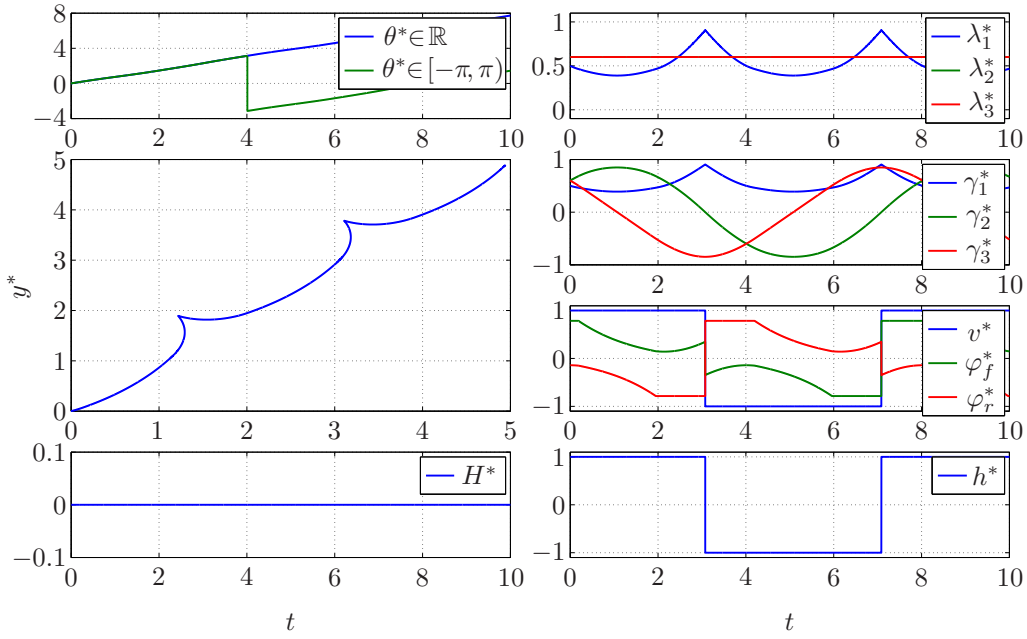


Figure 6.3: Normal regular extremal of the RKM of type M.

are at most two times at which $\varphi^*$ reaches or leaves bd $\Phi$ so that $\varphi^*$ changes from $\varphi_i$ to $\varphi_j$.

## 6.5 Analysis of normal singular extremals

Normal singular extremals result from normalized initial conditions of case C4 which are $\tilde{\gamma}_0 = (\pm 1/(\sin(2\,\hat{\varphi})\;\hat{v}), 0, 0)$.

**Lemma 6.5.1** *(Properties of normal singular extremals of the RKM) For normal singular extremals of the RKM, the following properties hold:*

***NS1:*** *The input $u^* = (v^*, \varphi^*)$ can be chosen at each time $t$ from*

$$\begin{aligned} u_I &= (-\operatorname{sgn}(\tilde{\gamma}_{10})\,\hat{v}, \varphi_2)\,, \\ u_{II} &= (\operatorname{sgn}(\tilde{\gamma}_{10})\,\hat{v}, \varphi_3)\,. \end{aligned} \tag{6.34}$$

***NS2:*** *Let $q^*(t_1) = (\theta^*(t_1), x^*(t_1), y^*(t_1))$ be the configuration at time $t_1$ and $u^* \in \{u_I, u_{II}\}$ the constant input over $I = [t_1, t_2]$. For $u^* = u_I$, set $\sigma_u = 1$, and for $u^* = u_{II}$, set $\sigma_u = -1$. Then, at time $t_2$, the configuration is*

$$q^*(t_2) = \begin{bmatrix} \theta^*(t_1) + \operatorname{sgn}(\tilde{\gamma}_{10})\,\hat{v}\,(t_2 - t_1) \\ x^*(t_1) - \frac{1}{2}\,\sigma_u\big(\sin(\theta^*(t_1) + \operatorname{sgn}(\tilde{\gamma}_{10})\,\hat{v}\,(t_2 - t_1)) - \sin(\theta^*(t_1))\big) \\ y^*(t_1) + \frac{1}{2}\,\sigma_u\big(\cos(\theta^*(t_1) + \operatorname{sgn}(\tilde{\gamma}_{10})\,\hat{v}\,(t_2 - t_1)) - \cos(\theta^*(t_1))\big) \end{bmatrix}. \tag{6.35}$$

**Proof**

**NS1:** By Theorem 6.3.4, normal singular extremals arise from normalized initial conditions $\tilde{\gamma}_0$ of case C4. Due to property E2, for an initial condition of case C4, $\gamma^*(t)$ is of case C4 for all $t \in I$. Then, $|b|$ is maximized by $\varphi_I^{C4} = \varphi_2$ and $\varphi_{II}^{C4} = \varphi_3$. For $\gamma^*(t)$ of case C4, $\gamma_1^* = \tilde{\gamma}_{10} \neq 0$ and $\gamma_2^* = \gamma_3^* = 0$ holds. Thus, $v^* = \operatorname{sgn}(b^*)\;\hat{v} = \operatorname{sgn}\left(\tilde{\gamma}_{10} \sin\left(\varphi_f^* - \varphi_r^*\right)\right)\hat{v}$

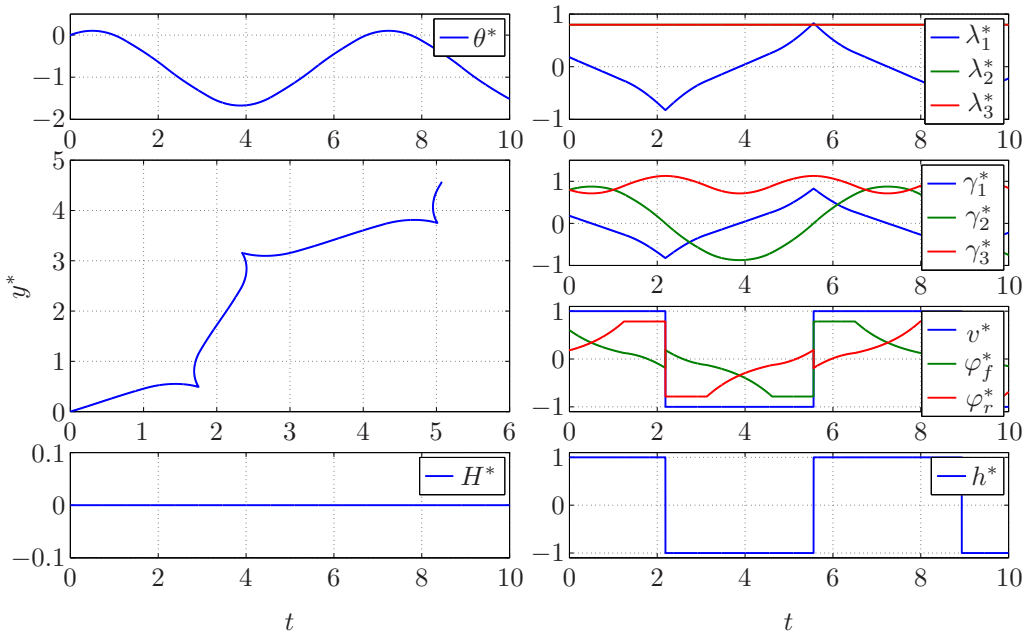


Figure 6.4: Normal regular extremal of the RKM of type P.

is true. For $\hat{\varphi} = \frac{\pi}{4}$, the input $u_I = (-\operatorname{sgn}(\tilde{\gamma}_{10})\,\hat{v}, \varphi_2)$ results from $\varphi_I^{C4} = \varphi_2 = (-\hat{\varphi}, \hat{\varphi})$, and the input $u_{II} = (\operatorname{sgn}(\tilde{\gamma}_{10})\,\hat{v}, \varphi_3)$ results from $\varphi_{II}^{C4} = \varphi_3 = (\hat{\varphi}, -\hat{\varphi})$.

**NS2:** For a fixed input $u^* \in \{u_I, u_{II}\}$ and the corresponding $\sigma_u$, the RKM (5.4) yields

$$\begin{aligned} \dot{\theta}^* &= \operatorname{sgn}(\tilde{\gamma}_{10})\,\hat{v}, \\ \dot{x}^* &= -\tfrac{1}{2}\,\sigma_u\,\operatorname{sgn}(\tilde{\gamma}_{10})\cos(\theta^*)\,\hat{v}, \\ \dot{y}^* &= -\tfrac{1}{2}\,\sigma_u\,\operatorname{sgn}(\tilde{\gamma}_{10})\sin(\theta^*)\,\hat{v}. \end{aligned} \tag{6.36}$$

By analytical integration of (6.36) over $[t_1, t_2]$ starting from $q^*(t_1)$, (6.35) results. ■

For a normal singular extremal arising from an initial condition $\tilde{\gamma}_0$ of case C4, the input $u^*$ can be chosen at each time from $\{u_I, u_{II}\}$. If a constant input $u^*$ is applied over a time interval, an arc of a circle of minimal turning radius $R$ is obtained. By Lemma 5.3.7, for $\hat{\varphi} = \frac{\pi}{4}$, $R = \frac{1}{2}$ results. The transition of the configuration along this arc is given by (6.35). The normal singular extremals of the RKM are concatenations of such arcs. For fixed $q_0$, $T$, $\hat{\varphi}$, and $\hat{v}$, different extremals result depending on the sign of $\tilde{\gamma}_{10}$ and the intervals over which $u^* = u_I$ and $u^* = u_{II}$ is used. Since the transition of the configuration along each arc can be represented by (6.35), closed-form representations and end-point maps 2.1.5 of the normal singular extremals can be derived. Every time the input switches from $u_I$ to $u_{II}$ or vice versa, a cusp occurs.

Figure 6.5 shows a normal singular extremal of the RKM consisting of three arcs of circles. To generate the figure, $q_0 = (0, 0, 0)$, $\tilde{\gamma}_0 = (1, 0, 0)$, $\hat{v} = 1$, and $T = 6$ was used. For the figure, the input $u_{II}$ was set over the interval $[0, 2.5)$, the input $u_I$ over $[2.5, 4.5)$, and the input $u_{II}$ over $[4.5, 6]$. This way, a normal singular extremal with cusps at $t_1 = 2.5$ and $t_2 = 4.5$ resulted.

## 6.6 Discussion of the extremals

For the RKM, normal regular and normal singular extremals exist by Theorem 6.3.5 and 6.3.4. These extremals were discussed in Section 6.4 and 6.5. They are generated by piecewise differen-

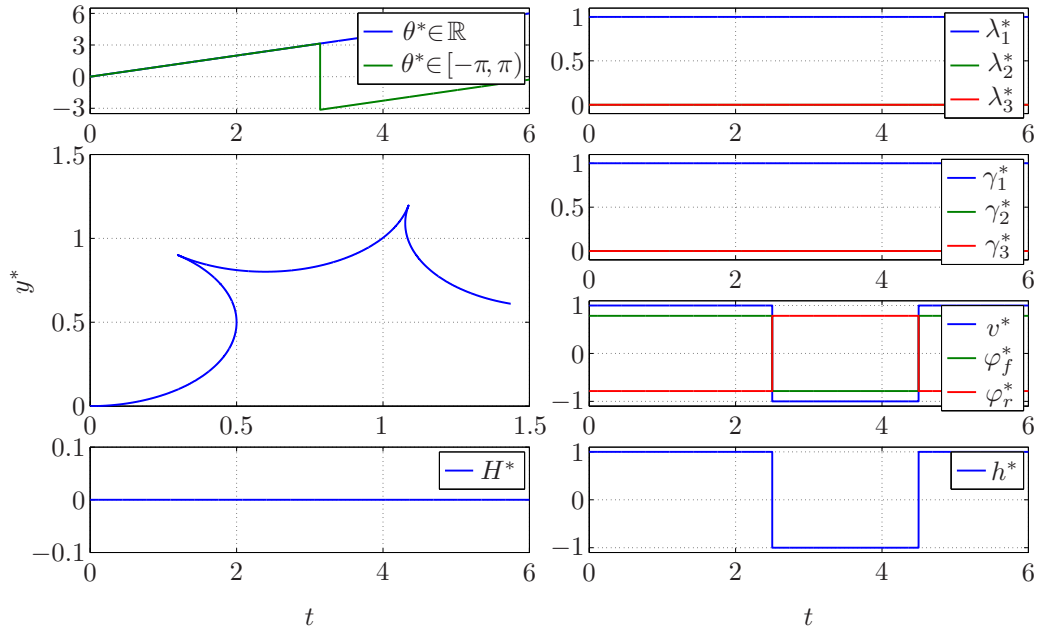


Figure 6.5: Normal singular extremal of the RKM.

tiable steering inputs $\varphi^*$ and piecewise constant driving inputs $v^*$. Switchings of $v^*$ cause cusps, i. e., reversals of the driving direction. Normal regular extremals of type M and P and normal singular extremals may have cusps, whereas normal regular extremals of type S have none. Over each compact interval $I$, the extremals can only have finitely many cusps. Depending on the trajectory of $\theta^*$, each normal regular extremal is of type S, M, or P.

The extremals of the RKM, the car-like robot, and the differential drive show differences and similarities. Reeds-Shepp paths, i. e., shortest paths of the car-like robot driving forward and backward, are equivalent to time-optimal solutions, as the absolute translational velocity $|v_t| = \sqrt{\dot{x}^2 + \dot{y}^2}$ is constant. These paths consist of straight line segments and arcs of circles of minimal turning radius, see [94, 108, 120]. The extremals for time-optimal control of the differential drive in [9, 10, 60] comprise straight line segments and turns on the spot. Similarly simple extremals of the RKM are the normal regular extremals of type S which are straight line segments and the normal singular extremals which consist of arcs of circles. As for the car-like robot and the differential drive, no abnormal extremals exist for the RKM by Theorem 6.3.3.

The turning rate $\dot{\theta}^*$ of the extremals of the car-like robot and the differential drive is zero or piecewise constant. Thus, closed-form representations of their extremals and end-point maps 2.1.5 can be given depending on a finite parameter set. These closed-form solutions simplify the path planning and the optimality analysis based on derivatives of the end-point map, see [94, 108, 120]. In contrast, for the RKM, closed-form representations only exist for normal regular extremals of type S, which are given by (6.27), and for normal singular extremals, which result from the concatenation of transitions (6.35). For normal regular extremals of type M and P, such representations are not available, as the extremal turning rate $\dot{\theta}^*$ is not piecewise constant but varies continuously. While $v^*$ is piecewise constant, $\varphi^*$ obtained from the maximization of $|b|$ can vary continuously. In particular, no closed-form solutions of the extremals can be derived based on the concatenation of flows under constant inputs 2.1.6, as the extremal steering inputs are not piecewise constant. Hence, normal regular extremals of type M and P can only be integrated numerically, which makes their analysis challenging.

# Part III

# Path planning and optimality

# 7 Approach for time-optimal control

This chapter introduces our approach for time-optimal control. It gives time-optimal or near time-optimal solutions from an initial state $x_0$ to a desired state $x_d$ based on normal regular extremals. To find such solutions, the path planning is performed iteratively over a decreasing time horizon until an optimal solution is found or the iteration is terminated. The path planning searches for an initial condition $\lambda(0)$ of the adjoint state which give rise to a normal regular extremal from $x_0$ to $x_d$. Here, $\lambda(0)$ is determined by local optimization initialized to a random starting point. In this chapter, the optimization problem for the initial condition is analyzed and algorithms for path planning and time-optimal control are given, followed by an analysis of the convergence of the approach.

**Definition 7.0.1** *(Path planning problem using normal regular extremals) For a time-optimal control problem 2.2.3, let $(x^*(\cdot), \lambda^*(\cdot), u^*(\cdot))$ be normal regular extremals which satisfy the necessary optimality conditions of the Maximum Principle 4.2.2, and $\Lambda_{x_0}$ the search space 4.3.4. Fix a constant $\varepsilon_x > 0$. The problem to find an end time $\tau$ and an initial condition $\lambda_0^{PP} \in \Lambda_{x_0}$ such that for an extremal satisfying $x^*(0) = x_0$ and $\lambda^*(0) = \lambda_0^{PP}$, there holds $\|x^*(\tau) - x_d\| \leq \varepsilon_x$ is called path planning problem using normal regular extremals. Any solution $(\lambda_0^{PP}, \tau)$ is called solution to the path planning problem.*

The path planning problem is a modified version of the boundary value problem 4.4.1 of the time-optimal control problem with free end time. In contrast to problem 4.4.1, for problem 7.0.1, only normal regular extremals are considered, and the desired state $x_d$ has to be reached only within the tolerance $\varepsilon_x$. Here, $\|\cdot\| : M \to \mathbb{R}_{\geq 0}$ is the Euclidean norm. If $\|x^*(\tau) - x_d\| \leq \varepsilon_x$ holds for small $\varepsilon_x$, then $x^*(\tau)$ is close to $x_d$. The search space $\Lambda_{x_0}$ consists of all initial conditions $\lambda_0$ of the adjoint state for which there are normal regular extremals satisfying $x^*(0) = x_0$ and $\lambda^*(0) = \lambda_0$. Thus, $\lambda_0^{PP} \in \Lambda_{x_0}$ has to hold.

Due to the restriction to normal regular extremals, there may be no solution to problem 7.0.1 for specific $x_0$, $x_d$, and $\varepsilon_x$, even if the system is controllable and time-optimal solutions exist. This is true since some $x_d$ may be reachable from $x_0$ within the tolerance $\varepsilon_x$ only by abnormal or singular extremals.

**Definition 7.0.2** *(Near time-optimal control problem using normal regular extremals) For a time-optimal control problem 2.2.3, let $\tau^{to}$ be the end time of a time-optimal solution, $(x^*(\cdot), \lambda^*(\cdot), u^*(\cdot))$ normal regular extremals which satisfy the necessary optimality conditions of the Maximum Principle 4.2.2, and $\Lambda_{x_0}$ the search space 4.3.4. Fix constants $k \geq 1$ and $\varepsilon_x > 0$. The problem to find an end time $\tilde{\tau}^{to} \leq k\,\tau^{to}$ and an initial condition $\lambda_0^{to} \in \Lambda_{x_0}$ such that for an extremal satisfying $x^*(0) = x_0$ and $\lambda^*(0) = \lambda_0^{to}$, there holds $\|x^*(\tilde{\tau}^{to}) - x_d\| \leq \varepsilon_x$ is called near time-optimal control problem using normal regular extremals. Any solution $(\lambda_0^{to}, \tilde{\tau}^{to})$ is called solution to the near time-optimal control problem.*

The near time-optimal control problem results from the path planning problem 7.0.1 by the requirement that the solution has to be a near time-optimal solution 2.2.5 satisfying $\tilde{\tau}^{to} \leq k\,\tau^{to}$. If only normal regular extremals exist for a time-optimal control problem, solutions to problem 7.0.2 can be time-optimal, i. e., $k = 1$ can hold. For general control problems, there are not only normal regular extremals, but also abnormal or singular ones. Solutions to problem 7.0.2 do not always exist. If there are solutions, they are not time-optimal in general.

In the following, path planning and time-optimal control using exclusively normal regular extremals is covered. The problems 7.0.1 and 7.0.2 are referred to as the path planning and near time-optimal control problem without stressing each time that normal regular extremals are

applied. The normal regular extremals are simply referred to as extremals, as neither normal singular nor abnormal extremals are taken into account. Since only extremals $(x^*(\cdot), \lambda^*(\cdot), u^*(\cdot))$ are considered, the superscript $^*$ is omitted for the trajectories of $x$, $\lambda$, and $u$.

## 7.1 Simplification of the path planning problem

In this section, approaches are given to simplify a path planning problem by reducing its complexity and scope. Such simplifications are often applied before a path planning problem is solved, see [10, 13, 60, 94, 106, 107, 108]. In particular, the simplifications are beneficial for practical application of path planning methods. At first, for a control system with affine input $v$ and non-affine input $w$, a scaling of the affine input is addressed. This scaling based on a time transformation allows to normalize the affine input $v$ so that for one input variable $v_i$ with symmetric input space, $v_i \in [-1, 1]$ results. Then, the transformation of the initial state of a left-invariant control system 3.1.4 to the origin of the configuration space is discussed. Further simplifications not mentioned here arise from symmetry properties of optimal paths. Such properties are studied for the car-like robot in [13, 106, 108].

**Theorem 7.1.1** *(Affine input scaling) Let $U = V \times W$ be an input space with*

$$V = [-\hat{v}_1, \hat{v}_1] \times \cdots \times [-\hat{v}_{m_1}, \hat{v}_{m_1}],$$

*$m_1 > 0$, $\hat{v}_j > 0$, and $W$ a compact subset of $\mathbb{R}^{m_2}$, $m_2 \geq 0$. For a control system*

$$\dot{x}(t) = f(x(t), u(t)) = f_0(x(t), w(t)) + \sum_{j=1}^{m_1} g_j(x(t), w(t))\, v_j(t) \tag{7.1}$$

*with input $u = (v_1, \ldots, v_{m_1}, w_1, \ldots, w_{m_2}) \in U$, let $(\tau, x(\cdot), u(\cdot))$ be an admissible solution $S(x_0, x_d)$ over the time interval $I = [0, \tau]$.*

*Choose one input variable $v_i$ from $(v_1, \ldots, v_{m_1})$. Then, for the control system*

$$\check{x}'(s) = \check{f}(\check{x}(s), \check{u}(s)) = \frac{1}{\hat{v}_i} f_0(\check{x}(s), \check{w}(s)) + \sum_{j=1}^{m_1} g_j(\check{x}(s), \check{w}(s))\, \check{v}_j(s) \tag{7.2}$$

*with the scaled input space $\check{U} = \check{V} \times W$,*

$$\check{V} = \left[-\frac{\hat{v}_1}{\hat{v}_i}, \frac{\hat{v}_1}{\hat{v}_i}\right] \times \cdots \times \left[-\frac{\hat{v}_{i-1}}{\hat{v}_i}, \frac{\hat{v}_{i-1}}{\hat{v}_i}\right] \times [-1, 1] \times \left[-\frac{\hat{v}_{i+1}}{\hat{v}_i}, \frac{\hat{v}_{i+1}}{\hat{v}_i}\right] \times \cdots \times \left[-\frac{\hat{v}_{m_1}}{\hat{v}_i}, \frac{\hat{v}_{m_1}}{\hat{v}_i}\right],$$

*and*

$$\check{v}(s) := \frac{1}{\hat{v}_i} v\left(\tfrac{1}{\hat{v}_i}\, s\right) = \frac{1}{\hat{v}_i} v(t), \quad \check{w}(s) := w\left(\tfrac{1}{\hat{v}_i}\, s\right) = w(t), \tag{7.3}$$

*$(\sigma, \check{x}(\cdot), \check{u}(\cdot))$ is an admissible solution $\check{S}(x_0, x_d)$ over the time interval $\check{I} = [0, \sigma]$ for $\sigma = \hat{v}_i\, \tau$.*

**Proof** Using the time transformation $s = \hat{v}_i\, t$ and plugging in $\check{x}(s) := x\left(\frac{1}{\hat{v}_i}\, s\right) = x(t)$, the derivative of $\check{x}(s)$ with respect to time $s$ is $\check{x}'(s) = \mathrm{d}\check{x}(s)/\mathrm{d}s = \frac{1}{\hat{v}_i}\, \dot{x}(t)$. From $\dot{x}(t)$ given by (7.1) and $t = \frac{1}{\hat{v}_i}\, s$,

$$\check{x}'(s) = \frac{1}{\hat{v}_i}\left(f_0\left(x\left(\tfrac{1}{\hat{v}_i}\, s\right), w\left(\tfrac{1}{\hat{v}_i}\, s\right)\right) + \sum_{j=1}^{m_1} g_j\left(x\left(\tfrac{1}{\hat{v}_i}\, s\right), w\left(\tfrac{1}{\hat{v}_i}\, s\right)\right) v_j\left(\tfrac{1}{\hat{v}_i}\, s\right)\right)$$

is obtained, and (7.3) gives (7.2).

Recall Definition 2.2.1 of an admissible solution $S(x_0, x_d)$ of a control system $\dot{x} = f(x, u)$ with state space $M$, initial state $x_0$, desired state $x_d$, and input space $U$. Each admissible

solution consists of the end time $\tau$ of an interval $I = [0, \tau]$, an input map $u\colon I \to U$, and a state trajectory $x\colon I \to M$ such that $x(0) = x_0$, $\dot{x} = f(x, u)$ for almost all $t \in I$, and $x(\tau) = x_d$ holds. Thus, for an admissible solution of system (7.1) with $x(0) = x_0$ and $x(\tau) = x_d$,

$$x(t) = x_0 + \int_0^t f(x(\xi)\,, u(\xi))\ \mathrm{d}\xi$$

and $u(t) \in U$ is true for all $t \in I$. Then, by inspection, the integration of system (7.2) with initial condition $\check{x}(0) = x_0$ gives

$$\check{x}(s) = x_0 + \int_0^s \check{f}(\check{x}(\zeta)\,, \check{u}(\zeta))\ \mathrm{d}\zeta,$$

which holds for all $s \in \check{I}$, and $\check{x}(\sigma) = x_d$. Because of (7.3), if $u(t) \in U$ and $v(t) \in V$ is true for all $t \in I$, then $\check{u}(s) \in \check{U}$ and $\check{v}(s) \in \check{V}$ is true for all $s \in \check{I}$ as well. Thus, $(\sigma, \check{x}(\cdot)\,, \check{u}(\cdot))$ is an admissible solution $\check{S}(x_0, x_d)$ from $x_0$ to $x_d$. ■

The purpose of the input scaling 7.1.1 is to obtain the scaled input space $\check{V}$ with a normalized input variable $\check{v}_i \in [-1, 1]$. If there is a solution $(\sigma, \check{x}(\cdot)\,, \check{u}(\cdot))$ from $x_0$ to $x_d$ for system (7.2) with scaled input space $\check{V}$ and end time $\sigma$, then there is a solution $(\tau, x(\cdot)\,, u(\cdot))$ from $x_0$ to $x_d$ for system (7.1) with original input space $V$ and end time $\tau = \frac{1}{\check{v}_i}\,\sigma$. In general, no equivalent scaling can be given for non-affine inputs $w$.

System (7.1) is more general than the affine control system $\dot{x} = f_0(x) + \sum_{i=1}^m g_i(x)\,u_i$, as it may have both affine and non-affine inputs. It is similar to system (4.17), for which local second-order sufficient optimality conditions are considered in Section 4.6.2. However, for system (4.17), $W = \mathbb{R}^{m_2}$ holds, whereas for system (7.1), $W$ is a compact subset of $\mathbb{R}^{m_2}$.

**Theorem 7.1.2** *(Transformation of the initial state) For a left-invariant control system 3.1.4 on a matrix Lie group $G$, let $g \in G$ be the state, $E$ the identity element of $G$, $g_0 \in G$ the initial state, and $g_d \in G$ the desired state. Let $(\tau, g(\cdot)\,, u(\cdot))$ be an admissible solution $S(g_0, g_d)$ over the time interval $[0, \tau]$. Then, for $\tilde{g}(t) := g_0^{-1}\,g(t)$, $(\tau, \tilde{g}(\cdot)\,, u(\cdot))$ is an admissible solution $\tilde{S}(\tilde{g}_0, \tilde{g}_d)$ over $[0, \tau]$ which satisfies $\tilde{g}_0 = E$ and $\tilde{g}_d = g_0^{-1}\,g_d$.*

**Proof** According to Definition 3.1.4, a left-invariant control system on a matrix Lie group $G$ with state $g \in G$ is given by $\dot{g} = g \sum_{i=1}^r w_i(u)\,e_i = g\,V(u)$. Here, $w_i\colon U \to \mathbb{R}$ are real analytic functions, and $e_i \in T_E G$ are linearly independent vectors of the Lie algebra. For an admissible solution $(\tau, g(\cdot)\,, u(\cdot))$ of a system with initial condition $g(0) = g_0$, there holds $u(t) \in U$ and

$$g(t) = g_0 + \int_{\xi=0}^t g(\xi)\,V(u(\xi))\ \mathrm{d}\xi \tag{7.4}$$

for all $t \in [0, \tau]$. At time $\tau$, $g(\tau) = g_d$ is true. Left multiplication of (7.4) by $g_0^{-1}$ gives

$$\begin{aligned} g_0^{-1}\,g(t) &= g_0^{-1}\left(g_0 + \int_{\xi=0}^t g(\xi)\,V(u(\xi))\ \mathrm{d}\xi\right) \\ &= g_0^{-1}\,g_0 + g_0^{-1}\int_{\xi=0}^t g(\xi)\,V(u(\xi))\ \mathrm{d}\xi \\ &= E + \int_{\xi=0}^t g_0^{-1}\,g(\xi)\,V(u(\xi))\ \mathrm{d}\xi, \end{aligned}$$

since $g_0^{-1}$ is constant. Thus, for the new state $\tilde{g} = g_0^{-1}\,g$, the new initial state $\tilde{g}_0 = g_0^{-1}\,g_0 = E$, and the new desired state $\tilde{g}_d = g_0^{-1}\,g_d$, $(\tau, \tilde{g}(\cdot)\,, u(\cdot))$ is an admissible solution of the new control system $\dot{\tilde{g}} = \tilde{g}\,V(u)$ which satisfies $u(t) \in U$ for all $t \in [0, \tau]$, $\tilde{g}(0) = E$, and $\tilde{g}(\tau) = \tilde{g}_d$. ■

The transformation of a trajectory $g(\cdot)$ starting from $g_0$ to a trajectory $\tilde{g}(\cdot)$ starting from $E$ simplifies the path planning problem, as only solutions with initial state $E$ have to be determined. If a trajectory $\tilde{g}(\cdot)$ from $E$ to $\tilde{g}_d$ generated by an input $u(\cdot)$ is known, the same input gives a trajectory $g(\cdot)$ from $g_0$ to $g_d$. Theorem 7.1.2 is used in Section 7.4 about modifications of the time-optimal control for practical application. By considering only paths starting from $E$ which represents the origin of the configuration space, the number of precomputed solutions is reduced. Transformations like in Theorem 7.1.2 are applied in [41, 60].

## 7.2 Path planning using normal regular extremals

This section addresses the path planning using normal regular extremals. It is performed iteratively in Section 7.3 to obtain near time-optimal solutions. The path planning problem is translated into an optimization problem, a solution approach for this problem is given, and its convergence is analyzed. Then, an algorithm which implements the path planning is presented.

### 7.2.1 Path planning as optimization problem

The path planning is implemented as an optimization problem for the initial condition $\lambda(0) = \lambda_0 \in \Lambda_{x_0}$ of the adjoint state. Here, $\Lambda_{x_0}$ is the search space from Definition 4.3.4. The initial condition $\lambda_0$ results from the minimizing of the deviation between the state $x(\tau)$ and the desired state $x_d$ at some end time $\tau$. In the following, sometimes $x_{\lambda_0}(t) := x(t, \lambda_0)$ is written instead of $x(t)$ to stress that the extremal state $x$ at time $t$ depends on $\lambda_0$.

**Definition 7.2.1** *(Optimization problem for path planning) For the path planning problem 7.0.1, let $(x_{\lambda_0}(\cdot), \lambda(\cdot), u(\cdot))$ be normal regular extremals which satisfy $x_{\lambda_0}(0) = x_0$ and $\lambda(0) = \lambda_0$, $\Lambda_{x_0}$ the search space, and $I = [0, T]$ a time interval with sufficiently large $T$.*

*Let $D\colon \Lambda_{x_0} \times I \to \mathbb{R}_{\geq 0}$, $(\lambda_0, t) \mapsto D(\lambda_0, t)$,*

$$D(\lambda_0, t) := \|x_{\lambda_0}(t) - x_d\| \tag{7.5}$$

*be the deviation between $x_{\lambda_0}(t)$ and $x_d$ over $\lambda_0 \in \Lambda_{x_0}$ and $t \in I$. Let $d\colon \Lambda_{x_0} \to \mathbb{R}_{\geq 0}$, $\lambda_0 \mapsto d(\lambda_0)$,*

$$d(\lambda_0) := D(\lambda_0, t_i^m) = \min_{t \in I} D(\lambda_0, t) \tag{7.6}$$

*be the minimal deviation between $x_{\lambda_0}(t)$ and $x_d$ over $\lambda_0 \in \Lambda_{x_0}$ at $t_i^m \in I$. Let*

$$T^m := \{t_i^m \in I \,|\, D(\lambda_0, t_i^m) = d(\lambda_0)\} \tag{7.7}$$

*be the set of all times $t_i^m$ which satisfy (7.6). Choose the minimal time*

$$t^m := \min T^m. \tag{7.8}$$

*The problem to find any initial condition $\lambda_0^m$ for which*

$$d(\lambda_0^m) = \inf_{\lambda_0 \in \Lambda_{x_0}} d(\lambda_0) \tag{7.9}$$

*holds is called optimization problem for path planning.*

As discussed below, for a bounded search space $\Lambda_{x_0}$, the set $T^m$ is finite and discrete. By (7.8), the minimal time $t^m$ is chosen from $T^m$, since in Section 7.3, near time-optimal solutions are determined by solving the optimization problem for path planning iteratively. Taking the minimal time for $t^m$ gives faster convergence. For varying $\lambda_0$, the times $t_i^m$ and $t^m$ may change. The infimum in (7.9) gives the greatest lower bound on $d$ for $\lambda_0 \in \Lambda_{x_0}$. As the search space $\Lambda_{x_0}$ does not have to be bounded or closed, there may be no point in $\Lambda_{x_0}$ at which $d$ attains its infimum, i. e., there may be no minimum of $d$ in $\Lambda_{x_0}$. Hence, the infimum of $d$ is used in (7.9). To deal with the minimum of $d$ instead of the infimum, the following assumption is made.

**Assumption 7.2.2** *(Minimum of d) There is at least one minimum of d in the search space* $\Lambda_{x_0}$ *such that (7.9) can be replaced by*

$$d(\lambda_0^m) = \min_{\lambda_0 \in \Lambda_{x_0}} d(\lambda_0)\,. \tag{7.10}$$

Assumption 7.2.2 holds e. g. if $\Lambda_{x_0}$ is compact and $d$ is continuous as shown below. There may be several minima satisfying (7.10). Then, any of these minima can be chosen. In the next section, the minimization of $d$ is implemented by local optimization. For several minima meeting (7.10), the resultant minimum $\lambda_0^m$ depends on the initialization of the optimization.

**Lemma 7.2.3** *(Solution to the path planning problem) For the optimization problem 7.2.1 and* $\varepsilon_x > 0$*, let*

$$D(\lambda_0^m, t^m) \leq \varepsilon_x \tag{7.11}$$

*be satisfied for an initial condition* $\lambda_0^m \in \Lambda_{x_0}$ *and a time* $t^m \in I$*. Then,* $\lambda_0^{PP} = \lambda_0^m$ *and* $\tau = t^m$ *give a solution to the path planning problem 7.0.1.*

**Proof** According to Definition 7.2.1, $D(\lambda_0^m, t^m) = \|x_{\lambda_0}(t^m) - x_d\|$ holds for a normal regular extremal $(x_{\lambda_0}(\cdot)\,, \lambda(\cdot)\,, u(\cdot))$ which satisfies $x_{\lambda_0}(0) = x_0$ and $\lambda(0) = \lambda_0^m$. Thus, for $\lambda_0^{PP} = \lambda_0^m$ and $\tau = t^m$, the condition $D(\lambda_0^{PP}, \tau) = \|x_{\lambda_0}(\tau) - x_d\| \leq \varepsilon_x$ is satisfied, and $(\lambda_0^{PP}, \tau)$ is a solution to the path planning problem 7.0.1. ■

A solution to path planning problem 7.0.1 exists if there is a normal regular extremal which goes from $x_0$ to $x(t^m)$ such that $\|x(t^m) - x_d\| \leq \varepsilon_x$ and $t^m \leq T$ holds. Hence, in Definition 7.2.1, the final time $T$ of the interval $I = [0, T]$ is assumed to be sufficiently large to ensure that no solution is missed if $\|x(t^m) - x_d\| \leq \varepsilon_x$ would hold only for a time $t^m > T$.

**Definition 7.2.4** *(Solution minimum) An initial condition* $\lambda_0^m \in \Lambda_{x_0}$ *such that* $D(\lambda_0^m, t^m) \leq \varepsilon_x$ *holds for the time* $t^m$ *obtained from (7.8) is called solution minimum.*

**Lemma 7.2.5** *(Properties of the optimization problem for path planning) For the optimization problem for path planning 7.2.1, the following properties hold:*

**O1:** *The minimal deviation d satisfies* $0 \leq d(\lambda_0) \leq \hat{d}$ *for all* $\lambda_0 \in \Lambda_{x_0}$ *and*

$$\hat{d} = \|x_0 - x_d\| > 0.$$

**O2:** *The minimal deviation d is continuous in* $\lambda_0$ *for all* $\lambda_0 \in \Lambda_{x_0}$*, but it need not be differentiable everywhere in* $\Lambda_{x_0}$*.*

**O3:** *Let* $\dot{x}(t) \neq 0$ *hold for almost all* $t \in I$*. Assume that the search space* $\Lambda_{x_0}$ *is bounded and*

$$(x(t) - x_d)^\top \dot{x}(t) = 0 \tag{7.12}$$

*does not hold over any proper interval in I. Then, the union*

$$T^m_{\Lambda_{x_0}} = \bigcup_{\lambda_0^m \in \Lambda_{x_0}} T^m \tag{7.13}$$

*of the sets* $T^m$ *over all solution minima* $\lambda_0^m$ *in* $\Lambda_{x_0}$ *is finite and discrete.*

**Proof**

**O1:** As $d$ gives the minimal value of $D$ with respect to $t$ and $D$ is the Euclidean norm of $x - x_d$, the minimal deviation $d$ is non-negative. If $D(\lambda_0, t) > D(\lambda_0, 0)$ holds for all $t \in (0, T]$, then $\hat{d} = D(\lambda_0, 0)$ is the minimal value of $d$. Thus, $d(\lambda_0) \leq \hat{d}$ holds for all $\lambda_0 \in \Lambda_{x_0}$. Since $x_0 \neq x_d$ holds for the control problem 2.2.1 underlying problem 7.0.1, $\hat{d} > 0$ is true.

**O2:** For a fixed initial condition $\lambda_0$, the deviation $D = \|x - x_d\|$ is continuous in $t$, as $x$ is absolutely continuous in $t$ according to Definition 2.1.3, and the Euclidean norm $\|\cdot\|$ is continuous. Likewise, for a fixed time $t$, $D$ is continuous in $\lambda_0$. This is true since the extremal adjoint state $\lambda(t)$ at the fixed time $t$ depends continuously on its initial condition $\lambda_0$. Hence, the extremal input $u$ obtained from the maximization of the Hamiltonian function $H(x, \mu, \lambda, u) = -\mu + \lambda^\top f(x, u)$ and thus the extremal state $x$ resulting from $\dot{x} = f(x, u)$ depend continuously on $\lambda_0$ at the fixed time $t$. The minimal deviation $d(\lambda_0) = \min_{t \in I} D(\lambda_0, t)$ is continuous in $\lambda_0$ for all $\lambda_0 \in \Lambda_{x_0}$, as $D$ is continuous in $t$ and $\lambda_0$, and the minimum of $D$ over $t \in I$ is continuous as well.

To show that $d$ need not be differentiable with respect to $\lambda_0$ for all $\lambda_0 \in \Lambda_{x_0}$, it is assumed that for some $\lambda_0$, the minimal deviation $d$ is obtained at time $t^m = t_1$, i. e., $d(\lambda_0) = D(\lambda_0, t_1)$ holds for $t_1$ from (7.8). For $\lambda_0'$ close to $\lambda_0$, $t_1'$ close to $t_1$, and $t_2 < t_1'$, it is assumed that $d(\lambda_0') = D(\lambda_0', t_1') = D(\lambda_0', t_2)$ holds, which implies $x(t_1') = x(t_2)$. If during the minimization of $d$, the initial condition changes from $\lambda_0$ to $\lambda_0'$, the time $t^m$ does not change from $t_1$ to $t_1'$, but to $t_2$ due to $t_2 < t_1'$, and $t^m$ is the minimal time of the set $T^m$. If $t_2$ is not close to $t_1$, i. e., if the time $t^m$ changes discontinuously from $t_1$ to $t_2$, then $\dot{x}(t_1') = \dot{x}(t_2)$ does not result from $x(t_1') = x(t_2)$ in general. Thus, if $t^m$ changes discontinuously, $d$ need not be differentiable with respect to $\lambda_0$.

**O3:** To show property O3, at first, it is assumed that there is only one solution minimum $\lambda_0^m$ in $\Lambda_{x_0}$. Instead of $D$ given by (7.5),

$$\bar{D}(\lambda_0, t) = \frac{1}{2} \sum_{i=1}^{n} (x(t) - x_d)^2 \tag{7.14}$$

is analyzed. If $D$ is constant over a proper time interval in $I$, then $\bar{D}$ is constant, and vice versa. For $\bar{D}$ to be constant,

$$\dot{\bar{D}} = \sum_{i=1}^{n} \dot{x}_i \, (x(t) - x_d) = (x(t) - x_d)^\top \, \dot{x}(t) = 0$$

has to hold. If $\dot{x}(t) \neq 0$ holds for almost all $t \in I$ and $(x(t) - x_d)^\top \, \dot{x}(t) = 0$ does not hold over any proper interval in $I$, then $(x(t) - x_d)^\top \, \dot{x}(t) \neq 0$ holds for almost all $t \in I$. Hence, $\bar{D}$ and $D$ are not constant. Therefore, if at $\lambda_0^m$ and $t^m$, there is a minimum of $D$, then $D$ cannot take the constant minimal value $D(\lambda_0^m, t^m)$ over a proper interval in $I$. Thus, the set $T^m$ of times $t_i^m$ given by (7.7) is discrete. As the deviation $D = \|x - x_d\|$ is continuous in $t$ and the time interval $I = [0, T]$ is compact, the number of times $t_i^m$ which satisfy (7.6) is finite. Thus, set $T^m$ of times $t_i^m$ is finite and discrete.

In general, there are multiple solution minima in $\Lambda_{x_0}$, called $\lambda_{0_j}^m$ in the following for $j \in \mathbb{N}_{>0}$. According to property O2, $d$ is continuous everywhere in $\Lambda_{x_0}$. Thus, the region of attraction $\Omega_j \subset \Lambda_{x_0}$ of each solution minimum $\lambda_{0_j}^m$ cannot be arbitrarily small. As the search space $\Lambda_{x_0}$ is assumed to be bounded, there is only a finite number of regions of attraction and of solution minima in $\Lambda_{x_0}$. The set $T_{\Lambda_{x_0}}^m$ as in (7.13) is the union of the sets $T_j^m$ taken over all solution minima $\lambda_{0_j}^m \in \Lambda_{x_0}$. Since each $T_j^m$ is finite and discrete as shown above, $T_{\Lambda_{x_0}}^m$ is finite and discrete as well, and property O3 holds. ■

The upper bound $\hat{d}$ on $d$ from property O1 is considered in Section 7.2.4 with respect to improvements of the path planning. If $d(\lambda_0) = \hat{d}$ holds for an extremal, the system moves away from $x_d$ for all $t \in I$, and $x(0) = x_0$ has the minimal deviation from $x_d$. According to property O2, $d$ is continuous, but need not be differentiable everywhere in $\Lambda_{x_0}$. Thus, the optimization problem 7.2.1 can be nonsmooth. The condition $(x(t) - x_d)^\top \, \dot{x}(t) = 0$ as in (7.12) means that

there is no non-constant trajectory $x(t)$ for which $\|x(t) - x_d\|$ is constant over a proper time interval. A system for which condition (7.12) can hold over a proper time interval is $\dot{x} = (u_1, u_2)$ for the state $x = (x_1, x_2)$, state space $M = \mathbb{R}^2$, input $u = (u_1, u_2)$, and input space $U = \mathbb{R}^2$. For $x_d = (0,0)$, $x_0 \neq (0,0)$, $u_1 = x_2$, und $u_2 = -x_1$, the state $x$ evolves on a circle around $(0,0)$, and (7.12) is satisfied for all time.

During the minimization of $d$, the times $t_i^m \in T^m$ can change discontinuously. The minimal deviation $d$ may have several minima in $\Lambda_{x_0}$, which can be local or global minima. In general, depending on the value of $\varepsilon_x$, not all minima satisfy condition (7.11). To solve the optimization problem 7.2.1, it is required to find not any minimum of $d$, but a solution minimum 7.2.4. Thus, problem 7.2.1 is a global optimization problem.

For illustration, simulation results are given here for path planning for the RKM 5.0.2 covered in detail in Chapter 8. Figure 7.1 shows $d$, $t^m$, and $\tilde{\lambda}_0 = \left(\tilde{\lambda}_{10}, \tilde{\lambda}_{20}, \tilde{\lambda}_{30}\right)$ over $\alpha_1 \in [1, 2.5]$. A parameterization of the search space is given by Theorem 8.2.1. Using this parameterization, the normalized initial conditions $\tilde{\lambda}_0 \in \Lambda_{q_0}$ are represented as $\tilde{\lambda}_0 = \tilde{\lambda}_0(\alpha)$ for $\alpha = (\alpha_1, \alpha_2)$. Figure 7.2 gives a plot of the two-dimensional surface obtained from $d$ over $\Lambda_{q_0}$. For the simulation, the initial configuration $q_0 = (0,0,0)$, desired configuration $q_d = \left(-\frac{\pi}{2}, 4, 2\right)$, final time $T = 8.614$, and maximal velocity $\hat{v} = 1$ was used. In Figure 7.1, the varying initial condition $\tilde{\lambda}_0(\alpha)$ results from $\alpha = (\alpha_1, 0.45)$ for $\alpha_1 \in [1, 2.5]$. At $\alpha_1 = 1.309$ and $\alpha_1 = 2.036$, the time $t^m$ changes discontinuously, and $d$ is not differentiable but only continuous. In Figure 7.2, there are several minima of $d$ over $\Lambda_{q_0}$, including three solution minima. Over a large domain $\Psi$ of $\Lambda_{q_0}$, there holds $d(\lambda_0) = \hat{d}$. Simulations for many desired configurations $q_d$ show that the search space $\Lambda_{q_0}$ consists of regions of attraction $\Omega$ of one or several minima, which may be solution minima satisfying condition (7.11) or other minima which do not meet (7.11), and a domain $\Psi$ where $d(\lambda_0) = \hat{d}$ is true. In the interior of the regions of attraction $\Omega$ and the domain $\Psi$, the minimal deviation $d$ is differentiable with respect to $\tilde{\lambda}_0$. At the boundaries between the regions of attraction $\Omega$ and the domain $\Psi$, i. e., on a set of measure zero, $d$ is only continuous. In Figure 7.2, the points $\alpha = (1.309, 0.45)$ and $\alpha = (2.036, 0.45)$ where $t^m$ changes discontinuously lie on the boundaries between the regions of attraction of the minima of $d$.

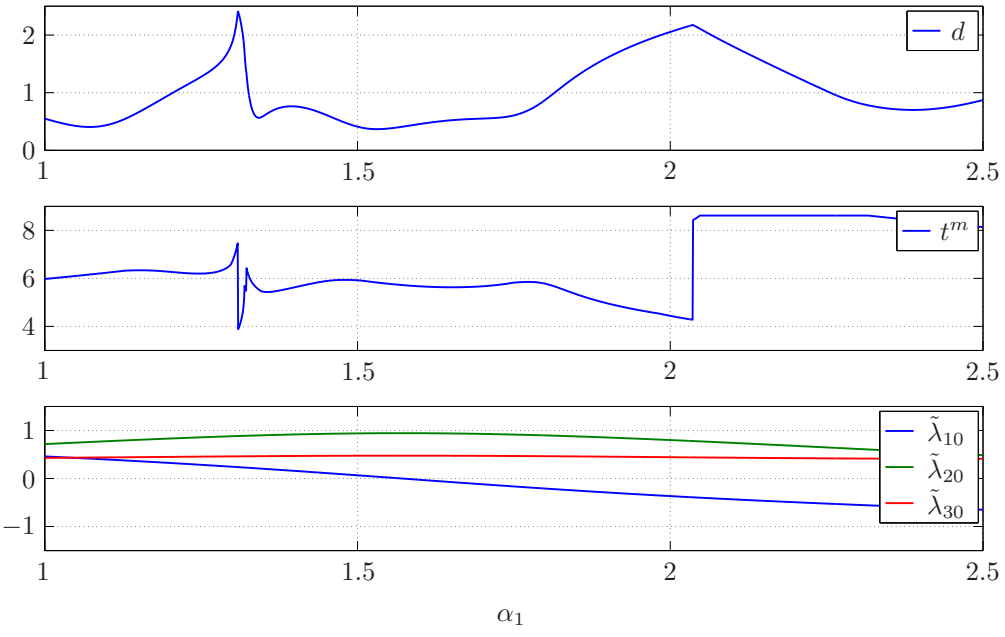


Figure 7.1: Simulation results of the path planning.

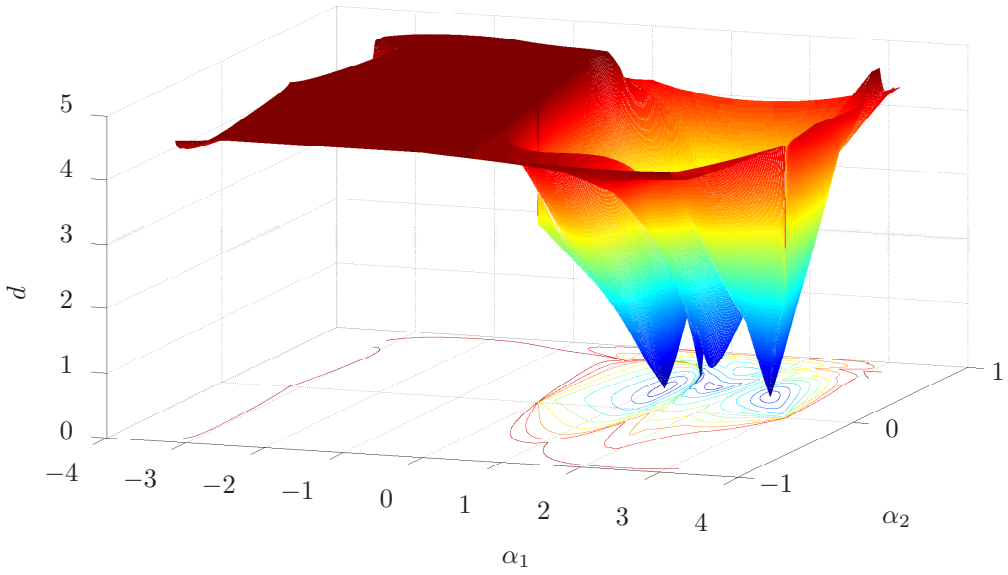


Figure 7.2: Deviation $d$ over the search space.

### 7.2.2 Solution to the optimization problem for path planning

In this section, our solution approach to the optimization problem for path planning 7.2.1 is given which is based on local optimization initialized to a random starting point. If condition $D(\lambda_0^m, t^m) \leq \varepsilon_x$ as in (7.11) holds, a solution is found. The generation of random starting points and the local optimization is repeated if required, as the optimization may converge to a minimum which is no solution minimum and does not solve the path planning problem. To control the local optimization and the path planning, exit conditions are defined. These conditions are required since for some path planning problems, there may be no solution to the optimization problem due to the restriction to normal regular extremals.

**Approach 7.2.6** *(Path planning by local optimization with random initialization) To obtain a solution $(\lambda_0^{PP}, \tau)$ to the path planning problem 7.0.1, a solution $(\lambda_0^m, t^m)$ to the optimization problem 7.2.1 is determined. For $I = [0, T]$ with sufficiently large $T$, the following steps are repeated until condition (7.11) holds or the path planning is terminated by an exit condition:*

***Step 1:*** *Generate a random starting point $\lambda_0^{SP} \in \Lambda_{x_0}$ with uniform probability distribution.*

***Step 2:*** *Perform a local optimization initialized to $\lambda_0^{SP}$ to minimize $d$ over $\lambda_0 \in \Lambda_{x_0}$ until condition (7.11) holds or the optimization is terminated.*

*If condition (7.11) holds, set $\lambda_0^{PP} = \lambda_0^m$ and $\tau = t^m$.*

The exit conditions for the local optimization and the path planning are defined below. An algorithm to implement the path planning 7.2.6 is given in Section 7.2.3. For the local optimization in Approach 7.2.6, a standard method for nonlinear optimization is used. For each evaluation of $d$, the extremal is simulated over the interval $I$ by numerical integration of the control system starting from $x_0$ and the adjoint equation starting from the current $\lambda_0$. For the resultant extremal, the trajectory of the deviation $D = \|x - x_d\|$ is computed, and the minimal deviation $d$ is chosen as in (7.6). Then, $d$ is minimized over $\lambda_0 \in \Lambda_{x_0}$ according to (7.10) so that $\lambda_0$ and $t^m$ obtained from (7.7) and (7.8) result. It can be necessary to start the local optimization several times with different $\lambda_0^{SP}$, as the optimization may be trapped in a minimum not meeting condition (7.11) or may not converge at all.

As the location of the solution minima $\lambda_0^m$ is unknown, random samples from $\Lambda_{x_0}$ are chosen as starting points $\lambda_0^{SP}$ for the local optimizations. Suitable random sampling leads to probabilistic completeness as shown below. The probability distribution is uniform and independent. If information about the solution minima is available, $\lambda_0^{SP}$ can be chosen from a subset of the search space $\Lambda_{x_0}$ as discussed in Section 7.2.4. A selection of starting points based on a deterministic sampling of $\Lambda_{x_0}$ requires an analysis of the location of the solution minima in $\Lambda_{x_0}$. Otherwise, either ineffective starting points are chosen if the resolution of the sampling is too fine, or not all regions of attraction are covered if the resolution is too coarse. For deterministic sampling without an analysis, an iterative refinement of the sampling can be applied. However, such refinements are not efficient for most applications, see [60].

For applicable and efficient path planning, it is necessary to control the individual optimizations in Step 2 and the overall path planning. Hence, the following exit conditions are applied, which evaluate the number of simulated extremals as a measure of the computational cost.

**Definition 7.2.7** *(Exit condition for local optimization) To control the path planning 7.2.6, the following exit condition is used to terminate the individual local optimizations:*

***EC1:*** *The number $n_{Sim}^{LO}$ of simulated extremals for the current local optimization satisfies $n_{Sim}^{LO} \geq \hat{n}_{Sim}^{LO}$ for a bound $\hat{n}_{Sim}^{LO} > 0$.*

If exit condition EC1 holds, the current local optimization is terminated. Then, at least $\hat{n}_{Sim}^{LO}$ extremals were simulated without finding a solution. This is the case if the optimization is trapped in a minimum where condition (7.11) does not hold or if it does not converge.

**Definition 7.2.8** *(Exit condition for path planning) To control the path planning 7.2.6, the following exit condition is used to terminate the overall path planning:*

***EC2:*** *The number $n_{Sim}^{PP}$ of simulated extremals for the path planning satisfies $n_{Sim}^{PP} \geq \hat{n}_{Sim}^{PP}$ for a bound $\hat{n}_{Sim}^{PP} > 0$.*

If no solution to the path planning problem exists, the generation of random starting points and the local optimization would be executed again and again. The prevent this, the number of simulated extremals for the path planning is bounded by exit condition EC2.

The following definition of probabilistic completeness can be found e. g. in [59].

**Definition 7.2.9** *(Probabilistic completeness) An algorithm is probabilistically complete if it includes random decisions and is guaranteed to find any existing solution in finite time.*

Algorithms can be complete, resolution complete, probabilistically complete, or neither. If an algorithm is complete, it finds a solution or correctly reports that no solution exists in finite time. In general, completeness can only be achieved if the whole search space is scanned. If this takes too long, e. g. for a global optimization problem, a search can be done which explores the search space with a sampling scheme. The sampling can be deterministic or random. Using deterministic sampling, an algorithm is called resolution complete if it samples densely such that it finds any existing solution in finite time. Neither resolution nor probabilistically complete algorithms can determine in finite time that no solution exists. For details on probabilistic completeness and path planning, see [58, 59, 60, 121]. The path planning 7.2.6 utilizes random sampling to generate the starting points $\lambda_0^{SP}$. Thus, probabilistic completeness is studied.

**Definition 7.2.10** *(Probability of convergence) For the path planning problem 7.0.1, let $\lambda_0^m \in \Lambda_{x_0}$ be a solution minimum 7.2.4 and $\Omega$ its region of attraction. The probability that a local optimization initialized to a starting point $\lambda_0^{SP} \in \Omega$ converges so that condition (7.11) holds is called probability of convergence $P_C(\lambda_0^{SP})$ for the starting point $\lambda_0^{SP}$. The mean value of $P_C(\lambda_0^{SP})$ over all $\lambda_0^{SP} \in \Omega$ is called probability of convergence $P_C$ for the solution minimum $\lambda_0^m$.*

As a solution minimum is assumed in Definition 7.2.10, there is at least one solution 7.2.3 to problem 7.0.1. For $P_C$, local optimizations starting from points $\lambda_0^{SP}$ in the region of attraction $\Omega$ of a solution minimum $\lambda_0^m$ are studied. For a specific $\lambda_0^{SP}$, $P_C(\lambda_0^{SP})$ specifies how probable an optimization starting from $\lambda_0^{SP}$ converges to $\lambda_0^m$. In this case, a solution to optimization problem 7.2.1 and thus to path planning problem 7.0.1 is found. The mean value of $P_C(\lambda_0^{SP})$ over all $\lambda_0^{SP} \in \Omega$ gives the probability of convergence $P_C$ for the solution minimum $\lambda_0^m$. It should be noted that the probability of convergence $P_C$ does not give the probability of successful path planning for an arbitrary point $\lambda_0^{SP} \in \Lambda_{x_0}$, since for $P_C$, only random starting points $\lambda_0^{SP}$ in the region of attraction of a solution minimum are considered. In general, the regions of attraction of the solution minima are unknown for a specific path planning problem.

For the following theorem on convergence of the path planning, $P_C > 0$ is assumed. Among others, $P_C$ depends on the applied method for local optimization and the bound $\hat{n}_{Sim}^{LO}$ for exit condition EC1. If a suitable method for local optimization is used and $\hat{n}_{Sim}^{LO}$ is sufficiently large, $P_C > 0$ is true. In general, convergence is not always achieved, but $P_C < 1$ holds due to two reasons. First, if condition (7.11) is true for some solution minimum $\lambda_0^m$, an optimization converging too slowly to $\lambda_0^m$ is terminated by exit condition EC1 as it requires too many simulated extremals. Second, the optimization problem 7.2.1 can be nonsmooth, since according to property O2, $d$ need not be differentiable everywhere in $\Lambda_{x_0}$. At a point where derivatives change discontinuously, a derivative-based method for local optimization may fail to converge.

**Theorem 7.2.11** *(Convergence of the path planning) The path planning 7.2.6 is applied to path planning problem 7.0.1. The local optimizations and the path planning are controlled by the exit conditions EC1 and EC2 for a sufficiently large bound $\hat{n}_{Sim}^{PP}$. Assume that the search space $\Lambda_{x_0}$ is bounded. If there is at least one solution to problem 7.0.1, let the probability of convergence for each solution minimum satisfy $P_C > 0$. Then, any existing solution to problem 7.0.1 is found after a finite number of simulated extremals. The path planning is probabilistically complete.*

**Proof** Provided that at least one solution to the path planning problem exists, it is assumed that there is exactly one solution and thus one solution minimum $\lambda_0^m$ in $\Lambda_{x_0}$. If several solutions and several solution minima exist, Theorem 7.2.11 can be shown analogously. A solution minimum $\lambda_0^m$ from Definition 7.2.4 is a minimum of $d$ such that $\lambda_0^m \in \Lambda_{x_0}$ and $d(\lambda_0^m) \leq \varepsilon_x$ is true. Hence, there is a minimum of $d$ in $\Lambda_{x_0}$, and Assumption 7.2.2 holds.

If a solution to the path planning problem 7.0.1 exists, the region of attraction $\Omega \subset \Lambda_{x_0}$ of the corresponding solution minimum $\lambda_0^m$ cannot be not arbitrarily small, as $d$ is continuous everywhere in $\Lambda_{x_0}$, see property O2 of Lemma 7.2.5. As the search space $\Lambda_{x_0}$ is assumed to be bounded and the region of attraction $\Omega$ is not arbitrarily small, $\Omega$ is hit by a random starting point $\lambda_0^{SP}$ after a finite number of starting points, since the points are uniformly distributed over $\Lambda_{x_0}$. For a random starting point $\lambda_0^{SP}$ located in $\Omega$, the local optimization initialized to $\lambda_0^{SP}$ converges on average with probability $P_C > 0$ so that condition (7.11) holds and a solution to the path planning problem is found. As it takes only a finite number of random starting points $\lambda_0^{SP}$ to hit $\Omega$ and each $\lambda_0^{SP} \in \Omega$ leads on average with probability $P_C > 0$ to convergence so that condition (7.11) is true, convergence is obtained after a finite number of random starting points $\lambda_0^{SP}$. This number is denoted by $n_{SP}$.

For each of the $n_{SP}$ starting points, one run of the local optimization is done. Each local optimization is terminated if condition (7.11) holds or if exit condition EC1 is true, i. e., the number $n_{Sim}^{LO}$ of simulated extremals satisfies $n_{Sim}^{LO} \geq \hat{n}_{Sim}^{LO}$ for finite $\hat{n}_{Sim}^{LO}$. If a solution to the path planning problem exists, it is found after $n_{Sim}^{PP} \leq \hat{n}_{Sim}^{LO}\, n_{SP}$ simulated extremals. Thus, $n_{Sim}^{PP}$ is finite. As $\hat{n}_{Sim}^{PP}$ is assumed to be sufficiently large, $n_{Sim}^{PP} < \hat{n}_{Sim}^{PP}$ holds, and the path planning is not terminated by exit condition EC2 before a solution is found. As it takes only a finite time to simulate $n_{Sim}^{PP}$ extremals, the path planning is probabilistically complete. ■

For the proof of Theorem 7.2.11, it was assumed that only one solution and one solution minimum exists. If there are several solution minima, a solution to the path planning problem

is obtained after a smaller number of random starting points $\lambda_0^{SP}$ in general, as it takes fewer points $\lambda_0^{SP}$ to hit the region of attraction of a solution minimum.

As discussed in [60, 121], for path planning problems which are global optimization problems, an analysis of the rate of convergence is either expensive or requires restrictive assumptions. Hence, the rate of convergence of the path planning 7.2.6 is not analyzed. In particular, no expected number of random starting points or simulated extremals for a solution is given, as this would require a detailed analysis of the minima of $d$ over the search space $\Lambda_{x_0}$ for the specific path planning problem. To characterize the rate of convergence, it would be necessary to know the coverage of $\Lambda_{x_0}$ by regions of attraction of solution minima. If this coverage would be known, an expected number of random starting points to solve the path planning problem could be given. From this number, an expected number of simulated extremals would result.

For a textbook example of path planning solved by the randomized potential field method, the rate of convergence is analyzed in [58]. This method also addressed in [60] combines gradient descent and random walk to escape from local minima. For each minimum of the potential field, the region of attraction is explicitly specified. Minima leading to a solution of the path planning problem are identified, and the transition probability between minima which solve the problem and those which do not are calculated. Finally, an expected number of random walks required to arrive at a solution minimum is given. For nontrivial problems like path planning for the RKM, it is impossible to specify the regions of attraction and to determine which minima solve the problem without a computationally expensive analysis.

### 7.2.3 Algorithm for path planning

An implementation of the path planning 7.2.6 is given in Algorithm 7.1. A detailed representation of the algorithm in form of a listing in MATLAB-like code can be found in Section A.1.

**Parameters:** $x_0, x_d, \varepsilon_x, \Lambda_{x_0}, T, \hat{n}_{Sim}^{LO}, \hat{n}_{Sim}^{PP}$

**Output variables:** $\lambda_0^{PP}, \tau$

**Initialization:** Set $n_{Sim}^{PP} = 0$.

**Step 1:** Choose a random starting point $\lambda_0^{SP}$ from the search space $\Lambda_{x_0}$.

**Step 2:** Minimize $d$ over $\lambda_0 \in \Lambda_{x_0}$ starting from $\lambda_0 = \lambda_0^{SP}$. To calculate $d(\lambda_0)$,

- simulate the extremal $x(\cdot)$ obtained for $x(0) = x_0$, $\lambda(0) = \lambda_0$ over $I = [0, T]$,
- calculate $D(\lambda_0, \cdot) = \|x(\cdot) - x_d\|$,
- set $d = \min_{t \in I} D(\lambda_0, t)$ and $t^m = \min T^m$ for $T^m = \{t_i^m \in I \,|D(\lambda_0, t_i^m) = d\}$.

Let $n_{Sim}^{LO}$ be the number of simulated extremals for the optimization.
If $d \leq \varepsilon_x$ or $n_{Sim}^{LO} \geq \hat{n}_{Sim}^{LO}$ holds, terminate the optimization. Set $n_{Sim}^{PP} = n_{Sim}^{PP} + n_{Sim}^{LO}$.

If $d \leq \varepsilon_x$ or $n_{Sim}^{PP} \geq \hat{n}_{Sim}^{PP}$ holds, terminate the path planning and, if $d \leq \varepsilon_x$ holds, set $\lambda_0^{PP} = \lambda_0$ and $\tau = t^m$. Otherwise, go to **Step 1**.

Algorithm 7.1: Algorithm for path planning.

The parameters of Algorithm 7.1 are the initial and desired state $x_0$ and $x_d$, the tolerance $\varepsilon_x$, a representation of the search space $\Lambda_{x_0}$, the final time $T$ of the interval $I = [0, T]$, and the maximal number of simulated extremals for each run of the local optimization and the path

planning, $\hat{n}_{Sim}^{LO}$ and $\hat{n}_{Sim}^{PP}$. The algorithm returns the initial condition $\lambda_0^{PP}$ and the end time $\tau$ which solve the path planning problem.

For initialization, the counter $n_{Sim}^{PP}$ for the total number of simulated extremals for the path planning is set to zero. Then, Step 1 and Step 2 are executed iteratively until the path planning is terminated. Step 1 and 2 of Algorithm 7.1 correspond to Step 1 and 2 of Approach 7.2.6. In Step 1, a random starting point $\lambda_0^{SP}$ is chosen from the search space $\Lambda_{x_0}$. In Step 2, the deviation $d$ is minimized over $\lambda_0 \in \Lambda_{x_0}$ as in (7.10). The local optimization for the minimization is initialized to $\lambda_0^{SP}$. To calculate the value $d(\lambda_0)$ for the minimization, the normal regular extremal obtained for the initial conditions $x(0) = x_0$ and $\lambda(0) = \lambda_0$ is simulated over the interval $I$, and the deviation $D$ as in (7.5) is computed. Then, the minimal deviation $d(\lambda_0)$ is chosen according to (7.6). It gives the value of $d$ for the minimization. Besides, the end time $t^m$ results from (7.7) and (7.8). The minimization is terminated if $d \leq \varepsilon_x$ or $n_{Sim}^{LO} \geq \hat{n}_{Sim}^{LO}$ holds. Here, $d \leq \varepsilon_x$ means that condition (7.11) is true for $\lambda_0^m = \lambda_0$. If $n_{Sim}^{LO} \geq \hat{n}_{Sim}^{LO}$ applies, exit condition EC1 holds, i. e., the maximal number of simulated extremals is used for the current local optimization. Finally, the number $n_{Sim}^{PP}$ of simulated extremals for the path planning is incremented by the number $n_{Sim}^{LO}$ of simulations done for the local optimization.

The path planning is terminated if the minimal deviation satisfies $d \leq \varepsilon_x$ or if the total number of simulated extremals meets $n_{Sim}^{PP} \geq \hat{n}_{Sim}^{PP}$. If $d \leq \varepsilon_x$ is true, condition (7.11) holds for $\lambda_0^m = \lambda_0$, and the path planning problem is solved. If $n_{Sim}^{PP} \geq \hat{n}_{Sim}^{PP}$ is true, exit condition EC2 holds, and the path planning is terminated unsuccessfully, i. e., without finding a solution. If the path planning is terminated due to $d \leq \varepsilon_x$, the output variables $\lambda_0^{PP}$ and $\tau$ are set to the values of $\lambda_0$ and $t^m$ from the last run of Step 2.

To simulate an extremal over the interval $I = [0, T]$, the ordinary differential equations of the control system and the adjoint equation driven by the extremal inputs from the maximization of the Hamiltonian function are integrated numerically. To compute and represent the trajectories of $x$ and $D$ in an efficient way, the interval $I$ is discretized using a discretization interval $\triangle t > 0$. This gives the time vector

$$I_\triangle = \left[ t_i \,\middle|\, t_i = i\,\triangle t,\ i{=}0,...,n_T,\ n_T = T/\triangle t \right] . \tag{7.15}$$

Here, $T = n_T\,\triangle t$ is assumed for $n_T \in \mathbb{N}_{>0}$. The vector

$$x(I_\triangle) = \left[ x_i \,\middle|\, x_i = x(t_i),\ t_i \in I_\triangle \right]$$

results from the numerical integration for the extremal state $x$ at the times $I_\triangle$. Based on $x(I_\triangle)$,

$$D(I_\triangle) = \left[ D_i \,\middle|\, D_i = \|x(t_i) - x_d\|,\ t_i \in I_\triangle \right]$$

is the deviation $D$ at the times $I_\triangle$. From $D(I_\triangle)$, the minimal element is chosen for (7.6). The end time $t^m$ is the element of $I_\triangle$ which meets (7.8). Thus, the resolution of $t^m$ and $\tau$ is $\triangle t$.

The discretization interval $\triangle t$ is chosen depending on the tolerance $\varepsilon_x$. On the one hand, $\triangle t$ must be short enough for a fine resolution of $t^m$ so that solutions satisfying condition (7.11) for the specific $\varepsilon_x$ can be found. Thus, for a smaller value of $\varepsilon_x$, a smaller discretization interval $\triangle t$ is required. On the other hand, $\triangle t$ should not be too short to keep the computational effort low. Because of the discretization of $I$ for $\triangle t > 0$, desired states $x_d$ cannot be reached with arbitrarily small deviation in general. For time-optimal control of the BSR, a value for $\triangle t$ is given depending on $\varepsilon_x$ by Theorem 8.2.2.

The parameters of the algorithm for path planning are summarized in Table 7.1. There are different types of parameters, parameters belonging to the problem data of the path planning problem, parameters resulting from the path planning problem, and design parameters. The parameters of the problem data are the initial and desired state $x_0$ and $x_d$ and the tolerance $\varepsilon_x$ for condition (7.11). The parameters from the path planning problem comprise $\Lambda_{x_0}$, $\triangle t$, and $T$. The search space $\Lambda_{x_0}$ is represented by a suitable parameter set. The discretization interval $\triangle t$ has to be chosen depending on $\varepsilon_x$ as discussed above. The final time $T$ of $I$ must satisfy $T = n_T\,\triangle t$ for $n_T \in \mathbb{N}_{>0}$. Besides, $T$ must be as short as possible to obtain a vector

$I_\triangle$ with minimal number of elements to reduce the computational effort. However, $T$ has to be sufficiently large to ensure that if there is a solution with end time $\tau$, this solution is not missed due to $T < \tau$. The design parameters $\hat{n}_{Sim}^{LO}$ and $\hat{n}_{Sim}^{PP}$ are selected to adjust the path planning. For a high probability of convergence $P_C$ of the local optimization, $\hat{n}_{Sim}^{LO}$ should be large, but to prevent the local optimizations from wasting computational effort without yielding convergence, $\hat{n}_{Sim}^{LO}$ should be small. The same is true for $\hat{n}_{Sim}^{PP}$, which should be large to make it possible to find a solution, but not too large to keep the cost low if no solution can be found. The parameter $\hat{n}_{Sim}^{PP}$ defines the maximal computational cost of the path planning. To set the parameters $\Lambda_{x_0}$, $\triangle t$, and $T$, an analysis of the path planning problem is required.

| parameter | description | type |
|---|---|---|
| $x_0$ | initial state | problem data |
| $x_d$ | desired state | problem data |
| $\varepsilon_x$ | tolerance for condition (7.11) | problem data |
| $\Lambda_{x_0}$ | parameter set to represent the search space | from path planning problem |
| $\triangle t$ | discretization interval | from path planning problem |
| $T$ | final time of the interval $I = [0, T]$ | from path planning problem |
| $\hat{n}_{Sim}^{LO}$ | maximal number of simulated extremals for each run of the local optimization | design parameter |
| $\hat{n}_{Sim}^{PP}$ | maximal number of simulated extremals for path planning in total | design parameter |

Table 7.1: Parameters of the algorithm for path planning.

### 7.2.4 Discussion of the path planning

Approach 7.2.6 for path planning uses extremals of the time-optimal control problem, as the goal of the time-optimal control based on the path planning is to find time-optimal solutions. For path planning, only normal regular extremals are considered. Abnormal extremals are not included, since they are in some way degenerate, as the Lagrangian is not taken into account. Besides, non-constant abnormal extremals do not exist for most nonholonomic kinematic systems, see [117, 120]. In contrast to abnormal extremals, normal singular extremals are relevant for optimal control of nonholonomic systems. However, such extremals are not studied here, as they are more complicated than regular extremals in general. Only for specific classes of control systems, singular inputs can be determined directly. Moreover, such extremals are numerically difficult to handle. For the RKM, singular extremals give optimal solutions only for some configurations $q_d$ which are not reachable by regular extremals, see Section 9.6.

To find a solution $(\lambda_0^{PP}, \tau)$ to the path planning problem 7.0.1, the optimization problem 7.2.1 is solved by Approach 7.2.6. This optimization problem is a boundary value problem with free end time as in Definition 4.4.1. As discussed in Section 4.4, standard solvers for boundary value problems require a fixed end time. For this, a time transformation can be applied to obtain a control problem with new time $s = \frac{1}{\tau} t \in [0, 1]$. The unknown end time $\tau$ of the original system is modeled as additional state variable, resulting in a problem of higher dimension which is more costly to solve. Besides, a good initial guess of $\tau$ is needed, which may be difficult to give. In contrast, for the path planning 7.2.6, no time transformation is required. Moreover, no guess of $\tau$ must be provided, but only an upper bound on the final time $T$ of $I = [0, T]$.

Aside from the time transformation, standard solvers for boundary value problems rely on a good guess of the solution for initialization. Otherwise, no solution is found in general, as the solvers can only find solutions close to the initial guess. For good initial guesses, a detailed analysis of the boundary value problem is required. As discussed in Section 9.4, even for time-optimal solutions to nearby desired states, the initial conditions $\lambda_0$ of the adjoint state may be completely different. Apart from $\lambda_0$, the initialization of the state variable for $\tau$ is important.

As standard solvers can only find solutions with $\tau$ close to its initialization value, no solution is found if an initialization value of $\tau$ is set for which no solution with a nearby value exists. In contrast, for Approach 7.2.6, a random starting point $\lambda_0^{SP}$ is used for the initialization of $\lambda_0$, and no initialization value of $\tau$ is needed.

The path planning can be easily adapted to specific problems. To implement it, the equations of the control system, the adjoint equation, the extremal inputs, and the parameters of Table 7.1 have to be given. In particular, no knowledge of the minima of the optimization problem for path planning is required, as random starting points are used for initialization and the path planning is probabilistically complete. The maximal computational cost can be set by $\hat{n}_{Sim}^{PP}$.

Depending on the control problem, the search space $\Lambda_{x_0}$ for optimization problem 7.2.1 can be narrowed down to a subset containing all initial conditions which solve the path planning problem. This subset can be given based on knowledge of the minima of $d$ or heuristic rules. Besides exit condition EC1 and EC2, further conditions may be used for the local optimizations and the path planning. An exit condition can check whether a starting point $\lambda_0^{SP}$ yields $d(\lambda_0^{SP}) = \hat{d} = \|x_0 - x_d\|$. Then, this point is discarded, as $d(\lambda_0) = \hat{d}$ may hold for all $\lambda_0$ in the neighborhood of $\lambda_0^{SP}$, impeding convergence of derivative-based optimization methods. Another exit condition can prevent the optimization from converging to known minima which do not solve the path planning problem. For this, all minima of $d$ found so far are stored, and the distance of the current $\lambda_0$ to the these minima is monitored. If the distance to some minimum falls below a threshold, the optimization is terminated.

As problem 7.2.1 is a global optimization problem, global optimization methods may be used. Such methods can escape from minima which do not meet condition (7.11). An example of a global optimization method is the hybrid approach in [127] which combines simulated annealing to escape from local minima with gradient descent for faster convergence. This approach is applied in [36] for time-optimal control of spin systems. Another example is the randomized potential field method in [58, 60] which implements path planning by gradient descent and random walk. Global optimization methods may yield convergence to solution minima which satisfy condition (7.11). However, they typically require a detailed analysis of the optimization problem, as discussed for the randomized potential field method at the end of Section 7.2.2.

According to property O2 of Lemma 7.2.5, problem 7.2.1 can be nonsmooth, as $d$ need not be differentiable everywhere in $\Lambda_{x_0}$. For nonsmooth problems, derivative-based optimization methods may fail to converge at points of the search space where derivatives change discontinuously. Optimization methods for nonsmooth problems exist, but their efficiency depends strongly on the particular problem. Moreover, smoothing approximations like in [126] may be used to obtain a smooth optimization problem which can be solved by a standard method for local optimization. From solutions to this new problem, solutions to the original nonsmooth problem can be derived. Neither optimization methods for nonsmooth problems nor smoothing approximations are used for the optimization problem 7.2.1, as standard optimization methods yield good convergence in almost all simulations performed for this thesis.

## 7.3 Time-optimal control by iterated path planning

This section covers our approach for time-optimal control which performs the path planning from Section 7.2 iteratively over a decreasing time horizon to solve the near time-optimal control problem 7.0.2. Like in Section 7.2, the approach is described, its convergence is analyzed, and an algorithm which implements the time-optimal control is given.

### 7.3.1 Iterated path planning over a decreasing time horizon

**Definition 7.3.1** *(Time horizon, feasible time horizon, decreasing time horizon) The optimization problem for path planning 7.2.1 is considered. For some final time $T > 0$, the time interval $I = [0, T]$ is called time horizon. A time horizon $I$ is called feasible if there is an initial condition $\lambda_0^m$ and a time $t^m \in I$ resulting from (7.8) such that condition (7.11) holds. For a*

*new final time $T' < T$, let $I' = [0, T']$ be the new time horizon. A time horizon changing from $I$ to $I' \subset I$ is called decreasing time horizon.*

**Approach 7.3.2** *(Time-optimal control by iterated path planning over a decreasing time horizon) To obtain a solution $(\lambda_0^{to}, \tilde{\tau}^{to})$ to the near time-optimal control problem 7.0.2, solutions to the path planning problem 7.0.1 are determined iteratively over a decreasing time horizon. Starting from an initial time horizon $I = [0, \hat{T}]$ with sufficiently large $\hat{T}$, the following steps are iterated until a near time-optimal solution is found or the near time-optimal control is terminated by an exit condition:*

***Step 1:*** *Perform the path planning 7.2.6 over the time horizon $I$ until a solution $(\lambda_0^{PP}, \tau)$ is found or the path planning is terminated.*

***Step 2:*** *If a solution $(\lambda_0^{PP}, \tau)$ is found, set $\lambda_0^{to} = \lambda_0^{PP}$ and $\tilde{\tau}^{to} = \tau$, let*

$$T' := \tau - \triangle t$$

*be the final time of the new time horizon $I' = [0, T']$, and set $I := I'$.*

To terminate the path planning in Step 1, exit condition EC2 is used. An exit condition for the near time-optimal control is defined below. An algorithm which implements Approach 7.3.2 is presented in Section 7.3.2. For a solution $(\lambda_0^{PP}, \tau)$ to the path planning problem, $\tau \in I$ holds, which implies $\tau \leq T$. Thus, for $\triangle t > 0$, the new final time $T' = \tau - \triangle t$ satisfies $T' < T$. Hence, each time horizon changing from $I$ to $I'$ is a decreasing time horizon 7.3.1. To obtain the new final time $T'$, the end time $\tau$ is decreased by the period $\triangle t$. This period equals the discretization interval $\triangle t$ used for the discretization $I_\triangle$ (7.15) of the time horizon $I$. For convergence of the time-optimal control, $\triangle t$ must be sufficiently small, see Theorem 7.3.4 below. Using the discretization $I_\triangle$, the interval $\triangle t$ is the minimal possible value for the decrease of $\tau$. In Approach 7.3.2, the end time $\tilde{\tau}^{to}$ is determined by iterated path planning over a decreasing time horizon and not by a direct optimization. The motivation for this iterative procedure is given in Section 7.3.3.

According to Definition 2.2.5, a solution is near time-optimal if its end time $\tilde{\tau}^{to}$ satisfies $\tilde{\tau}^{to} \leq k\,\tau^{to}$ for a constant $k \geq 1$ and the end time $\tau^{to}$ of a time-optimal solution. If the end time $\tau^{to}$ is known, $\tilde{\tau}^{to} \leq k\,\tau^{to}$ can be directly checked. However, in general, $\tau^{to}$ is unknown. Thus, it is assumed in the following that an optimality condition can be given which is true if a solution is near time-optimal. If this condition holds, the near time-optimal control 7.3.2 is terminated. Such a condition, called condition for near time-optimality in the following, can be based on the optimality conditions given in Section 4.5 and 4.6. For the BSR, conditions for near time-optimality are addressed in Chapter 9.

In Figure 7.3, the decreasing time horizon is shown exemplary for a run of the time-optimal control with disproportionately large $\triangle t$. The iterated path planning is performed over the time horizons $I_1$, $I_2$, and $I_3$. For the initial time horizon $I_1 = [0, T_1]$ with $T_1 = \hat{T}$, one run of the path planning gives a solution with end time $\tau_1$. Then, the time horizon $I_2 = [0, T_2]$ with final time $T_2 = \tau_1 - \triangle t$ is used. For this time horizon, a solution to the path planning problem with end time $\tau_2$ results. Finally, the time horizon $I_3 = [0, T_3]$ with $T_3 = \tau_2 - \triangle t$ is applied. The solution obtained for this time horizon has the end time $\tau_3$. For the example in Figure 7.3, this solution is assumed to satisfy a condition for near time-optimality. Hence, $\tau_3$ is the end time of a near time-optimal solution, i. e., $\tau_3 = \tilde{\tau}^{to}$ holds.

Like the path planning, the time-optimal control has to be controlled for applicability and efficiency. For this, the following exit condition is applied to terminate the time-optimal control depending on the number of simulated extremals.

**Definition 7.3.3** *(Exit condition for time-optimal control) To control the time-optimal control 7.3.2, the following exit condition is used:*

***EC3:*** *The number $n_{Sim}^{to}$ of simulated extremals for the time-optimal control satisfies $n_{Sim}^{to} \geq \hat{n}_{Sim}^{to}$ for a bound $\hat{n}_{Sim}^{to} > 0$.*

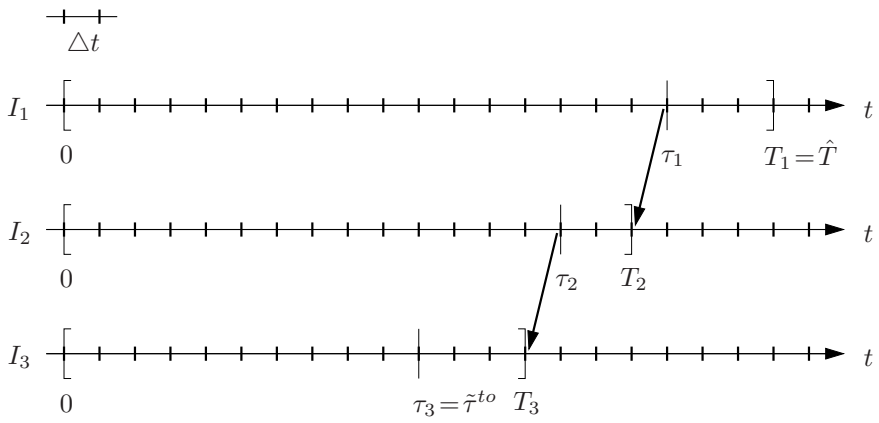


Figure 7.3: Decreasing time horizon.

Exit condition EC3 restricts the total number $n^{to}_{Sim}$ of simulated extremals for the time-optimal control which is the sum of the number of simulated extremals over all runs of the path planning. It is applied to prevent the time-optimal control from running ad infinitum if no near time-optimal solution is found.

**Theorem 7.3.4** *(Convergence of the time-optimal control) The time-optimal control 7.3.2 is applied to the near time-optimal control problem 7.0.2. The local optimizations, the path planning, and the time-optimal control are controlled by the exit conditions EC1, EC2, and EC3 for a sufficiently large bound $\hat{n}^{to}_{Sim}$. The bound $\hat{n}^{PP}_{Sim}$ for exit condition EC2 is set to*

$$\hat{n}^{PP}_{Sim} = \hat{n}^{to}_{Sim} - n^{to}_{Sim}. \tag{7.16}$$

*Assume that the search space $\Lambda_{x_0}$ is bounded. If there is at least one solution to problem 7.0.2, let the probability of convergence for each solution minimum satisfy $P_C > 0$, let condition (7.12) for property O3 of Lemma 7.2.5 be satisfied, and let the discretization interval $\triangle t$ be sufficiently small. Then, any existing solution to problem 7.0.2 is found after a finite number of simulated extremals. The time-optimal control is probabilistically complete.*

**Proof** The time-optimal control executes the path planning 7.2.6 iteratively over the decreasing time horizon $I$. Each solution to problem 7.0.2 is also a solution to the path planning problem 7.0.1. Thus, if the assumptions of Theorem 7.3.4 hold and the bound $\hat{n}^{PP}_{Sim}$ for exit condition EC2 is sufficiently large, the assumptions of Theorem 7.2.11 for convergence of the path planning hold as well. Due to (7.16), for each run of the path planning, all remaining simulations $\hat{n}^{to}_{Sim} - n^{to}_{Sim}$ are allocated. The bound $\hat{n}^{to}_{Sim}$ is assumed to be sufficiently large. Hence, $\hat{n}^{PP}_{Sim}$ is sufficiently large. Then, due to $P_C > 0$, a solution to the path planning problem is found after a finite number of simulated extremals for each feasible time horizon $I$.

The set $T^m_{\Lambda_{x_0}}$ given by (7.13) is the union of the sets $T^m$ of times $t^m$ which give the minimal deviation $d$, taken over all solution minima $\lambda^m_0 \in \Lambda_{x_0}$. In Theorem 7.3.4, it is assumed that condition (7.12) holds. Hence, the set $T^m_{\Lambda_{x_0}}$ is discrete by property O3. Thus, there is a sufficiently small discretization interval $\triangle t$ for which $T' = \tau - \triangle t$ is so large that no near time-optimal solution is missed. That is, no final time $T'$ results such that $T' < \tilde{\tau}^{to}$ can hold for the end time $\tilde{\tau}^{to}$ of any near time-optimal solution. As discussed above, a solution to the path planning problem is found for each feasible time horizon. Thus, if at least one near time-optimal solution exists, such a solution is found in the end, since the bound $\hat{n}^{to}_{Sim}$ for exit condition EC3 is assumed to be sufficiently large.

For each solution to the path planning problem, the final time $T'$ of the new time horizon satisfies $T' < T$ because of $\tau \leq T$ and $\triangle t > 0$. Thus, if a new solution with new end time $\tau' \in I'$ is found, $\tau' < \tau$ holds. As $T' = \tau - \triangle t$ is strictly decreasing for each new end time $\tau$, the path

planning gives at most one solution for each final time $T'$. The number of time horizons $I$ for which the path planning is executed is finite. Since a solution to each path planning problem is found after a finite number of simulated extremals, a near time-optimal solution is found after a finite number $n^{to}_{Sim}$ of simulated extremals. As it takes only a finite time to simulate $n^{to}_{Sim}$ extremals, the time-optimal control 7.3.2 is probabilistically complete. ■

According to Theorem 7.3.4, the time-optimal control 7.3.2 finds an existing near time-optimal solution after $n^{to}_{Sim}$ simulated extremals, provided that $P_C > 0$ holds for each solution minimum, condition (7.12) for property O3 is true, $\triangle t$ is sufficiently small, and $\hat{n}^{to}_{Sim}$ is sufficiently large. Then, for each feasible time horizon, a solution to the path planning is found as $\hat{n}^{PP}_{Sim} = \hat{n}^{to}_{Sim} - n^{to}_{Sim}$ is sufficiently large for sufficiently large $\hat{n}^{to}_{Sim}$. Due to condition (7.12), for sufficiently small $\triangle t$, no near time-optimal solution is missed because of a too short time horizon for path planning. Since for each run of the path planning, the number $n^{PP}_{Sim}$ of simulated extremals is finite, and the path planning is performed only finitely often, the number $n^{to}_{Sim}$ of simulated extremals for a near time-optimal solution is finite.

As for the path planning, the rate of convergence of the time-optimal control is not analyzed here. In particular, no expected number of runs of the path planning or of simulated extremals for a near time-optimal solution is given. For this, an analysis of the minima of $d$ over the search space $\Lambda_{x_0}$ would be necessary for each new time horizon $I$, as the minima change with $I$. Thus, the analysis would be very expensive.

### 7.3.2 Algorithm for time-optimal control

An implementation of the time-optimal control 7.3.2 is given in Algorithm 7.2. A detailed representation of the algorithm in MATLAB-like code can be found in Section A.2.

**Parameters:** $x_0, x_d, \varepsilon_x, \Lambda_{x_0}, \triangle t, \hat{T}, \hat{n}^{LO}_{Sim}, \hat{n}^{to}_{Sim}$

**Output variables:** $\lambda^{to}_0, \tilde{\tau}^{to}$

**Initialization:** Set $n^{to}_{Sim} = 0$, $\hat{n}^{PP}_{Sim} = \hat{n}^{to}_{Sim}$, and $T = \hat{T}$.

**Step 1:** Perform the path planning 7.2.6 from $x_0$ to $x_d$ over $I = [0, T]$, using $\Lambda_{x_0}$ and $\hat{n}^{LO}_{Sim}$. Let $d$ be the minimal deviation (7.10) and $n^{PP}_{Sim}$ the number of simulated extremals. If $d \leq \varepsilon_x$ or $n^{PP}_{Sim} \geq \hat{n}^{PP}_{Sim}$ holds, terminate the path planning and, if $d \leq \varepsilon_x$ holds, set $\lambda^{PP}_0 = \lambda_0$ and $\tau = t^m$. Set $n^{to}_{Sim} = n^{to}_{Sim} + n^{PP}_{Sim}$ and $\hat{n}^{PP}_{Sim} = \hat{n}^{to}_{Sim} - n^{to}_{Sim}$.

**Step 2:** If $d \leq \varepsilon_x$ holds, set $\lambda^{to}_0 = \lambda^{PP}_0$, $\tilde{\tau}^{to} = \tau$, and $T = \tau - \triangle t$.

If a near time-optimal solution is found or $n^{to}_{Sim} \geq \hat{n}^{to}_{Sim}$ holds, terminate the time-optimal control. Otherwise, go to **Step 1**.

Algorithm 7.2: Algorithm for time-optimal control.

The parameters of Algorithm 7.2 include $x_0$, $x_d$, $\varepsilon_x$, $\Lambda_{x_0}$, and $\hat{n}^{LO}_{Sim}$ which are also parameters of Algorithm 7.1, the discretization interval $\triangle t$, the final time $\hat{T}$ of the initial time horizon, and the maximal number $\hat{n}^{to}_{Sim}$ of simulated extremals for the time-optimal control. The output variables are the initial condition $\lambda^{to}_0$ and the end time $\tilde{\tau}^{to}$ of a near time-optimal solution. As the time vector (7.15) is used for the underlying path planning, the resolution of $\tilde{\tau}^{to}$ is $\triangle t$.

For initialization, the counter $n^{to}_{Sim}$ for the total number of simulated extremals for time-optimal control is set to zero, the maximal number $\hat{n}^{PP}_{Sim}$ of simulated extremals for the next run of the path planning is set to $\hat{n}^{to}_{Sim}$, and the final time $T$ of $I$ is set to $\hat{T}$. Then, Step 1 and

Step 2 corresponding to Step 1 and 2 of Approach 7.3.2 are executed iteratively until the time-optimal control is terminated. In Step 1, the path planning 7.2.6 is performed from $x_0$ to $x_d$ over the time interval $I = [0, T]$. For this, the search space $\Lambda_{x_0}$ and the maximal number $\hat{n}^{LO}_{Sim}$ of simulated extremals for each run of the local optimization are required. The path planning is terminated if $d \leq \varepsilon_x$ or $n^{PP}_{Sim} \geq \hat{n}^{PP}_{Sim}$ holds. If $d \leq \varepsilon_x$ is true for the minimal deviation $d$ as in (7.10), the path planning problem is solved for the current time horizon $I$. Then, the variables $\lambda_0^{PP} = \lambda_0$ and $\tau = t^m$ are assigned. If $n^{PP}_{Sim} \geq \hat{n}^{PP}_{Sim}$ holds, the path planning is terminated by exit condition EC2, i. e., the maximal number of simulated extremals is used. At the end of Step 1, the variables $n^{to}_{Sim}$ and $\hat{n}^{PP}_{Sim}$ are updated by $n^{to}_{Sim} = n^{to}_{Sim} + n^{PP}_{Sim}$ and $\hat{n}^{PP}_{Sim} = \hat{n}^{to}_{Sim} - n^{to}_{Sim}$. In Step 2, provided that $d \leq \varepsilon_x$ holds, the output variables $\lambda_0^{to}$ and $\tilde{\tau}^{to}$ are set to the values of $\lambda_0^{PP}$ and $\tau$, and the final time of the new time horizon is set to $T = \tau - \triangle t$.

The time-optimal control is terminated if a near time-optimal solution is found or the total number of simulated extremals meets $n^{to}_{Sim} \geq \hat{n}^{to}_{Sim}$. To determine whether a solution in near time-optimal, a condition for near time-optimality is evaluated. For the BSR, such conditions are discussed in Chapter 9. If $n^{to}_{Sim} \geq \hat{n}^{to}_{Sim}$ is satisfied, exit condition EC3 holds, and the time-optimal control is terminated unsuccessfully, i. e., no near time-optimal solution was found.

The parameters of the algorithm for time-optimal control are given in Table 7.2. There are different types of parameters, parameters of the problem data, parameters resulting from the control problem, and design parameters. The parameters of the problem data are $x_0$, $x_d$, and $\varepsilon_x$. The parameters from the control problem are $\Lambda_{x_0}$, $\triangle t$, and $\hat{T}$. Here, $x_0$, $x_d$, $\varepsilon_x$, $\Lambda_{x_0}$, and $\triangle t$ are the same parameters as for Algorithm 7.1. For $\hat{T}$, the requirements given for $T$ in Section 7.2.3 hold, i. e., $\hat{T} = n_{\hat{T}} \triangle t$ must be true for $n_{\hat{T}} \in \mathbb{N}_{>0}$. Moreover, $\hat{T}$ should be large enough to make it possible to find a solution, but not too large to keep the computational cost low. For time-optimal control of the BSR, a value for $\hat{T}$ is derived in Section 8.2.3. The design parameters $\hat{n}^{LO}_{Sim}$ and $\hat{n}^{to}_{Sim}$ are used to adjust the time-optimal control. The value of $\hat{n}^{LO}_{Sim}$ has to be set as described in Section 7.2.3. The parameter $\hat{n}^{to}_{Sim}$ defines the maximal computational effort for the time-optimal control.

| parameter | description | type |
|---|---|---|
| $x_0$ | initial state | problem data |
| $x_d$ | desired state | problem data |
| $\varepsilon_x$ | tolerance for condition (7.11) | problem data |
| $\Lambda_{x_0}$ | parameter set to represent the search space | from time-optimal control problem |
| $\triangle t$ | discretization interval | from time-optimal control problem |
| $\hat{T}$ | final time of the initial time horizon | from time-optimal control problem |
| $\hat{n}^{LO}_{Sim}$ | maximal number of simulated extremals for each run of the local optimization | design parameter |
| $\hat{n}^{to}_{Sim}$ | maximal number of simulated extremals for time-optimal control in total | design parameter |

Table 7.2: Parameters of the algorithm for time-optimal control.

### 7.3.3 Discussion of the time-optimal control

The time-optimal control 7.3.2 relies on a strictly monotonic decrease of the time horizon $I$ from one solution of the path planning problem to the next. This way, a near time-optimal solution with end time $\tilde{\tau}^{to}$ is obtained in the end. Starting from a first solution to the path planning problem, for each new solution, a better approximation of $\tilde{\tau}^{to}$ is provided until the solution is near time-optimal. According to Theorem 7.3.4, this is the case after a finite number of simulated extremals. In principle, the quality of the approximation increases with computational effort, which is important for many applications. In addition, as soon as the first solution

to the path planning problem is found, at least any solution is available even if it is not near time-optimal, which is important for practical applications as well.

The time-optimal control is based on three layered optimizations. The first one is the maximization of the Hamiltonian function to obtain extremals for time-optimal control. The second one tackles the optimization problem 7.2.1 to find a solution to the path planning problem 7.0.1. The third one iterates the path planning to minimize the end time and solve the near time-optimal control problem 7.0.2. The results of the underlying problems are required to solve the respective optimization problems. However, each optimization problem can be solved independently from each other. If, for example, the extremals can directly be given, the optimization problems for path planning and time-optimal control are not affected. Thus, our approach is flexible and adjustable to various control problems, for which the individual problems may be solved in different ways.

The end time $\tilde{\tau}^{to}$ of a near time-optimal solution is not determined by a direct optimization, but by iterated path planning. If $\tilde{\tau}^{to}$ should directly be optimized, the minimization of $d$ has to be replaced by a minimization of $\tau$ subject to condition (7.11), which is now a constraint of the optimization problem. Simulations show that it is hard to find a solution with end time $\tilde{\tau}^{to}$ this way without initializing $\tau$ close to $\tilde{\tau}^{to}$. Thus, $\tilde{\tau}^{to}$ is not directly optimized here.

As addressed in Section 2.3, direct and indirect methods for time-optimal control are distinguished. Direct methods are based on a discretization of the state and input space or on a finite parameterization of the inputs, followed by a direct computation of the optimal inputs. Indirect methods rely on extremals which are candidates for optimal solutions. The extremals are defined by the necessary optimality conditions of the Maximum Principle and lead to a boundary value problem with free end time. The time-optimal control 7.3.2 is based on path planning using normal regular extremals and is thus an indirect method. No direct method is applied, as for complex systems like the RKM, it is questionable whether time-optimal solutions can be found this way, since mostly, only locally optimal solutions are obtained. Moreover, no finite parameterization of the optimal inputs can be given. Hence, an indirect method is utilized. As discussed in Section 7.2.4, no standard solver for boundary value problems is used, since for such solvers, a good initial guess of the solution is required.

Besides exit condition EC1, EC2, and EC3, additional exit conditions may be used for the time-optimal control. The location of all minima found so far over all runs of the path planning can be stored. If a minimum does not satisfy condition (7.11) for some time horizon $I = [0, T]$, it cannot satisfy the condition for $I' = [0, T']$ with $T' < T$. Thus, if the distance of the current initial condition $\lambda_0$ to one of the minima falls below a threshold, the optimization is terminated. The time-optimal control is well suited for parallelization, as the individual runs of the path planning are independent from each other and can be executed in parallel. Between the nodes running the path planning, only the minimal end time $\tau$ obtained so far has to be shared. This time is required to define the time horizon $I$ for the next run of the path planning.

## 7.4 Modifications for practical application

For practical application of the path planning and time-optimal control to real-world systems, the algorithms in Section 7.2.3 and 7.3.2 are not directly suitable. This is the case as both algorithms do not satisfy requirements on real-time systems like deterministic response times, as the Theorems 7.2.11 and 7.3.4 give probabilistic completeness, but no upper bounds on the computational effort required for a solution. Since the path planning depends on random starting points to initialize the local optimizations, it is hardly possible to give such bounds.

In this section, it is assumed that a time-optimal control should be realized for a specific control system $\dot{x} = f(x, u)$ with state space $M$ and input space $U$. For this, initial conditions $\lambda_0$ can be computed based on a deterministic sampling scheme and stored in a lookup table. In a first approach, sampling can be performed over $M \times M$ to consider all possible pairs of initial and desired states $x_0$ and $x_d$. The generation of the table is computationally costly, but can be done offline before the time-optimal control is in operation. In addition, the final

time $\hat{T}$ of the initial time horizon has to be stored for each sampling point. To obtain a solution for a particular pair $(x_0, x_d)$, the precomputed initial condition $\lambda_0$ and the final time $\hat{T}$ are interpolated to obtain a starting point and a final time for the subsequent online local optimization. This optimization is required to reach exactly $x_d$ from $x_0$, since in general, $x_0$ and $x_d$ are no sampling points.

The resolution of the sampling has to be chosen depending on the current control problem. In general, for larger values of $\varepsilon_x$, a coarser resolution is sufficient. Depending on memory capacity, sampling points can be used such that for each pair $(x_0, x_d)$, a near time-optimal solution or just any solution is obtained from the local optimization. If it is sufficient to find just any solution for each pair $(x_0, x_d)$, much less sampling points are needed, leading to significantly reduced memory requirements compared to a sampling for near time-optimal solutions. Besides, approaches to simplify the path planning problem from Section 7.1 can be applied. By an affine input scaling 7.1.1, the final times $\hat{T}$ can be computed for different scaled input spaces $\check{U}$ which may result from gear changes of the drive actuating one of the affine inputs. Theorem 7.1.2 can be applied to left-invariant control systems on a matrix Lie group $G$. For such systems, only initial conditions $\lambda_0$ have to be considered for trajectories $x(\cdot)$ which start from the initial state $x_0$ represented by the identity element $E$ of $G$. Trajectories with other initial states can be computed from these trajectories by transformation. This way, it is possible to reduce the number of sampling points, since for a fixed initial state $x_0$, a sampling over $M$ is sufficient which incorporates all desired states $x_d$ instead of all pairs $(x_0, x_d)$.

# 8 Time-optimal control of the bi-steerable robot

In this chapter, the time-optimal control from Chapter 7 is applied to the RKM of the BSR. Recalling Definition 5.0.2, the RKM is given by the driftless control system $\dot{q} = g(\theta, \varphi)\, v$ for the configuration $q = (\theta, x, y)$, configuration space $Q = SE(2)$, input $u = (v, \varphi_f, \varphi_r)$, and input space $U = [-\hat{v}, \hat{v}] \times [-\hat{\varphi}, \hat{\varphi}] \times [-\hat{\varphi}, \hat{\varphi}]$. The RKM should be steered from an initial configuration $q_0 = (\theta_0, x_0, y_0)$ to a desired configuration $q_d = (\theta_d, x_d, y_d)$ in minimal time. For this, the path planning problem and the near time-optimal control problem for the RKM are considered and the convergence of the time-optimal control is analyzed. Then, the algorithm for time-optimal control is applied to the RKM and simulation results are presented. Since only extremals $(q^*(\cdot)\,, \lambda^*(\cdot)\,, u^*(\cdot))$ of the configuration, the adjoint state, and the input of the RKM are considered in the following, the superscript $^*$ is omitted for the extremals.

**Definition 8.0.1** *(Path planning problem for the RKM) For the time-optimal control problem for the RKM 6.0.2, let $(q(\cdot)\,, \lambda(\cdot)\,, u(\cdot))$ be normal regular extremals which satisfy the necessary optimality conditions of Theorem 6.1.1, and $\Lambda_{q_0}$ the search space 6.3.6. Fix a constant $\varepsilon_q > 0$. The problem to find an end time $\tau$ and an initial condition $\tilde{\lambda}_0^{PP} \in \Lambda_{q_0}$ such that for an extremal satisfying $q(0) = q_0$ and $\lambda(0) = \tilde{\lambda}_0^{PP}$, there holds $\|q(\tau) - q_d\| \leq \varepsilon_q$ is called path planning problem for the RKM. Any solution $\left(\tilde{\lambda}_0^{PP}, \tau\right)$ is called solution to the path planning problem.*

The path planning problem for the RKM arises from the path planning problem 7.0.1 underlying the time-optimal control problem 6.0.2. In contrast to problem 7.0.1, the initial condition of the adjoint state is denoted by $\tilde{\lambda}_0$ as it is a normalized initial condition 6.3.2. The search space $\Lambda_{q_0}$ given by Corollary 6.3.6 consists of all normalized initial conditions $\tilde{\lambda}_0$ of case C2, C3, C5, and C6, i. e., all initial conditions for which there are normal regular extremals which satisfy $q(0) = q_0$ and $\lambda(0) = \tilde{\lambda}_0$. Thus, $\tilde{\lambda}_0^{PP} \in \Lambda_{q_0}$ has to hold.

**Definition 8.0.2** *(Near time-optimal control problem for the RKM) For the time-optimal control problem for the RKM 6.0.2, let $\tau^{to}$ be the end time of a time-optimal solution, $(q(\cdot), \lambda(\cdot), u(\cdot))$ normal regular extremals which satisfy the necessary optimality conditions of Theorem 6.1.1, and $\Lambda_{q_0}$ the search space 6.3.6. Fix constants $k \geq 1$ and $\varepsilon_q > 0$. The problem to find an end time $\tilde{\tau}^{to} \leq k\, \tau^{to}$ and an initial condition $\tilde{\lambda}_0^{to} \in \Lambda_{q_0}$ such that for an extremal satisfying $q(0) = q_0$ and $\lambda(0) = \tilde{\lambda}_0^{to}$, there holds $\|q(\tilde{\tau}^{to}) - q_d\| \leq \varepsilon_q$ is called near time-optimal control problem for the RKM. Any solution $\left(\tilde{\lambda}_0^{to}, \tilde{\tau}^{to}\right)$ is called solution to the near time-optimal control problem.*

The near time-optimal control problem for the RKM arises from the near time-optimal control problem 7.0.2 applied to problem 6.0.2. In contrast to problem 6.0.2, only normal regular extremals are considered as candidates for solutions, and the desired configuration $q_d$ has to be reached within the tolerance $\varepsilon_q$. For problem 6.0.2, solutions exist by Theorem 6.2.1. The extremals include normal regular and normal singular extremals according to Theorem 6.3.4 and 6.3.5. For the problems 8.0.1 and 8.0.2, the existence of solutions is not discussed here, since in general, it is unknown which desired configurations $q_d$ are reachable within $\varepsilon_q$ by normal regular extremals. Thus, it is assumed that solutions exist. If this is not the case for some specific $q_d$, the time-optimal control is terminated by an exit condition.

For the heading angle $\theta$ of the RKM, values $\theta$ and $\theta + 2\,k\,\pi$ with $k \in \mathbb{Z}$ are identified, as they give the same orientation of the robot. Thus, for $(\theta(\tau), x(\tau), y(\tau))$ and $(\theta(\tau) + 2\,k\,\pi, x(\tau), y(\tau))$, the Euclidean norm $\|q(\tau) - q_d\|$ has the same result. For the path planning problem 8.0.1, it

is irrelevant how many complete turns the BSR makes until it reaches $q_d$. For the near time-optimal control problem 8.0.2, additional turns cause larger end times.

## 8.1 Simplification of the path planning problem

In this section, the approaches from Section 7.1 are applied to simplify the path planning problem and the near time-optimal control problem for the RKM. The space of the admissible steering angles $\varphi = (\varphi_f, \varphi_r)$ is $\Phi = \left[-\frac{\pi}{4}, \frac{\pi}{4}\right] \times \left[-\frac{\pi}{4}, \frac{\pi}{4}\right]$ as in (6.1).

**Corollary 8.1.1** *(Affine input scaling for the RKM) For the control system*

$$\dot{q}(t) = g(\theta(t), \varphi(t))\, v(t) \tag{8.1}$$

*of the RKM 5.0.2 with input $u = (v, \varphi_f, \varphi_r)$ and input space $U = [-\hat{v}, \hat{v}] \times \Phi$, let $(\tau, q(\cdot), u(\cdot))$ be an admissible solution $S(q_0, q_d)$ over the time interval $I = [0, \tau]$.*

*Then, for the control system*

$$\check{q}'(s) = \frac{1}{\hat{v}}\, g\big(\check{\theta}(s), \check{\varphi}(s)\big)\, \check{v}(s) \tag{8.2}$$

*with the scaled input space*

$$\check{U} = [-1, 1] \times \Phi$$

*and*

$$\check{v}(s) := \frac{1}{\hat{v}} v\big(\tfrac{1}{\hat{v}}\, s\big) = \frac{1}{\hat{v}} v(t), \quad \check{\varphi}(s) := \varphi\big(\tfrac{1}{\hat{v}}\, s\big) = \varphi(t),$$

*$(\sigma, \check{q}(\cdot), \check{u}(\cdot))$ is an admissible solution $\check{S}(q_0, q_d)$ over the time interval $\check{I} = [0, \sigma]$ for $\sigma = \hat{v}\,\tau$.*

**Proof** Corollary 8.1.1 results from Theorem 7.1.1 applied to the control system (8.1) of the RKM with input space $U = [-\hat{v}, \hat{v}] \times \Phi$. Using the notation of Theorem 7.1.1, system (8.1) represents system (7.1) with input $u = (v_1, w_1, w_2) = (v, \varphi_f, \varphi_r) \in U$, input space $U = V \times W$ for $V = [-\hat{v}, \hat{v}]$, $W = \Phi$, $m_1 = 1$, and $m_2 = 2$, and vector fields $f_0(x, w) = 0$ and $g_1(x, w) = g(\theta, \varphi)$. System (8.2) is the transformed system (7.2) with scaled input space $\check{U} = \check{V} \times W = [-1, 1] \times \Phi$. ■

Due to Corollary 8.1.1, it is sufficient to consider the problems 8.0.1 and 8.0.2 for the input space $\check{U}$, i. e., for $\check{v} \in [-1, 1]$. Solutions for other values of $\hat{v}$ result from those for $\hat{v} = 1$. The inputs $(\varphi_f, \varphi_r)$ cannot be scaled, as they enter the RKM nonlinearly. In Corollary 8.1.1 and throughout this thesis, the RKM is denoted by $\dot{q} = g(\theta, \varphi)\, v$. Only in the next corollary, $g$ is used for a Lie group element which represents the configuration $q$ of the RKM.

**Corollary 8.1.2** *(Transformation of the initial configuration of the RKM) For the RKM 5.0.2, let $(\tau, q(\cdot), u(\cdot))$ be an admissible solution $S(q(0), q(\tau))$ over the time interval $I = [0, \tau]$ from $q(0) = (\theta_0, x_0, y_0)$ and $q(\tau) = (\theta_d, x_d, y_d)$.*

*Then, for*

$$\tilde{q}(t) := \begin{bmatrix} \theta(t) & - & \theta_0 \\ (x(t) - x_0)\cos(\theta_0) & + & (y(t) - y_0)\sin(\theta_0) \\ -(x(t) - x_0)\sin(\theta_0) & + & (y(t) - y_0)\cos(\theta_0) \end{bmatrix}, \tag{8.3}$$

*$(\tau, \tilde{q}(\cdot), u(\cdot))$ is an admissible solution $\tilde{S}(\tilde{q}(0), \tilde{q}(\tau))$ over $I$ from $\tilde{q}(0) = (0, 0, 0)$ to*

$$\tilde{q}(\tau) = \begin{bmatrix} \theta_d & - & \theta_0 \\ (x_d - x_0)\cos(\theta_0) & + & (y_d - y_0)\sin(\theta_0) \\ -(x_d - x_0)\sin(\theta_0) & + & (y_d - y_0)\cos(\theta_0) \end{bmatrix}. \tag{8.4}$$

**Proof** By Lemma 5.3.8, the RKM can be written as left-invariant control system $\dot{g} = g\left(w_1(u)\, e_1 + w_2(u)\, e_2 + w_3(u)\, e_3\right)$ on $G = SE(2)$ for the basis vectors $e_i$ of the Lie algebra $\mathfrak{se}(2)$ given by (5.29) and the functions $w_i(u)$ as in (5.31). The configuration $q = (\theta, x, y)$ is represented by the Lie group element

$$g = \begin{bmatrix} \cos(\theta) & -\sin(\theta) & x \\ \sin(\theta) & \cos(\theta) & y \\ 0 & 0 & 1 \end{bmatrix}.$$

Assume that $(\tau, g(\cdot), u(\cdot))$ is an admissible solution over the time interval $[0, \tau]$ from $g(0)$ to $g(\tau)$ given by

$$g(0) = \begin{bmatrix} \cos(\theta_0) & -\sin(\theta_0) & x_0 \\ \sin(\theta_0) & \cos(\theta_0) & y_0 \\ 0 & 0 & 1 \end{bmatrix}, \quad g(\tau) = \begin{bmatrix} \cos(\theta(\tau)) & -\sin(\theta(\tau)) & x(\tau) \\ \sin(\theta(\tau)) & \cos(\theta(\tau)) & y(\tau) \\ 0 & 0 & 1 \end{bmatrix}.$$

Then, if $\tilde{g}(t) = g_0^{-1}\, g(t)$ is applied, $(\tau, \tilde{g}(\cdot), u(\cdot))$ is an admissible solution over $[0, \tau]$ from $\tilde{g}(0) = E$ to $\tilde{g}(\tau) = g_0^{-1}\, g_d$ by Theorem 7.1.2. Here, the configuration $\tilde{q} = \left(\tilde{\theta}, \tilde{x}, \tilde{y}\right)$ is represented by the Lie group element $\tilde{g}$. The identity element

$$E = \begin{bmatrix} 1 & 0 & 0 \\ 0 & 1 & 0 \\ 0 & 0 & 1 \end{bmatrix}$$

of $SE(2)$ corresponds to the initial configuration $\tilde{q}(0) = (0, 0, 0)$. For

$$\tilde{g}(t) = g_0^{-1}\, g(t) = \begin{bmatrix} \cos(\theta(t) - \theta_0) & -\sin(\theta(t) - \theta_0) & (x(t) - x_0)\cos(\theta_0) + (y(t) - y_0)\sin(\theta_0) \\ \sin(\theta(t) - \theta_0) & \cos(\theta(t) - \theta_0) & -(x(t) - x_0)\sin(\theta_0) + (y(t) - y_0)\cos(\theta_0) \\ 0 & 0 & 1 \end{bmatrix},$$

(8.3) results, and for

$$\tilde{g}(\tau) = g_0^{-1}\, g_d = \begin{bmatrix} \cos(\theta_d - \theta_0) & -\sin(\theta_d - \theta_0) & (x_d - x_0)\cos(\theta_0) + (y_d - y_0)\sin(\theta_0) \\ \sin(\theta_d - \theta_0) & \cos(\theta_d - \theta_0) & -(x_d - x_0)\sin(\theta_0) + (y_d - y_0)\cos(\theta_0) \\ 0 & 0 & 1 \end{bmatrix},$$

(8.4) is obtained. Thus, Corollary 8.1.2 holds. ■

According to the corollary, if a solution $q(\cdot)$ goes from $q_0$ to $q_d$, then the solution $\tilde{q}(\cdot)$ goes from $(0, 0, 0)$ to $\tilde{q}(\tau)$. Hence, it is sufficient to study the problems 8.0.1 and 8.0.2 for the fixed initial configuration $(0, 0, 0)$.

In the following, the scaled input space $[-1, 1] \times \Phi$ is denoted by $U$ instead of $\check{U}$. The initial configuration $(0, 0, 0)$ is denoted by $q_0$. Due to $\theta_0 = 0$ at $q_0$, there holds $\tilde{\lambda}_0 = \tilde{\gamma}_0$ for the normalized initial conditions of the adjoint state $\lambda$ and the transformed adjoint state $\gamma$. Thus, only initial conditions $\tilde{\lambda}_0$ are considered. The simplified versions of the path planning problem and the near time-optimal control problem for the RKM are as follows:

**Definition 8.1.3** *(Simplified path planning problem for the RKM) For the time-optimal control problem for the RKM 6.0.2 with initial configuration $q_0 = (0, 0, 0)$ and input space $U = [-1, 1] \times \Phi$, let $(q(\cdot), \lambda(\cdot), u(\cdot))$ be normal regular extremals which satisfy the necessary optimality conditions of Theorem 6.1.1, and $\Lambda_{q_0}$ the search space 6.3.6. Fix a constant $\varepsilon_q > 0$. The problem to find an end time $\tau$ and an initial condition $\tilde{\lambda}_0^{PP} \in \Lambda_{q_0}$ such that for an extremal satisfying $q(0) = q_0$ and $\lambda(0) = \tilde{\lambda}_0^{PP}$, there holds $\|q(\tau) - q_d\| \leq \varepsilon_q$ is called simplified path planning problem for the RKM. Any solution $\left(\tilde{\lambda}_0^{PP}, \tau\right)$ is called solution to the simplified path planning problem.*

**Definition 8.1.4** *(Simplified near time-optimal control problem for the RKM) For the time-optimal control problem for the RKM 6.0.2 with initial configuration $q_0 = (0,0,0)$ and input space $U = [-1,1] \times \Phi$, let $\tau^{to}$ be the end time of a time-optimal solution, $(q(\cdot), \lambda(\cdot), u(\cdot))$ normal regular extremals which satisfy the necessary optimality conditions of Theorem 6.1.1, and $\Lambda_{q_0}$ the search space 6.3.6. Fix constants $k \geq 1$ and $\varepsilon_q > 0$. The problem to find an end time $\tilde{\tau}^{to} \leq k\,\tau^{to}$ and an initial condition $\tilde{\lambda}_0^{to} \in \Lambda_{q_0}$ such that for an extremal satisfying $q(0) = q_0$ and $\lambda(0) = \tilde{\lambda}_0^{to}$, there holds $\|q(\tilde{\tau}^{to}) - q_d\| \leq \varepsilon_q$ is called simplified near time-optimal control problem for the RKM. Any solution $\left(\tilde{\lambda}_0^{to}, \tilde{\tau}^{to}\right)$ is called solution to the simplified near time-optimal control problem.*

In the following, the simplified problems 8.1.3 and 8.1.4 are considered, which are referred to as path planning problem and near time-optimal control problem for the RKM.

## 8.2 Implementation of the approach for time-optimal control

In this section, implementation aspects for the application of the time-optimal control 7.3.2 and the underlying path planning 7.2.6 to the near time-optimal control problem 8.1.4 are addressed. To implement the time-optimal control, the control system of the RKM, the adjoint equation, the extremal inputs, the parameters of Table 7.2, and a condition for near time-optimality to terminate the time-optimal control are required. Moreover, a parameterization of the search space $\Lambda_{q_0}$, a discretization interval $\triangle t$ for the representation of $I$ by the time vector $I_\triangle$, and a final time $\hat{T}$ of the initial time horizon have to be specified, which is done in the following.

### 8.2.1 Parameterization of the search space

To represent the search space $\Lambda_{q_0}$ as in Corollary 6.3.6, consider the parameter sets

$$\hat{A} = \left\{(\alpha_1, \alpha_2) \in \mathbb{R}^2 \mid -\pi \leq \alpha_1 < \pi, |\alpha_2| \leq 1\right\}$$

and

$$A = \hat{A} \backslash \left\{(-\pi, 0), (0,0)\right\}. \tag{8.5}$$

For $\alpha \in A$, let $\lambda_0 = \lambda_0(\alpha)$ be given by the map

$$\lambda_0 \colon A \to \mathbb{R}^3,\ \lambda_0(\alpha) = \begin{bmatrix} \lambda_{10}(\alpha) \\ \lambda_{20}(\alpha) \\ \lambda_{30}(\alpha) \end{bmatrix} = \begin{bmatrix} \sqrt{1-\alpha_2^2}\,\cos(\alpha_1) \\ \sqrt{1-\alpha_2^2}\,\sin(\alpha_1) \\ \alpha_2 \end{bmatrix}. \tag{8.6}$$

For $\hat{v} = 1$, a normalized initial condition $\tilde{\lambda}_0 = \tilde{\lambda}_0(\alpha)$ as in Definition 6.3.2 is obtained for

$$\tilde{\lambda}_0(\alpha) = \frac{1}{|b(\lambda_0(\alpha), \varphi^*(0))|}\ \lambda_0(\alpha). \tag{8.7}$$

Here, $b(\lambda_0(\alpha), \varphi^*(0))$ is the function $b(\gamma, \varphi)$ (6.8) evaluated at $\gamma = \lambda_0(\alpha)$ with $\gamma = \lambda$ because of $\theta_0 = 0$, and $\varphi = \varphi^*(0)$.

**Theorem 8.2.1** *(Parameterization of the search space $\Lambda_{q_0}$) The near time-optimal control problem 8.1.4 with the search space $\Lambda_{q_0}$ given by Corollary 6.3.6 is considered. For the parameter set $A$ (8.5), the map $\lambda_0$ (8.6), and $\alpha \in A$, let $\tilde{\lambda}_0(\alpha)$ be the normalized initial condition (8.7). Then, a parameterization of the search space is $\Lambda_{q_0} = \left\{\tilde{\lambda}_0(\alpha) \,\middle|\, \alpha \in A\right\}$.*

**Proof** According to Corollary 6.3.6, the search space $\Lambda_{q_0}$ consists of all normalized initial conditions $\tilde{\lambda}_0$ of case C2, C3, C5, and C6. For $\hat{v} = 1$, normalized initial conditions $\tilde{\lambda}_0$ result from (8.7) for initial conditions $\lambda_0 = \lambda_0(\alpha) \neq 0$.

By Theorem 6.1.4, initial conditions $\lambda_0$ of case C2 have to satisfy $\lambda_{10} = \lambda_{20} = 0$, $\lambda_{30} \neq 0$. These initial conditions arise from (8.6) for $\alpha = (\alpha_1, \alpha_2)$ with arbitrary $\alpha_1 \in [-\pi, \pi)$ and $\alpha_2 = \pm 1$. Initial conditions $\lambda_0$ of case C3 meeting $\lambda_{10} = 0$, $\lambda_{20} \neq 0$, $\lambda_{30} = 0$ are obtained from (8.6) for $\alpha_1 = \pm\frac{\pi}{2}$ and $\alpha_2 = 0$. For $\alpha_1 \in \{-\pi, 0\}$ and $0 < |\alpha_2| < 1$, (8.6) gives initial conditions $\lambda_0$ of case C5 with $\lambda_{10} \neq 0$, $\lambda_{20} = 0$, $\lambda_{30} \neq 0$. For $\alpha_1 \notin \{-\pi, 0\}$ and $|\alpha_2| < 1$, initial conditions of case C6 result from (8.6), for which $\lambda_{20} \neq 0$ and $\lambda_{10}^2 + \lambda_{30}^2 > 0$ is true. The union of the domains of $\alpha$ for initial conditions of case C2, C3, C5, and C6 gives the parameter set $A$.

Initial conditions of case C1 with $\lambda_{10} = \lambda_{20} = \lambda_{30} = 0$ are not relevant for time-optimal control. Such initial conditions do not result from any $\alpha \in A$, as for (8.6), $\|\lambda_0(\alpha)\| = 1$ holds. Initial conditions of case C4 with $\lambda_{10} \neq 0$, $\lambda_{20} = \lambda_{30} = 0$ leading to normal singular extremals result from $\alpha = (-\pi, 0)$ and $\alpha = (0, 0)$. For the parameter set $A$, these values of $\alpha$ are excluded. Thus, $\left\{ \tilde{\lambda}_0(\alpha) \,\middle|\, \alpha \in A \right\}$ gives a parameterization of the search space $\Lambda_{q_0}$. ■

Figure 8.1 shows the search space $\Lambda_{q_0}$. It looks like a 2-sphere deformed by the normalization (8.7). The red arrows point at the two excluded initial conditions which belong to normal singular extremals. The parameterization $\tilde{\lambda}_0(\alpha)$ of $\Lambda_{q_0}$ can be used for the path planning 7.2.6. Then, from a randomly chosen $\alpha^{SP} \in A$, a starting point $\tilde{\lambda}_0^{SP} = \tilde{\lambda}_0(\alpha^{SP}) \in \Lambda_{q_0}$ results, and the minimization $\min_{\alpha \in A} d\big(\tilde{\lambda}_0(\alpha)\big)$ over $A$ implements the minimization $\min_{\tilde{\lambda}_0 \in \Lambda_{q_0}} d\big(\tilde{\lambda}_0\big)$ over $\Lambda_{q_0}$.

Without the normalization (8.7), the image of $A$ under the map (8.6) is the unit 2-sphere minus two points. Other parameterizations of the 2-sphere like spherical coordinates with azimuth and polar angle are common as well. Parameterization 8.2.1 is used since the surface element $\mathrm{d}S = \mathrm{d}\alpha_1 \, \mathrm{d}\alpha_2$ is independent of $\alpha$. If the probability distribution on the parameter set $A$ is uniform, it is also uniform on the 2-sphere as the image of $A$ under (8.6). This is not true for spherical coordinates. If no knowledge of the minima of $d$ is available, the uniform distribution is advantageous, since random starting points $\tilde{\lambda}_0^{SP} = \tilde{\lambda}_0(\alpha^{SP})$ from $\alpha^{SP} \in A$ are located everywhere on the 2-sphere with same probability. As the normalization (8.7) deforms the 2-sphere, a uniform distribution on $A$ gives a distribution on the 2-sphere which is approximately uniform. This does not affect the probabilistic completeness of the path planning.

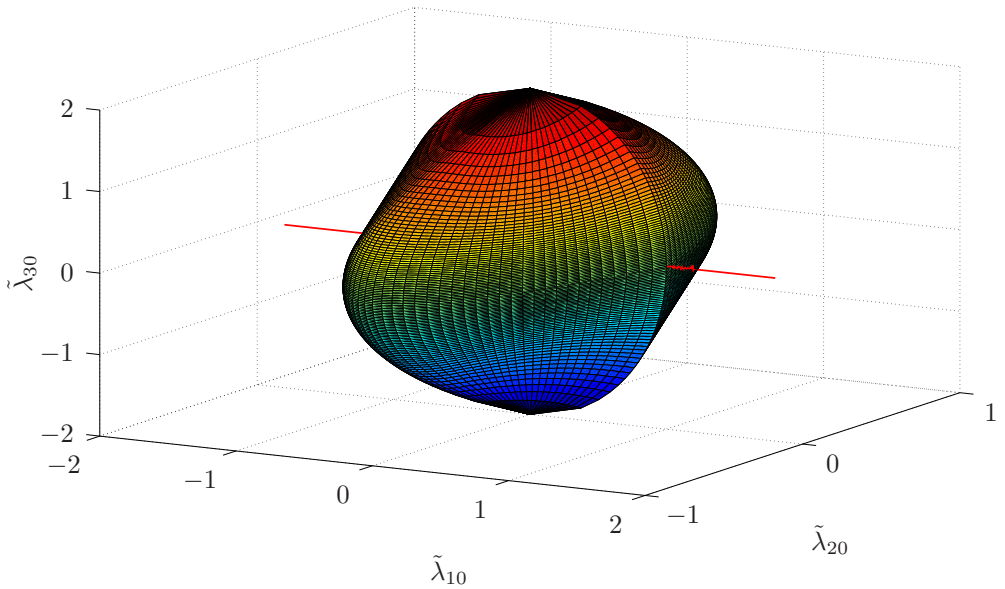


Figure 8.1: Search space $\Lambda_{q_0}$.

If instead of $A$, the parameter set $\hat{A}$ given by (8.5) is considered, the set

$$\hat{\Lambda}_{q_0} = \left\{ \tilde{\lambda}_0 \in \mathbb{R}^3 \,\middle|\, -1 + \tilde{\lambda}_0^\top g(\theta_0, \varphi(0))\, v(0) = 0 \right\} \tag{8.8}$$

results, which is a deformed 2-sphere and thus compact. In contrast, the search space $\Lambda_{q_0}$ is a deformed 2-sphere minus two points. Hence, $\Lambda_{q_0}$ is not compact but only bounded. The set $\hat{\Lambda}_{q_0}$ corresponds to the set $\hat{\Lambda}_{x_0}$ (4.6) for the RKM $\dot{q} = g(\theta, \varphi)\, v$ with the extremal inputs $\varphi(0)$ and $v(0)$ at time $t = 0$. It contains all initial conditions for which there are normal extremals meeting the necessary optimality conditions of Theorem 6.1.1 for $q^*(0) = q_0$ and $\lambda^*(0) = \tilde{\lambda}_0$.

For practical reasons, $\alpha$ is not taken from $A$ for the generation of random starting points $\tilde{\lambda}_0^{SP} = \tilde{\lambda}_0(\alpha^{SP})$ and the minimization $\min_\alpha d\big(\tilde{\lambda}_0(\alpha)\big)$, but from its closure which is

$$\bar{A} = \big\{(\alpha_1, \alpha_2) \in \mathbb{R}^2 \;|\, |\alpha_1| \leq \pi, |\alpha_2| \leq 1\big\} \,.$$

Using $\bar{A}$ instead of $A$ makes it possible to select $\alpha$ from a compact set. As $A$ and $\bar{A}$ differ only in a set of measure zero, almost all randomly chosen $\alpha \in \bar{A}$ satisfy $\alpha \in A$. A few normal singular extremals obtained for $\alpha = (-\pi, 0)$ or $\alpha = (0, 0)$ do not affect the time-optimal control.

### 8.2.2 Discretization interval

**Theorem 8.2.2** *(Discretization interval $\triangle t$) The near time-optimal control problem 8.1.4 is considered for a fixed tolerance $\varepsilon_q > 0$. For a discretization interval $\triangle t > 0$, $n_T \in \mathbb{N}_{>0}$, and $T = n_T\, \triangle t$, let*

$$I_\triangle = \big[\, t_i \;\big|\; t_i = i\, \triangle t,\; i = 0, \ldots, n_T,\; n_T = T/\triangle t \,\big]$$

*be the discretization of the time horizon $I = [0, T]$ as in (7.15) with sufficiently large $T$. If $\triangle t \leq \sqrt{3}\, \varepsilon_q$ holds, any existing solution to problem 8.1.4 can be found.*

**Proof** For the discretization

$$q(I_\triangle) = \big[\, q_i \;\big|\; q_i = q(t_i),\; t_i \in I_\triangle \,\big]$$

of the configuration at the times $I_\triangle$, the distance $\delta_i = \|q(t_i) - q(t_i + \triangle t)\|$ between two consecutive configurations is considered. By Lemma 5.3.5, the right-hand side of the RKM satisfies

$$\hat{v} \leq \|g(\theta, \varphi)\; v\| \leq \frac{2}{\sqrt{3}}\, \hat{v}$$

for $|v| = \hat{v}$ and $\hat{\varphi} = \frac{\pi}{4}$. Thus, $\|g(\theta, \varphi)\; v\| \leq 2/\sqrt{3}$ results for $\hat{v} = 1$, and the distance $\delta_i$ meets

$$\delta_i \leq \hat{\delta} = \frac{2}{\sqrt{3}}\, \triangle t. \tag{8.9}$$

If for a desired configuration $q_d$, at least one solution to problem 8.1.4 exists, it is assumed that there is a normal regular extremal given by $q(I_\triangle)$, a time $t_i \in I_\triangle$, and $c \in [0, 1]$ such that

$$q_d = q(t_i) + c\,(q(t_i + \triangle t) - q(t_i)) \tag{8.10}$$

holds. As (8.10) is true for some $c \in [0, 1]$, $q_d$ lies on the line between $q(t_i)$ and $q(t_i + \triangle t)$. If the distance $\delta_i = \|q(t_i) - q(t_i + \triangle t)\|$ satisfies $\delta_i \leq 2\, \varepsilon_q$, a solution to the path planning problem is found, since at $\tau = t_i$ or $\tau = t_i + \triangle t$, there holds $\|q(\tau) - q_d\| \leq \varepsilon_q$. To reach $q_d$ within $\varepsilon_q$ in the worst case, i. e., if the distance $\delta_i$ covered in the interval $\triangle t$ equals the maximal distance $\hat{\delta} = 2/\sqrt{3}\, \triangle t$ according to (8.9), $\hat{\delta} \leq 2\, \varepsilon_q$ has to hold. From this, $\triangle t \leq \sqrt{3}\, \varepsilon_q$ results. ■

For $\delta_i = 2\, \varepsilon_q$, an extremal meeting (8.10) is shown in Figure 8.2 on the left. A situation where (8.10) is true but $\delta_i \leq 2\, \varepsilon_q$ does not hold is shown in Figure 8.2 in the middle. Here, $\|q(\tau) - q_d\| \leq \varepsilon_q$ is true neither at $\tau = t_i$ nor at $\tau = t_i + \triangle t$. Depending on $q_d$, the assumption that a normal regular extremal satisfying (8.10) exists may be too strong. There are solutions for which $\|q(\tau) - q_d\| \leq \varepsilon_q$ is true even if (8.10) does not hold, see Figure 8.2 on the right. For the implementation of the time-optimal control, a slightly smaller value than $\sqrt{3}\, \varepsilon_q$ is set to ensure that no solutions are missed due to numerical errors.

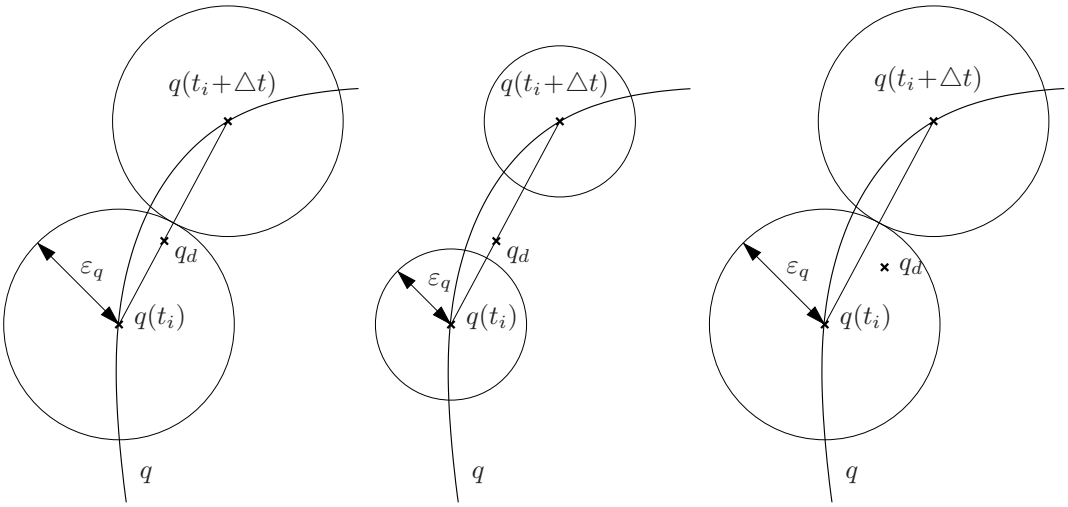


Figure 8.2: Solution with $q_d = q(t_i)+c\,(q(t_i+\triangle t)-q(t_i))$, $\hat{\delta}=2\,\varepsilon_q$ (left) and $\hat{\delta}>2\,\varepsilon_q$ (middle), solution with $q_d \neq q(t_i)+c\,(q(t_i+\triangle t)-q(t_i))$ and $\hat{\delta}=2\,\varepsilon_q$ (right).

### 8.2.3 Final time of the initial time horizon

In the following, $\lceil T \rceil_{\triangle t}$ means that $T$ is rounded up to the next integer multiple of $\triangle t$.

**Theorem 8.2.3** *(Final time $\hat{T}$ of the initial time horizon) The near time-optimal control problem 8.1.4 is considered for a desired configuration $q_d=(\theta_d,x_d,y_d)$. For $0<\triangle t\leq\sqrt{3}\,\varepsilon_q$ and $n_{\hat{T}}\in\mathbb{N}_{>0}$, let $\hat{T}=n_{\hat{T}}\,\triangle t$ be the final time of the initial time horizon $I=\left[0,\hat{T}\right]$. If*

$$\hat{T}=\max\left\{\left\lceil\frac{5\,\pi}{2}\right\rceil_{\triangle t},\left\lceil\pi+\sqrt{x_d^2+y_d^2}+1\right\rceil_{\triangle t}\right\} \tag{8.11}$$

*holds, any existing solution to problem 8.1.4 can be found.*

Before Theorem 8.2.3 is proved, some properties of Dubins paths are given. Dubins paths are the shortest paths of the simplified model (3.16) of the car-like robot which drives forward at constant velocity and has fixed positive minimal turning radius. These paths are used in the following to derive the upper bound (8.11). The paths consist of up to three pieces which are straight line segments $S$ or arcs of circles $C$ of radius $R$. Dubins paths are of type $CSC$ or $CCC$, where one or more pieces may vanish. They can be reproduced by the RKM, although they are no extremals for time-optimal control in general. Figure 8.3 shows Dubins paths of type $CCC$ and $CSC$. The angles of the arcs of the first, second, and third circle are called $\triangle\theta_1$, $\triangle\theta_2$, and $\triangle\theta_3$. As shown in [19], for Dubins paths of type $CCC$,

$$\begin{aligned}&\pi<|\triangle\theta_2|<2\,\pi,\\&0\leq|\triangle\theta_1|\leq|\triangle\theta_2|\ \text{ and }\ 0\leq|\triangle\theta_3|\leq|\triangle\theta_2|\,,\\&0\leq|\triangle\theta_1|<|\triangle\theta_2|-\pi\ \text{ or }\ 0\leq|\triangle\theta_3|<|\triangle\theta_2|-\pi\end{aligned} \tag{8.12}$$

holds. For Dubins paths of type $CSC$, $l$ is the length of the straight line segment. According to [19], the angles $\triangle\theta_1$ and $\triangle\theta_2$ of the first and second circle of a path of type $CSC$ satisfy

$$|\triangle\theta_1|+|\triangle\theta_2|\leq 2\,\pi. \tag{8.13}$$

**Proof** To obtain (8.11), the maximal times $\hat{T}_{CCC}$ and $\hat{T}_{CSC}$ required to pass Dubins paths of type $CCC$ and $CSC$ are determined. For paths of type $CCC$, the minimal turning radius $R$ and

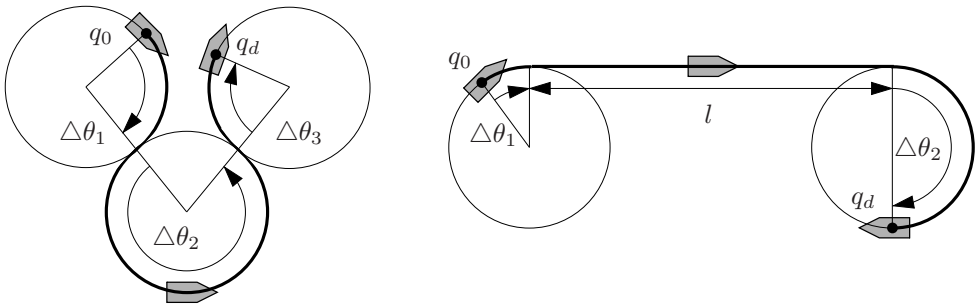


Figure 8.3: Dubins paths of type $CCC$ (left) and $CSC$ (right) with dimensions.

the maximal velocity $\hat{v}$ are taken into account. The time it takes to drive an arc of a circle of radius $R$ and angle $|\triangle\theta|$ with velocity $\hat{v}$ is $T = |\triangle\theta|\ R/\hat{v}$. From (8.12), $|\triangle\theta_1| + |\triangle\theta_2| + |\triangle\theta_3| \leq 5\,\pi$ results. Thus, the maximal time $\hat{T}_{CCC}$ for a path of type $CCC$ is

$$\hat{T}_{CCC} = \frac{5\,\pi\,R}{\hat{v}}. \tag{8.14}$$

For paths of type $CSC$ from $q_0 = (\theta_0, x_0, y_0)$ to $q_d = (\theta_d, x_d, y_d)$, the distance

$$d_{xy} = \sqrt{(x_d - x_0)^2 + (y_d - y_0)^2}$$

is considered. For the length of the straight line segment, $l \leq d_{xy} + 2\,R$ holds, as it has to be tangent to both circles at the points of contact. From the maximal time $2\,\pi\,R/\hat{v}$ required for the two arcs of circles which satisfy (8.13) and $(d_{xy} + 2\,R)\,/\hat{v}$ for the straight line segment,

$$\hat{T}_{CSC} = \frac{1}{\hat{v}}\left(2\,\pi\,R + \sqrt{(x_d - x_0)^2 + (y_d - y_0)^2} + 2\,R\right) \tag{8.15}$$

results. The final time $\hat{T}$ is the maximum of $\hat{T}_{CCC}$ and $\hat{T}_{CSC}$ according to

$$\hat{T} = \max\left\{\hat{T}_{CCC}, \hat{T}_{CSC}\right\}. \tag{8.16}$$

For a final time $\hat{T} = n_{\hat{T}}\,\triangle t$ with $n_{\hat{T}} \in \mathbb{N}_{>0}$, the times $\hat{T}_{CCC}$ and $\hat{T}_{CSC}$ are rounded up to the next integer multiple of $\triangle t$. Using (8.14), (8.15), and (8.16) gives

$$\hat{T} = \max\left\{\left\lceil\frac{5\,\pi\,R}{\hat{v}}\right\rceil_{\triangle t}, \left\lceil\frac{1}{\hat{v}}\left(2\,\pi\,R + \sqrt{(x_d - x_0)^2 + (y_d - y_0)^2} + 2\,R\right)\right\rceil_{\triangle t}\right\}.$$

For the minimal turning radius $R = \frac{1}{2}$ given by Lemma 5.3.7 for $\hat{\varphi} = \frac{\pi}{4}$, $\hat{v} = 1$, and $x_0 = y_0 = 0$, (8.11) holds. ■

The conditions (8.12) and (8.13) are also discussed in [2, 106, 120]. The time $\hat{T}$ given by (8.11) is used as final time of the initial time horizon $I = [0, \hat{T}]$ for the time-optimal control. It was derived based on Dubins paths from $q_0 = (0, 0, 0)$ to $q_d = (\theta_d, x_d, y_d)$. For the BSR, shorter final times $\hat{T}$ than (8.11) can be obtained, since in contrast to the car-like robot considered for Dubins paths, the BSR can drive forward and backward and has two steerable axles. Shorter final times may be determined based on Reeds-Shepp paths, see [94].

## 8.3 Analysis of the convergence

In this section, the convergence of the time-optimal control is studied for the near time-optimal control problem 8.1.4. For this, condition (7.12) for property O3 of Lemma 7.2.5 is analyzed,

and probabilistic completeness of the time-optimal control is established by Theorem 7.3.4 and the results from Section 8.2.1.

**Lemma 8.3.1** *(Condition (7.12) for property O3 of Lemma 7.2.5) For the time-optimal control problem for the RKM 6.0.2, let* $(q(\cdot), \lambda(\cdot), u(\cdot))$ *be normal regular extremals which satisfy the necessary optimality conditions of Theorem 6.1.1 over the time interval* $I = [0, \tau]$*, and let* $\|q(t) - q_d\|$ *be sufficiently small for all* $t \in I$*. Then,* $\dot{q}(t) \neq 0$ *holds for almost all* $t \in I$*, and*

$$(q(t) - q_d)^\top \dot{q}(t) = 0 \tag{8.17}$$

*does not hold over any proper time interval in* $I$*.*

**Proof** According to property E7 of Lemma 6.3.1, $q$ is non-constant for all extremals. Thus, $\dot{q}(t) \neq 0$ holds for almost all $t \in I$. Using the deviation $\bar{D} = \frac{1}{2}\|\triangle q\|^2 = \frac{1}{2}\triangle q^\top \triangle q$ as in (7.14) for $\triangle q = q - q_d$, $\triangle\theta = \theta - \theta_d$, $\triangle x = x - x_d$, and $\triangle y = y - y_d$, (8.17) can be written as

$$\dot{\bar{D}} = \triangle q^\top \dot{q} = \triangle\theta\,\dot{\theta} + \triangle x\,\dot{x} + \triangle y\,\dot{y} = 0.$$

As discussed in Section 6.4.3, the extremal velocities $v$ are constant between cusps and discontinuous at the cusps. In each compact time interval $I$, only a finite number of cusps can occur. The extremal steering angles $\varphi$ are piecewise differentiable, continuous if $\varphi$ enters or leaves bd $\Phi$, and discontinuous at the cusps. Between two cusps, $\varphi$ reaches or leaves bd $\Phi$ at most twice. Thus, the inputs $v$ and $\varphi$ are differentiable for almost all $t \in I$.

As from now, the inputs $v$ and $\varphi$ are assumed to be differentiable, since the times at which $v$ is not constant or $\varphi$ is not differentiable do not affect whether (8.17) holds over a proper interval or not. Then, the time derivative $\dot{q}$ from $\dot{q} = g(\theta, \varphi)\, v$ is continuously differentiable, and the second time derivative $\ddot{\bar{D}}$ of $\bar{D} = \frac{1}{2}\|\triangle q\|^2$ exists and is

$$\ddot{\bar{D}} = \dot{q}^\top \dot{q} + \triangle q^\top \ddot{q} = \dot{\theta}^2 + \dot{x}^2 + \dot{y}^2 + \triangle\theta\,\ddot{\theta} + \triangle x\,\ddot{x} + \triangle y\,\ddot{y}.$$

For (8.17) to hold over a proper interval in $I$, $\dot{\bar{D}} = 0$ and $\ddot{\bar{D}} = 0$ must hold at all times of the interval at which the inputs $v$ and $\varphi$ are differentiable. This is true since (8.17) is equivalent to $\dot{\bar{D}} = 0$, and for $\dot{\bar{D}} = 0$ to hold over a proper interval, $\ddot{\bar{D}} = 0$ must hold there as well. However, in the following it is shown that if $\dot{\bar{D}} = 0$ and $\ddot{\bar{D}} = 0$ holds at some time $t_1$, then $\dot{\bar{D}} = 0$ and $\ddot{\bar{D}} = 0$ cannot be true over any proper interval starting from $t_1$ for sufficiently small $\triangle q$. Here, $\triangle q = q - q_d$ is sufficiently small, as $\|q(t) - q_d\|$ is assumed in Lemma 8.3.1 to be sufficiently small for all $t \in I$.

The first term of $\ddot{\bar{D}} = \dot{q}^\top \dot{q} + \triangle q^\top \ddot{q}$ is the squared norm of the right-hand side of the RKM $\dot{q} = g(\theta, \varphi)\, v$, i. e., $\dot{q}^\top \dot{q} = \|g(\theta, \varphi)\ v\|^2$ applies. Due to Lemma 5.3.5, for $|v| = \hat{v}$ and $\hat{\varphi} = \frac{\pi}{4}$,

$$\hat{v} \leq \|g(\theta, \varphi)\ v\| \leq \frac{2}{\sqrt{3}}\,\hat{v}$$

holds. Thus, $\dot{q}^\top \dot{q} \geq 1$ is true for $\hat{v} = 1$. For $\dot{q} = g(\theta, \varphi)\, v$ and $\frac{\mathrm{d}}{\mathrm{d}t} v = 0$ since $v$ is constant between two cusps, the second time derivatives of $(\theta, x, y)$ are

$$\begin{aligned}
\ddot{\theta} &= (\dot{\varphi}_f - \dot{\varphi}_r)\cos(\varphi_f - \varphi_r)\, v, \\
\ddot{x} &= -\tfrac{1}{2}\, v \Big( \dot{\varphi}_f \left(\sin(\varphi_f)\cos(\theta + \varphi_r) + \cos(\varphi_r)\sin(\theta + \varphi_f)\right) \\
&\quad + \dot{\varphi}_r \left(\cos(\varphi_f)\sin(\theta + \varphi_r) + \sin(\varphi_r)\cos(\theta + \varphi_f)\right) \\
&\quad + \sin(\varphi_f - \varphi_r)\left(\cos(\varphi_f)\sin(\theta + \varphi_r) + \cos(\varphi_r)\sin(\theta + \varphi_f)\right) v \Big), \\
\ddot{y} &= \tfrac{1}{2}\, v \Big( \dot{\varphi}_f \left(-\sin(\varphi_f)\sin(\theta + \varphi_r) + \cos(\varphi_r)\cos(\theta + \varphi_f)\right) \\
&\quad + \dot{\varphi}_r \left(\cos(\varphi_f)\cos(\theta + \varphi_r) - \sin(\varphi_r)\sin(\theta + \varphi_f)\right) \\
&\quad + \sin(\varphi_f - \varphi_r)\left(\cos(\varphi_f)\cos(\theta + \varphi_r) + \cos(\varphi_r)\cos(\theta + \varphi_f)\right) v \Big)
\end{aligned}$$

with $\dot{\varphi}_f = \frac{\mathrm{d}}{\mathrm{d}t}\varphi_f$ and $\dot{\varphi}_r = \frac{\mathrm{d}}{\mathrm{d}t}\varphi_r$. For these second time derivatives,

$$\left|\ddot{\theta}\right| \leq \left|\dot{\varphi}_f - \dot{\varphi}_r\right| |v|\,, \quad |\ddot{x}| \leq \frac{1}{2}\left(|\dot{\varphi}_f| + |\dot{\varphi}_r| + 2\,|v|\right)|v|\,, \quad |\ddot{y}| \leq \frac{1}{2}\left(|\dot{\varphi}_f| + |\dot{\varphi}_r| + 2\,|v|\right)|v|$$

holds. Thus, for $|v| = \hat{v} = 1$, they satisfy

$$\left|\ddot{\theta}\right| \leq \left|\dot{\varphi}_f - \dot{\varphi}_r\right|, \quad |\ddot{x}| \leq \frac{1}{2}\left(|\dot{\varphi}_f| + |\dot{\varphi}_r| + 2\right), \quad |\ddot{y}| \leq \frac{1}{2}\left(|\dot{\varphi}_f| + |\dot{\varphi}_r| + 2\right). \tag{8.18}$$

The extremal inputs $\varphi_i$, $i = 1,...,9$ from Theorem 6.1.3 are either constant or result from (6.11) to (6.15). For $\varphi_9 = (\varphi_{f_9}, \varphi_{r_9})$ as in (6.15), $\dot{\varphi}_9 = (\dot{\varphi}_{f_9}, \dot{\varphi}_{r_9})$ is given by

$$\begin{aligned} \dot{\varphi}_{f_9} &= \tfrac{1}{2}\left(\frac{2\left(-\gamma_1\,\dot{\gamma}_2 + \gamma_2\,\dot{\gamma}_1\right)}{4\,\gamma_1^2 + \gamma_2^2} + \frac{\gamma_2\,\dot{\gamma}_3 - \gamma_3\,\dot{\gamma}_2}{\gamma_2^2 + \gamma_3^2}\right), \\ \dot{\varphi}_{r_9} &= \tfrac{1}{2}\left(\frac{2\left(\gamma_1\,\dot{\gamma}_2 - \gamma_2\,\dot{\gamma}_1\right)}{4\,\gamma_1^2 + \gamma_2^2} + \frac{\gamma_2\,\dot{\gamma}_3 - \gamma_3\,\dot{\gamma}_2}{\gamma_2^2 + \gamma_3^2}\right). \end{aligned} \tag{8.19}$$

As $v$ is assumed to be differentiable and thus constant, no cusps occur at which $v$ changes from $\pm\hat{v}$ to $\mp\hat{v}$. Thus, $\gamma_2 \neq 0$ is true, since cusps take place at the zero-crossing of $\gamma_2$ according to property NR5 of Lemma 6.4.3. Since $\gamma_2 \neq 0$ holds, $\gamma$ is bounded, and $\dot{\gamma}$ as in (6.10) is bounded for bounded $\gamma$ and bounded $v$, the time derivatives $(\dot{\varphi}_{f_9}, \dot{\varphi}_{r_9})$ given by (8.19) are bounded. The derivatives $\dot{\varphi}_i$ of the other extremal inputs $\varphi_i$, $i = 1,...,8$ are bounded as well.

All in all, $\dot{q}^\top \dot{q} \geq 1$ holds, the second time derivatives satisfy (8.18), and $\dot{\varphi}_i$ is bounded for $i = 1,...,9$. Hence, $\ddot{D} > 0$ holds for sufficiently small $\triangle q$. Since the deviation $\|q(t) - q_d\|$ is assumed to be sufficiently small for all $t \in I$, $\triangle q = q - q_d$ is sufficiently small. Thus, $\ddot{D} \neq 0$ is true for $\dot{D} = 0$, and $(q(t) - q_d)^\top \dot{q}(t) = 0$ does not hold over any proper time interval. ■

To show Lemma 8.3.1 without assuming a sufficiently small $\triangle q$, closed-form representations of $q$, $v$, and $\varphi$ would be required. According to simulations, the lemma holds for arbitrary $\triangle q$.

**Corollary 8.3.2** *(Convergence of the time-optimal control of the RKM) The time-optimal control 7.3.2 is applied to the near time-optimal control problem 8.1.4. The local optimizations, the path planning, and the time-optimal control are controlled by the exit conditions EC1, EC2, and EC3 for a sufficiently large bound $\hat{n}^{to}_{Sim}$. The bound $\hat{n}^{PP}_{Sim}$ for exit condition EC2 is set to $\hat{n}^{PP}_{Sim} = \hat{n}^{to}_{Sim} - n^{to}_{Sim}$. If there is at least one solution to problem 8.1.4, let the probability of convergence for each solution minimum satisfy $P_C > 0$, let $\|q(t) - q_d\|$ be sufficiently small for all time $t$, and let the discretization interval $\triangle t$ be sufficiently small. Then, any existing solution to problem 8.1.4 is found after a finite number of simulated extremals. The time-optimal control is probabilistically complete.*

**Proof** Corollary 8.3.2 results from Theorem 7.3.4 applied to the near time-optimal control problem for the RKM. As discussed in Section 8.2.1, the search space $\Lambda_{q_0}$ is bounded, since $\Lambda_{q_0}$ is a deformed 2-sphere minus two points. By Lemma 8.3.1, if the deviation $\|q(t) - q_d\|$ is sufficiently small for all $t$, condition (7.12) for property O3 is satisfied. Thus, if the assumptions of Corollary 8.3.2 are satisfied, the assumptions of Theorem 7.3.4 hold as well. Hence, if at least one solution to problem 8.1.4 exists, a solution is found after a finite number of simulated extremals, and the time-optimal control is probabilistically complete. ■

According to Corollary 8.3.2, for probabilistic completeness of the time-optimal control of the RKM, the probability of convergence $P_C$ must be positive for each solution minimum, the deviation $\|q(t) - q_d\|$ must be sufficiently small for all $t$, the discretization interval $\triangle t$ for the final time $T' = \tau - \triangle t$ must be sufficiently small, and the bound $\hat{n}^{to}_{Sim}$ for exit condition EC3 must be sufficiently large. According to simulations, Lemma 8.3.1 holds for arbitrary $\triangle q$. Thus, condition (7.12) for property O3 is true without requiring that $\|q(t) - q_d\|$ is sufficiently small.

## 8.4 Simulation results

This section gives simulation data of the time-optimal control 7.3.2 applied to the near time-optimal control problem 8.1.4. For this, the setup of the simulation is described, results on the probability of convergence $P_C$ of the local optimization are discussed, and simulations of the time-optimal control for two desired configurations $q_d$ are presented.

### 8.4.1 Setup of the simulation

To use the discretization interval

$$\triangle t = 0.001, \tag{8.20}$$

the tolerance $\varepsilon_q$ for the condition $\|q(\tau) - q_d\| \leq \varepsilon_q$ is set to

$$\varepsilon_q = 0.00058. \tag{8.21}$$

For $(x, y)$ given in m and $\theta$ in rad, $\varepsilon_q = 0.00058$ corresponds to a net translational deviation of 0.00058 m = 0.58 mm or a net rotational deviation of 0.00058 rad = 0.033°. For comparison, the length of Mustang MK I and the CyCab robot from Chapter 5 is 2.15 m and 1.9 m, respectively. By Theorem 8.2.2, the discretization interval $\triangle t$ has to satisfy $\triangle t \leq \sqrt{3}\,\varepsilon_q = 0.001005$ for $\varepsilon_q = 0.00058$. Thus, $\triangle t = 0.001$ is feasible.

Table 8.1 lists the values and references for the parameters of Table 7.2 for time-optimal control of the RKM. No values for $q_d$ and $\hat{T}$ are given, as the desired configuration $q_d$ is specified for each individual control problem and the final time $\hat{T}$ results from (8.11) for $q_d$. The value of $\hat{n}_{Sim}^{LO}$ for the maximal number of simulated extremals for each run of the local optimization is derived in Section 8.4.2. For $\hat{n}_{Sim}^{to}$, a sufficiently large value is chosen so that the time-optimal control is not terminated by exit condition EC3.

| parameter | value | reference |
|---|---|---|
| $q_0$ | $(0, 0, 0)$ | - |
| $\varepsilon_q$ | 0.00058 | (8.21) |
| $\Lambda_{q_0}$ | - | Theorem 8.2.1 |
| $\triangle t$ | 0.001 | (8.20) |
| $\hat{n}_{Sim}^{LO}$ | 150 | Table 8.2 |
| $\hat{n}_{Sim}^{to}$ | 1000 | - |

Table 8.1: Parameters for time-optimal control of the reduced kinematic model.

For local optimization, the MATLAB function **fmincon** was used, which applies sequential quadratic programming (SQP) for medium-scale optimization problems. For the numerical integration of the equations of the RKM and the adjoint equation (6.4) driven by the extremal inputs (6.5) and (6.6), the function MATLAB function **ode45** was applied. It implements a Runge-Kutta solver of fifth order.

### 8.4.2 Probability of convergence of the local optimization

The probability of convergence $P_C$ from Definition 7.2.10 is analyzed in the following for the local optimization method used for path planning for the RKM. For convergence of the path planning and the time-optimal control, $P_C > 0$ has to hold for each solution minimum. In Table 8.2, simulation results for $P_C$ are listed. The simulation data is given for different values of $\hat{n}_{Sim}^{LO}$, i. e., different maximal numbers of simulated extremals for each run of the local optimization. Among others, the value of $P_C$ depends on $\hat{n}_{Sim}^{LO}$. If the number $n_{Sim}^{LO}$ of simulated extremals for a local optimization satisfies $n_{Sim}^{LO} \geq \hat{n}_{Sim}^{LO}$, the optimization is terminated by exit condition EC1.

For larger $\hat{n}_{Sim}^{LO}$, the probability of convergence is greater, as more extremals can be simulated for each optimization until a solution is found or the optimization is terminated.

For the results of Table 8.2, local optimizations were performed for random starting points $\tilde{\lambda}_0^{SP} = \tilde{\lambda}_0(\alpha^{SP})$ in the region of attraction of solution minima. The desired configurations

$$Q_d = \left\{ q_d = (\theta_d, x_d, y_d) \,\middle|\, \theta_d \in \left\{ -\pi, -\frac{\pi}{2}, 0, \frac{\pi}{2} \right\}, x_d \in \{0, 2, 4\}, y_d \in \{0, 2, 4\}, x_d + y_d > 0 \right\}$$

and the corresponding final times $\hat{T}$ (8.11) were used. Due to $x_d + y_d > 0$, the configuration $q_d = (0, 0, 0)$ was excluded, as $q_0 \neq q_d$ should hold. The configurations $(-\pi, 0, 0)$, $\left(-\frac{\pi}{2}, 0, 0\right)$, and $\left(\frac{\pi}{2}, 0, 0\right)$ were excluded by $x_d + y_d > 0$, as they are not reachable by normal regular extremals, see Section 9.4. For each desired configuration $q_d \in Q_d$, 150 local optimizations initialized to different starting points $\tilde{\lambda}_0^{SP}$ were performed. The random starting points $\tilde{\lambda}_0^{SP} = \tilde{\lambda}_0(\alpha^{SP})$ were represented by the parameterization 8.2.1. For different values of $\hat{n}_{Sim}^{LO}$, the ratio of local optimizations for which $\|q(\tau) - q_d\| \leq \varepsilon_q$ holds for $\tau \leq \hat{T}$ was taken as value for $P_C$.

| $\hat{n}_{Sim}^{LO}$ | $P_C$ | $n_{LO}$ | $P$ | $n_{Sim}$ | $\hat{n}_{Sim}^{LO}$ | $P_C$ | $n_{LO}$ | $P$ | $n_{Sim}$ |
|---|---|---|---|---|---|---|---|---|---|
| 50 | 0.081 | 55 | 0.990 | 2750 | 180 | 0.938 | 2 | 0.996 | 360 |
| 60 | 0.239 | 17 | 0.990 | 1020 | 190 | 0.941 | 2 | 0.996 | 380 |
| 70 | 0.459 | 8 | 0.992 | 560 | 200 | 0.950 | 2 | 0.997 | 400 |
| 80 | 0.635 | 5 | 0.993 | 400 | 210 | 0.957 | 2 | 0.998 | 420 |
| 90 | 0.735 | 4 | 0.995 | 360 | 220 | 0.959 | 2 | 0.998 | 440 |
| 100 | 0.793 | 3 | 0.991 | 300 | 230 | 0.964 | 2 | 0.998 | 460 |
| 110 | 0.829 | 3 | 0.994 | 330 | 240 | 0.969 | 2 | 0.999 | 480 |
| 120 | 0.854 | 3 | 0.996 | 360 | 250 | 0.971 | 2 | 0.999 | 500 |
| 130 | 0.878 | 3 | 0.998 | 390 | 260 | 0.973 | 2 | 0.999 | 520 |
| 140 | 0.893 | 3 | 0.998 | 420 | 270 | 0.976 | 2 | 0.999 | 540 |
| 150 | 0.913 | 2 | 0.992 | 300 | 280 | 0.978 | 2 | 0.999 | 560 |
| 160 | 0.922 | 2 | 0.993 | 320 | 290 | 0.984 | 2 | 0.999 | 580 |
| 170 | 0.932 | 2 | 0.995 | 340 | 300 | 0.984 | 2 | 0.999 | 600 |

Table 8.2: Probability of convergence $P_C$ of the local optimization for path planning.

In Table 8.2, the expected number $n_{LO}$ of local optimizations is listed such that after $n_{LO}$ optimizations, a solution to the path planning problem is found with probability $P > 0.99$. For example, for $\hat{n}_{Sim}^{LO} = 100$, Table 8.2 gives $P_C = 0.793$. To achieve $P > 0.99$, at least $n_{LO} = 3$ local optimizations have to be performed, since after 3 optimizations,

$$P = P_C + (1 - P_C) P_C + (1 - P_C)^2 P_C = 0.991 > 0.99$$

is true. Here, $P$ is the sum of the probabilities $P_C$, $(1 - P_C) P_C$, and $(1 - P_C)^2 P_C$ that a solution is found for the first, second, and third random starting point $\tilde{\lambda}_0^{SP}$, respectively.

From $\hat{n}_{Sim}^{LO}$ and $n_{LO}$, the expected number $n_{Sim} = \hat{n}_{Sim}^{LO} n_{LO}$ of simulated extremals results, i. e., $n_{Sim}$ simulated extremals are required to find a solution with probability $P > 0.99$, provided that only random starting points $\tilde{\lambda}_0^{SP}$ in the regions of attraction of solution minima are chosen. A small value of $n_{Sim}$ is desirable to keep the computational effort for path planning low. According to Table 8.2, the minimal value $n_{Sim} = 300$ results for $\hat{n}_{Sim}^{LO} = 100$ and $\hat{n}_{Sim}^{LO} = 150$. Because of the greater value of $P$, $\hat{n}_{Sim}^{LO} = 150$ is used in the following, for which $P_C = 0.913 > 0$ holds. It should be noted that the value for $P$ in Table 8.2 does not give the probability that a solution to the path planning problem is found after $n_{Sim}$ simulated extremals for arbitrary starting points $\tilde{\lambda}_0^{SP} \in \Lambda_{q_0}$, since for Table 8.2, only random starting points $\tilde{\lambda}_0^{SP}$ in the regions of attraction of solution minima are considered. However, in general, the regions of attraction of the solution minima are unknown for a specific path planning problem.

### 8.4.3 Simulation results of the time-optimal control

In the following, simulation results of the time-optimal control 7.3.2 applied to the near time-optimal control problem 8.1.4 are presented for the desired configurations $q_d = \left(-\frac{\pi}{2}, 4, 2\right)$ and $q_d = (0, 2, -4)$. For $q_d = \left(-\frac{\pi}{2}, 4, 2\right)$, the final time $\hat{T}$ is 8.614. In Table 8.3, a sequence of solutions generated by the time-optimal control is listed. Each row of the table gives one solution of the path planning 7.2.6.

| $n_S$ | $T$ | $n_{SP}$ | $n_{Sim}^{PP}$ | $\alpha^{SP}$ | $\tilde{\lambda}_0^{SP}$ | $\alpha^{PP}$ | $\tilde{\lambda}_0^{PP}$ | $\tau$ | $n_c$ |
|---|---|---|---|---|---|---|---|---|---|
| S1 | 8.614 | 1 | 78 | $\begin{pmatrix} 2.7143 \\ 0.3136 \end{pmatrix}$ | $\begin{pmatrix} -0.8641 \\ 0.3934 \\ 0.3136 \end{pmatrix}$ | $\begin{pmatrix} 2.4780 \\ 0.3237 \end{pmatrix}$ | $\begin{pmatrix} -0.7453 \\ 0.5827 \\ 0.3237 \end{pmatrix}$ | 8.528 | 3 |
| S2 | 8.527 | 6 | 572 | $\begin{pmatrix} 1.9759 \\ 0.5998 \end{pmatrix}$ | $\begin{pmatrix} -0.3153 \\ 0.7353 \\ 0.5998 \end{pmatrix}$ | $\begin{pmatrix} 1.0979 \\ 0.3510 \end{pmatrix}$ | $\begin{pmatrix} 0.4264 \\ 0.8335 \\ 0.3510 \end{pmatrix}$ | 6.249 | 1 |
| S3 | 6.248 | 8 | 770 | $\begin{pmatrix} 2.1323 \\ -0.5433 \end{pmatrix}$ | $\begin{pmatrix} -0.4469 \\ 0.7106 \\ -0.5433 \end{pmatrix}$ | $\begin{pmatrix} 1.2545 \\ 0.5581 \end{pmatrix}$ | $\begin{pmatrix} 0.2581 \\ 0.7886 \\ 0.5581 \end{pmatrix}$ | 5.492 | 1 |

Table 8.3: Solutions generated by the time-optimal control for $q_d = \left(-\frac{\pi}{2}, 4, 2\right)$.

The columns of Table 8.3 list $n_S$, $T$, $n_{SP}$, $n_{Sim}^{PP}$, $\alpha^{SP}$, $\tilde{\lambda}_0^{SP}$, $\alpha^{PP}$, $\tilde{\lambda}_0^{PP}$, $\tau$, and $n_c$. Here, $n_S$ is the number of the solution, $T$ the final time of the time horizon $I = [0, T]$, $n_{SP}$ the number of random starting points, and $n_{Sim}^{PP}$ the number of extremals simulated so far. From the random value $\alpha^{SP}$, the initial condition $\tilde{\lambda}_0^{SP} = \tilde{\lambda}(\alpha^{SP})$ is obtained. The local optimization $\min_{\alpha \in \bar{A}} d\big(\tilde{\lambda}_0(\alpha)\big)$ results in $\alpha^{PP}$, which gives the initial condition $\tilde{\lambda}_0^{PP} = \tilde{\lambda}(\alpha^{PP})$ that solves the path planning problem. The end time of the solution is $\tau$ and the number of cusps is $n_c$. From solution S1 to solution S3, the number of random starting points $n_{SP}$ and simulated extremals $n_{Sim}^{PP}$ increases. The end time $\tau$ decreases, and the number of cusps $n_c$ decreases or stays constant. The first, sixth and eighth random value $\alpha^{SP}$ gives a solution to the path planning problem. For the other $\alpha^{SP}$, no solution is obtained, and the local optimization is terminated by exit condition EC1. The solutions S2 and S3 are near time-optimal solutions, as they have the minimal number of cusps, see Section 9.5. Solution S3 is a time-optimal normal regular extremal.

The solutions S1 and S3 are depicted in Figure 8.4 and 8.5. Each figure consists of a time plot of the orientation angle $\theta \in \mathbb{R}$ and $\theta \in [-\pi, \pi)$ with angles $\theta$ and $\theta + 2\,k\,\pi$ identified for $k \in \mathbb{Z}$, a time plot of the adjoint state $\big(\tilde{\lambda}_1, \tilde{\lambda}_2, \tilde{\lambda}_3\big)$, an $(x, y)$ plot, and time plots of the input $\big(v, \varphi_f, \varphi_r\big)$, the function $h$ (6.3), the Hamiltonian function $H$ (6.2), and the deviation $D = \|q - q_d\|$ as in (7.5) for fixed $\tilde{\lambda}_0^{PP}$. Figure 8.6 contains $(x, y)$ plots of the three solutions. The green, blue, and red pentagons represent $q_0$, $q_d$, and $q(\tau)$. Due to $\varepsilon_q > 0$, the blue and red pentagons differ slightly. The arrowheads of the pentagons point in the forward direction of the BSR. Besides, snapshots of the BSR at equal time intervals are shown. The light continuous curves give the path of the center of mass of the BSR. The thick bars on the front and rear indicate the steering angles. Regarding the types 6.4.1 of normal regular extremals, the solutions S1 and S2 are of type M, and solution S3 is of type P. In Figure 8.6, the decrease of the end time $\tau$ over the solutions is clearly visible.

The Figures 8.7 and 8.8 show plots of the two-dimensional surface obtained from the minimal deviation $d$ for $T = 8.614$. In Figure 8.7, $d\big(\tilde{\lambda}_0(\alpha)\big)$ is depicted over the search space $\Lambda_{q_0}$ obtained for $\alpha \in \bar{A}$. In Figure 8.8, $d\big(\tilde{\lambda}_0(\alpha)\big)$ is given over a subset of $\Lambda_{q_0}$ which results for $\alpha \in \big\{(\alpha_1, \alpha_2) \in \mathbb{R}^2 \mid 0 \le \alpha_1 \le \pi, 0 \le \alpha_2 \le 1\big\}$. According to the figures, the search space $\Lambda_{q_0}$ consists of one domain $\Psi$ where $d = \hat{d}$ holds for $\hat{d} = \|q_0 - q_d\| = 4.740$, and the regions of attraction $\Omega$ of four minima. Three of the four minima of $d$ are solution minima which result in the solutions in Table 8.3. For the remaining minimum, $\|q(\tau) - q_d\| \le \varepsilon_q$ cannot be achieved.

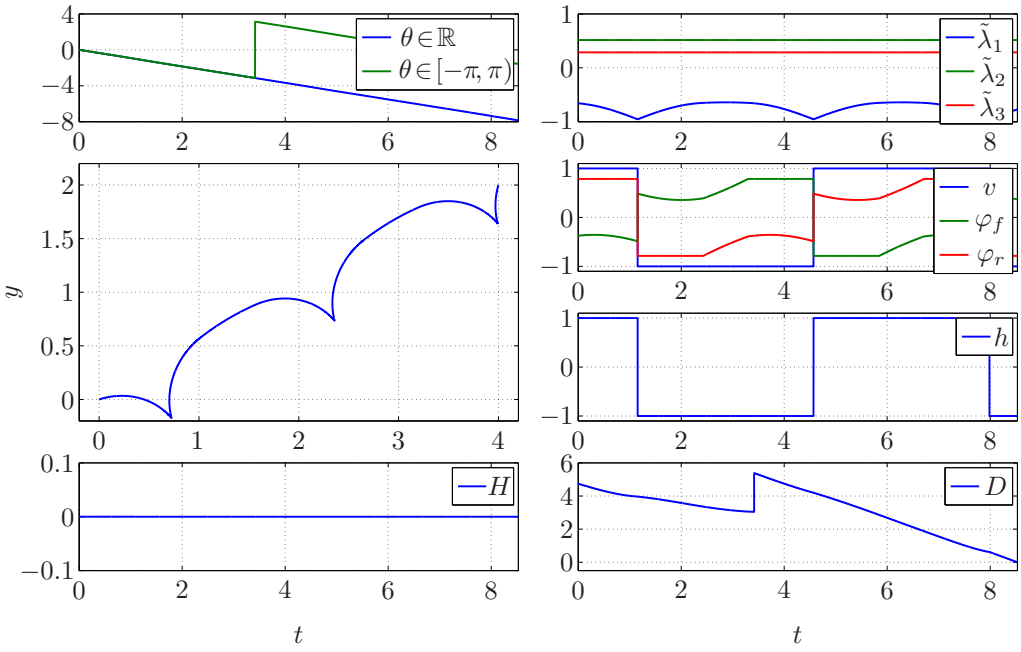


Figure 8.4: Solution S1 for $q_d = \left(-\frac{\pi}{2}, 4, 2\right)$.

As the sequence of solutions in the table consists of three solutions, all three solution minima are found during the run of the time-optimal control.

For the desired configuration $q_d = (0, 2, -4)$, the final time $\hat{T}$ is 8.614 as well. In Table 8.4, a sequence of solutions generated by the time-optimal control is listed. Three solutions S1, S2, and S3 are found. Solution S3 is a near time-optimal solution because of $n_c = 0$ and a time-optimal normal regular extremal. Figure 8.9 shows $(x, y)$ plots of the solutions of Table 8.4. Solution S1 is of type M, and the solutions S2 and S3 are of type P. The end time $\tau$ decreases over the solutions, and the number of cusps $n_c$ stays constant or decrease. In Figure 8.10, the minimal deviation $d\big(\tilde{\lambda}_0(\alpha)\big)$ for $\hat{T} = 8.614$ is shown over the search space $\Lambda_{q_0}$ for $\alpha \in \bar{A}$. The search space $\Lambda_{q_0}$ comprises one domain $\Psi$ where $d = \hat{d} = 4.472$ holds, and the regions of attraction $\Omega$ of multiple minima including several solution minima. Three of them lead to the solutions in Table 8.4.

| $n_S$ | $T$ | $n_{SP}$ | $n_{Sim}^{PP}$ | $\alpha^{SP}$ | $\tilde{\lambda}_0^{SP}$ | $\alpha^{PP}$ | $\tilde{\lambda}_0^{PP}$ | $\tau$ | $n_c$ |
|---|---|---|---|---|---|---|---|---|---|
| S1 | 8.614 | 1 | 74 | $\begin{pmatrix} 0.1704 \\ -0.5487 \end{pmatrix}$ | $\begin{pmatrix} 0.8238 \\ 0.1418 \\ -0.5487 \end{pmatrix}$ | $\begin{pmatrix} 0.4396 \\ -0.6482 \end{pmatrix}$ | $\begin{pmatrix} 0.6890 \\ 0.3240 \\ -0.6482 \end{pmatrix}$ | 7.324 | 2 |
| S2 | 7.323 | 5 | 332 | $\begin{pmatrix} 0.9431 \\ 0.3909 \end{pmatrix}$ | $\begin{pmatrix} 0.5404 \\ 0.7450 \\ 0.3909 \end{pmatrix}$ | $\begin{pmatrix} 2.4439 \\ -0.8988 \end{pmatrix}$ | $\begin{pmatrix} -0.3358 \\ 0.2815 \\ -0.8988 \end{pmatrix}$ | 6.776 | 2 |
| S3 | 6.775 | 9 | 433 | $\begin{pmatrix} 2.9907 \\ -0.2658 \end{pmatrix}$ | $\begin{pmatrix} -0.9530 \\ 0.1449 \\ -0.2658 \end{pmatrix}$ | $\begin{pmatrix} 2.9761 \\ -0.7961 \end{pmatrix}$ | $\begin{pmatrix} -0.5968 \\ 0.0997 \\ -0.7961 \end{pmatrix}$ | 5.198 | 0 |

Table 8.4: Solutions generated by the time-optimal control for $q_d = (0, 2, -4)$.

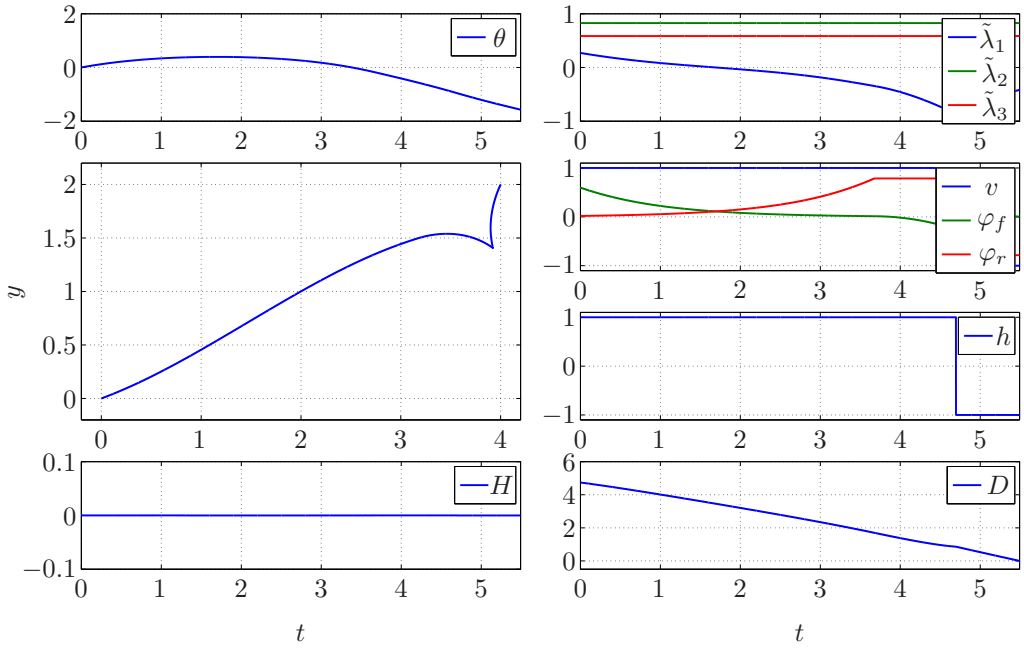


Figure 8.5: Solution S3 for $q_d = \left(-\frac{\pi}{2}, 4, 2\right)$.

## 8.5 Optimal solutions of the bi-steerable and the car-like robot

As addressed in Chapter 5, one advantage of the BSR is that is can go from one configuration to another with maybe shorter path length than other wheeled mobile robots. To demonstrate this, the simulation results on time-optimal normal regular extremals of Table 8.3 and 8.4 are compared to Reeds-Shepp paths, i. e., shortest paths of the simplified model (3.16) of the car-like robot. The solutions are compared with respect to the path length $l = \int_0^\tau |v_t(\xi)| \, \mathrm{d}\xi$ instead of the end time $\tau$. The absolute translational velocity $|v_t| = \sqrt{\dot{x}^2 + \dot{y}^2}$ of the RKM given by (5.18) is not constant but depends on $(\varphi_f, \varphi_r)$. Thus, time-optimal solutions of the RKM are in general no shortest paths, see [108, 120, 124]. However, for the desired configurations $q_d = \left(-\frac{\pi}{2}, 4, 2\right)$ and $q_d = (0, 2, -4)$, time-optimal normal regular extremals of the RKM have shorter path length than the Reeds-Shepp paths.

As discussed in Section 1.1, shortest paths of the car-like robot driving forward and backward at constant absolute velocity consist of arcs of circles $C$ and straight line segments $S$. They have at most two cusps denoted by $|$ and are of type $C|CSC|C$ or $CC|CC$, where not all pieces and cusps must exist. The Reeds-Shepp paths are obtained for the simplified model (3.16) of the car-like robot with input space $U_{RS} = [-1, 1] \times \{-1, 1\}$. For details, see [94, 108, 120]. For the car-like robot, shortest paths are also time-optimal, as the absolute translational velocity $|v_t| = \sqrt{\dot{x}^2 + \dot{y}^2}$ satisfies $|v_t| = |v_2|$ and is constant for constant $|v_2|$.

In Figure 8.11 and 8.12, time-optimal normal regular extremals of the BSR and shortest paths of the car-like robot from $q_0 = (0, 0, 0)$ to $q_d = \left(-\frac{\pi}{2}, 4, 2\right)$ and $q_d = (0, 2, -4)$ are shown. The initial configuration is represented by a green pentagon and the final configuration by a blue one. The path of the center of mass as well as snapshots at equal time intervals are plotted for the BSR in black and for the car-like robot in red. In Table 8.5, the time-optimal normal regular extremals of the BSR and shortest paths of the car-like robot are compared. For the extremals of the BSR, references to the solutions in Table 8.3 and 8.4 are given, and the path length $l_{BSR}$ is stated. For the shortest paths of the car-like robot, the path type and path length $l_{RS}$ is listed. Besides, the ratio $l_{BSR}/l_{RS}$ is given.

In Table 8.5, for both desired configurations, $l_{BSR}/l_{RS} < 1$ holds, i. e., time-optimal normal

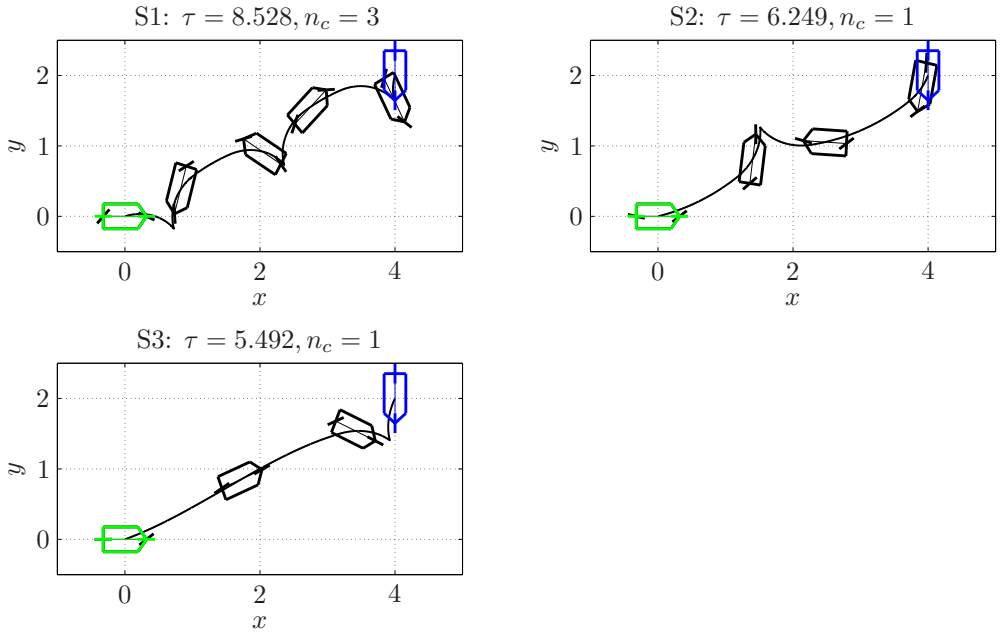


Figure 8.6: Solutions for $q_d = \left(-\frac{\pi}{2}, 4, 2\right)$.

| desired configuration $q_d$ | BSR | | car-like robot | | $\frac{l_{BSR}}{l_{RS}}$ |
|---|---|---|---|---|---|
| | solution | $l_{BSR}$ | path type | $l_{RS}$ | |
| $\left(-\frac{\pi}{2}, 4, 2\right)$ | S3 of Table 8.3 | 4.908 | $CSC\|C$ | 5.679 | 0.864 |
| $(0, 2, -4)$ | S3 of Table 8.4 | 4.607 | $CSC$ | 5.140 | 0.896 |

Table 8.5: Comparison of time-optimal normal regular extremals of the bi-steerable robot and shortest paths of the car-like robot.

regular extremals of the BSR have shorter path length than Reeds-Shepp paths. One reason for this is that the BSR can go through curves of smaller turning radius than the car-like robot, provided that both robots have the same maximal steering angles. In addition, the BSR can perform diagonal motions which are beneficial as well. Further simulations show that $l_{BSR}/l_{RS} \leq 1$ holds for all desired configurations. Hence, compared to Reeds-Shepp paths, time-optimal solutions of the RKM are of equal or shorter path length. For $q_d = \left(-\frac{\pi}{2}, 4, 2\right)$ and $q_d = (0, 2, -4)$, the optimal solutions of the BSR and the car-like robot have the same number of cusps $n_c$.

## 8.6 Discussion of the time-optimal control

The simulations of Section 8.4.3 demonstrate the successful operation of the time-optimal control 7.3.2 applied to the near time-optimal control problem 8.1.4. Over the sequences of solutions, the end time $\tau$ decreases. For the given results, the end times $\tau$ of the solutions of a sequence differ by at least several intervals $\triangle t = 0.001$. There are no normal regular extremals which lie close together and have almost the same end time $\tau$. This is confirmed by additional simulations of the time-optimal control for other desired configurations. Extremals which lie close together and have almost the same end time are ruled out by the Maximum Principle which ensures Pontryagin optimality, see Section 4.2.3.

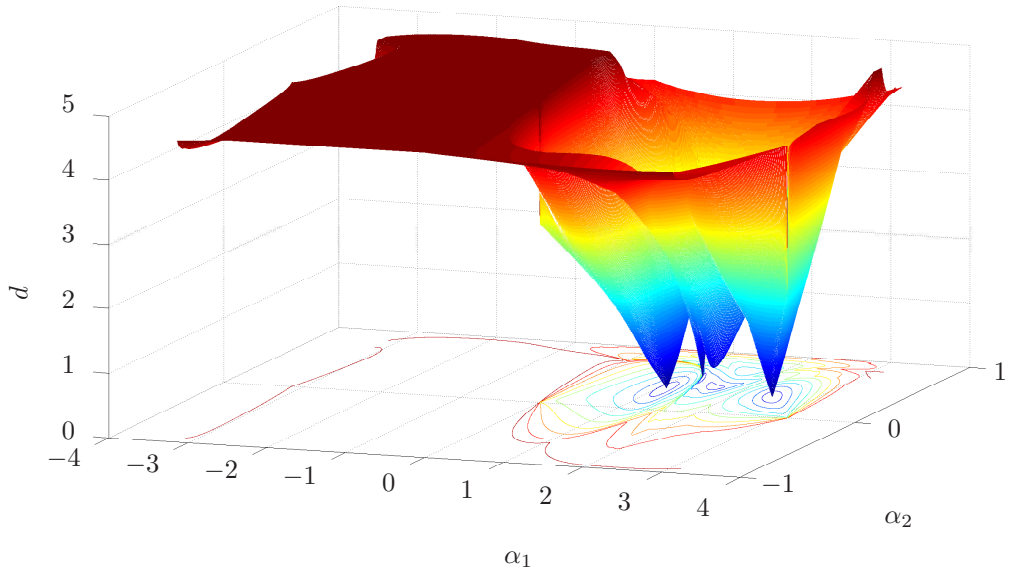


Figure 8.7: Deviation $d\big(\tilde{\lambda}_0(\alpha)\big)$ over $\alpha \in \bar{A}$ for $q_d = \big(-\frac{\pi}{2}, 4, 2\big)$.

For an increasing number $n_{Sim}^{PP}$ of simulated extremals, i. e., for more computational effort, solutions with shorter end time $\tau$ are obtained. Thus, a time-optimal solution is approximated better and better. Finally, if the time-optimal control is not terminated by a condition for near time-optimality or exit condition EC3, a time-optimal normal regular extremal is found. The relation between the number of cusps and the optimality of a solution is discussed in the next chapter. Over the sequence of solutions of the time-optimal control, the type of the extremals can change.

The plots of the two-dimensional surfaces of the minimal deviation $d$ over the search space $\Lambda_{q_0}$ in Figure 8.7 and 8.10 and over the subset of $\Lambda_{q_0}$ in Figure 8.8 show that the minimization of $d$ over $\tilde{\lambda}_0 \in \Lambda_{q_0}$ is a global optimization problem. This is true as the search space $\Lambda_{q_0}$ consists of the domain $\Psi$ where $d = \hat{d} = \|q_0 - q_d\|$ holds as well as regions of attraction $\Omega$ of several minima which may be solution minima such that $\|q(\tau) - q_d\| \leq \varepsilon_q$ holds. A random starting point $\tilde{\lambda}_0^{SP}$ in the region of attraction of a solution minimum gives rise to a solution, provided that the optimization converges before it is terminated by exit condition EC1. In contrast, a starting point $\tilde{\lambda}_0^{SP}$ in the domain $\Psi$ or in the region of attraction of a minimum for which $\|q(\tau) - q_d\| \leq \varepsilon_q$ cannot be achieved does not result in a solution. As could be seen from the Figures 8.7, 8.8, and 8.10, the deviation $d$ is differentiable in the interior of the domain $\Psi$ and the regions $\Omega$ of attraction. At the boundaries between the regions of attraction, the minimal deviation $d$ is only continuous, which agrees with property O2 of Lemma 7.2.5.

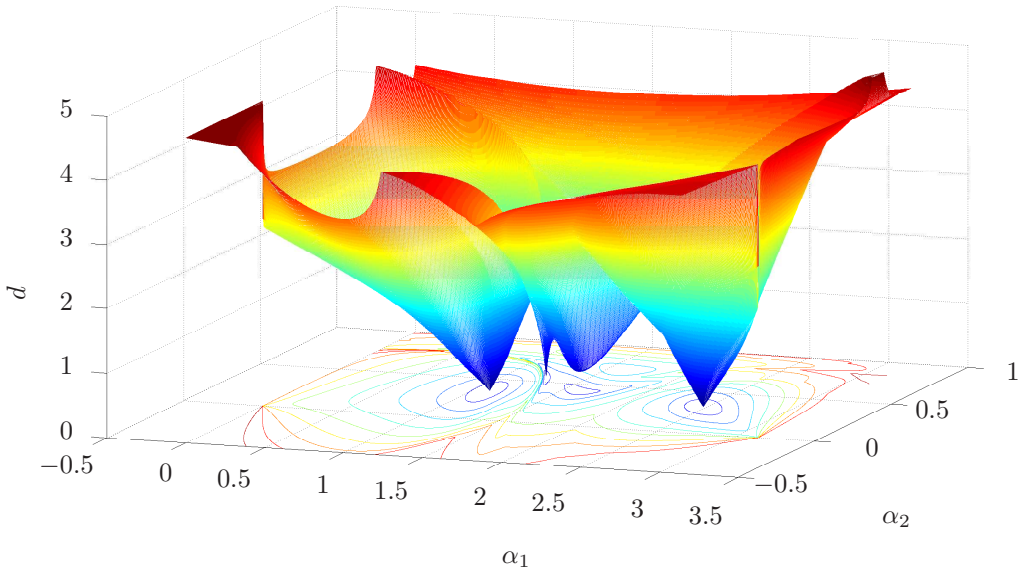


Figure 8.8: Deviation $d\big(\tilde{\lambda}_0(\alpha)\big)$ over $\big\{\alpha \in \mathbb{R}^2 \,|\, 0 \leq \alpha_1 \leq \pi, -0.5 \leq \alpha_2 \leq 1\big\}$ for $q_d = \big(-\frac{\pi}{2}, 4, 2\big)$.

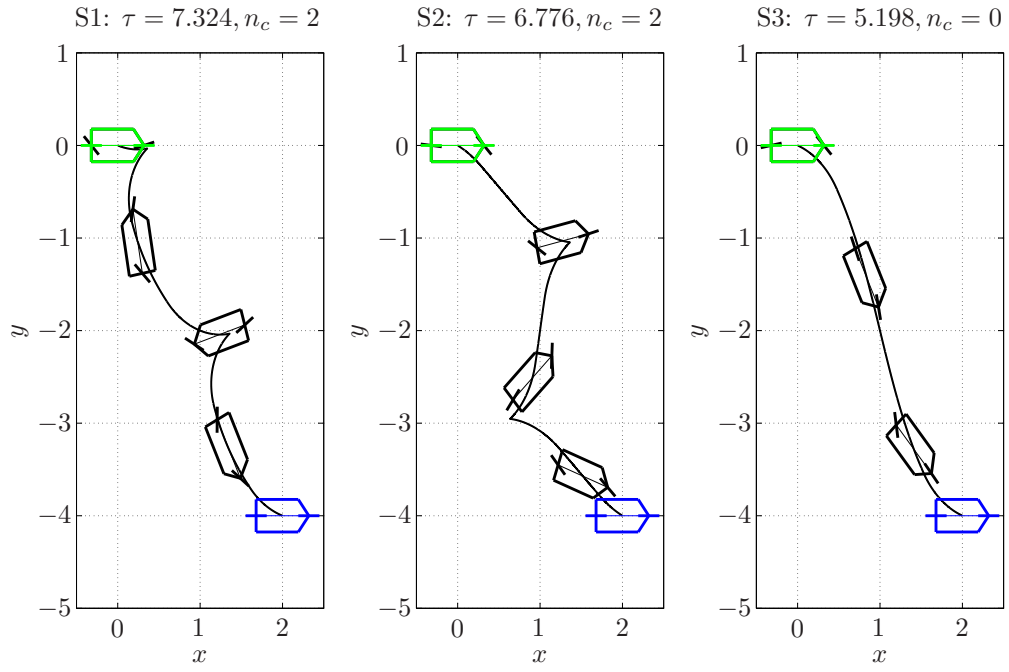


Figure 8.9: Solutions for $q_d = (0, 2, -4)$.

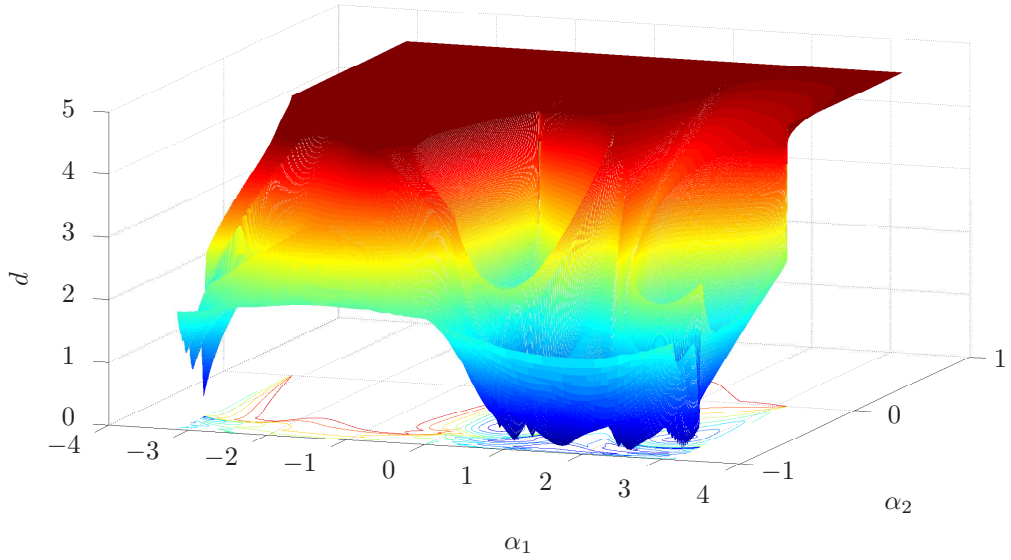


Figure 8.10: Deviation $d\big(\tilde{\lambda}_0(\alpha)\big)$ over $\alpha \in \bar{A}$ for $q_d = (0, 2, -4)$.

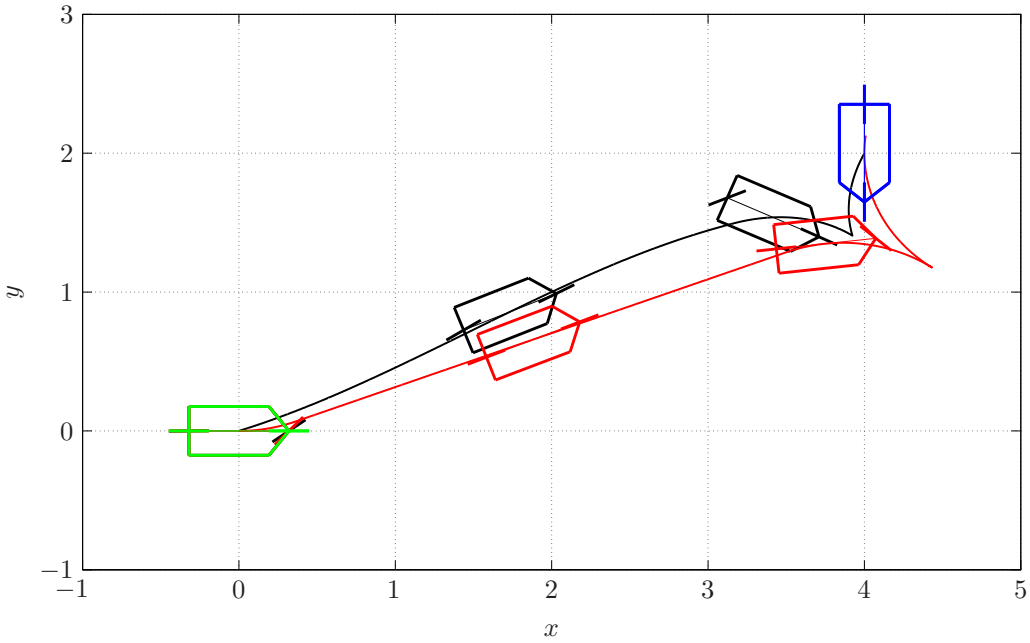


Figure 8.11: Time-optimal normal regular extremal of the BSR (black) and shortest path of the car-like robot (red) for $q_d = \big(-\frac{\pi}{2}, 4, 2\big)$.

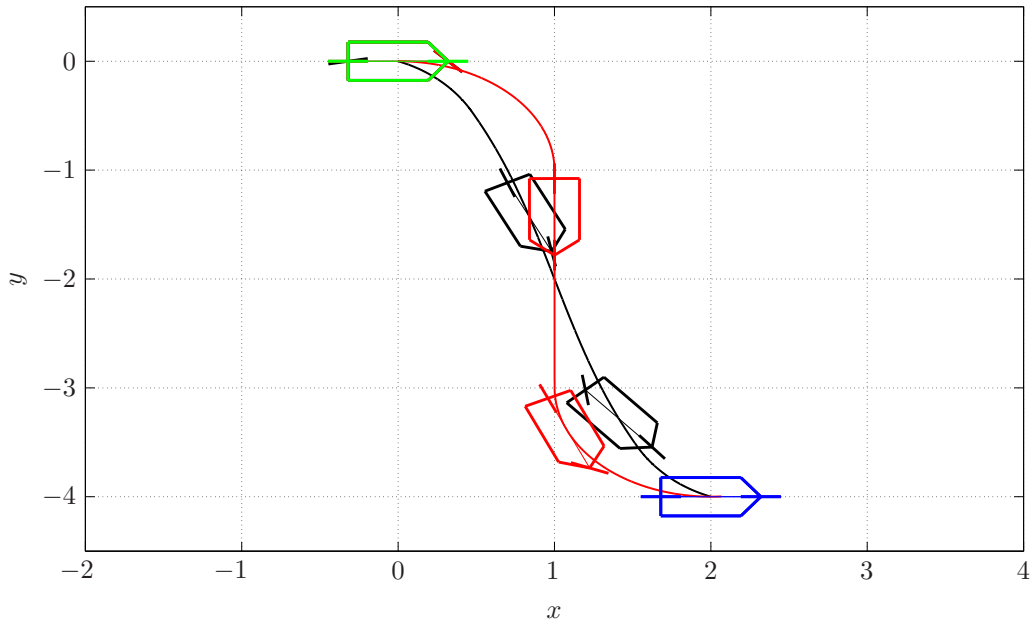


Figure 8.12: Time-optimal normal regular extremal of the BSR (black) and shortest path of the car-like robot (red) for $q_d = (0, 2, -4)$.

# 9 Optimality of normal regular extremals of the bi-steerable robot

In this chapter, the optimality of normal regular extremals for time-optimal control of the RKM is analyzed. In particular, optimality conditions are addressed which allow to terminate the time-optimal control 7.3.2 when a near time-optimal solution is found. Moreover, time-optimal normal regular and normal singular extremals of the RKM are compared.

**Definition 9.0.1** *(Condition for near time-optimality for the RKM) The near time-optimal control problem 8.1.4 is considered for a desired configuration $q_d = (\theta_d, x_d, y_d)$. Let $\tau^{to}$ be the end time of a time-optimal solution, $k \geq 1$ a constant, and $\left(\tilde{\lambda}_0^{PP}, \tau\right)$ a solution to the path planning problem 8.1.3 underlying problem 8.1.4. A condition which is true if $\tau \leq k\,\tau^{to}$ holds is called condition for near time-optimality for the RKM.*

In Definition 9.0.1, the optimality of a solution to the path planning problem is addressed for a specific desired configuration $q_d$. In principle, instead of $q_d$, the resultant final configuration $q(\tau)$ has to be considered. However, the path planning is performed until $\|q(\tau) - q_d\| \leq \varepsilon_q$ holds for small $\varepsilon_q$. For the discretization interval $\triangle t = 0.001$, the difference in the end time of extremals which lie close together and have different final configurations $q(\tau)$ satisfying $\|q(\tau) - q_d\| \leq \varepsilon_q$ is at most one discretization interval $\triangle t$. In contrast, as discussed in Section 8.6, the end time $\tau$ of consecutive solutions generated by the time-optimal control differs by at least several intervals $\triangle t$. Thus, to simplify the analysis, the optimality of solutions is studied with respect to the desired configuration $q_d$ instead of the final configuration $q(\tau)$. Since only normalized initial conditions 6.3.2 are considered in this chapter, they are denoted by $\lambda_0$ instead of $\tilde{\lambda}_0$ to simplify the notation.

If a condition for near time-optimality holds for a solution, the time-optimal control 7.3.2 can be terminated, as it is done in Algorithm 7.2. Without this condition, the algorithm would execute the path planning until exit condition EC3 is true, i. e., the number of simulated extremals exceeds $\hat{n}_{Sim}^{to}$. In order to integrate a condition for near time-optimality into the time-optimal control, the condition should be easy to apply and computationally cheap.

Conditions for near time-optimality depend on the specific control problem. To obtain a condition for the normal regular extremals of the RKM, necessary and sufficient optimality conditions are studied in Section 9.1 and 9.3. As no condition for near time-optimality results from these conditions, a necessary optimality condition is derived in Section 9.5 which is based on simulation results on time-optimal normal regular extremals given in Section 9.4. In the following, both time-optimal and near time-optimal normal regular extremals of the RKM are considered. Time-optimal normal regular extremals give time-optimal solutions if only normal regular extremals exist for a control problem. Near time-optimal normal regular extremals are near time-optimal solutions 2.2.5 among the normal regular extremals. For control problems with normal regular and normal singular extremals, time-optimal normal regular extremals are in general no time-optimal solutions, as such solutions may be normal singular extremals.

## 9.1 Application of necessary optimality conditions

In this section, the necessary optimality conditions from Section 4.5 are analyzed for the time-optimal control problem 6.0.2 to find a condition for near time-optimality for the RKM.

The Legendre-Clebsch condition $H_{uu} \leq 0$ given by (4.8) and the strengthened Legendre-Clebsch condition $u^\top H_{uu} u \leq -\alpha \|u\|^2$ as in (4.9) for $\alpha > 0$ are necessary optimality conditions

for systems with non-compact input space $U$. Thus, they cannot be applied to the RKM with compact input space $U = [-\hat{v}, \hat{v}] \times \left[-\frac{\pi}{4}, \frac{\pi}{4}\right] \times \left[-\frac{\pi}{4}, \frac{\pi}{4}\right]$. As a workaround, the Lagrangian $L(x,u) = 1$ for time-optimal control can be replaced by $L(x,u) = 1 + \sum_{i=1}^{m} \alpha_i \, u_i^2$ for $\alpha_i > 0$, see [8]. For sufficiently large $\alpha_i$, there holds $u(t) \in \operatorname{int} U$ for all $t \in I$. Then, the conditions (4.8) and (4.9) can be applied. However, if the Lagrangian

$$L(x,u) = 1 + \alpha_1 \, v^2 + \alpha_2 \, \varphi_f^2 + \alpha_3 \, \varphi_r^2$$

is used and sufficiently large $\alpha_i$ are chosen such that $u(t) \in \operatorname{int} U$ holds for all $t \in I$, extremal velocities $v$ with $|v| < \hat{v}$ result which give solutions that are far from time-optimal.

In contrast to condition (4.8) and (4.9), the modified Legendre-Clebsch condition

$$H_{ww} \leq 0 \tag{9.1}$$

given by (4.10) and the strengthened modified Legendre-Clebsch condition

$$w^\top H_{ww} w \leq -\alpha \, \|w\|^2 \tag{9.2}$$

according to (4.11) for $\alpha > 0$ are applicable to the RKM. For these conditions, the modified input vector $w$ is considered which consists of the input variables $u_i$ which do not lie on $\operatorname{bd} U$, see Definition 3.1.3. For the extremal input $u = (v, \varphi_f, \varphi_r)$ of the RKM, $v = \pm\hat{v}$, $|\varphi_f| \leq \hat{\varphi}$, and $|\varphi_r| \leq \hat{\varphi}$ holds. The modified input vector is $w = \varphi = (\varphi_f, \varphi_r)$ for $|\varphi_f| < \hat{\varphi}$ and $|\varphi_r| < \hat{\varphi}$, $w = \varphi_f$ for $|\varphi_f| < \hat{\varphi}$ and $|\varphi_r| = \hat{\varphi}$, $w = \varphi_r$ for $|\varphi_f| = \hat{\varphi}$ and $|\varphi_r| < \hat{\varphi}$, and $w = \emptyset$ for $|\varphi_f| = |\varphi_r| = \hat{\varphi}$. Using the Hamiltonian function $H$ (6.2) and the function $h$ (6.3),

$$H_{\varphi_f \varphi_f} = H_{\varphi_r \varphi_r} = -v \, h$$

results for $w = \varphi_f$ and $w = \varphi_r$. For $w = \varphi$ and

$$\begin{aligned} h_{\varphi_f \varphi_r} = h_{\varphi_r \varphi_f} = {} & \lambda_1 \sin(\varphi_f - \varphi_r) + (\cos(\theta) \, \lambda_2 + \sin(\theta) \, \lambda_3) \sin(\varphi_f) \sin(\varphi_r) \\ & - \tfrac{1}{2} \, (-\sin(\theta) \, \lambda_2 + \cos(\theta) \, \lambda_3) \sin(\varphi_f + \varphi_r) \, , \end{aligned}$$

the matrix

$$H_{\varphi\varphi} = \begin{bmatrix} -v \, h & v \, h_{\varphi_f \varphi_r} \\ v \, h_{\varphi_r \varphi_f} & -v \, h \end{bmatrix}$$

is obtained. Simulations show that the conditions (9.1) and (9.2) are satisfied for all normal regular extremals of the RKM. For solution S1 and S3 of Table 8.3, time plots of the input $u$, the modified input vector $w$, $w^\top H_{ww} w$, and $-\alpha \, \|w\|^2$ are given in Figure 9.1 and 9.2 for $\alpha = 0.5$. In both figures, condition (9.2) holds. Thus, condition (9.1) holds as well. Hence, for the solutions S1 and S3, the two conditions give no condition for near time-optimality 9.0.1, as they are true for both solutions, although they have strongly different end times $\tau = 8.528$ and $\tau = 5.492$. Further simulations show that the conditions (9.1) and (9.2) hold for all normal regular extremals, independent of the number of cusps $n_c$ and the end time $\tau$.

Switchings of the velocity input $v$ of the RKM give rise to cusps as discussed in Section 6.4.3. In Section 4.5.2, bounds on the number of switchings $n_s$ are addressed for linear time-invariant systems $\dot{x} = A \, x + B \, u$, single-input affine systems $\dot{x} = f(x) + g(x) \, u$, and other specific control systems considered e. g. in [28, 32, 37, 48, 68, 94]. However, the RKM $\dot{q} = g(\theta, \varphi) \, v$ belongs to none of the classes of control systems for which bounds on the number of switchings $n_s$ are available. Thus, no bound on the number of cusps $n_c$ for normal regular extremals of the RKM can be given, and no condition for near time-optimality is obtained.

In Section 4.5.3, necessary optimality conditions derived from a generalization of the theory of envelopes are addressed. For details, see [110, 115, 120]. In these references, end-point maps 2.1.5 are used to analyze the optimality of bang-bang extremals. As discussed in Section 6.6, for normal regular extremals of the RKM of type M and P, no end-point maps are available,

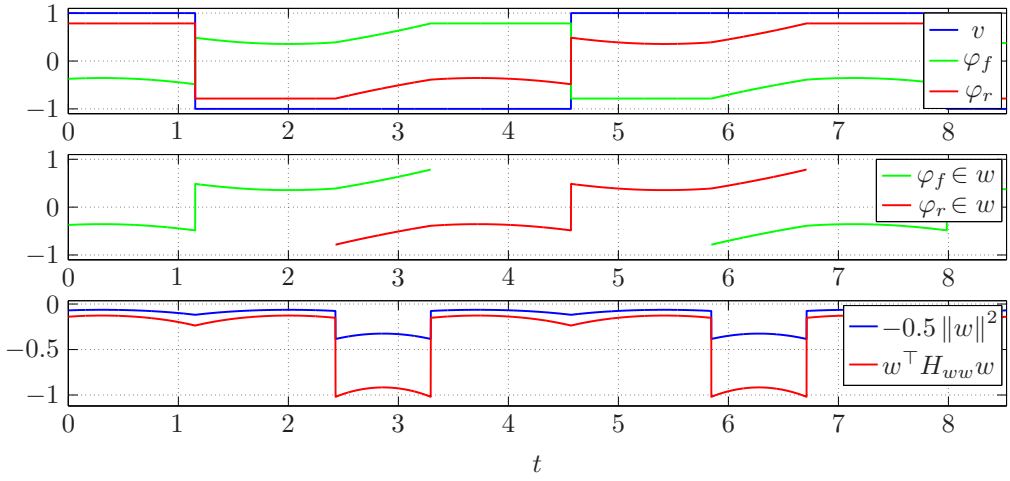


Figure 9.1: Input $u$, modified input $w$, $w^\top H_{ww} w$, and $-0.5\,\|w\|^2$ for solution S1 of Table 8.3.

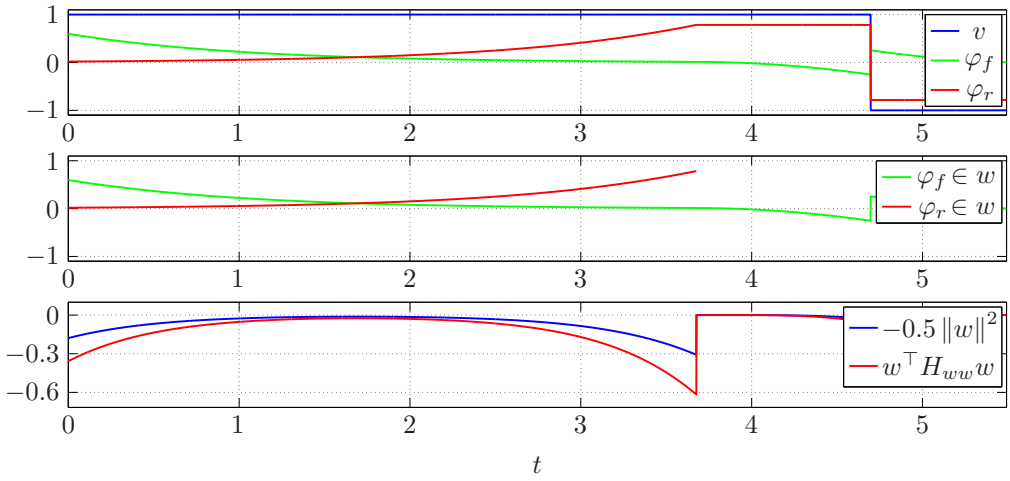


Figure 9.2: Input $u$, modified input $w$, $w^\top H_{ww} w$, and $-0.5\,\|w\|^2$ for solution S3 of Table 8.3.

as the extremal turning rate $\dot{\theta}$ of the RKM is not piecewise constant but varies continuously depending on the extremal inputs $v$ and $\varphi$. Thus, the generalization of the theory of envelopes from [110, 115, 120] cannot be applied to obtain a necessary optimality condition for the RKM which gives a condition for near time-optimality 9.0.1.

All in all, no condition for near time-optimality for the RKM results from the necessary optimality conditions described in Section 4.5.

## 9.2 Transformed time-optimal control problem

Before the sufficient optimality conditions from Section 4.6 are studied in the next section, the transformed time-optimal control problem 2.2.4 with fixed end time is considered for the RKM, as some of the sufficient conditions are usually applied to this problem. The transformed problem 2.2.4 results from the time-optimal control problem 2.2.3 with free end time by the time transformation $s = \frac{1}{\tau} t$ for constant $\tau > 0$. Here, $\tau$ corresponds to the unknown end time of problem 2.2.3. For problem 2.2.4, solutions $\left(\check{X}^{to}(\cdot), \check{u}^{to}(\cdot)\right)$ of the extended control system

$\check{X}' = \check{f}\big(\check{X}, \check{u}\big)$ as in (2.4) are studied over the fixed interval $\check{I} = [0,1]$. For the extended state $\check{X} = (\check{x}, z)$ of dimension $\check{n} = n+1$ and the input $\check{u}$, there holds $\check{x}(s) := x\big(\tau\, s\big) = x(t)$ and $\check{u}(s) := u\big(\tau\, s\big) = u(t)$. The extended adjoint state $\check{\Lambda} = \big(\check{\lambda}, \check{\lambda}_{\check{n}}\big) \in \mathbb{R}^{\check{n}}$ is used to formulate the necessary optimality conditions of the Maximum Principle for problem 2.2.4. Here, $\check{\Lambda} = \big(\check{\lambda}, \check{\lambda}_{\check{n}}\big)$ consists of $\check{\lambda}$ with $\check{\lambda}(s) := \lambda\big(\tau\, s\big) = \lambda(t)$ and the adjoint state variable $\check{\lambda}_{\check{n}}$ related to $z$.

In the following, the Maximum Principle is applied to the transformed time-optimal control problem 2.2.4 for the RKM. Like in Chapter 6, extremals are denoted by the superscript $^*$, which is omitted in the remaining chapter. No proofs are given in this section, as they can be easily derived from the proofs in Chapter 6.

**Definition 9.2.1** *(Extended reduced kinematic model of the BSR) Let $\check{M} = SE(2) \times \mathbb{R}_{>0}$ be the state space, $\check{X} = (\check{q}, z) \in \check{M}$ the state with $\check{q} = (\check{\theta}, \check{x}, \check{y})$, and $g_{11} = g_{11}\big(\check{\theta}, \check{\varphi}\big)$, $g_{12} = g_{12}\big(\check{\theta}, \check{\varphi}\big)$, and $g_{13} = g_{13}\big(\check{\theta}, \check{\varphi}\big)$ the real-valued functions (5.3). The driftless control system*

$$\check{X}' = \begin{bmatrix} \check{\theta}' \\ \check{x}' \\ \check{y}' \\ z' \end{bmatrix} = \begin{bmatrix} z\, g_1\big(\check{\theta}, \check{\varphi}\big) \\ z\, g_2\big(\check{\theta}, \check{\varphi}\big) \\ z\, g_3\big(\check{\theta}, \check{\varphi}\big) \\ 0 \end{bmatrix} \check{v} = \check{g}\big(\tau, \check{\theta}, \check{\varphi}\big)\, \check{v} \tag{9.3}$$

*with input space $U = [-\hat{v}, \hat{v}] \times [-\hat{\varphi}, \hat{\varphi}] \times [-\hat{\varphi}, \hat{\varphi}]$, $\hat{v} > 0$, $\hat{\varphi} < \frac{\pi}{2}$, and input $\check{u} = (\check{v}, \check{\varphi}_f, \check{\varphi}_r) \in U$ is called extended RKM of the BSR.*

System (9.3) is the extended system (2.4) of the RKM 5.0.2. The space of the admissible steering angles $\check{\varphi} = (\check{\varphi}_f, \check{\varphi}_r)$ is $\Phi = \left[-\frac{\pi}{4}, \frac{\pi}{4}\right] \times \left[-\frac{\pi}{4}, \frac{\pi}{4}\right]$ as in (6.1).

**Definition 9.2.2** *(Transformed time-optimal control problem for the RKM) The transformed time-optimal control problem 2.2.4 for the extended RKM with initial state $\check{X}_0 = (q_0, \tau)$, desired state $\check{X}_d = (q_d, \tau)$, and input space $U = [-\hat{v}, \hat{v}] \times \Phi$, $\hat{v} > 0$, is called transformed time-optimal control problem for the RKM.*

Problem 9.2.2 is the transformed time-optimal control problem which arises from the time-optimal control problem for the RKM as in Definition 6.0.2.

**Theorem 9.2.3** *(Necessary optimality conditions for the transformed time-optimal control problem for the RKM) The transformed time-optimal control problem 9.2.2 is considered. Let $\check{\Lambda} = \big(\check{\lambda}_1, \check{\lambda}_2, \check{\lambda}_3, \check{\lambda}_4\big)$ be the extended adjoint state and $\mu \in \{0,1\}$ a constant. Then, the Hamiltonian function*

$$\check{H}\big(\check{X}, \mu, \check{\Lambda}, \check{u}\big) = -\mu\, z + z\, \check{h}\big(\check{X}, \check{\Lambda}, \check{\varphi}\big)\, \check{v} \tag{9.4}$$

*results with*

$$\begin{aligned} \check{h}\big(\check{X}, \check{\Lambda}, \check{\varphi}\big) \;=\; & \check{\lambda}_1 \sin(\check{\varphi}_f - \check{\varphi}_r) + \big(\cos\big(\check{\theta}\big)\, \check{\lambda}_2 + \sin\big(\check{\theta}\big)\, \check{\lambda}_3\big) \cos(\check{\varphi}_f) \cos(\check{\varphi}_r) \\ & + \tfrac{1}{2}\, \big(-\sin\big(\check{\theta}\big)\, \check{\lambda}_2 + \cos\big(\check{\theta}\big)\, \check{\lambda}_3\big) \sin(\check{\varphi}_f + \check{\varphi}_r)\,. \end{aligned}$$

*Let $\big(\check{X}^*(\cdot)\,, \check{\Lambda}^*(\cdot)\,, \check{u}^*(\cdot)\big)$ be an extremal and $\check{H}^*(\cdot) := \check{H}\big(\check{X}^*(\cdot)\,, \mu, \check{\Lambda}^*(\cdot)\,, \check{u}^*(\cdot)\big)$ the extremal Hamiltonian function over the time interval $\check{I} = [0,1]$. Then, the following conditions hold:*

**N1′:** *For all $s \in \check{I}$, $\big(\mu, \check{\Lambda}^*(s)\big) \neq 0$ is true.*

**N2′:** *For almost all $s \in \check{I}$, there holds the adjoint equation*

$$\begin{aligned}
\check{\lambda}_1'^* &= z^* \left( \tfrac{1}{2} \cos\left(\check{\theta}^*\right) \sin\left(\check{\varphi}_f^* + \check{\varphi}_r^*\right) + \sin\left(\check{\theta}^*\right) \cos\left(\check{\varphi}_f^*\right) \cos\left(\check{\varphi}_r^*\right) \right) \check{\lambda}_2^* \, \check{v}^* \\
&\quad + z^* \left( \tfrac{1}{2} \sin\left(\check{\theta}^*\right) \sin\left(\check{\varphi}_f^* + \check{\varphi}_r^*\right) - \cos\left(\check{\theta}^*\right) \cos\left(\check{\varphi}_f^*\right) \cos\left(\check{\varphi}_r^*\right) \right) \check{\lambda}_3^* \, \check{v}^*, \\
\check{\lambda}_2'^* &= 0, \\
\check{\lambda}_3'^* &= 0, \\
\check{\lambda}_4'^* &= -\frac{1}{z^*} \, \check{H}^*.
\end{aligned}$$

**N3′:** *For almost all $s \in \check{I}$, $\check{u}^* = (\check{v}^*, \check{\varphi}^*)$ satisfies $\left|\check{h}\left(\check{X}^*, \check{\Lambda}^*, \check{\varphi}^*\right)\right| = \max_{\check{\varphi} \in \Phi} \left|\check{h}\left(\check{X}^*, \check{\Lambda}^*, \check{\varphi}\right)\right|$ and $\check{v}^* = \operatorname{sgn}\left(\check{h}^*\right) \hat{v}$.*

**N4′:** *For almost all $s \in \check{I}$, $\check{H}^*(s) = 0$ holds.*

**N5′:** *There holds $\check{\lambda}_4(0) = \check{\lambda}_4(1) = 0$.*

Theorem 9.2.3 results from the Maximum Principle 4.2.3 applied to problem 9.2.2. The function $\check{h}$ corresponds to the function $h$ (6.3).

**Theorem 9.2.4** *(Normal extremal of the transformed time-optimal control problem) For the time-optimal control problem 6.0.2, let $(q^*(\cdot), \lambda^*(\cdot), u^*(\cdot))$ be a normal extremal over $I = [0, \tau]$ which satisfies the optimality conditions of Theorem 6.1.1 for $q^*(0) = q_0$ and $q^*(\tau) = q_d$.*

*Then, for the transformed problem 9.2.2, $\left(\check{X}^*(\cdot), \check{\Lambda}^*(\cdot), \check{u}^*(\cdot)\right)$ with $\check{X}^*(s) := \left(q^*\left(\tau\, s\right), \tau\right) = \left(q^*(t), \tau\right)$, $\check{\Lambda}^*(s) := \left(\lambda^*\left(\tau\, s\right), 0\right) = \left(\lambda^*(t), 0\right)$, and $\check{u}^*(s) := u^*\left(\tau\, s\right) = u^*(t)$ is a normal extremal over $\check{I} = [0, 1]$ which satisfies the optimality conditions of Theorem 9.2.3 for $\check{X}^*(0) = (q_0, \tau)$ and $\check{X}^*(1) = (q_d, \tau)$.*

To prove the theorem, it can be shown that if an extremal $(q^*(\cdot), \lambda^*(\cdot), u^*(\cdot))$ over $I = [0, \tau]$ satisfies the conditions of Theorem 6.1.1 and goes from $q_0$ to $q_d$, then $\left(\check{X}^*(\cdot), \check{\Lambda}^*(\cdot), \check{u}^*(\cdot)\right)$ over $\check{I} = [0, 1]$ meets the conditions of Theorem 9.2.3 and goes from $(q_0, \tau)$ to $(q_d, \tau)$. Due to $\check{\lambda}_4(0) = 0$ from condition N5′ and $\check{\lambda}_4'^* = -\frac{1}{z^*} H^* = 0$ from condition N2′ and N4′, $\check{\lambda}_4^*(s) = 0$ is true for all $s \in \check{I}$.

By Theorem 9.2.4, an extremal $(q^*(\cdot), \lambda^*(\cdot), u^*(\cdot))$ of problem 6.0.2 corresponds to an extremal $\left(\check{X}^*(\cdot), \check{\Lambda}^*(\cdot), \check{u}^*(\cdot)\right)$ of problem 9.2.2. Figure 9.3 shows the solution to the transformed control problem obtained from solution S1 of Table 8.3 for $q_d = \left(-\frac{\pi}{2}, 4, 2\right)$ with $\check{D} = \|\check{q} - q_d\|$. The Figures 8.4 and 9.3 give the same plots except for the different times $t$ and $s$. Sufficient optimality conditions for fixed end time problems are applied next to extremals of the transformed time-optimal control problem 9.2.2 to analyze extremals of the time-optimal control problem 6.0.2.

## 9.3 Application of sufficient optimality conditions

In this section, the sufficient optimality conditions from Section 4.6 are studied for the time-optimal control problem 6.0.2 and the transformed problem 9.2.2, respectively, to find a condition for near time-optimality for the RKM. The application of the local second-order sufficient conditions with Riccati equation from Section 4.6.2 is discussed in detail in Section 9.3.1.

The Arrow and Mangasarian conditions from Section 4.6.1 are sufficient optimality conditions for normal extremals of transformed time-optimal control problems with fixed end time. These conditions hold if for $\mu = 1$, the extremal Hamiltonian function $\check{H} = \check{H}\left(\check{X}, \mu, \check{\Lambda}, \check{u}\right)$ is concave in $\check{X}$ on the whole state space. To analyze the concavity of the extremal Hamiltonian function $\check{H}$ given by (9.4), the Hessian

$$\check{H}_{\check{X}\check{X}} = \frac{\partial^2 \check{H}}{\partial \check{X}^2}\left(\check{X}, \mu, \check{\Lambda}, \check{u}\right)$$

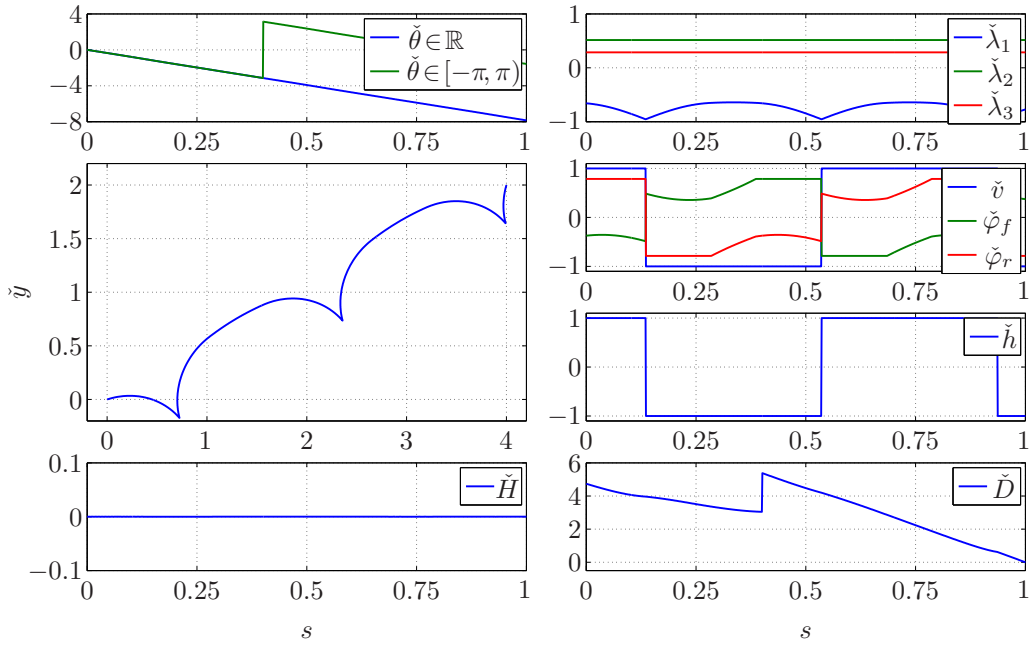


Figure 9.3: Solution to the transformed control problem obtained from solution S1 of Table 8.3 for $q_d = \left(-\frac{\pi}{2}, 4, 2\right)$.

is studied for normal regular extremals $\left(\check{X}(\cdot), \check{\Lambda}(\cdot), \check{u}(\cdot)\right)$ of the transformed time-optimal control problem 9.2.2. In simulations of different extremals including time-optimal ones, the eigenvalues $\{\sigma_1, \sigma_2, \sigma_3, \sigma_4, \}$ of $\check{H}_{\check{X}\check{X}}$ satisfy $\sigma_1 < 0$, $\sigma_2 > 0$, $\sigma_3 = \sigma_4 = 0$ for all $s \in \check{I}$. So, $\check{H}_{\check{X}\check{X}}$ is not negative semidefinite, and $\check{H}$ is not concave in $\check{X}$. Thus, the Arrow and Mangasarian conditions are not satisfied and give no condition for near time-optimality.

If the local second-order sufficient conditions from Section 4.6.3 are satisfied, they give strong local time-optimality for bang-bang extremals. The normal regular extremals of the time-optimal control problem 6.0.2 are no bang-bang extremals, as the RKM is no affine control system. Only the input $v$ enters the RKM affinely, whereas the input $\varphi$ enters by trigonometric functions. Hence, for normal regular extremals, $v(\cdot)$ is a bang-bang input, but $\varphi(\cdot)$ can vary continuously. Thus, the sufficient conditions from Section 4.6.3 do not apply to problem 6.0.2.

Boltyanskii's sufficient condition from Section 4.6.4 ensures optimality if a piecewise smooth feedback $u = u(t, x)$ can be found which generates solutions that satisfy the necessary optimality conditions of the Maximum Principle and additional regularity conditions. The additional regularity conditions are analyzed in [105, 106] based on a partition of the configuration space $Q$ into cells which are submanifolds of $Q$. For this, closed-form solutions of extremals are used to obtain the partition of $Q$. For the normal regular extremals of the time-optimal control problem 6.0.2, it is not possible to generate a partition of the configuration space $Q$ the way it is done in [105, 106], since no closed-form solutions can be derived for extremals of type M and P, see Section 6.6. Thus, no condition for near time-optimality is obtained from Boltyanskii's sufficient condition along the lines of [105, 106].

To sum up, no condition for near time-optimality for the RKM results from the sufficient optimality conditions given in Section 4.6.1, 4.6.3, and 4.6.4.

### 9.3.1 Local second-order sufficient conditions with Riccati equation

The local second-order sufficient conditions with Riccati equation from Section 4.6.2 can be used to check strong local optimality or weak local optimality of extremals of optimal control

problems with fixed end time. Hence, the transformed time-optimal control problem is considered. Provided that specific regularity conditions hold, an extremal is locally optimal if a bounded solution $Q(\cdot)$ to a Riccati equation exists which meets specific boundary conditions.

In the following, the local second-order sufficient conditions are studied for normal regular extremals of the transformed time-optimal control problem 9.2.2. The condition for strong local optimality with Riccati equation (4.12) cannot be used for problem 9.2.2, as it requires the strengthened Legendre-Clebsch condition $u^\top H_{uu} u \leq -\alpha \|u\|^2$ to hold for $\alpha > 0$. As discussed in Section 9.1, this condition is not applicable due to the compact input space $U$ of the RKM.

The local second-order sufficient condition for control systems (4.17) given by

$$\dot{x} = f_0(x, w) + \sum_{i=1}^{m_1} g_i(x, w)\, v_i \tag{9.5}$$

with affine input $v \in V$, non-affine input $w \in W$, compact input space $V \subset \mathbb{R}^{m_1}$, and $W = \mathbb{R}^{m_2}$ from [86] does not apply, too. Although the extended RKM is a control system (9.5) with $f_0(x, w) = 0$, $g_1(x, w) = \check{g}\big(\tau, \check{\theta}, \check{\varphi}\big)$, affine input $\check{v}$, and non-affine input $\check{\varphi}$, the input $\check{\varphi}$ takes values in $\left[-\frac{\pi}{4}, \frac{\pi}{4}\right] \times \left[-\frac{\pi}{4}, \frac{\pi}{4}\right]$, which is a compact subset of $\mathbb{R}^2$.

The second-order sufficient conditions from [65, 72, 75] give weak local optimality for systems with compact input space described by an input constraint $c(u) \leq 0$ as in Definition 3.1.3. These conditions can be applied to the normal regular extremals of the transformed time-optimal control problem 9.2.2. For this, the input space $U = [-\hat{v}, \hat{v}] \times [-\hat{\varphi}, \hat{\varphi}] \times [-\hat{\varphi}, \hat{\varphi}]$ is written as $U = \left\{\check{u} \in \mathbb{R}^3 \mid c(\check{u}) \leq 0\right\}$ for the input constraint

$$c(\check{u}) = \begin{pmatrix} -\check{v} & - & \hat{v} \\ \check{v} & - & \hat{v} \\ -\check{\varphi}_f & - & \hat{\varphi} \\ \check{\varphi}_f & - & \hat{\varphi} \\ -\check{\varphi}_r & - & \hat{\varphi} \\ \check{\varphi}_r & - & \hat{\varphi} \end{pmatrix} \leq 0. \tag{9.6}$$

The strengthened modified Legendre-Clebsch condition $\check{w}^\top \check{H}_{\check{w}\check{w}} \check{w} \leq -\alpha \|\check{w}\|^2$ as in (9.2) is satisfied for normal regular extremals of the transformed time-optimal control problem 9.2.2, as this condition holds for the normal regular extremals of the time-optimal control problem 6.0.2, see Section 9.1, and $\check{H}\big(\check{X}, \mu, \check{\Lambda}, \check{u}\big) = z\, H\big(\check{x}, \mu, \check{\lambda}, \check{u}\big)$ as in (4.5) is true for $z = \tau > 0$.

For weak local optimality, a bounded solution $Q(\cdot)$ to the Riccati equation (4.14) given by

$$Q' = -Q\, \check{f}_{\check{X}} - \check{f}_{\check{X}}^\top Q - \check{H}_{\check{X}\check{X}} + \big(\check{H}_{\check{X}\check{u}} + Q\, \check{f}_{\check{u}}\big)\, P \left(P^\top\, \check{H}_{\check{u}\check{u}}\, P\right)^{-1} P^\top \left(\check{H}_{\check{X}\check{u}} + Q\, \check{f}_{\check{u}}\right)^\top$$

has to exist which is continuous at the switching times of the right-hand side of the Riccati equation and meets the boundary conditions $q_{\check{n}\check{n}}(0) > 0$ and $q_{\check{n}\check{n}}(1) < 0$. To compute the right-hand side of the Riccati equation depending on the active input constraints 3.1.3, the $m \times (m - n_a(s))$ matrix $P$ is required. Here, $n_a(s) = |I(s)|$ is the number of active input constraints with $0 \leq n_a(s) \leq m$. The matrix $P$ has to meet $C_{\check{u}} P = 0$ for the matrix $C_{\check{u}}$ (4.15) which depends on the active input constraints.

For the normal regular extremals of the RKM, the first or second input constraint of (9.6) is active for all $s \in \check{I}$ because of $\check{v} = \pm\hat{v}$. Thus, $n_a(s) \geq 1$ holds. The input constraints on $\check{\varphi}_f$ and $\check{\varphi}_r$ may be true or not at each time $s \in \check{I}$. If $|\check{\varphi}_f(s)| < \hat{\varphi}$ and $|\check{\varphi}_r(s)| < \hat{\varphi}$ holds at some time $s$, then $n_a(s) = 1$ results, the $1 \times 3$ matrix $C_{\check{u}}$ is

$$C_{\check{u}} = \begin{bmatrix} \pm 1 & 0 & 0 \end{bmatrix},$$

and a $3 \times 2$ matrix satisfying $C_{\check{u}} P = 0$ is

$$P = \begin{bmatrix} 0 & 0 \\ 1 & 0 \\ 0 & 1 \end{bmatrix}. \tag{9.7}$$

If $|\check{\varphi}_f(s)| = \hat{\varphi}$ and $|\check{\varphi}_r(s)| < \hat{\varphi}$ holds at $s$, then $n_a(s) = 2$ is obtained, the $2 \times 3$ matrix $C_{\check{u}}$ is

$$C_{\check{u}} = \begin{bmatrix} \pm 1 & 0 & 0 \\ 0 & \pm 1 & 0 \end{bmatrix},$$

and a $3 \times 1$ matrix meeting $C_{\check{u}} P = 0$ is

$$P = \begin{bmatrix} 0 \\ 0 \\ 1 \end{bmatrix}. \tag{9.8}$$

If $|\check{\varphi}_f(s)| < \hat{\varphi}$ and $|\check{\varphi}_r(s)| = \hat{\varphi}$ is satisfied at $s$, then $n_a(s) = 2$ results, the $2 \times 3$ matrix $C_{\check{u}}$ is

$$C_{\check{u}} = \begin{bmatrix} \pm 1 & 0 & 0 \\ 0 & 0 & \pm 1 \end{bmatrix},$$

and a $3 \times 1$ matrix such that $C_{\check{u}} P = 0$ holds is

$$P = \begin{bmatrix} 0 \\ 1 \\ 0 \end{bmatrix}. \tag{9.9}$$

If $|\check{\varphi}_f(s)| = |\check{\varphi}_r(s)| = \hat{\varphi}$ holds at $s$, then $n_a(s) = 3$ is true, the $3 \times 3$ matrix $C_{\check{u}}$ is

$$C_{\check{u}} = \begin{bmatrix} \pm 1 & 0 & 0 \\ 0 & \pm 1 & 0 \\ 0 & 0 & \pm 1 \end{bmatrix},$$

and there is no matrix $P$ for $C_{\check{u}} P = 0$. For $P$ as in (9.7), (9.8), or (9.9), the corresponding Riccati equation (4.14) results. For $|\check{\varphi}_f(s)| = |\check{\varphi}_r(s)| = \hat{\varphi}$ and $n_a(s) = 3$, the Riccati equation $Q' = -Q\,\check{f}_{\check{X}} - \check{f}_{\check{X}}^{\top} Q - \check{H}_{\check{X}\check{X}}$ is obtained. To analyze whether a bounded solution $Q(\cdot)$ with $q_{\check{n}\check{n}}(0) > 0$ and $q_{\check{n}\check{n}}(1) < 0$ exists, an initial condition $Q(0)$ with $q_{\check{n}\check{n}}(0) > 0$ is chosen, the Riccati equation for the current active input constraints is integrated, and the boundedness of $Q(\cdot)$ as well as $q_{\check{n}\check{n}}(1) < 0$ are checked. If no weak local optimality follows from the initial condition, a new one is selected until local optimality is shown or the analysis is terminated.

In the following, solutions to the transformed control problem obtained from solution S1 and S3 of Table 8.3 for $q_d = \left(-\frac{\pi}{2}, 4, 2\right)$ are considered. Bounded solutions $Q(\cdot)$ exist for

$$Q(0) = \begin{bmatrix} 0 & 0 & 0 & 0 \\ 0 & 0 & 0 & 0 \\ 0 & 0 & 0 & 1 \\ 0 & 0 & 1 & 3 \end{bmatrix}.$$

Obviously, $q_{\check{n}\check{n}}(0) > 0$ holds. At $s = 1$, the solutions obtained for S1 and S3 are

$$Q(1) = \begin{bmatrix} 1.2829 & 0 & 0 & -1.6429 \\ 0 & 0 & 0 & 0 \\ 0 & 0 & 0 & 1 \\ -1.6429 & 0 & 1 & -1.2666 \end{bmatrix} \tag{9.10}$$

and

$$Q(1) = \begin{bmatrix} 0.8551 & 0 & 0 & -0.8354 \\ 0 & 0 & 0 & 0 \\ 0 & 0 & 0 & 1 \\ -0.8354 & 0 & 1 & -1.1229 \end{bmatrix}, \tag{9.11}$$

respectively. As $q_{\check{n}\check{n}}(1) < 0$ is true for (9.10) and (9.11), both solutions are locally optimal. Simulations show that suitable solutions $Q(\cdot)$ exist for all normal regular extremals of the RKM, independent of the number of cusps $n_c$ and the end time $\tau$. Thus, the sufficient conditions from [65, 72, 75] give no condition for near time-optimality for the RKM, as they do not single out extremals with too large end time $\tau$. This is the case as for weak local optimality 2.2.6, solutions in an $\varepsilon$-neighborhood with respect to $\tau$, $x$, and $u$ are considered. Hence, two normal regular extremals with different end times $\tau$ can both be locally optimal.

## 9.4 Simulations on time-optimal normal regular extremals

As the optimality conditions from Section 9.1 and 9.3 gave no condition for near time-optimality, simulation data on time-optimal normal regular extremals is presented in this section. The simulation results provide the motivation and basis for the necessary optimality condition for the RKM discussed in the next section.

To generate the simulation data, the time-optimal control 7.3.2 was applied to the near time-optimal control problem 8.1.4. The parameters of Table 8.1 were used, except for the maximal number of simulated extremals $\hat{n}^{to}_{Sim}$ for time-optimal control which was set to $\hat{n}^{to}_{Sim} = 10\,000$. Moreover, no condition for near time-optimality was included to terminate the time-optimal control. This way, time-optimal normal regular extremals were obtained for almost all desired configurations $q_d$ which are reachable by normal regular extremals.

The MATLAB functions **fmincon** and **ode45** were applied for optimization and numerical integration. For the simulations, 13 447 desired configurations

$$Q_d = \left\{ q_d = (\theta_d, x_d, y_d) \;\middle|\; \theta_d \in \Theta_d,\, x_d \in X_d,\, y_d \in Y_d,\, q_d \neq (0,0,0) \right\} \tag{9.12}$$

were considered obtained for

$$\begin{aligned} \Theta_d &= \left\{ -\pi, -\tfrac{3\pi}{4}, -\tfrac{\pi}{2}, -\tfrac{\pi}{4}, 0, \tfrac{\pi}{4}, \tfrac{\pi}{2}, \tfrac{3\pi}{4} \right\}, \\ X_d &= \{0.0,\, 0.1,\, \ldots,\, 3.9,\, 4.0\}, \\ Y_d &= \{0.0,\, 0.1,\, \ldots,\, 3.9,\, 4.0\}. \end{aligned} \tag{9.13}$$

The 13 447 desired configurations $q_d \in Q_d$ arise from 8 values for $\theta_d$ and 41 values for $x_d$ and $y_d$ minus $q_d = (0,0,0)$, which is excluded because of $q_0 = (0,0,0)$ and $q_0 \neq q_d$. Time-optimal normal regular solutions were simulated for desired configurations $q_d$ with $x_d \geq 0$ and $y_d \geq 0$, as solutions for $x_d < 0$ or $y_d < 0$ result from these solutions via symmetry properties not discussed here. No desired configurations with $x_d > 4$ or $y_d > 4$ were considered, as all interesting properties of time-optimal normal regular extremals regarding the end time $\tau$ and the number of cusps $n_c$ can be seen for $0 \leq x_d \leq 4$ and $0 \leq y_d \leq 4$ as discussed below. For each desired configuration, the final time $\hat{T}$ of the initial time horizon given by (8.11) was used.

In Figure 9.4, simulation data on the end time $\tau^{tor}$ of time-optimal normal regular extremals is shown. The superscript *tor* stands for *t*ime-*o*ptimal *r*egular, as $\tau^{tor}$ is the end time of an extremal which is time-optimal among all normal regular extremals to a specific desired configuration $q_d$. For each $\theta_d \in \Theta_d$ (9.13), a contour plot of the end time $\tau^{tor}$ over $(x_d, y_d) \in X_d \times Y_d$ is given in Figure 9.4. Each line in the figure is an isometric line of constant $\tau^{tor}$. Desired configurations are colored in black if they are not reachable by normal regular extremals. As $q_d = (0,0,0)$ is excluded from $Q_d$, this configuration is black as well.

Results similar to Figure 9.4 are given in [10, 60, 106, 107]. In [10], a contour plot of the end time of time-optimal paths of the differential drive is presented. In [107], lines of constant end time are depicted for time-optimal paths of the car-like robot with free final orientation $\theta(\tau)$. For Dubins paths, contour plots of the path length are shown in [60, 106].

To validate the final time $\hat{T}$ of the initial time horizon, the mean value of $\hat{T}/\tau^{tor}$ over all solutions was computed, resulting in 2.36 for the simulations in Figure 9.4. Hence, the final time $\hat{T}$ of the initial time horizon for the first run of the path planning is on average more than

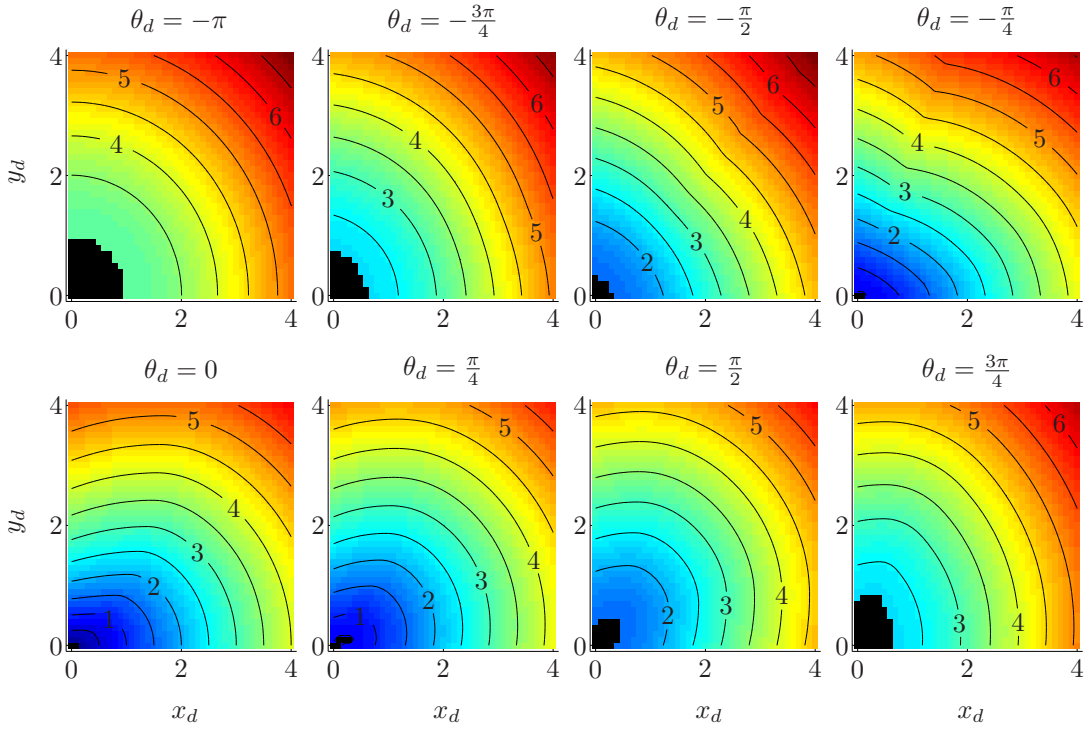


Figure 9.4: End time $\tau^{tor}$ of time-optimal normal regular extremals to $q_d \in Q_d$.

two times longer than the end time of a time-optimal normal regular extremal. Shorter final times $\hat{T}$ than (8.11) for smaller mean values of $\hat{T}/\tau^{tor}$ can be derived from Reeds-Shepp paths.

In Figure 9.5, simulation data on the number of cusps of time-optimal normal regular extremals is given for the desired configurations $q_d \in Q_d$ (9.12). According to Corollary 9.5.2 below, a time-optimal normal regular extremal to a desired configuration $q_d$ has the minimal number of cusps among all normal regular extremals to $q_d$. This minimal number called $n_c^m$ in the following is fundamental for the results on near time-optimality in the next section. In Figure 9.5, $n_c^m$ is shown for the desired configurations $q_d \in Q_d$. For each $\theta_d \in \Theta_d$, an $(x, y)$ plot is given for $(x_d, y_d) \in X_d \times Y_d$. In the $(x, y)$ plots, domains of different minimal number of cusps $n_c^m$ are marked in different colors. The desired configurations $q_d$ in green, yellow, and red domains are reached by time-optimal normal regular extremals with $n_c^m(q_d) = 0$, $n_c^m(q_d) = 1$, and $n_c^m(q_d) = 2$, respectively. Solutions with $n_c^m(q_d) = 2$ only exist for $\theta_d = 0$. Domains colored in black indicate that no normal regular extremals exists to the specific $q_d$. More detailed results than in Figure 9.5 can be given which do not only show the minimal number of cusps $n_c^m$ but also the type of the time-optimal normal regular extremal to $q_d$.

In Figure 9.4, the end time of the time-optimal normal regular extremals satisfies $\tau^{tor} \leq 6.899$ for all $q_d \in Q_d$. The time $\tau^{tor}$ increases approximately for growing $\|(x_d, y_d)\|$, as it takes longer to reach more distant positions. As could be seen in Figure 9.5, time-optimal normal regular extremals to nearby configurations $q_{d_1}$ and $q_{d_2}$ can be quite different. For example, for extremals to configurations $q_{d_1} = (\theta_{d_1}, x_{d_1}, y_{d_1})$ and $q_{d_2} = (\theta_{d_2}, x_{d_2}, y_{d_2})$ with $\theta_{d_1} = \theta_{d_2} = 0$, $y_{d_1} = y_{d_2}$, and $x_{d_1} < x_{d_2}$ close together, $n_c^m(q_{d_1}) = 2$ and $n_c^m(q_{d_2}) = 0$ can hold. Correspondingly, the initial conditions $\lambda_0$ of the adjoint state for time-optimal normal regular extremals to nearby configurations may have completely different values. Hence, in general, it is impossible to determine the initial condition $\lambda_0$ for a time-optimal extremal to a configuration $q_d$ based on the initial condition $\lambda_0$ for an extremal to a configuration close to $q_d$.

The results of Figure 9.4 and 9.5 were obtained for time-optimal normal regular extremals. For all configurations $q_d$ marked in black which are not reachable by such extremals, $\|(x_d, y_d)\|$

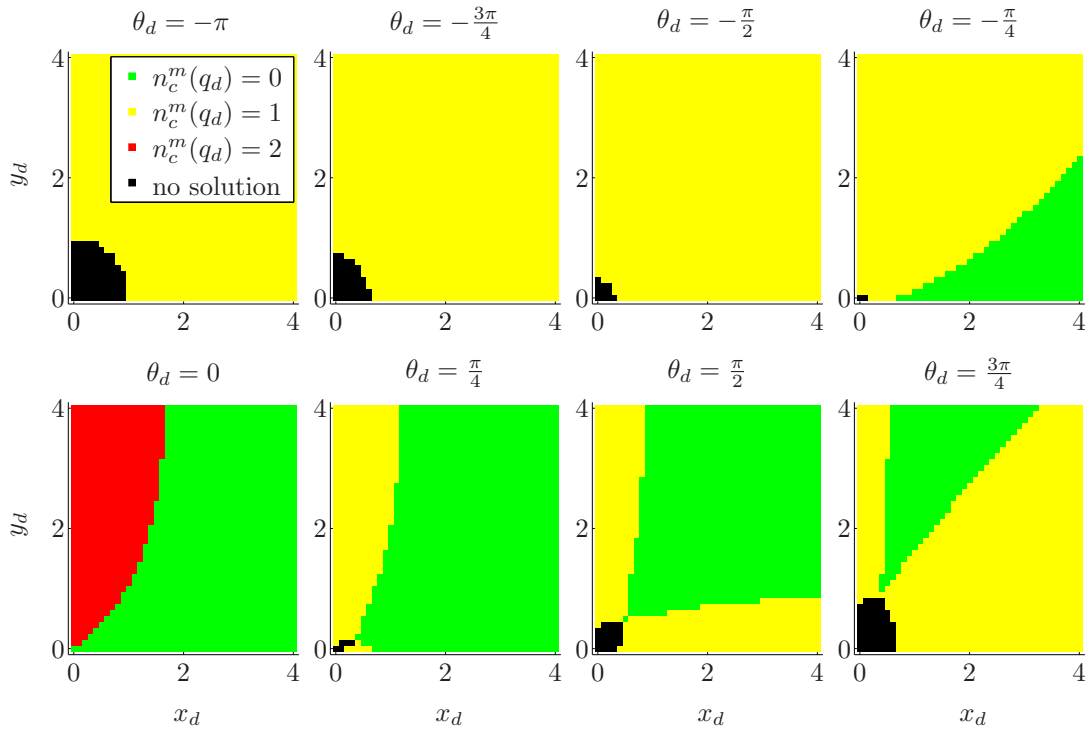


Figure 9.5: Minimal number of cusps $n_c^m$ of time-optimal normal regular extremals to $q_d \in Q_d$.

is small. Thus, for sufficiently large $\|(x_d, y_d)\|$, each configuration $q_d$ can be reached by a normal regular extremal. As discussed in Section 9.6, configurations not reachable by normal regular extremals can be reached by normal singular ones. For $X_d$ and $Y_d$ given by (9.13), desired configurations with $x_d \leq 4$ and $y_d \leq 4$ were studied, as only for small $\|(x_d, y_d)\|$, there are configurations not reachable by normal regular extremals. All relevant domains of different $n_c^m$ exist for $x_d \leq 4$ and $y_d \leq 4$. Thus, for $X_d$ and $Y_d$, all interesting properties of time-optimal normal regular extremals can be seen. In Figure 9.5, the domains of different $n_c^m$ are slightly affected by the discretization of $x_d$ and $y_d$ as in (9.13) and the tolerance $\varepsilon_q$.

## 9.5 Time-optimality and number of cusps

As no condition for near time-optimality resulted from the optimality conditions in Section 9.1 and 9.3, a necessary optimality condition is derived in the following based on simulation data on the minimal number of cusps $n_c^m$ from Section 9.4. For this, a theorem on the number of cusps and the end time of normal regular extremals is stated, from which the necessary optimality condition is derived. Simulation results on normal regular extremals satisfying this condition are presented. For a given desired configuration $q_d$, the necessary optimality condition can be used to terminate the time-optimal control 7.3.2 for the RKM when a solution is found which provides a good approximation of a time-optimal solution.

For each desired configuration $q_d$, the minimal number of cusps $n_c^m$ is the smallest existing number of cusps among all normal regular extremals to $q_d$. According to Figure 9.5, $n_c^m(q_d) \leq 2$ holds for the time-optimal normal regular extremals of the RKM to the configurations $q_d \in Q_d$ which are reachable by normal regular extremals. Aside from simulations, it is hardly possible to show $n_c^m(q_d) \leq 2$ without closed-form solutions. To make $n_c^m(q_d) \leq 2$ plausible, results on the number of cusps and switchings are reviewed for related optimal control problems. For the RKM with configuration $q$ of dimension $p = 3$, the number of cusps of time-optimal normal regular extremals satisfies $n_c \leq p - 1 = 2$. Thus, to reach a configuration $q_d = (\theta_d, x_d, y_d)$

specified by three configuration variables, each time-optimal normal regular extremal consists of up to three pieces of constant velocity. Reeds-Shepp paths, i. e., shortest paths of the car-like robot which drives forward and backward and has the same configuration as the RKM, have at most two cusps and three pieces of constant velocity as well, see [94, 108, 120]. In Section 8.5, time-optimal normal regular extremals of the BSR and shortest paths of the car-like robot were compared. The optimal solutions of both systems had the same number of cusps for the configurations $q_d = \left(-\frac{\pi}{2}, 4, 2\right)$ and $q_d = (0, 2, -4)$. Time-optimal solutions of the differential drive with a configuration of dimension $p = 3$ are addressed in [9, 10]. The optimal solutions have at most two cusps. In [48], near time-optimal solutions of the snakeboard with minimal number of switchings $n_s$ between motion primitives are analyzed. The snakeboard has a configuration of dimension $p = 5$. For each configuration $q_d$, the minimal number of switchings among all solutions satisfies $n_s \leq p - 1 = 4$.

As no closed-form representations of normal regular extremals of type M and P are available, the domains of different $n_c^m$ and their boundaries cannot be described analytically. To determine the minimal number of cusps for a specific configuration $q_d$, simulation data like in Figure 9.5 can be stored in a lookup table, and $n_c^m(q_d)$ can be computed approximately by nearest-neighbor interpolation, as the interpolated number has to be integer. The boundaries of the domains colored in black in Figure 9.5 consist of all configurations not reachable by normal regular extremals. These boundaries can be given analytically, as the configurations can be reached by normal singular extremals for which closed-form solutions exit, see Section 9.6.

### 9.5.1 Number of cusps and end time

The following result relates the number of cusps $n_c$ and the end time $\tau$ of normal regular extremals to a desired configuration $q_d$. It can be shown analytically for some sequences of types of extremals. For the remaining sequences, it is verified by extensive simulations.

**Theorem 9.5.1** *(Number of cusps and end time of normal regular extremals) The time-optimal control problem for the RKM 6.0.2 is considered for the initial configuration* $q_0 = (0, 0, 0)$ *and a desired configuration* $q_d = (\theta_d, x_d, y_d)$*. Let S1 and S2 be normal regular extremals from* $q_0$ *to* $q_d$ *with* $n_{c_1}$ *and* $n_{c_2}$ *cusps and end times* $\tau_1$ *and* $\tau_2$*, and let* $|\theta_d|$ *or* $|x_d|$ *be sufficiently large. Then,* $n_{c_1} > n_{c_2}$ *implies* $\tau_1 > \tau_2$*.*

**Proof** For the types 6.4.1 of normal regular extremals of the RKM, the following sequences of extremals S1 and S2 can be considered:

**S-S:** Extremal S1 is of type S and extremal S2 is of type S.

**S-M:** Extremal S1 is of type S and extremal S2 is of type M.

**S-P:** Extremal S1 is of type S and extremal S2 is of type P.

**M-S:** Extremal S1 is of type M and extremal S2 is of type S.

**M-M:** Extremal S1 is of type M and extremal S2 is of type M.

**M-P:** Extremal S1 is of type M and extremal S2 is of type P.

**P-S:** Extremal S1 is of type P and extremal S2 is of type S.

**P-M:** Extremal S1 is of type P and extremal S2 is of type M.

**P-P:** Extremal S1 is of type P and extremal S2 is of type P.

For each sequence of extremals S1 and S2, either $n_{c_1} > n_{c_2}$ cannot hold, i. e., the sequence of extremals does not exist, or Theorem 9.5.1 is true. In the following, this is shown for the sequences S-S, S-M, S-P, M-S, and P-S. For the remaining sequences M-M, M-P, P-M, and P-P, Theorem 9.5.1 is verified by simulations as discussed below.

According to property NR2 of Lemma 6.4.3, extremals of type S have no cusps. Thus, for an extremal S1 of type S, $n_{c_1} = 0$ holds, and there is no extremal S2 with $n_{c_2} < n_{c_1}$ cusps, as $n_{c_2}$ cannot be negative. Hence, $n_{c_1} > n_{c_2}$ cannot hold for the sequences S-S, S-M, and S-P for any desired configuration $q_d$.

By property NR3, extremals of type S are straight line segments from $q_0$ to $q_d$. Thus, their path length $l_S$ is minimal among all extremals. As $l_S$ is minimal, the path length $l_M$ and $l_P$ of extremals of type M and P satisfies $l_M \geq l_S$ and $l_P \geq l_S$. For extremals of type S, $\varphi = (0, 0)$ holds for all $t$. This is true since by property E3 of Lemma 6.3.1, the extremal adjoint state $\lambda(t)$ is of case C3 for all $t$ if it is of this case for some $t$, and by Theorem 6.1.4, for $\lambda(t)$ of case C3, the Hamiltonian function is maximized by $\varphi_0 = (0, 0)$. For extremals with $\varphi(t) = (0, 0)$ for all $t$, the absolute translational velocity $|v_t|$ given by (5.18) is maximal by Lemma 5.3.4. In contrast, for extremals of type M and P,

$$\dot{\theta}(t) = \sin(\varphi_f(t) - \varphi_r(t))\, v(t) \neq 0 \tag{9.14}$$

holds for almost all $t$, as the orientation $\theta$ of the extremals is not constant, see Definition 6.4.1. Thus, because of $v(t) \neq 0$ for almost all $t$, $\varphi_f^2(t) + \varphi_r^2(t) > 0$ results from (9.14), and the absolute translational velocity $|v_t|$ is not maximal for almost all $t$. As an extremal of type S has minimal path length $l_S$ and its absolute translational velocity $|v_t|$ takes its maximal value of all $t$, it has a shorter end time $\tau_2$ than an extremal of type M or P with end time $\tau_1$. Hence, Theorem 9.5.1 holds for the sequences M-S and P-S for any desired configuration $q_d$. ■

For the sequences M-S and P-S, the proof of Theorem 9.5.1 is independent of the number of cusps of the extremals of type M and P and of the configuration $q_d$. According to extensive simulations for $q_d \in Q_d$ (9.12), Theorem 9.5.1 holds for the sequences M-M, M-P, and P-P for all configurations $q_d$. In contrast, for the sequence P-M, there are extremals to configurations $q_d$ with small values of $|\theta_d|$ and $|x_d|$ for which $n_{c_1} > n_{c_2}$ does not imply $\tau_1 > \tau_2$. In general, the type of the extremals to a specific $q_d$ is unknown. Thus, for Theorem 9.5.1 to hold for any sequence of extremals, the configuration $q_d$ must have sufficiently large values of $|\theta_d|$ or $|x_d|$. In the simulations, the theorem does not hold for some configurations $q_d$ with $|\theta_d| \leq \frac{\pi}{4}$ and $|x_d| \leq 0.5$, but it is true for all configurations $q_d$ with $|\theta_d| > \frac{\pi}{4}$ or $|x_d| > 0.5$. For example, for $q_d = \left(-\frac{\pi}{4}, 0.5, 3.7\right)$ and $q_d = (0, 0.4, 3.2)$, there are sequences P-M with $n_{c_1} > n_{c_2}$ and $\tau_1 < \tau_2$.

To proof Theorem 9.5.1 for the sequences M-M, M-P, P-M, and P-P analytically, closed-form representations of the extremals of type M and P would be required to give the path length $l$ and the total change $\triangle\theta$ of the orientation of extremals from $q_0$ to $q_d$. For an extremal from $q_0$ to $q_d$ with end time $\tau$, the path length

$$l = \int_0^\tau |v_t(\xi)| \, \mathrm{d}\xi$$

is the distance the RKM has to travel. The total change of the orientation

$$\triangle\theta = \int_0^\tau \left|\dot{\theta}(\xi)\right| \mathrm{d}\xi$$

is the total angular distance of the orientation the RKM has to cover. To compare the end times $\tau_1$ and $\tau_2$ of extremals S1 and S2 with path length $l_1$ and $l_2$ and total change of the orientation $\triangle\theta_1$ and $\triangle\theta_2$, the absolute translational velocity $|v_t|$ given by (5.18) and the absolute rate of change of the orientation $\left|\dot{\theta}\right| = |\sin(\varphi_f - \varphi_r)|\, \hat{v}$ obtained from $\dot{\theta} = \sin(\varphi_f - \varphi_r)\, v$ for $|v| = \hat{v}$ have to be considered. However, closed-form representations of extremals of type M and P are not available. Thus, it is not possible to determine $l$ and $\triangle\theta$ analytically for extremals from $q_0$ to $q_d$ with different values of $n_c$ to compare the end times.

By Theorem 9.5.1, normal regular extremals to a desired configuration $q_d$ with sufficiently large $|\theta_d|$ or $|x_d|$ have shorter end times if they have fewer cusps. For a wheeled mobile robot which can drive forward and backward, it is an intuitive result that fewer cusps lead to shorter

end times. However, for the RKM, this is not true for extremals S1 and S2 of type P and M and for some configurations $q_d$. To make it plausible that $n_{c_1} > n_{c_2}$ does not imply $\tau_1 > \tau_2$ for particular configurations $q_d$ with small $|\theta_d|$ and $|x_d|$, for extremals S1 and S2 of type P and M with $n_{c_1} > n_{c_2}$, the change of the orientation $\triangle\theta_c$ between two consecutive cusps is considered. As discussed in Section 6.4.3, for extremals of type P and M, $0 < \triangle\theta_c < \pi$ and $\triangle\theta_c = \pi$ holds, respectively. Thus, for the extremals S1 and S2, $\triangle\theta_{c_1} < \triangle\theta_{c_2}$ is always true. Hence, even if $n_{c_1} > n_{c_2}$ is true, $\triangle\theta_1 < \triangle\theta_2$ may result. Then, for suitable path length $l_1$ and $l_2$ of the extremals, $\triangle\theta_1 < \triangle\theta_2$ may give rise to $\tau_1 < \tau_2$ despite of $n_{c_1} > n_{c_2}$.

The sequence M-M of solution S1 and S2 of Table 8.3 and the sequence P-P of solution S2 and S3 of Table 8.4 agree with Theorem 9.5.1, since for the desired configurations $q_d$ considered there, normal regular extremals with fewer cusps have shorter end times. In contrast, extremals with shorter end times do not always have fewer cusps, i. e., $\tau_1 > \tau_2$ does not imply $n_{c_1} > n_{c_2}$, but only $n_{c_1} \geq n_{c_2}$. There are solutions with $\tau_1 > \tau_2$ and $n_{c_1} = n_{c_2}$, like solution S2 and S3 of Table 8.3 and solution S1 and S2 of Table 8.4.

### 9.5.2 Necessary optimality condition on the number of cusps

Based on Theorem 9.5.1, the following necessary optimality condition on the number of cusps is obtained for the normal regular extremals of the RKM.

**Corollary 9.5.2** *(Necessary optimality condition on the number of cusps) The time-optimal control problem for the RKM 6.0.2 is considered for the initial configuration $q_0 = (0, 0, 0)$ and a desired configuration $q_d = (\theta_d, x_d, y_d)$. Let $n_c^m(q_d)$ be the minimal number of cusps among all normal regular extremals from $q_0$ to $q_d$, and let $|\theta_d|$ or $|x_d|$ be sufficiently large. Then, if a normal regular extremal from $q_0$ to $q_d$ is time-optimal, it has $n_c^m(q_d)$ cusps.*

**Proof** A desired configuration $q_d$ with sufficiently large $|\theta_d|$ or $|x_d|$ is considered. Thus, Theorem 9.5.1 applies. Let S1 be a time-optimal normal regular extremal to $q_d$ with $n_{c_1} > n_c^m(q_d)$ cusps and end time $\tau_1$. Then, by Theorem 9.5.1, there is another normal regular extremal S2 to $q_d$ with $n_{c_2} = n_c^m(q_d)$ cusps which has a shorter end time $\tau_2 < \tau_1$. Thus, the extremal S1 cannot be time-optimal, and Corollary 9.5.2 holds. ■

According to Corollary 9.5.2, for a desired configuration $q_d$ with sufficiently large $|\theta_d|$ or $|x_d|$, a normal regular extremal can only be time-optimal if its number of cusps $n_c$ is the minimal number of cusps $n_c^m$ among all normal regular extremals to $q_d$. Corollary 9.5.2 gives a necessary optimality condition, i. e., it characterizes candidates for time-optimal normal regular extremals. It is no sufficient optimality condition, as there are normal regular extremals which satisfy $n_c = n_c^m(q_d)$ but are not time-optimal. For example, $n_c = n_c^m(q_d)$ holds for solution S2 and S3 of Table 8.3, but solution S2 has a larger end time than solution S3.

As discussed in Section 9.4, the minimal number of cusps for a specific configuration $q_d$ can be approximated by a nearest-neighbor interpolation of simulation data on $n_c^m$ stored in a lookup table. Besides condition 9.5.2, there are other necessary optimality conditions for the normal regular extremals of the RKM which depend on the number of cusps $n_c$. As all time-optimal normal regular extremals have at most two cusps as addressed in Section 9.4, extremals with $n_c > 2$ cannot be optimal. Thus, $n_c \leq 2$ can be used instead of $n_c = n_c^m(q_d)$. This way, a weaker necessary condition is obtained for which no simulation data is needed. A stronger necessary condition than condition 9.5.2 results if in addition to $n_c = n_c^m(q_d)$, the normal regular extremal must have the same type as a time-optimal extremal to $q_d$. For the implementation of this condition, simulation data on the optimal type has to be stored.

### 9.5.3 Simulation results and condition for near time-optimality

The necessary optimality condition 9.5.2 is no condition for near time-optimality in the sense of Definition 9.0.1. A condition 9.0.1 holds if the end time of a normal regular extremal to $q_d$

satisfies $\tau \leq k\,\tau^{to}$ for a fixed quality factor $k \geq 1$ and the end time $\tau^{to}$ of a time-optimal normal regular extremal to $q_d$. Condition 9.5.2 allows to single out extremals which have too many cusps and thus larger end times than a time-optimal normal regular extremal to $q_d$. However, the condition does not take the quality factor $k$ and the minimal end time $\tau^{to}$ into account.

In the following, simulation data on normal regular extremals satisfying condition 9.5.2 is discussed. The condition is applied to solutions $\left(\lambda_0^{PP}, \tau\right)$ to the path planning problem 8.1.3, i. e., to normal regular extremals which reach the desired configuration $q_d$ within the tolerance $\varepsilon_q$. As discussed above, in principle, the final configuration $q(\tau)$ has to be considered for optimality instead of $q_d$, i. e., $n_c = n_c^m(q(\tau))$ has to be checked instead of $n_c = n_c^m(q_d)$. However, $n_c = n_c^m(q_d)$ is used to simplify the analysis.

Solutions to the path planning problem 8.1.3 which satisfy $n_c = n_c^m(q_d)$ give good approximations of time-optimal normal regular extremals as shown below in this section. Hence, and since no condition for near time-optimality 9.0.1 was found for the RKM, solutions with $n_c = n_c^m(q_d)$ are defined to be near time-optimal as from now. Their end time is denoted by $\tilde{\tau}^{to}$ and the resultant quality factor $k := \tilde{\tau}^{to}/\tau^{tor}$ is used to rate the approximation.

In Table 9.1, near time-optimal solutions with $n_c = n_c^m(q_d)$ and time-optimal normal regular extremals of Table 8.3 and 8.4 are compared. For the desired configurations $q_d = \left(-\frac{\pi}{2}, 4, 2\right)$ and $q_d = (0, 2, -4)$, references to the near time-optimal and time-optimal solutions are given, the end times $\tilde{\tau}^{to}$ and $\tau^{tor}$ are listed, and the resultant quality factor $k = \tilde{\tau}^{to}/\tau^{tor}$ is stated. For $q_d = (0, 2, -4)$, $k = 1$ holds, as the near time-optimal solution S3 is time-optimal as well. For $q_d = \left(-\frac{\pi}{2}, 4, 2\right)$, $k = 1.138$ results, as the end time $\tilde{\tau}^{to}$ of the near time-optimal solution S2 is larger than the end time $\tau^{tor}$ of the time-optimal normal regular extremal S3. Since $k$ is small, the near time-optimal solution S2 gives a good approximation of the time-optimal extremal S3 with respect to the end time.

| desired configuration $q_d$ | near time-optimal solution | | time-optimal normal regular extremal | | resultant quality factor $k$ |
|---|---|---|---|---|---|
| | solution | $\tilde{\tau}^{to}$ | solution | $\tau^{tor}$ | |
| $\left(-\frac{\pi}{2}, 4, 2\right)$ | S2 of Table 8.3 | 6.249 | S3 of Table 8.3 | 5.492 | 1.138 |
| $(0, 2, -4)$ | S3 of Table 8.4 | 5.198 | S3 of Table 8.4 | 5.198 | 1.000 |

Table 9.1: Comparison of near time-optimal solutions and time-optimal normal regular extremals.

In Table 9.2, near time-optimal solutions to all desired configurations $q_d \in Q_d$ (9.12) are considered. According to simulations, condition 9.5.2 holds for all configurations $q_d \in Q_d$ independent of $|\theta_d|$ and $|x_d|$. Thus, all configurations $q_d \in Q_d$ are used for the results in Table 9.2. For $Q_d$ consisting of 13 447 configurations, the number and percentage of configurations reachable by normal regular extremals are given. Most configurations $q_d \in Q_d$ can be reached by normal regular extremals. As discussed in the next section, the remaining configurations are reachable by normal singular extremals. From the configurations reachable by normal regular extremals, the number and percentage of solutions with $n_c = n_c^m(q_d)$ and $\tilde{\tau}^{to} = \tau^{tor}$ are given. For these configurations, solutions are time-optimal if $n_c = n_c^m(q_d)$ holds. As could be seen from Table 9.2, this is the case for the majority of configurations $q_d \in Q_d$. Besides, the number and percentage of the remaining configurations are stated. For these configurations, near time-optimal solutions with $n_c = n_c^m(q_d)$ and $\tilde{\tau}^{to} > \tau^{tor}$ are obtained.

Condition 9.5.2 gives no information about the quality factor $k$. Thus, simulation data on the minimal, mean, and maximal value of the resultant quality factor $k$ is given in Table 9.2 for near time-optimal solutions to $q_d \in Q_d$. Most often, $k = 1$ is attained for near time-optimal solutions which are in fact time-optimal. As $k$ has the mean value 1.029, the end times $\tilde{\tau}^{to}$ of near time-optimal solutions are on average 2.9 % larger than the end times $\tau^{tor}$ of time-optimal extremals. Thus, near time-optimal solutions provide good approximations of time-optimal normal regular extremals on average. Moreover, they give good approximations of all time-optimal solutions,

as there are no configurations $q_d$ reachable by normal regular extremals which can be reached by normal singular extremals with shorter end times as discussed in the next section. Large values of $k$ occur for configurations with $\theta_d = 0$.

| | | |
|---|---|---|
| desired configurations $q_d$ | reference | $Q_d$ (9.12) |
| | number | 13 447 |
| $q_d$ reachable by normal regular extremals | number | 13 222 |
| | percentage | 98.32 % |
| $n_c = n_c^m(q_d)$ and $\tilde{\tau}^{to} = \tau^{tor}$ | number | 10 038 |
| | percentage | 75.92 % |
| $n_c = n_c^m(q_d)$ and $\tilde{\tau}^{to} > \tau^{tor}$ | number | 3184 |
| | percentage | 24.08 % |
| resultant quality factor $k$ | minimal | 1.000 |
| | mean | 1.029 |
| | maximal | 2.357 |

Table 9.2: Near time-optimal solutions for $q_d \in Q_d$.

For a mean value of $k$ close to 1, the end times $\tilde{\tau}^{to}$ of near time-optimal solutions are on average only slightly larger than the end times $\tau^{tor}$ of time-optimal normal regular solutions extremals. Thus, near time-optimal solutions give good approximations of time-optimal solutions for the RKM. Hence, it is appropriate to use the necessary optimality condition 9.5.2 to terminate the time-optimal control 7.3.2 when an extremal with $n_c = n_c^m(q_d)$ is determined.

As discussed above, to integrate an optimality condition into the time-optimal control 7.3.2, the condition should be easy to apply and computationally cheap. Condition 9.5.2 meets these requirements, as the simulation data on $n_c^m$ for the lookup table is generated offline before the time-optimal control is executed, the nearest-neighbor interpolation to obtain $n_c^m$ for a specific configuration $q_d$ is cheap, and $n_c = n_c^m(q_d)$ can be easily checked. This should be compared to other optimality conditions like the second-order sufficient conditions with Riccati equation in Section 4.6.2 and 9.3.1, which require that a suitable solution $Q(\cdot)$ to a Riccati equation is found. For each configuration $q_d$, $n_c^m(q_d) \in \{0, 1, 2\}$ holds. Thus, the value of $n_c^m$ can be stored with a small number of bits for each $q_d$, and the memory capacity needed for the lookup table is low. In particular, it is much lower than for a lookup table which contains initial conditions $\lambda_0^{to}$ for a sampling of the configuration space $Q$ such that for any $q_d$, an initial condition for a near time-optimal solution results by interpolation.

The percentage of near time-optimal solutions in Table 9.2 which are time-optimal depends on the final time $\hat{T}$ (8.11) of the initial time horizon. For larger values of $\hat{T}$, a higher percentage of near time-optimal solutions which are not time-optimal is obtained. In contrast, the effect of the discretization interval $\triangle t = 0.001$ on the percentage of near time-optimal solutions which are time-optimal is negligible. This is true as the end times $\tau$ of two subsequent solutions to the path planning problem differ by at least several intervals $\triangle t$, see Section 8.6.

## 9.6 Time-optimal normal regular and normal singular extremals

For completeness, time-optimal normal singular extremals are compared in this section to the time-optimal normal regular extremals from Section 9.4. Normal singular extremals are relevant for two reasons: First, they provide solutions to configurations $q_d$ with small $\|(x_d, y_d)\|$ which are not reachable by normal regular extremals. Second, they may give solutions with shorter end time than normal regular extremals for some configurations $q_d$. As shown below, this is not true for time-optimal control of the RKM. The end time of time-optimal normal singular extremals is called $\tau^{tos}$. The superscript $tos$ stands for $t$ime-$o$ptimal $s$ingular, as $\tau^{tos}$ is the end time of an extremal which is time-optimal among all normal singular extremals to $q_d$.

As our approach for time-optimal control is based on normal regular extremals, normal singular extremals cannot be determined this way. Instead, closed-form representations of the trajectories $q(\cdot)$ of normal singular extremals were used to generate the simulation results. The trajectories were represented as vectors

$$q(I_\triangle) = \left[\, q_i \,\middle|\, q_i = q(t_i),\, t_i \in I_\triangle \,\right]$$

for the times $I_\triangle$ (7.15). The closed-form solutions arise from the concatenation of transitions (6.35) of the configuration for the arcs of circles of the normal singular extremals.

As $\tau^{tor} \leq 6.899$ holds for all time-optimal normal regular extremals in Figure 9.4, normal singular extremals with end times up to 6.899 are considered for solutions comparable to those of Section 9.4. The time-optimal normal regular extremals have at most two cusps. Thus, normal singular extremals are studied in the following which consist of at most three arcs of circles. By a brute force method, closed-form representations $q(I_\triangle)$ of all normal singular extremals over the times $I_\triangle$ with one, two, or three arcs were computed. For $\triangle t = 0.001$, the time vector $I_\triangle$ for the interval $I = [0, 6.899]$ has 6900 elements. Because of $\theta_0 = 0$ for $q_0 = (0, 0, 0)$, there holds $\lambda_0 = \gamma_0$ for the normalized initial conditions of the adjoint state $\lambda$ and the transformed adjoint state $\gamma$. Then, by Theorem 6.3.4, normal singular extremals result from initial conditions $\lambda_0 = \big(\lambda_{10}, 0, 0\big)$ with $\lambda_{10} = \pm 1$ for $\hat{v} = 1$ and $\hat{\varphi} = \frac{\pi}{4}$. According to property NS1 of Lemma 6.5.1, the input of a normal singular extremal can be chosen at each time $t$ from $\{u_I, u_{II}\}$ as in (6.34). For $\hat{v} = 1$ and $\hat{\varphi} = \frac{\pi}{4}$, this gives

$$\begin{aligned} u_I &= \big(-\operatorname{sgn}(\lambda_{10}), -\tfrac{\pi}{4}, \tfrac{\pi}{4}\big), \\ u_{II} &= \big(\operatorname{sgn}(\lambda_{10}), \tfrac{\pi}{4}, -\tfrac{\pi}{4}\big). \end{aligned}$$

For the initial input at time $t = 0$, there holds $u(0) \in \{u_I, u_{II}\}$.

Due to $\lambda_{10} = \pm 1$ and $u(0) \in \{u_I, u_{II}\}$, there are 4 different normal singular extremals without cusps which consist of one arc over the whole time interval $I = [0, 6.899]$. For normal singular extremals with more than one arc, each arc is at least one interval $\triangle t$ long. Hence,

$$4 \cdot 6898 = 27\,592$$

normal singular extremals exist with one cusp and two arcs, as $\lambda_{10} = \pm 1$ and $u(0) \in \{u_I, u_{II}\}$ holds and the cusp can take place at $t_c = i \triangle t$ for $i = 1, \ldots, 6898$. Here, $i \in \{0, 6899\}$ is excluded to rule out arcs of length zero. For normal singular extremal with two cusps and three arcs,

$$4 \cdot \frac{1}{2} \cdot 6898 \cdot 6897 = 95\,151\,012 \tag{9.15}$$

different solutions exist. Here, $\lambda_{10} = \pm 1$ and $u(0) \in \{u_I, u_{II}\}$ holds, the first cusp can occur at $t_1 = i_1 \triangle t$ for $i_1 = 1, \ldots, 6897$, and the second cusp at $t_2 = i_2 \triangle t$ for $i_2 = i_1 + 1, \ldots, 6898$. Using the Gaussian sum formula, (9.15) is obtained. In total, vectors $q(I_\triangle)$ for

$$4 + 27\,592 + 95\,151\,012 = 95\,178\,608$$

normal singular extremals are computed.

For the simulation data on $\tau^{tos}$, the configurations $q_d \in Q_d$ (9.12) were considered. For each $q_d$, all normal singular extremals with $\big\|q(\tau) - q_d\big\| \leq \varepsilon_q$ for some end time $\tau \in I_\triangle$ were determined. Then, an extremal with minimal end time $\tau^{tos}$ was chosen. In the simulations, no shorter end times $\tau^{tos}$ were obtained for normal singular extremals with more than two cusps and three arcs. This confirms that time-optimal extremals of the RKM have at most two cusps.

Like the end time $\tau^{tor}$ of time-optimal normal regular extremals in Figure 9.4, the end time $\tau^{tos}$ of time-optimal normal singular extremals is depicted in Figure 9.6. For this, contour plots of $\tau^{tos}$ over $(x_d, y_d) \in X_d \times Y_d$ are given for each $\theta_d \in \Theta_d$. As $\tau^{tos}$ is almost constant over large domains, a color bar is shown in the first plot. Large domains in Figure 9.6 are colored in black as the desired configurations are not reachable by normal singular extremals over $I = [0, 6.899]$.

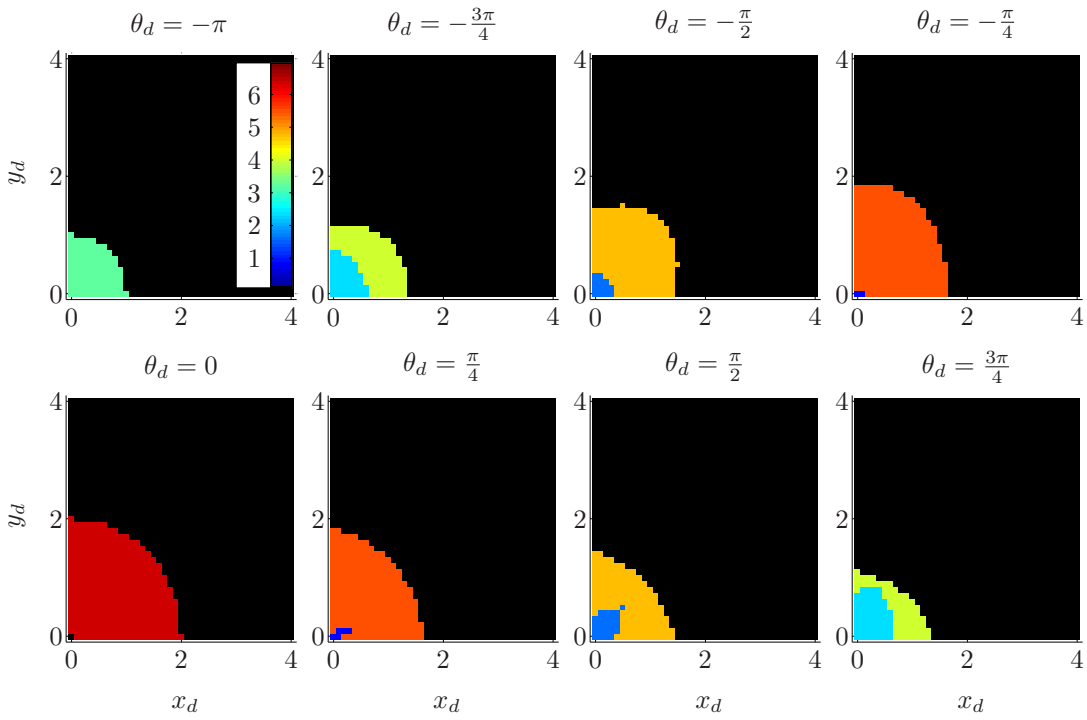


Figure 9.6: End time $\tau^{tos}$ of time-optimal normal singular extremals to $q_d \in Q_d$.

To compare the simulation data on the end times $\tau^{tor}$ of time-optimal normal regular extremals and $\tau^{tos}$ of time-optimal normal singular extremals, for each $q_d \in Q_d$, the end times are contrasted in Figure 9.7. Domains colored in red contain desired configurations which are not reachable by normal regular but only by normal singular extremals (NSE). Configurations depicted in yellow are reachable by both normal regular and normal singular extremals. Here, the normal regular extremals give equal or shorter end times, i. e., $\tau^{tor} \leq \tau^{tos}$ holds. Domains colored in green comprise configurations which can only be reached by normal regular extremals (NRE), but not by normal singular ones. There are no configurations reachable by normal regular and normal singular extremals where singular extremals give shorter end times.

Table 9.3 shows results on reachable desired configurations of normal regular and normal singular extremals. For the 13 447 desired configurations $q_d \in Q_d$, the number and percentage of configurations reachable by normal regular or normal singular extremals are given. Moreover, the number and percentage of configurations are stated which can only be reached by normal regular extremals and by normal regular and normal singular ones, respectively. In addition, the number and percentage of configurations which are time-optimally reachable by normal singular extremals are listed. These configurations correspond to those colored in red in Figure 9.7. All ratios of Table 9.3 are given with respect to the 13 447 configurations $q_d \in Q_d$.

According to Figure 9.7, all desired configurations $q_d$ not reachable by normal regular extremals can be reached by normal singular ones. Hence, in Table 9.3, the ratio of configurations reachable by normal regular or normal singular extremals is 1. Thus, an approach for time-optimal control of the RKM which applies both normal regular and normal singular extremals can find time-optimal solutions to all $q_d$. In Figure 9.7, for all configurations marked in yellow which are reachable by both normal regular and normal singular extremals, $\tau^{tor} \leq \tau^{tos}$ applies, i. e., normal regular extremals give equal or shorter end times than normal singular extremals. There are no configurations which can be reached by normal regular and normal singular extremals with $\tau^{tor} > \tau^{tos}$. The configurations $q_d$ which can be reached time-optimally by normal singular extremals are not reachable by normal regular ones. Hence, for all $q_d$ reach-

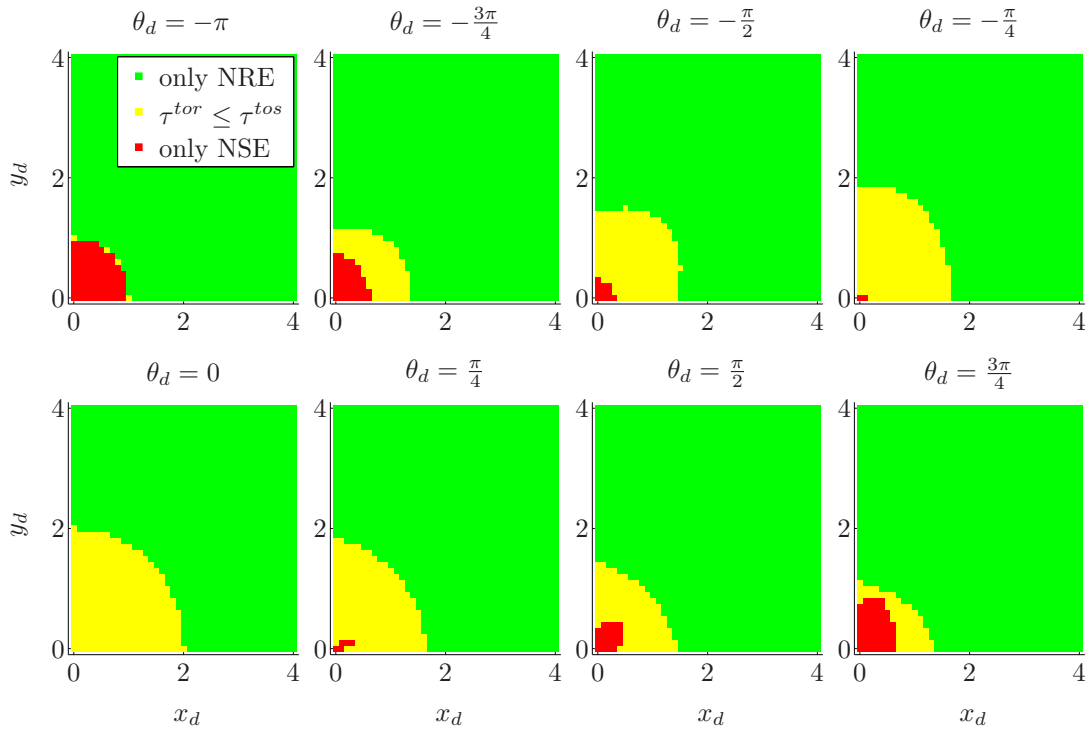


Figure 9.7: Comparison of time-optimal normal regular and normal singular extremals.

able by normal regular extremals, a control method using exclusively time-optimal normal regular extremals gives time-optimal solutions. Even the time-optimal control 7.3.2 leads to time-optimal solutions for most configurations, as most near time-optimal solutions are time-optimal as discussed in Section 9.5.3. Like in Figure 9.5, the domains in Figure 9.6 and 9.7 are slightly affected by the discretization of $x_d$ and $y_d$ and the tolerance $\varepsilon_q$.

## 9.7 Discussion of the optimality results

Aside from theoretical interest, the motivation to analyze the optimality of normal regular extremals of the RKM arises from the need for a condition for near time-optimality 9.0.1. Such a condition is required to terminate the time-optimal control 7.3.2 when a near time-optimal solution is found, i. e., a solution with end time $\tilde{\tau}^{to}$ close to the end time $\tau^{tor}$ of a time-optimal

| | | |
|---|---|---|
| desired configurations $q_d$ | reference | $Q_d$ (9.12) |
| | number | 13 447 |
| $q_d$ reachable by normal regular or normal singular extremals | number | 13 447 |
| | percentage | 100.00 % |
| $q_d$ reachable only by normal regular extremals | number | 13 222 |
| | percentage | 98.32 % |
| $q_d$ reachable by normal regular and normal singular extremals | number | 1353 |
| | percentage | 10.06 % |
| $q_d$ time-optimally reachable by normal singular extremals | number | 225 |
| | percentage | 1.67 % |

Table 9.3: Comparison of time-optimal normal regular and normal singular extremals.

normal regular extremal. As discussed in Section 9.1 and 9.3, neither the necessary conditions from Section 4.5 nor the sufficient conditions from Section 4.6 gave such a condition.

To find a suitable optimality condition for the RKM, extensive simulations of time-optimal normal regular extremals to the desired configurations $q_d \in Q_d$ (9.12) were performed and simulation data on the end time $\tau^{tor}$ and the minimal number of cusps $n_c^m$ was analyzed. According to these results, most desired configurations $q_d$ can be reached by normal regular extremals. For the minimal number of cusps, $n_c^m(q_d) \leq 2$ holds. By Theorem 9.5.1, for most desired configurations, normal regular extremals with fewer cusps have shorter end times. Based on the theorem, the necessary optimality condition 9.5.2 on the number of cusps was obtained. By this condition, normal regular extremals to a desired configuration $q_d$ can only be time-optimal if they have the minimal number of cusps $n_c^m$. This condition can be used to terminate the time-optimal control 7.3.2, as a solution which satisfies this condition gives a good approximation of a time-optimal solution for most $q_d$. According to simulations, for the majority of desired configurations $q_d$, solutions which satisfy condition 9.5.2 are in fact time-optimal solutions. For the desired configurations $q_d \in Q_d$, the mean value of the resultant quality factor $k = \tilde{\tau}^{to}/\tau^{tor}$ is 1.029. That is, on average, the end times of the solutions are only 2.9 % larger than those of time-optimal normal regular extremals.

Simulation data on time-optimal normal singular extremals was given and compared to the results on time-optimal normal regular extremals. In the simulations, all desired configurations $q_d$ not reachable by normal regular extremals can be reached by normal singular extremal. Some configurations $q_d$ can be reached by both normal regular and normal singular extremals. For all of these configurations, normal regular extremals give equal or shorter end times than normal singular ones.

All in all, most desired configurations $q_d$ can be reached by normal regular extremals, the remaining configurations are reachable by normal singular extremals, and some configurations can be reached by both. For the latter desired configurations $q_d$, normal regular extremals give equal or shorter end times. Most normal regular extremals which satisfy the necessary optimality condition 9.5.2 are time-optimal. On average, the end times of extremals satisfying the condition are only 2.9 % larger than end times of time-optimal normal regular extremals. Thus, the necessary optimality condition guarantees a good approximation of time-optimal solutions of the RKM for most desired configurations $q_d$. Hence, it can be used as condition to terminate the time-optimal control 7.3.2.

# 10 Conclusion

In this thesis, several aspects of time-optimal control of the BSR have been addressed. At the end, a summary of the original contributions and an overview of future work are given.

## 10.1 Summary

The main new contributions of this thesis are as follows:

- **Modeling and analysis of the BSR with independently steerable axles.** The FKM 5.0.1 and RKM 5.0.2 of the BSR were derived and studied in Chapter 5. Based on the kinematics of the bicycle model and its velocity constraint (5.10), the FKM 5.0.1 of the BSR was obtained. By using the steering angles $\varphi = (\varphi_f, \varphi_r)$ as input variables instead of state variables, the RKM resulted. Controllability of the two models was proved by Theorem 5.3.1 and 5.3.2, and it was shown by Corollary 5.3.3 that the constraint (5.10) is completely nonholonomic. Properties of the RKM relevant for time-optimal control were analyzed, including its absolute translational velocity, minimal turning radius, and representation as left-invariant control system on $SE(2)$. In contrast to the studies on the RKM in [11, 78, 97, 125] where the rear steering angle is a function of the front steering, all findings in this thesis apply to the RKM with independently steerable axles.

- **Extremals for time-optimal control.** In Chapter 6, the extremals for time-optimal control of the RKM were analyzed, and the existence of time-optimal solutions was shown. The necessary optimality conditions of the Maximum Principle were stated in Theorem 6.1.1, followed by the analytical maximization of the Hamiltonian function in Theorem 6.1.3 and 6.1.4. The analytical maximization reveals essential properties of the extremals and allows to simulate them at low computational cost. The extremals of the RKM were classified into normal, abnormal, regular, and singular extremals, and the normal regular and normal singular extremals relevant for time-optimal control of the RKM were analyzed. In particular, the types S, M, and P of normal regular extremals were defined, and properties of normal regular and normal singular extremals were given by Lemma 6.4.3 and 6.5.1. Simulation data on the extremals was presented and discussed. The results of Chapter 6 are original contributions, as there is no published work on extremals for time-optimal control of the BSR.

- **Optimality of the extremals.** Optimality results on normal regular and normal singular extremals for time-optimal control of the RKM were presented in Chapter 9. In particular, the necessary optimality condition 9.5.2 was given which arises from Theorem 9.5.1. According to the theorem, for most desired configurations $q_d$, normal regular extremals with fewer cusps have shorter end times. The optimality condition 9.5.2 requires that a normal regular extremal to a desired configuration $q_d$ has the minimal number of cusps $n_c^m$, which is the number of cusps of a time-optimal normal regular extremal to $q_d$. Condition 9.5.2 is a necessary optimality condition, as for most configurations $q_d$, only normal regular extremals with minimal number of cusps can be time-optimal. In fact, normal regular extremals which meet the optimality condition provide time-optimal solutions for the majority of desired configurations. On average, the end times of solutions which satisfy the necessary optimality condition are only 2.9 % larger than the end times of time-optimal normal regular extremals. Thus, they give good approximations of time-optimal solutions. These optimality results are new contributions for the BSR, as there are no published findings on time-optimal solutions for this robot.

## 10.2 Future work

Many directions of work arise from the thesis. The following aspects are worth consideration:

- **Further study of the time-optimal control problem for the RKM.** For time-optimal control of the RKM, many open issues remain. In this thesis, the driving input $v$ is the longitudinal velocity instead of the instantaneous velocity $u_{CM}$ of the center of mass, see Section 5.2.3. As the absolute translational velocity $|v_t|$ given by (5.18) is not constant, time-optimal solutions of the RKM are in general no shortest paths. The effect of using $v$ instead of $u_{CM}$ should be analyzed. As discussed in Section 6.6, no closed-form solutions of normal regular extremals of type M and P could be derived. Such closed-form representations would be valuable for path planning and optimality analysis. In addition, the sets bd $R_T(q_0)$ of configurations reachable from $q_0$ by normal regular extremals within time $T$ could be described. In Figure 9.5, solutions with $n_c^m(q_d) = 2$ only exist for configurations $q_d$ with $\theta_d = 0$, but not for $|\theta_d| \geq \frac{\pi}{4}$. Thus, it is interesting to study solutions to configurations with small $|\theta_d|$. The configurations $q_d$ with small $|\theta_d|$ and $|x_d|$ for which Theorem 9.5.1 does not hold should be considered. Finally, the singular extremals should be analyzed further.

- **Time-optimal control of other models of the BSR.** Time-optimal control can be studied for other models than the RKM. Instead of $L_f = L_r = \frac{1}{2}$, distances $L_f \neq L_r$ can be considered. Likewise, instead of $\hat{\varphi} = \frac{\pi}{4}$, other maximal steering angles $0 < \hat{\varphi} < \frac{\pi}{2}$ can be used. As discussed in Chapter 6, a more complicated structure of the extremals is expected then. Time-optimal control can be addressed for the FKM. For bounded steering angles $(\varphi_f, \varphi_r)$ which are state variables of the FKM, the Maximum Principle for control systems with state constraints has to be applied. For references to this Maximum Principle, see [43]. Moreover, a reduced kinematic model with acceleration input and bounded velocity can be studied, obtained from the RKM for the longitudinal acceleration $a = \dot{v}$ as driving input. The resultant model with state $z = (q, v)$ is

$$\begin{bmatrix} \dot{q} \\ \dot{v} \end{bmatrix} = \begin{bmatrix} g(\theta, \varphi) \\ 0 \end{bmatrix} v + \begin{bmatrix} 0 \\ 1 \end{bmatrix} a. \tag{10.1}$$

  Bounded velocities $v$ are ensured by a state constraint. Model (10.1) is more realistic than the RKM, as it does not permit discontinuous velocities. For time-optimal control of system (10.1), cusps play an important role, as reversals of the driving direction contribute considerably to the end time of a solution due to acceleration and deceleration phases.

- **Framework for time-optimal control of nonholonomic systems.** Our approach for time-optimal control is a first step to a framework for time-optimal control of nonholonomic systems. Starting point is a reduced kinematic model for a system with directly steerable axles or rudders. Such a model makes sense if the dynamics of the axles or rudders is much faster than that of the system in position and orientation. Simplifications like in Section 7.1 can be applied if the system is left-invariant on $SO(n)$ or $SE(n)$. Besides wheeled mobile robots, the control can be used e. g. for underwater vehicles which are left-invariant on $SE(3)$ and have directly steerable rudders for roll, pitch, and yaw. For references to optimal control of underwater vehicles, see [28, 29, 30, 31, 32]. To implement the time-optimal control 7.3.2 to a specific problem, the equations of the control system, the adjoint equation, and the extremal inputs are required. The parameters of Table 7.2 have to be set to adjust the algorithm for time-optimal control, including a parameterization of the search space $\Lambda_{x_0}$. Finally, optimality conditions are needed to terminate the iterated path planning when a near time-optimal solution is found. To obtain a general framework for time-optimal control of nonholonomic systems, sets of candidates for the parameterization of the search space $\Lambda_{x_0}$ and for the optimality conditions are required. Elements from these sets can be chosen to tailor the approach to the problem at hand. This way, a versatile tool for optimal control of nonholonomic systems would arise.

# A Listings

In the following, listings are given for Algorithm 7.1 which implements the path planning 7.2.6 and Algorithm 7.2 which implements the time-optimal control 7.3.2. In the listings, the algorithms are written in MATLAB-like code. For convenience and in distinction from real MATLAB code, the original names of the objects like $x_0$ and $\varepsilon_x$ are used.

## A.1 Algorithm for path planning

The algorithm for the path planning 7.2.6 is given as MATLAB function **pathplanning** in Listing A.1. The parameters of the algorithm are the initial and desired state $x_0$ and $x_d$, the tolerance $\varepsilon_x$, a parameter set $A$ to represent the search space $\Lambda_{x_0}$, the interval $\triangle t$ for the discretization of $I = [0, T]$, the final time $T$ of $I$, and the maximal number of simulated extremals for each optimization and the path planning, $\hat{n}_{Sim}^{LO}$ and $\hat{n}_{Sim}^{PP}$. Here, $\triangle t > 0$ and $T = n_T \triangle t$ holds with $n_T \in \mathbb{N}_{>0}$. The algorithm returns the initial condition $\lambda_0^{PP}$ and the end time $\tau$ which solve the path planning problem as well as the number $n_{Sim}^{PP}$ of simulated extremals.

The function **pathplanning** consists of the definition of global variables, the initialization, the loop for path planning, and the assignment of output variables. The global variables comprise the end time $t^m$, the number $n_{Sim}^{LO}$ of simulated extremals for the optimization, and the flags SC and EC1. The flag SC (for *S*olution *C*ondition) indicates whether condition (7.11) for a solution to the path planning problem is satisfied. The flags EC1 and EC2 represent the exit conditions EC1 and EC2. The global variables are used to exchange data with the function **deviation** described below which can only return the value of the deviation $d(\lambda_0)$ directly. For initialization, the counter $n_{Sim}^{PP}$ for the total number of simulated extremals for the path planning is set to zero, the flags SC and EC2 are initialized to false, and the output variables $\lambda_0^{PP}$ and $\tau$ are set to [], i. e., they are defined, but no values are assigned.

The loop for path planning is executed until flag SC or EC2 is true. Flag SC is false as long as the path planning problem is not solved, i. e., condition (7.11) is not true. Flag EC2 is false as long as the number $n_{Sim}^{PP}$ of simulated extremals is less than $\hat{n}_{Sim}^{PP}$. In the loop, a random starting point $\lambda_0^{SP}$ in the search space $\Lambda_{x_0}$ represented by the parameter set $A$ is generated by the function **random** not detailed here. Then, the minimization of $d$ as in (7.10) is performed by calling the local optimization method **opt**. The flag EC1, which is set to true in function **deviation** if the number $n_{Sim}^{LO}$ of extremals for the local optimization is greater or equal to $\hat{n}_{Sim}^{LO}$, is initialized to false, and $n_{Sim}^{LO}$ is set to zero. The local optimization is initialized to $\lambda_0^{SP}$. Then, it minimizes $d$ over $\lambda_0 \in \Lambda_{x_0}$ with $d(\lambda_0)$ provided by **deviation**. The input argument @**exit**(SC||EC1) of **opt** represents a handler to a function **exit** which terminates the optimization if SC or EC1 is true. The output of the optimization is the initial condition $\lambda_0^m$ which gives the minimal value of $d$.

After the optimization, the number $n_{Sim}^{PP}$ of simulated extremals for the path planning is incremented by $n_{Sim}^{LO}$. If $n_{Sim}^{PP}$ is greater or equal to $\hat{n}_{Sim}^{PP}$, EC2 is set to true. If SC is true as the path planning problem is solved, the output variables $\lambda_0^{PP}$ and $\tau$ are assigned. If SC is false, [] is returned for $\lambda_0^{PP}$ and $\tau$ to indicate that no solution was found.

In Listing A.2, the function **deviation** is given. This function returns $d(\lambda_0)$ for the minimization (7.10). It consists of the definition of global variables, the computation of $d(\lambda_0)$, and the assignment of global variables. The global variables are required as **deviation** can only return the value of $d(\lambda_0)$ directly, but not the variables $t^m$, $n_{Sim}^{LO}$, SC, and EC1 also required by

```
function [λ_0^PP, τ, n_Sim^PP] = pathplanning(x_0, x_d, ε_x, A, △t, T, n̂_Sim^LO, n̂_Sim^PP)

% global variables
global t^m n_Sim^LO SC EC1;

% initialization
n_Sim^PP = 0;
SC = false; % condition D(λ_0^m, t^m) ≤ ε_x not satisfied
EC2 = false; % n_Sim^PP < n̂_Sim^PP
λ_0^PP = [];
τ = [];

% loop for path planning
while ((SC == false) && (EC2 == false))
    λ_0^SP = random(A);
    n_Sim^LO = 0;
    EC1 = false; % n_Sim^LO < n̂_Sim^LO
    λ_0^m = opt(deviation(x_0, x_d, λ_0, △t, T, n̂_Sim^LO), λ_0^SP, A, @exit(SC||EC1));
    n_Sim^PP = n_Sim^PP + n_Sim^LO;
    if (n_Sim^PP ≥ n̂_Sim^PP)
        EC2 = true;
    end
end

% assignment of output variables
if (SC == true)
    λ_0^PP = λ_0^m;
    τ = t^m;
end
```

Listing A.1: Function **pathplanning** for path planning.

the function **pathplanning**. For the computation of $d(\lambda_0)$, the time vector

$$I_\triangle = \left[\, t_i \,\middle|\, t_i = i\,\triangle t,\ i{=}0,...,n_T,\ n_T = T/\triangle t \,\right]$$

is used which represents the discretized interval $I = [0, T]$. Besides the initial conditions $x_0$ and $\lambda_0$, the time vector $I_\triangle$ is an input of the function **extremal**. The function returns the vector

$$x(I_\triangle) = \left[\, x_i \,\middle|\, x_i = x(t_i),\ t_i \in I_\triangle \,\right]$$

which represents the extremal state $x$ at the times $I_\triangle$. The function **extremal** not discussed here in detail gives $x(I_\triangle)$ by numerical integration of the ordinary differential equations of the control system and the adjoint equation driven by the extremal inputs. For this, the differential equations are coded in **extremal**, and the maximization of the Hamiltonian function is implemented. Based on $x(I_\triangle)$, the vector

$$D(I_\triangle) = \left[\, D_i \,\middle|\, D_i = \|x(t_i) - x_d\|,\ t_i \in I_\triangle \,\right]$$

is generated which provides the deviation $D$ as in (7.5) at the times $I_\triangle$. From $D(I_\triangle)$, the minimal element is chosen according to (7.6), and the index $i_d$ of the corresponding element is

returned. Then, $t^m$ is set to the element of $I_\triangle$ with index $i_d$. By the MATLAB function **min**, $t^m = \min T^m$ as in (7.8) is automatically true. The number $n_{Sim}^{LO}$ of extremals is incremented by one. If condition (7.11) holds, SC is set to true. If $n_{Sim}^{LO}$ is greater or equal to $\hat{n}_{Sim}^{LO}$, EC1 is set to true.

```
function d = deviation(x_0, x_d, λ_0, △t, T, n̂_Sim^LO)

% global variables
global t^m n_Sim^LO SC EC1;

% computation of d(λ_0)
I_△ = 0:△t:T;
x(I_△) = extremal(x_0, λ_0, I_△);
D(I_△) = sqrt(sum((x(I_△) - x_d).^2));
[d, i_d] = min(D(I_△));

% assignment of global variables
t^m = I_△(i_d);
n_Sim^LO = n_Sim^LO + 1;
if (d ≤ ε_x)
    SC = true;
end
if (n_Sim^LO ≥ n̂_Sim^LO)
    EC1 = true;
end
```

Listing A.2: Function **deviation** for the computation of $d(\lambda_0)$.

## A.2 Algorithm for time-optimal control

In Listing A.3, the algorithm for the time-optimal control 7.3.2 is given as MATLAB function **tocontrol**. Its parameters include $x_0$, $x_d$, $\varepsilon_x$, $\triangle t$, $A$, and $\hat{n}_{Sim}^{LO}$ which are also inputs of the algorithm for path planning from Listing A.1, the final time $\hat{T}$ of the initial time horizon, and the maximal number $\hat{n}_{Sim}^{to}$ of simulated extremals for the time-optimal control. Here, $\hat{T} = n_{\hat{T}} \triangle t$ holds with $n_{\hat{T}} \in \mathbb{N}_{>0}$. The output variables of the algorithm are the initial condition $\lambda_0^{to}$ and the end time $\tilde{\tau}^{to}$ of a near time-optimal solution.

The function **tocontrol** consists of the initialization and the loop for time-optimal control. For initialization, the counter $n_{Sim}^{to}$ for the total number of simulated extremals for time-optimal control is set to zero. The maximal number $\hat{n}_{Sim}^{PP}$ of simulated extremals for the path planning is initialized to $\hat{n}_{Sim}^{to}$. The flag OC (for *O*ptimality *C*ondition) for the condition for near time-optimality of the solution and the flag EC3 for exit condition EC3 are set to false. The final time $T$ of the time horizon $I_\triangle$ is set to $\hat{T}$. The output variables $\lambda_0^{to}$ and $\tilde{\tau}^{to}$ are set to $[]$.

The loop for time-optimal control is executed until flag OC or EC3 is true. The function **pathplanning** is called, which returns the initial condition $\lambda_0^{PP}$ and the end time $\tau$ if a solution to the path planning problem was found, as well as the number $n_{Sim}^{PP}$ of simulated extremals. The number $n_{Sim}^{to}$ of simulated extremals for time-optimal control is incremented by $n_{Sim}^{PP}$. The function **optimality** is called with the parameters $x_0$, $x_d$, $\lambda_0^{PP}$, and $\tau$ to check whether the condition for near time-optimality holds. If this condition is satisfied, the flag OC is set to true. If a solution to the path planning problem was found, then $\lambda_0^{PP}$ from the function **pathplanning**

```
function [λ_0^to, τ̃^to] = tocontrol(x_0, x_d, ε_x, A, △t, T̂, n̂_Sim^LO, n̂_Sim^to)

% initialization
n_Sim^to = 0;
n̂_Sim^PP = n̂_Sim^to;
OC = false; % condition for near time-optimality not satisfied
EC3 = false; % n_Sim^to < n̂_Sim^to
T = T̂;
λ_0^to = [];
τ̃^to = [];

% loop for time-optimal control
while ((OC == false) && (EC3 == false))
    [λ_0^PP, τ, n_Sim^PP] = pathplanning(x_0, x_d, A, ε_x, △t, T, n̂_Sim^LO, n̂_Sim^PP);
    n_Sim^to = n_Sim^to + n_Sim^PP;
    OC = optimality(x_0, x_d, λ_0^PP, τ);
    if (~isempty(λ_0^PP))
        λ_0^to = λ_0^PP;
        τ̃^to = τ;
        T = τ - △t;
        n̂_Sim^PP = n̂_Sim^to - n_Sim^to;
    end
    if (n_Sim^to ≥ n̂_Sim^to)
        EC3 = true;
    end
end
```

Listing A.3: Function **tocontrol** for time-optimal control.

is not empty, i. e., it is unequal to []. In this case, $\lambda_0^{PP}$ and $\tau$ are assigned to the output variables $\lambda_0^{to}$ and $\tilde{\tau}^{to}$, the final time $T$ is set to $\tau - \triangle t$, and the maximal number $\hat{n}_{Sim}^{PP}$ of simulated extremals for the next run of the path planning is set to $\hat{n}_{Sim}^{to} - n_{Sim}^{to}$. If $n_{Sim}^{to}$ is greater or equal to $\hat{n}_{Sim}^{to}$, EC3 is set to true to exit the loop without further runs of the path planning.

If the loop for time-optimal control terminates due to flag OC, the solution $(\lambda_0^{to}, \tilde{\tau}^{to})$ is near time-optimal. If the loop terminates due to flag EC3, then $(\lambda_0^{to}, \tilde{\tau}^{to})$ is the best solution obtained so far within $n_{Sim}^{to}$ simulated extremals, or both variables $\lambda_0^{to}$ and $\tilde{\tau}^{to}$ are [], indicating that no solution was found.

# Bibliography


[1] R. Abraham, J. E. Marsden, T. Ratiu (1988). *Manifolds, Tensor Analysis, and Applications*. New York, Berlin, Heidelberg: Springer.

[2] A. A. Agrachev, Y. L. Sachkov (2004). *Control Theory from the Geometric Viewpoint*. Berlin, Heidelberg, New York: Springer.

[3] A. A. Agrachev, G. Stefani, P. Zezza (2002). Strong Optimality for a Bang-Bang Trajectory. *SIAM Journal on Control and Optimization*, 41(4), 991-1014.

[4] J. C. Alexander, J. H. Maddocks (1988). On the maneuvering of vehicles. *SIAM Journal on Applied Mathematics*, 48(1), 38-51.

[5] J. C. Alexander, J. H. Maddocks, B. A. Michalowski (1998). Shortest Distance Paths for Wheeled Mobile Robots. *IEEE Transactions on Robotics and Automation*, 14(5), 657-662.

[6] D. A. Anisi (2003). Optimal Motion Control of a Ground Vehicle. *Research Report FOI-R-0961-SE*, Royal Institute of Technology, Stockholm, Sweden. Available: http://www.math.kth.se/~anisi/articles/foi-r-0961-se.pdf.

[7] V. I. Arnold (1989). *Mathematical Methods in Classical Mechanics*. Berlin, Heidelberg, New York: Springer.

[8] D. Augustin, H. Maurer (2001). Second Order Sufficient Conditions and Sensitivity Analysis for the Optimal Control of a Container Crane under State Constraints. *Optimization*, 49(4), 351-368.

[9] D. J. Balkcom, M. T. Mason (2000). Extremal trajectories for bounded velocity differential drive robots. *Proceedings of the 2000 IEEE International Conference on Robotics and Automation*, 3, 2479-2484.

[10] D. J. Balkcom, M. T. Mason (2000). Geometric construction of time optimal trajectories for differential drive robots. *Proceedings of the 4th Workshop on the Algorithmic Foundations of Robotics*, 1-13.

[11] L. C. Bento, U. Nunes, A. Mendes, M. Parent (2003). Path Tracking Controller of a bi-steerable Cybernetic Car using Fuzzy Logic. *Proceedings of the 11th IEEE International Conference on Advanced Robotics*, 3, 1556-1561.

[12] A. M. Bloch, J. Baillieul, P. E. Crouch, J. E. Marsden (2003). *Nonholonomic Mechanics and Control*. Berlin, Heidelberg, New York: Springer.

[13] J.-D. Boissonnat, A. Cerezo, J. Leblond (1992). Shortest paths of bounded curvature in the plane. *Proceedings of the 1992 IEEE International Conference on Robotics and Automation*, 3, 2315-2320.

[14] V. G. Boltyanskii (1966). Sufficient Conditions for Optimality and the Justification of the Dynamic Programming Method. *SIAM Journal on Control*, 4(2), 326-361.

[15] B. Bonnard, M. Chyba (2003). *Singular Trajectories and their Role in Control Theory*. Berlin, Heidelberg, New York: Springer.

[16] W. M. Boothby (2003). *An Introduction to Differential Manifolds and Riemannian Geometry*. Amsterdam, Boston, Heidelberg: Academic Press.

[17] A. Bressan (1985). A high order test for optimality of bang-bang controls. *SIAM Journal on Control and Optimization*, 23(1), 38-48.

[18] R. W. Brockett (1981). Control Theory and Singular Riemannian Geometry, 11-27 in: P. J. Hilton, G. S. Young (Ed.). *New Directions in Applied Mathematics*. Berlin, Heidelberg, New York: Springer.

[19] X.-N. Bui, J.-D. Boissonnat, P. Souères, J.-P. Laumond (1994). Shortest path synthesis for Dubins non-holonomic robot. *Proceedings of the 1994 IEEE International Conference on Robotics and Automation*, 1, 2-7.

[20] F. Bullo (2004). Trajectory design for mechanical control systems: from geometry to algorithms. *European Journal of Control*, 10(5), 397-410.

[21] F. Bullo, A. D. Lewis (2003). Kinematic controllability and motion planning for the snakeboard. *IEEE Transactions on Robotics and Automation*, 19(3), 494-498.

[22] F. Bullo, A. D. Lewis (2004). *Geometric Control of Mechanical Systems*. Berlin, Heidelberg, New York: Springer.

[23] L. G. Bushnell, D. M. Tilbury, S. S. Sastry (1995). Steering three-input nonholonomic systems: The fire truck example. *International Journal of Robotics Research*, 14(4), 366-381.

[24] C. Büskens, H. Maurer (2000). SQP-Methods for Solving Optimal Control Problems with Control and State Constraints: Adjoint Variables, Sensitivity Analysis and Real-Time Control. *Journal of Computational and Applied Mathematics*, 120(1), 85-108.

[25] G. Campion, G. Bastin, B. d'Andrea-Novel (1996). Structural Properties and Classification of Kinematic and Dynamic Models of Wheeled Mobile Robots. *IEEE Transactions on Robotics and Automation*, 12(1), 47-62.

[26] L. Cesari (1983). *Optimization - Theory and Applications*. Berlin, Heidelberg, New York: Springer.

[27] H. Chitsaz, S. M. LaValle, D. J. Balkcom, M. T. Mason (2006). Minimum Wheel-Rotation Paths for Differential-Drive Mobile Robots. *Proceedings of the 2006 IEEE International Conference on Robotics and Automation*, 4, 1616-1623.

[28] M. Chyba, T. Haberkorn (2005). Designing efficient trajectories for underwater vehicles using geometric control theory. *Proceedings of the 24th International Conference on Offshore Mechanics and Arctic Engineering*, 2, 637-645.

[29] M. Chyba, T. Haberkorn, R. N. Smith (2005). Controllability and Optimal Trajectories for Controlled Mechanical Systems: An Application to Underwater Vehicles. *Submitted to Systems & Control Letters*. Available: http://www.math.hawaii.edu/~mchyba/documents/publications/scl05.pdf.

[30] M. Chyba, T. Haberkorn, R. N. Smith (2006). Design of time efficient trajectories for a submerged rigid body. *Submitted to Discrete and Continuous Dynamical Systems*. Available: http://www.math.hawaii.edu/~mchyba/documents/publications/dcds06.pdf.

[31] M. Chyba, T. Haberkorn, R. N. Smith, S. Zhao, S. K. Choi (2006). Towards practical implementation of time optimal trajectories for underwater vehicles. *Proceedings of the 25th International Conference on Offshore Mechanics and Arctic Engineering*, 2, 183-190.

[32] M. Chyba, H. J. Sussmann, H. Maurer, G. Vossen (2004). Underwater vehicles: The minimum time problem. *Proceedings of the 43rd IEEE International Conference on Decision and Control*, 2, 1370-1375.

[33] J. Cortés (2008). Discontinuous dynamical systems. *IEEE Control Systems Magazine*, 28(3), 36-73.

[34] B. d'Andrea-Novel, G. Campion, G. Bastin (1995). Control of nonholonomic wheeled mobile robots by state feedback linearization. *The International Journal of Robotics Research*, 14(6), 543-559.

[35] A. De Luca, G. Oriolo (1995). Modeling and Control of Nonholonomic Mechanical Systems, 277-342 in: J. Angeles, A. Kecskemethy (Ed.). *Kinematics and Dynamics of Multi-Body Systems*. Berlin, Heidelberg, New York: Springer.

[36] G. Dirr, U. Helmke, K. Hüper, M. Kleinsteuber, Y. Liu (2006). Spin Dynamics: A Paradigm for Time Optimal Control on Compact Lie Groups. *Journal of Global Optimization*, 35(3), 443-474.

[37] L. E. Dubins (1957). On Curves of Minimal Length with a Constraint on Average Curvature, and with Prescribed Initial and Terminal Positions and Tangents. *American Journal of Mathematics*, 79(3), 497-516.

[38] H. Durrant-Whyte, D. Pagac, B. Rogers, M. Stevens, G. Nelmes (2007). An autonomous straddle carrier for movement of shipping containers. *IEEE Robotics and Automation Magazine*, 14(3), 14-23.

[39] M. Fliess, J. Lévine, P. Martin, P. Rouchon (1992). On differentially flat nonlinear systems, 159-163 in: M. Fliess (Ed.). *Nonlinear Control Systems Design*. Oxford: Pergamon Press.

[40] M. Fliess, J. Lévine, P. Martin, P. Rouchon (1995). Flatness and defect of nonlinear systems: Introductory theory and examples. *International Journal of Control*, 61(6), 1327-1361.

[41] E. Frazzoli, M. A. Dahleh, E. Feron (2005). Maneuver-based motion planning for nonlinear systems with symmetries. *IEEE Transactions on Robotics and Automation*, 21(6), 1077-1091.

[42] A. T. Fuller (1961). Relay control systems optimized for various performance criteria. *Automatic and remote control*, 1, 510-519.

[43] R. F. Hartl, S. P. Sethi, R. G. Vickson (1995). A Survey of the Maximum Principles for Optimal Control Problems with State Constraints. *SIAM Review*, 37(2), 181-218.

[44] J. Hermosillo, S. Sekhavat (2003). Feedback Control of a Bi-steerable Car Using Flatness Application to Trajectory Tracking. *Proceedings of the 2003 IEEE American Control Conference*, 4, 3567-3572.

[45] M. Hess (2010). *Motion coordination and control in systems of nonholonomic autonomous vehicles*. Ph.D. dissertation, University of Würzburg, Würzburg, Germany. Available: http://opus.bibliothek.uni-wuerzburg.de/volltexte/2010/4644/pdf/hessdiss.pdf.

[46] T. M. Howard, A. Kelly (2007). Optimal Rough Terrain Trajectory Generation for Wheeled Mobile Robots. *International Journal of Robotics Research*, 26(2), 141-166.

[47] I. I. Hussein (2005). *Motion Planning for Multi-Spacecraft Interferometric Imaging Systems*. Ph.D. dissertation, University of Michigan, Ann Arbor, MI, USA.

[48] S. Iannitti, K. M. Lynch (2004). Minimum control-switch motions for the snakeboard: a case study in kinematically controllable underactuated systems. *IEEE Transactions on Robotics*, 20(6), 994-1006.

[49] V. Jurdjevic (1997). *Geometric Control Theory*. Cambridge, New York, Melbourne: Cambridge University Press.

[50] M. I. Kamien, N. L. Schwartz (1971). Sufficient Conditions in Optimal Control Theory. *Journal of Economic Theory*, 3(2), 207-214.

[51] C. Y. Kaya, S. K. Lucas, S. T. Simakov (2004). Computations for bang-bang constrained optimal control using a mathematical programming formulation. *Optimal Control Applications and Methods*, 25(6), 295-308.

[52] J. Kierzenka, L. F. Shampine (2001). A BVP Solver based on Residual Control and the MATLAB PSE. *ACM Transactions on Mathematical Software*, 27(3), 299-316.

[53] I. Kolmanovsky, N. H. McClamroch (1995). Developments in Nonholonomic Control Problems. *IEEE Control Systems Magazine*, 15(6), 20-36.

[54] W.-S. Koon, J. E. Marsden (1997). Optimal Control for Holonomic and Nonholonomic Mechanical Systems with Symmetry and Lagrangian Reduction. *SIAM Journal on Control and Optimization*, 35(3), 901-929.

[55] T. Kopfstedt, M. Restle, W. Grimm (2010). Terrain Optimized Nonholonomic Following of Vehicle Tracks. *Proceedings of the 7th IFAC Symposium on Intelligent Autonomous Vehicles*.

[56] A. J. Krener (1977). The high order maximal principle and its application to singular extremals. *SIAM Journal on Control and Optimization*, 15(2), 256-293.

[57] G. Lafferriere, H. J. Sussmann (1991). Motion Planning for Controllable Systems without Drift. *Proceedings of the 1991 IEEE International Conference on Robotics and Automation*, 2, 1148-1153.

[58] F. Lamiraux, J.-P. Laumond (1996). On the expected complexity of random path planning. *Proceedings of the 1996 IEEE International Conference on Robotics and Automation*, 4, 3014-3019.

[59] J.-P. Laumond, S. Sekhavat, F. Lamiraux (1998). Guidelines in Nonholonomic Motion Planning for Mobile Robots, 1-53 in: J.-P. Laumond (Ed.). *Robot Motion Planning and Control*. Berlin, Heidelberg, New York: Springer.

[60] S. M. LaValle (2006). *Planning Algorithms*. Cambridge, New York, Melbourne: Cambridge University Press.

[61] W. Leroquais, B. d'Andrea-Novel (1995). Transformation of the kinematic models of restricted mobility wheeled mobile robots with a single platform into chain forms. *Proceedings of the 34th IEEE International Conference on Decision and Control*, 4, 3811-3816.

[62] A. D. Lewis (2000). Simple Mechanical Control Systems with Constraints. *IEEE Transactions on Automatic Control*, 45(8), 1420-1436.

[63] A. D. Lewis, J. P. Ostrowski, J. W. Burdick, R. M. Murray (1994). Nonholonomic mechanics and locomotion: The snakeboard example. *Proceedings of the 1994 IEEE International Conference on Robotics and Automation*, 3, 2391-2397.

[64] S.-J. Li, W. Respondek (2010). Describing and Calculating Flat Outputs of Two-Input Driftless Control Systems. *Proceedings of the 8th IFAC Symposium on Nonlinear Control Systems*, 1, 683-688.

[65] K. Malanowski, H. Maurer, S. Pickenhain (2004). Second-Order Sufficient Conditions for State-Constrained Optimal Control Problems. *Journal of Optimization Theory and Applications*, 123(3), 595-617.

[66] O. L. Mangasarian (1966). Sufficient conditions for the optimal control of nonlinear systems. *SIAM Journal on Control*, 4(1), 139-152.

[67] P. Martin, P. Rouchon (1995). Any (controllable) driftless system with $m$ inputs and $m + 2$ states is flat. *Proceedings of the 34th IEEE International Conference on Decision and Control*, 3, 2886-2891.

[68] S. Martínez, J. Cortés, F. Bullo (2003). A catalog of inverse-kinematics planners for underactuated systems on matrix Lie groups. *Proceedings of the 2003 IEEE/RSJ International Conference on Intelligent Robots and Systems*, 1, 625-630.

[69] M. Mauder (2008). Robust tracking control of nonholonomic dynamic systems with application to the bi-steerable mobile robot. *Automatica*, 44(10), 2588-2592.

[70] H. Maurer (1995). Second Order Sufficient Conditions for Control Problems with Free Final Time. *Proceedings of the 3rd IEEE European Control Conference*, 3602-3606.

[71] H. Maurer, I. Altrogge, N. Goris (2005). Optimization methods for solving bang-bang control problems with state constraints and the verification of sufficient conditions. *Proceedings of the 44th IEEE International Conference on Decision and Control*, 923-928.

[72] H. Maurer, D. Augustin (1995). Second Order Sufficient Conditions and Sensitivity Analysis for the Controlled Rayleigh Equation. *Proceedings of the 4th International Conference on Parametric Optimization and Related Topics*, 245-249.

[73] H. Maurer, C. Büskens, J.-H. R. Kim, C. Y. Kaya (2005). Optimization methods for the verification of second order sufficient conditions for bang-bang controls. *Optimal Control Applications and Methods*, 26(3), 129-156.

[74] H. Maurer, J.-H. R. Kim, G. Vossen (2005). On a State-Constrained Control Problem in Optimal Production and Maintenance, 289-308 in: C. Deissenberg, R. F. Hartl (Ed.). *Optimal Control and Dynamic Games: Applications in Finance, Management Science and Economics*. Berlin, Heidelberg, New York: Springer.

[75] H. Maurer, H. J. Oberle (2002). Second Order Sufficient Conditions for Optimal Control Problems with Free Final Time: The Riccati Approach. *SIAM Journal on Control and Optimization*, 41(2), 380-403.

[76] H. Maurer, N. P. Osmolovskii (2004). Second Order Sufficient Conditions for Time-Optimal Bang-Bang Control. *SIAM Journal on Control and Optimization*, 42(6), 2239-2263.

[77] J. P. McDanell, W. F. Powers (1971). Necessary conditions for joining optimal singular and nonsingular subarcs. *SIAM Journal on Control*, 9(2), 161-173.

[78] A. Mendes, L. C. Bento, U. Nunes (2003). Path-Tracking Controller with an Anti-collision Behaviour of a bi-steerable Cybernetic Car. *Proceedings of the 2003 IEEE International Conference on Emerging Technologies and Factory Automation*, 1, 613-619.

[79] J. C. Monforte (2002). *Geometric, Control and Numerical Aspects of Nonholonomic Systems*. Berlin, Heidelberg, New York: Springer.

[80] R. M. Murray, Z. Li, S. S. Sastry (1994). *A Mathematical Introduction to Robotic Manipulation*. Boca Raton, London, New York, Tokyo: CRC Press.

[81] R. M. Murray, S. S. Sastry (1993). Nonholonomic Motion Planning: Steering Using Sinusoids. *IEEE Transactions on Automatic Control*, 38(5), 700-716.

[82] W. S. Newman (1990). Robust Near Time-Optimal Control. *IEEE Transactions on Automatic Control*, 35(7), 841-844.

[83] H. Nijmeijer, A. van der Schaft (1990). *Nonlinear Dynamical Control Systems*. Berlin, Heidelberg, New York: Springer.

[84] P. J. Olver (1993). *Applications of Lie Groups to Differential Equations*. Berlin, Heidelberg, New York: Springer.

[85] N. P. Osmolovskii, H. Maurer (2005). Equivalence of second order optimality conditions for bang-bang control problems. Part 1: Main results. *Control and Cybernetics*, 34(3), 927-950.

[86] N. P. Osmolovskii, H. Maurer (2007). Second order sufficient optimality conditions for a control problem with continuous and bang-bang control components: Riccati approach, 411-429 in: A. Korytowski, K. Malanowski, W. Mitkowski, M. Szymkat (Ed.). *System Modeling and Optimization*. Berlin, Heidelberg, New York: Springer.

[87] J. Ostrowski, J. P. Desai, V. Kumar (1997). Optimal Gait Selection for Nonholonomic Locomotion Systems. *Proceedings of the 1997 IEEE International Conference on Robotics and Automation*, 1, 786-791.

[88] B. Piccoli, H. J. Sussmann (2000). Regular Synthesis and Sufficiency Conditions for Optimality. *SIAM Journal on Control and Optimization*, 39(2), 359-410.

[89] L. Poggiolini (2006). On local state optimality of bang-bang extremal. *Mathematical Journal of the University of Turin*, 64(1), 1-23.

[90] L. Poggiolini, G. Stefani (2002). Minimum time optimality of a bang-bang trajectory. *Proceedings of the 41st IEEE International Conference on Decision and Control*, 2, 1922-1925.

[91] L. Poggiolini, G. Stefani (2006). Sufficient optimality conditions for a bang-bang trajectory. *Proceedings of the 45th IEEE International Conference on Decision and Control*, 6624-6629.

[92] E. Polak (1973). An Historical Survey of Computational Methods in Optimal Control. *SIAM Review*, 15(2), 553-584.

[93] L. S. Pontryagin, V. G. Boltyanskii, R. V. Gamkrelidze, E. F. Mishchenko (1962). *The Mathematical Theory of Optimal Processes*. New York, London: John Wiley & Sons.

[94] J. A. Reeds, L. A. Shepp (1990). Optimal paths for a car that goes both forward and backward. *Pacific Journal of Mathematics*, 145(2), 367-393.

[95] H. M. Robbins (1967). A Generalized Legendre-Clebsch Condition for the Singular Cases of Optimal Control. *IBM Journal of Research and Development*, 11(4), 361-372.

[96] R. Rothfuß, J. Rudolph, M. Zeitz (1997). Flachheit: Ein neuer Zugang zur Steuerung und Regelung nichtlinearer Systeme. *Automatisierungstechnik*, 45(11), 517-525.

[97] S. Sanan, D. Santani, K. M. Krishna, H. Hexmoor (2006). Extension of Reeds & Shepp Paths to a Robot with Front and Rear Wheel Steer. *Proceedings of the 2006 IEEE International Conference on Robotics and Automation*, 9, 3730-3735.

[98] S. S. Sastry (1999). *Nonlinear Systems*. Berlin, Heidelberg, New York: Springer.

[99] H. M. Schättler (1988). On the local structure of time-optimal bang-bang trajectories in $R^{3*}$. *SIAM Journal on Control and Optimization*, 26(1), 186-204.

[100] H. M. Schättler (1988). The local structure of time-optimal trajectories in dimension three under generic conditions. *SIAM Journal on Control and Optimization*, 26(4), 899-918.

[101] S. Sekhavat, J. Hermosillo (2000). The Cycab Robot: a Differentially Flat System. *Proceedings of the 2000 IEEE/RSJ International Conference on Intelligent Robots and Systems*, 1, 312-317.

[102] S. Sekhavat, P. Rouchon, J. Hermosillo (2001). Computing the Flat Outputs of Engel Differential Systems: The Case Study of the Bi-steerable Car. *Proceedings of the 2001 IEEE American Control Conference*, 5, 3576-3581.

[103] E. D. Sontag (1998). A General Approach to Path Planning for Systems without Drift, 151-168 in: J. Baillieul, S. S. Sastry, H. J. Sussmann (Ed.). *Essays on Mathematical Robotics*. Berlin, Heidelberg, New York: Springer.

[104] E. D. Sontag (1998). *Mathematical Control Theory*. Berlin, Heidelberg, New York: Springer.

[105] P. Souères (2007). Minimum-Length Trajectories for a Car: An Example of the Use of Boltianskii's Sufficient Conditions for Optimality. *IEEE Transactions on Automatic Control*, 52(2), 323-327.

[106] P. Souères, J.-D. Boissonnat (1998). Optimal Trajectories for Nonholonomic Mobile Robots, 93-170 in: J.-P. Laumond (Ed.). *Robot Motion Planning and Control*. Berlin, Heidelberg, New York: Springer.

[107] P. Souères, J.-Y. Fourquet, J.-P. Laumond (1994). Set of reachable positions for a car. *IEEE Transactions on Automatic Control*, 39(8), 1626-1630.

[108] P. Souères, J.-P. Laumond (1996). Shortest Path Synthesis for a Car-Like Robot. *IEEE Transactions on Automatic Control*, 41(5), 672-688.

[109] R. S. Strichartz (1986). Sub-Riemannian Geometry. *Journal of Differential Geometry*, 24(2), 221-263.

[110] H. J. Sussmann (1986). Envelopes, Conjugate Points, and Optimal Bang-Bang Extremals, 325-346 in: M. Fliess, M. Hazewinkel (Ed.). *Algebraic and Geometric Methods in Nonlinear Control Theory*. Dordrecht, Boston: D. Reidel Publishing Company.

[111] H. J. Sussmann (1987). The Structure of Time-Optimal Trajectories for Single-Input Systems in the Plane: The $C^\infty$ Nonsingular Case. *SIAM Journal on Control and Optimization*, 25(2), 433-465.

[112] H. J. Sussmann (1987). The Structure of Time-Optimal Trajectories for Single-Input Systems in the Plane: The General Real Analytic Case. *SIAM Journal on Control and Optimization*, 25(4), 868-904.

[113] H. J. Sussmann (1987). Regular Synthesis for Time-Optimal Control of Single-Input Real Analytic Systems in the Plane. *SIAM Journal on Control and Optimization*, 25(5), 1145-1162.

[114] H. J. Sussmann (1988). Why real analyticity is important in control theory, 315-340 in: B. Jakubczyk, K. Malanowski, W. Respondek (Ed.). *Perspectives in control theory*. Boston: Birkäuser.

[115] H. J. Sussmann (1989). Envelopes, Higher-Order Optimality Conditions, and Lie Brackets. *Proceedings of the 28th IEEE International Conference on Decision and Control*, 2, 1107-1112.

[116] H. J. Sussmann (1996). From the Brachystochrone to the Maximum Principle. *Proceedings of the 35th IEEE International Conference on Decision and Control*, 2, 1588-1594.

[117] H. J. Sussmann (1997). An introduction to the coordinate-free Maximum Principle, 463-557 in: B. Jakubczyk, W. Respondek (Ed.). *Geometry of Feedback and Optimal Control*. New York: Marcel Dekker.

[118] H. J. Sussmann, V. Jurdjevic (1972). Controllability of Nonlinear Systems. *Journal of Differential Equations*, 12(1), 95-116.

[119] H. J. Sussmann, B. Piccoli (1999). Regular Presynthesis and Synthesis, and Optimality of Families of Extremals. *Proceedings of the 39th IEEE International Conference on Decision and Control*, 4, 3352-3357.

[120] H. J. Sussmann, G. Tang (1991). Shortest paths for the Reeds-Shepp car: a worked out example of the use of geometric techniques in nonlinear optimal control. *Research Report SYCON-91-10*, Rutgers University, New Brunswick, NJ, USA.

[121] P. Svestka, M. H. Overmars (1998). Probabilistic Path Planning, 255-304 in: J.-P. Laumond (Ed.). *Robot Motion Planning and Control*. Berlin, Heidelberg, New York: Springer.

[122] D. M. Tilbury, A. Chelouah (1993). Steering a three-input nonholonomic system using Multi-rate Controls. *Proceedings of the 2nd IEEE European Control Conference*, 1428-1431.

[123] B. Thuilot, B. d'Andrea-Novel, A. Micaelli (1996). Modeling and Feedback Control of Mobile Robots Equipped with Several Steering Wheels. *IEEE Transactions on Robotics and Automation*, 12(3), 375-390.

[124] H. Wang, Y. Chen, P. Souères (2009). A Geometric Algorithm to Compute Time-Optimal Trajectories for a Bidirectional Steered Robot. *IEEE Transactions on Robotics*, 25(2), 399-413.

[125] D. Wang, F. Qi (2001). Trajectory Planning for a Four-Wheel-Steering Vehicle. *Proceedings of the 2001 IEEE International Conference on Robotics and Automation*, 4, 3320-3325.

[126] X. Q. Yang (1994). Smoothing approximations to nonsmooth optimization problems. *Journal of the Australian Mathematical Society, Series B, Applied Mathematics*, 36, 274-285.

[127] K. F. C. Yiu, Y. Liu, K. L. Teo (2004). A Hybrid Descent Method for Global Optimization. *Journal of Global Optimization*, 28(2), 229-238.

# Index